A LOCAL MESH REFINEMENT SCHEME FOR FINITE DIFFERENCE SOLUTION OF MIXED BOUNDARY-VALUE ELASTIC PROBLEMS

by

Aminul Islam Khan

A thesis submitted in partial fulfillment of the requirements for the degree of

MASTER OF SCIENCE IN MECHANICAL ENGINEERING

Department of Mechanical Engineering
BANGLADESH UNIVERSITY OF ENGINEERING AND TECHNOLOGY
Dhaka 1000, Bangladesh.

August, 2014

This thesis titled "**A LOCAL MESH REFINEMENT SCHEME FOR FINITE DIFFERENCE SOLUTION OF MIXED BOUNDARY-VALUE ELASTIC PROBLEMS",** submitted by **Aminul Islam Khan**, Student No. **0411102073 P,** Session: **April 2011**, has been accepted as satisfactory in partial fulfillment of the requirements for the degree of MASTER OF SCIENCE IN MECHANICAL ENGINEERING on 27 August, 2014.

BOARD OF EXAMINERS

_____ Chairman (Supervisor)

Dr. Md. Abdus Salam Akanda
Professor
Department of Mechanical Engineering
BUET, Dhaka, Bangladesh.

_____ Member (Ex-Officio)

Dr. Md. Zahurul Haq
Professor and Head
Department of Mechanical Engineering
BUET, Dhaka, Bangladesh.

_____ Member

Dr. Shaikh Reaz Ahmed
Professor
Department of Mechanical Engineering
BUET, Dhaka, Bangladesh.

_____ Member (External)

Prof. Dr. M. Fazli Ilahi
Ex. Vice Chancellor
Islamic University of Technology (IUT)
Gazipur, Dhaka, Bangladesh.

CERTIFICATE OF RESEARCH

This is to certify that the work presented in this thesis is carried out by the author under the supervision of Dr. Md. Abdus Salam Akanda, Professor of the Department of Mechanical Engineering, Bangladesh University of Engineering and Technology, Dhaka, Bangladesh.

_____ _____

Dr. Md. Abdus Salam Akanda Aminul Islam Khan

DECLARATION

It is hereby declared that this thesis or any part of it has not been submitted elsewhere for the award of any degree or qualification.

_____ _____

Aminul Islam Khan Date

Author

Dedicated to My Parents

ACKNOWLEDGEMENTS

Thanks to most merciful, most gracious and the most cordial almighty Allah. The author would like to thank his parents, his elder sister and his loving wife for giving him unquestionable support and inspirations.

The author would like to express his gratefulness and deepest reverence to his thesis supervisor Dr. Md. Abdus Salam Akanda, Professor, Department of Mechanical Engineering, BUET for his constant guidance, cynosure, constructive criticism, encouragement, and careful supervision throughout the research work without which this thesis would not have egress.

The author gratefully acknowledges the assistance received at various stages of this work from Dr. Shaikh Reaz Ahmed, Professor, Department of Mechanical Engineering, BUET and the author also like to acknowledges Dr. Md. Zahurul Haq, Professor and Head, Department of Mechanical Engineering, BUET for giving support and encouragement .

Special thanks to all his colleagues, especially Kazi Arafat Rahman, Adnan Morshed and Md. Yeasin Bhuiyan for giving support and encouragement.

Finally, the author would like to express his gratitude to his all well wisher for their cooperation and support in the successful completion of this work.

Author

ABSTRACT

Some numerical simulations of multi-scale physical phenomena consume a significant amount of computational resources, since their domains are discretized on high resolution meshes. An enormous wastage of these resources occurs in refinement of sections of the domain where computation of the solution does not require high resolutions. This problem is effectively addressed by mesh refinement (MR) technique, a technique of local refinement of mesh only in sections where needed, thus allowing concentration of effort where it is required. Sections of the domain needing high resolution are generally determined by means of a criterion which may vary depending on the nature of the problem. Fairly straightforward criteria could include comparing the solution to a threshold or the gradient of a solution, that is, its local rate of change to a threshold or the presence of stress concentrator or stress riser, sharp change in cross section, void in material, cracks, holes etc. While the comparing of solution to a threshold is not particularly rigorous and hardly ever represents a physical phenomenon of interest, it is simple to implement. However, the gradient criterion is not as simple to implement as a direct comparison of values, but it is still quick and a good indicator of the effectiveness of the MR technique. The MR technique can be classified into two categories. One is *h*-refinement, where either the existing mesh is split into several smaller cells or additional nodes are inserted locally and the other one is *r*-refinement in which move the mesh points inside the domain in order to better capture the dynamic changes of solution. The objective of this thesis is to develop a MR algorithm for the solution of fourth order bi-harmonic equation using FDM. In the MR algorithm developed, a mesh of increasingly fine resolution permits high resolution computation in sub-domains of interest and low resolution in others. In this thesis work, the gradient of the solution has been considered as region selecting criteria and existing mesh is split into smaller meshes to achieve refine mesh. The developed MR algorithm has been applied for the solution of an embedded crack problem. The validity, effectiveness, soundness and superiority of this MR algorithm has been verified by the comparing of obtained solutions with uniform mesh results, FEM results and also with the well known published results of the same embedded crack problem having same material, geometry and loading conditions.

TABLE OF CONTENTS

NOMENCLATURE

Notation	Definition
E	Modulus of Elasticity
M	Poisson ratio
Ψ	Displacement potential function
σ_x, σ_y, σ_z	Normal stress component along x,y and z-direction respectively
σ_{xy}, σ_{yx}	Shear stress component in the xy plane
σ_{xz}, σ_{zx}	Shear stress component in the zx plane
σ_{yz}, σ_{zy}	Shear stress component in the yz plane
σ_n	Stress component normal to boundary
σ_t	Stress component tangential to boundary
ε_x ,ε_y ,ε_z	Strain components parallel to the co-ordinate axes.
$\gamma_{xy,}$ $\gamma_{yz,}$ γ_{zx}	Strain components acting on the planes xy, yz and zx planes respectively
u_n	Normal component of displacement
u_t	Tangential component
u	Displacement component along x-direction
v	Displacement component along y-direction
$\varphi(x,y)$	Airy's stress function
H	Mesh length along x-direction for uniform meshing
k	Mesh length along y-direction for uniform meshing
h_1,h_2,h_3	Mesh length along x-direction for mesh refinement scheme
k_1,k_2,k_3	Mesh length along x-direction for mesh refinement scheme
R	k/h
A	Length of the body
B	Width of the body
l, m	Direction cosine of the normal at any physical boundary point
t_n	Stress vector
$t_{x,}$ $t_{y,}$ t_z	Stress vector in x, y, z direction respectively
i, j ,k	The unit vectors along(x, y ,z) axes respectively
n	Normal vector
n_x, n_y, n_z	The components of the normal vector
X, Y, Z	The components of body force per unit volume of the element in x, y, and z-directions respectively

ABBREVIATIONS

Notation	Definition
PDE	Partial Differential Equation
FDM	Finite Difference Method
FEM	Finite Element Method
2D	Two space Dimension
MR	Mesh Refinement
RM	Refine Mesh
UM	Uniform Mesh
CPU	Central Processing Unit
BVP	Boundary Value Problem
ODE	Ordinary Differential Equation
GE	Governing Equation
BC	Boundary Condition

LIST OF TABLES

LIST OF FIGURES

CHAPTER 1
INTRODUCTION

1.1 General

Numerical analysis deals with the study of algorithms for the problems of continuous mathematics. These algorithms are routinely applied to many problems in science and engineering. Important applications include weather forecasting, climate models, the analysis and design of molecules, the design of structures like bridges and airplanes, locating oil reservoirs and the like. In addition to mathematical axioms, theorems and proofs, numerical analysis uses empirical results of computation runs to probe new methods and analyze problems.

Some of the problems analyzed by numerical analysis can be solved exactly by an algorithm. These methods are called direct methods. Significant examples of such algorithm are the simplex method in linear programming and the Gaussian elimination method for solving systems of linear equations. However, for a majority of the problems, direct methods do not exist. For such cases, iterative methods are usually employed. An iterative method begins with a guess and finds successive approximation that hopefully converges to a solution.

The iterative procedures consume a lot of computational resources. As a consequence, efficiency plays a very significant role and a heuristic method may be preferred above a method with a solid theoretic foundation.

1.2 Background of the study

Stress analysis is a classical topic in the field of engineering. During recent years the theory of elasticity has found considerable application in the solution of engineering problems. For the solution of the problem several methodologies can be followed, however, all of these methods can be classified in the following three general categories: experimental, analytical and numerical method. Though experimental methods give the most reliable results, it is very costly, as it requires special equipments, testing facilities etc. Analytical solution of every problem is almost impossible because of complex boundary conditions and shapes or geometry. For these reasons numerical methods had become the ultimate choice by the researchers in the

last few decades. Invention and rapid improvement of the computing machines i.e. sophisticated high performance computers, also played an important role for the increasing popularity of the numerical methods. For the numerical simulation of many practical problems in physics and engineering, it is often equivalent to solve a set of partial differential equations (PDEs), which represent the mathematical model of physical problem concerned. There are various methods available for the solution of partial differential equations, which are needed for the stress analysis of structures. Among them most popular methods are: finite difference method (FDM) and finite element method (FEM). The FDM is one of the oldest numerical methods known for solving PDE's. The difference equations that are used to model governing equations in FDM are very simple to computer code and the global coefficient matrix that is produced by FDM possesses a banded structure, which is very effective for good solution. But, somehow these stress analysis problems are suffering from a lot of shortcomings. We have often failed in establishing a very good correlation between analysis and observation. To make-up this lack of good correlation, we have conjectured the behavior of materials in terms of its ultimate strength, yield strength, endurance strength, and fracture strength, but still could not really satisfactorily account for the shortcomings. Two factors may really be responsible for it. Both these factors involve management of the boundary of elastic problems: one is the conditions and other is the boundary shape. The necessity of the management of boundary shape has lead to the invention of the FEM and it's over whelming popularity, specifically because of the side by side development of high power computer machines. Of course, the adaptations of the FEM relieved us from our major inability of managing odd boundary shapes but we are constantly aware of its lack of sophistication and doubtful quality of the solutions so obtained. The other factor of impediment to quality solutions of elastic problems is the treatment of the transition in boundary conditions. Elastic problems are either formulated in terms of deformation parameters or stress parameters. But, at the boundary, all the problems are invariably subjected to the mixture of both known deformations and known stress parameters. But neither of these two formulations would allow us to account fully both these two types of boundary conditions with equal sophistication in the region of transition where boundary conditions change from one type to other. Several attempts were made to overcome both these two difficulties faced in the management of boundaries by FDM [1-2]. Besides these above shortcomings, both FDM and FEM simulations are still suffered

by a shortcoming of consuming huge amount of computational resources because their domains are discretized into high resolution of meshes. The remedy of this shortcoming of FDM is constantly looked by several researchers [3-6] introducing a new technique called mesh refinement. But at present, the mesh refinement technique has limited application of solving the problems those are governed by two or less order of PDEs. So, in this thesis, a local mesh refinement scheme for fourth order bi-harmonic partial differential equation will be developed and this scheme will be applied to investigate the stress distribution of 2D elastic field having crack. This thesis is an attempt to overcome the shortcomings of FDM simulations of consuming large computational resources for solution of mixed boundary value elastic problem by local mesh refinement scheme. It uses a new formulation of two-dimensional elastic problems, which enables to maintain different scale of resolution at different sections of the domain depending on the accuracy level requirement of the solutions. The computational work in this formulation is the same magnitude as in the stress formulation, in case of numerical approach of solution.

The present work is confined to homogeneous, isotropic, elastic materials. The response of a solid body to external forces is influenced by the geometric configuration of the body as well as the mechanical and elastic properties of the material. It is found that most of the elastic bodies are homogeneous, that is, material is continuously distributed over its volume so that the smallest element cut from the body possesses the same specific physical properties as the body itself. By the term isotropic it is mean that in any part of the body, the elastic properties are the same in all directions. It is also found that almost all engineering material possesses to a certain extent the property of elasticity. Here interest is restricted to elastic materials in which the deformation and stress regain their original status with the removal of external forces, provided that the external forces do not exceed a certain limit.

The formulation of two dimensional elastic problems used here was first introduced by Uddin [7], later Idris [8] used it for obtaining analytical solutions of a number of mixed boundary value elastic problems, and Ahmed [9-10] extended its use where he obtained finite-difference solutions of a number of mixed boundary value problems of simple boundary shapes. This thesis simply extends the earlier works to include usability of mesh refinement technique to get a fast and better solution in the critical zone of a

structure. The rationality and the reliability of the formulation is thus checked repeatedly by comparing the results of mixed boundary value elastic problems obtained through this formulation with those available in the literature.

1.3 Objectives of the present study

Specific objectives are as follows:

(a) Development of a local mesh refinement scheme with special treatment of governing equation and boundary condition at the interface of the fine and coarse meshes of the domain concerned.

(b) To investigate the displacement and stress distribution of stress concentration zone by local mesh refinement scheme.

(c) To compare the results obtained by the finite difference and finite element methods.

Possible Outcomes are as follows:

(a) Improvement of the solution in the stress concentration zone.

(b) A new mesh refinement scheme for fourth order bi-harmonic equation (Governing equation for potential function approach of elastic field analysis).

(c) Memory savings and less computational efforts in terms of computer programming.

1.4 Literature Review

During recent years the theory of elasticity has found considerable application in the solution of engineering problems because there are many cases in which elementary methods of strength of materials are inadequate to provide satisfactory and accurate information regarding stress distribution in engineering structures. The elementary theory is insufficient to give information regarding local stresses near the loads and near the supports of structures. It fails also in the cases when the stress distribution in bodies, all the dimensions of which are of the same order, has to be investigated, and recourse must be made to more powerful methods of the theory of elasticity. Although the theory of elasticity had been established long before, solution of the practical problems started mainly after the introduction of stress function by Airy, G. B. [11].

The Airy's stress function is governed by a fourth order partial differential equation and the stress components are related to its various second order derivatives. Solutions were initially sought through various polynomial expressions of the stress function [12-13], but the success of this approach is very limited. Mesnager [12] solved two dimensional problems using stress functions in the form of polynomial and applied his results to several problems in bending of beams of narrow rectangular cross section. He showed that the elementary formulas of strength of materials give correct values for normal and shearing stresses in a cantilever, loaded at its free end. He also showed that the rigorous solution for a uniformly distributed loaded beam can be obtained with small corrections to the elementary formulas, which can be neglected for practical purposes. The problem of stress in masonary dams is of great practical interest and has been attempted by various authors [14-15] using polynomial expressions for the stress functions. But it should be noted that the solutions thus obtained do not satisfy the conditions at the bottom of the dam where it is connected with the foundation and would predict reasonable values of stress in the region far away from the foundation on account of Saint-Venant's principle [16-17]. For complex boundary shapes and difficulties in the management of boundary conditions of practical problems, analytical solutions of such problems become difficult. However, most of these difficulties, in most cases, can be surmounted by the use of experimental methods, such as, strain measurement by strain gauge, photo elastic method etc.

First application of finite difference equations, i.e. numerical method, in elasticity was done by Runge [18], who used this method in solving torsional problems. Subsequently finite difference method found very wide application in publications of stress analysis. Successful application of the stress function in conjunction with the finite difference method was reported in 1951 by Conway et al. [19]. The main shortcoming of the stress function formulation is that it accepts boundary conditions in terms of boundary loadings only. So problems containing boundary conditions in terms of restraints only or in terms of both loading and restraints (mixed boundary value problems) could not be solved by this stress function formulation. With a view to solving the problems of mixed boundary conditions, Uddin [7] proposed a formulation for the solution of two dimensional such mixed boundary value problems using the displacement potential function formulation and successfully applied this formulation for the solution of many two dimensional elastic mixed boundary value problems [1,2,8,20-22]. Not only that,

Hossain [23] extended the displacement potential function formulation for three dimensional elastic problems and obtained reliable solution for some classical problems of solid mechanics [24]. Solution of the two dimensional elastic problem with hole is successfully carried out by Rahman [25]. Beside the finite difference method, another numerical method namely finite element method was first successfully applied for the two dimensional elastic problem by Turner et al. [26] and Clough [27]. Afterwards it became very popular and reliable with the rapid development of the digital computers and used by many researchers in both two dimension and three dimension [28].

The elementary theory gives no means of investigating stresses in regions of sharp variation in cross section of structures. It is known that at reentrant corners a high stress concentration occurs and as a result of this cracks are likely to starts at such corners, especially if the structure is submitted to a reversal of stresses. The majority of fractures of machine parts in service can be attributed to such cracks. The finite difference method with Airy's stress function or potential function approach of such cases would provide a better result at the vicinity of stress concentration zone, if their domains could discretize on high resolution meshes. But this high resolution of meshes needs a significant amount of computational resources. In such cases, an enormous wastage of these resources occurs and a huge amount of computational efforts requires in refinement of sections of the domain where computation of the solution does not require high resolutions. As stated earlier in background study, this problem is effectively addressed by mesh refinement (MR) technique, a technique of local refinement of a mesh only in sections where needed, thus allowing concentration of effort where it is required that is a method of changing the accuracy of solutions in certain regions, where solutions of the problem have to be known very accurately. The literature for mesh refinement is extensive, dating back to approximately thirty years and continuing today as a rich field of research in a number of fields like computational fluid dynamics, computational astrophysics, structural dynamics, magnetics, thermal dynamics and microwave theory among others. Several approaches [29] exist to solve the finite-difference equations on uniform grids in the case of regular domains, as well as in the case of irregular domains [30-33]. The spacing of the grid points determines the local error and hence the accuracy of the solution. Many physical problems have variations in scale and when solving these problems numerically, high grid resolution in certain portions is needed to adequately solve the equations. Uniform grids in such

situations are inefficient in terms of storage and CPU requirements. Using a highly refined mesh in portions of the domain where high levels of refinement are not needed represents a waste of computational effort. Limitations on computational resources often force a compromise on grid resolution. By locally refining the mesh only where needed, adaptive mesh refinement allows concentration of effort where it is required, allowing better resolution of the problem [29]. In recent years, many researchers applied the mesh refinement technique to solve many challenging engineering problems. Bieniasz [34] applied MR technique to solve BVPs in singularly perturbed second-order ODEs. Unterweger et al. [35] applied Spacetree-Based adaptive mesh refinement for hyperbolic partial Differential equations. Hiester et al. [36] applied numerical simulation to evaluate the impact of adaptive meshes on the two-dimensional lock exchange flow.

Mesh refinement (MR) was originally developed by Berger et al. [3,5-6]. The method refines the mesh locally to focus computational effort where it is most needed. MR has found popularity in a wide range of fields such as computational fluid dynamics, astrophysics, oceanography, biophysics and many others [37]. In particular, it has been shown that the MR method is advantageous for physical systems with vastly different spatial scales. For example, the evolution of a hyperbolic equation often leads to local shocks, near which numerical methods can have large errors. These errors might propagate and further contaminate the solution across the entire domain. Moreover, the solution structures of different scales might interact, and the failure to address features on one scale can jeopardize the quality of the entire solution. The multi-resolution nature of the MR algorithm makes it ideal for these cases, where computational savings can be enormous [5]. The strategies of adaptive mesh refinement can fall into two categories from the viewpoint of way of multi-resolution of the domain concerned. The first category includes the adaptive algorithms involved local mesh refinement where either the existing mesh is split into several smaller cells or additional nodes are inserted locally usually referred as *h*-refinement. This group can be further categorized by the mesh type, i.e. hierarchical structured grid approach and unstructured mesh refinement approach. One representative of structured grid approaches is adaptive Cartesian mesh refinement proposed by Berger et al. [3,5-6]. They represented *h*-refinement by splitting the existing mesh into several smaller cells as shown in figure 1.1. Their approach is established on regular Cartesian meshes, but arranged

hierarchically with different resolutions. At the fine/coarse cell interfaces, special treatment is required for the communications between the meshes at different levels. Actually, they replaced the coarse cell value by the average of all the fine grid points in that cell for communications between different levels of meshes. Some other structured grid approaches of adaptive mesh refinement are represented by different researchers [38-39]. In this case, they inserted additional nodes locally to obtain *h*-refinement. Mehl and Hill [38] represented a new method of local grid refinement for two-dimensional block-centered finite-difference meshes in the context of steady-state groundwater-flow modeling. The method uses an iteration-based feedback with shared nodes to couple two separate grids shown in figure 1.2. They used Darcy's law in one dimension as governing equation for ground water system which can be given as $q = -K\frac{\partial h}{\partial x}$ where, q is the heat flux, K is the hydraulic conductivity and $\frac{\partial h}{\partial x}$, hydraulic gradient. Since the governing equation is first order, it is very easy to satisfy at different region of the domain concerned. A solution-adaptive algorithm was presented for the simulation of incompressible viscous flows by Ding and Shu [39]. Their framework consists of an adaptive local stencil refinement algorithm and 3-points central difference discretization. The adaptive local stencil refinement is designed in such a manner that 5-points symmetric stencil is guaranteed at each interior node, so that conventional finite difference formula can be easily constructed everywhere in the domain shown in figure 1.3. Since the governing equation for incompressible viscous flow is second order, the two types of stencil (figure 1.3) are sufficient to satisfy the domain shown in figure 1.4.

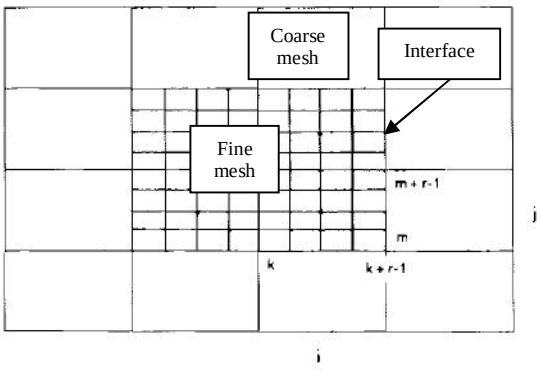

Figure 1.1: Structured grid approach of AMR technique obtained by splitting the existing cell into smaller one.

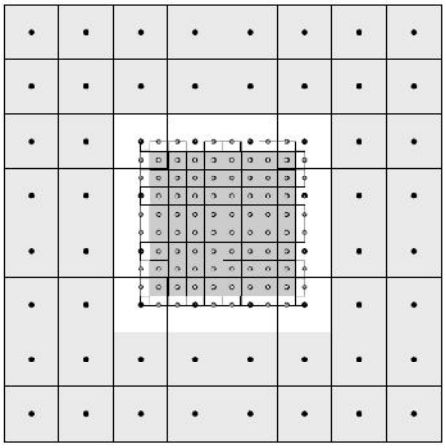

Figure 1.2: Structured grid approach of AMR technique obtained by inserting mesh locally. Darker shading is material represented by the child grid, lighter shading is material represented by the parent grid, and no shading is material at the interface.

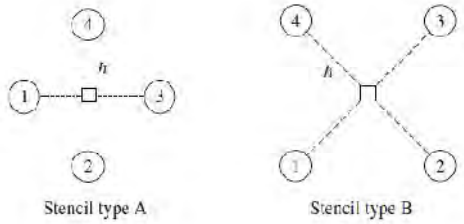

Figure 1.3: Two stencil configuration used by Ding and Shu for second order equation.

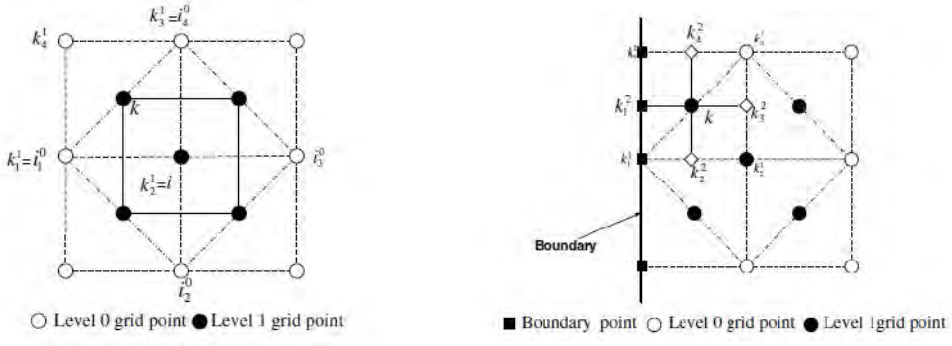

a) Only domain. b) Domain and boundary

Figure 1.4: Discretization of domain under AMR technique used by Ding and Shu.

With regard to the unstructured mesh refinement approach, Zienkiewicz reviewed the state-of-the-art of the automatic mesh refinement strategies in the finite element community in [28], and discussed the important role of error estimation and automatic

adaptation in the finite element analysis. Unlike the local refinement algorithm, the second category of adaptive algorithms involves global mesh-redistribution. These methods move the mesh points inside the domain in order to better capture the dynamic changes of solution. Therefore, such techniques are usually referred as moving mesh method or r-refinement. This group of adaptive methods is less popular than the first group. However, it can offer some distinct features. For example, they do not need to delete/insert nodes to coarsen/refine the local mesh. The practitioners also do not need to construct and maintain a hierarchical mesh structure. Applications of the moving mesh method have been extended to many challenging problems, such as the thin flame propagating [40], drop formation [41], non-breaking free surface wave [42].

1.5 Scope of the present study

This thesis consists of five chapters. A detail literature review is provided in Chapter 1. It illustrates the past research works showing various milestones and events that occurred in the field of stress analysis, theory of elasticity, application of various solution techniques and the evolution of mesh refinement technique in finite difference method.

In chapter 2, the relevant basic theories are recapitulated in brief to understand the theories of elasticity. The mathematical model, used for the finite difference scheme of the study is described for better understanding of displacement potential function formulation.

Chapter 3 depicts the numerical modeling of the problem, mainly the finite difference formulation of the fourth order partial differential governing equation and different boundary conditions. This chapter also describes the treatment of the formulation of governing equation and boundary conditions over non-uniform mesh for MR technique. Later in the chapter, a summary is also made on finite element method since finite element method is the supporting tool for the validation of finite difference results of the study.

In chapter 4, detailed analysis of results is presented accompanied by a validation. A similar problem is solved by the FDM and FEM. Both results are compared with each other. Another two problems are analyzed to show improvement of accuracy of solutions obtained by MR technique over uniform mesh (UM) technique. Results

obtained from the finite difference with MR technique for different boundary conditions are critically analyzed.

Finally in Chapter 5, the dissertation is completed with the main conclusions and the recommendations for future works.

CHAPTER 2
MATHEMATICAL MODEL

2.1 Introduction

One of the most important thing engineers and scientists do is to model physical phenomenon. Virtually every phenomenon in nature, whether aerospace, biological, chemical, geological or mechanical can be described, with the aid of the laws of physics or other fields in terms of algebraic, differential, and/or integral equations relating various quantities of interest. A mathematical model can be broadly defined as a set of equations that expresses the essential features of a physical system in terms of variables that describe the system. The mathematical models of a physical system are developed using assumptions concerning how the process works and using appropriate axioms or fundamental laws of physics such as the principle of conservation of mass, conservation of linear momentum, and conservation of energy, and they are often characterized by very complex differential and/or integral equations posed on geometrically complicated domains. Consequently, the processes to be studied, until the advent of electronic computation, were drastically simplified so that the governing equations can be solved analytically. Over the last few decades, however, computers have made it possible, with the help of suitable mathematical models and numerical methods, to solve many practical problems of engineering.

Almost all engineering materials possess to a certain extent the property of elasticity. If the external forces producing deformations do not exceed certain limit (elastic limit), the deformation disappears with the removal of forces. Throughout this thesis it will be assumed that the bodies undergoing the action of external forces are perfectly elastic, i.e. they resume their initial form completely after removal of the forces. Atomic structure will not be considered here. It will be assumed that the matter of an elastic body is homogeneous and continuously distributed over its volume so that the smallest element cut from the body possesses the same specific physical properties as the body. To simplify the discussion it will also assumed that for most of the body is isotropic i.e. that the elastic properties are the same in all directions.

2.2 Stresses at a Point

Under the action of external forces, internal forces are produced within the elastic body. The intensity i.e. internal forces per unit area of the surface on which they act is called stress. External forces may be of two types: surface force and body force. Forces distributed over the surface of a body, such as hydrostatic pressure, are called surface forces. Forces distributed over the volume of the body, such as gravitational force or inertia force, are called body force. As the effect of body forces as compared to the surface forces is very small, in most practical cases body forces are neglected. In the present study only the surface forces are taken into consideration.

The displacements, strains and stresses in a deformable body are interlinked. Additionally, they all depend on the geometry and material of the work piece, external forces and supports. The discussion is beginning on the governing equations with the concept of stress at a point. To understand the concept of stress at a point, consider a body subjected to external forces and supported in a suitable fashion, as shown in Figure 2.1. Note that, as soon as the forces are applied, the body gets deformed and sometimes displaced if the supports do not restrain the rigid body motion of the body. Thus, Figure 2.1 shows the deformed configuration. In fact, throughout this section, the configuration considered will be the deformed configuration. First, the stress vector (on a plane) is defined at point P of the body. For this, a plane (called as cutting plane) is passed through point P having a unit normal **n**. On each half of the body, there are distributed internal forces acting on the cutting plane and exerted by the other half. On the left half, a small area ΔA is considered around point P of the cutting plane. Let $\mathbf{\Delta F}$ be the resultant of the distributed internal forces (acting on ΔA) exerted by the right half. Then, the stress vector (or traction) at point P (on the plane with normal **n**) is defined as

$$\mathbf{t}_n = \lim_{\Delta A \to 0} \frac{\Delta \mathbf{F}}{\Delta A} \tag{2.1}$$

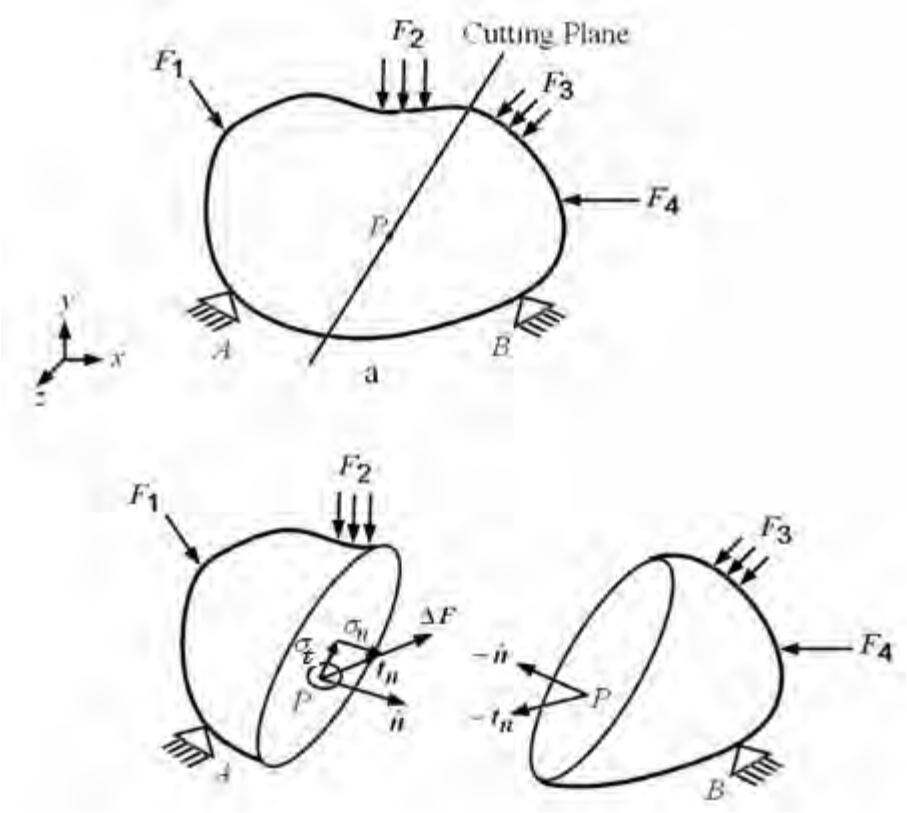

b

Figure 2.1: Stress vector at a point on a plane. (a) Cutting plane passing through point P of the deformed configuration, (b) Stress vector $\mathbf{t_n}$, normal stress component, σ_n and shear stress component, σ_t acting at point P on the cutting plane.

The component of $\mathbf{t_n}$ normal to the plane is called as the normal stress component. It is denoted by σ_n and The component of $\mathbf{t_n}$ along the plane is called as the shear stress component. It is denoted by σ_s. Note that, on the right half, the normal to the cutting plane will be **-n** and the stress vector at P will be $\mathbf{-t_n}$ as per the Newton's third law.

It can be shown that a stress vector on any arbitrary plane can be uniquely represented in terms of the stress vectors on three mutually orthogonal planes. To show this, we consider x, y and z planes as the three planes, having normal vectors along the three Cartesian directions x, y and z respectively. Let the stress vectors on x, y and z planes be denoted by $\mathbf{t_x}$, $\mathbf{t_y}$ and $\mathbf{t_z}$ respectively. Further, we denote their components along x, y and z directions as follows:

$$\mathbf{t_x} = \sigma_x \mathbf{.i} + \sigma_{xy}\mathbf{.j} + \sigma_{xz}\mathbf{.k} \quad (2.2)$$

$$\mathbf{t_y} = \sigma_{yx} \mathbf{.i} + \sigma_y\mathbf{.j} + \sigma y_z\mathbf{.k} \quad (2.3)$$

$$\mathbf{t_x} = \sigma_{zx} \mathbf{.i} + \sigma_{zy}\mathbf{.j} + \sigma_z\mathbf{.k} \quad (2.4)$$

where, (**i, j ,k**) are the unit vectors along(x, y ,z) axes. The stress vectors and their components are shown in Figure 2.2.To derive the above result, we consider a small element at point P whose shape is that of a tetrahedron. The three sides of the tetrahedron are chosen perpendicular to x, y and z axes and the slant face is chosen normal to vector **n**. Then, equilibrium of the tetrahedron in the limit as its size goes to zero leads to the following result:

$$\mathbf{t_n} = \mathbf{t_x} .n_x + \mathbf{t_y}. n_y + \mathbf{t_z}.n_z \quad (2.5)$$

Where n_x, n_y, and n_z are the components of the normal vector **n**. This result is true for every stress vector at point P no matter what the orientation of the normal vector **n** is. Further, this result remains valid even if the body forces are not zero or the body is accelerating.

Let the components of the stress vector $\mathbf{t_n}$ be

$$\mathbf{t_n} = (t_n)_x. \mathbf{i} + (t_n)_y. \mathbf{j} + (t_n)_z. \mathbf{k} \quad (2.6)$$

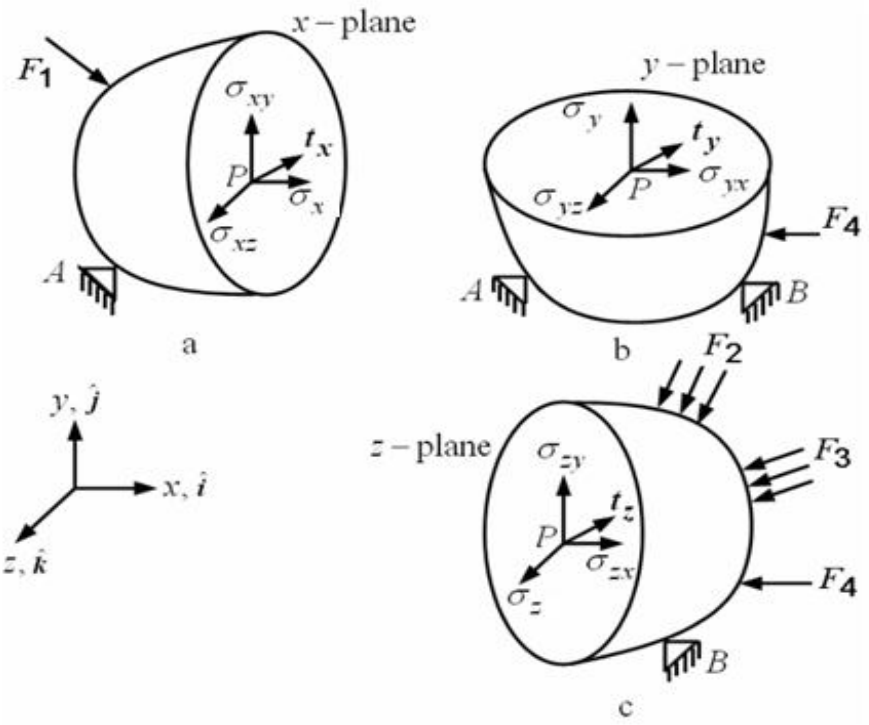

Figure 2.2: Stress vectors and their components on x, y, and z plane. (a) Stress vector and its components on x plane, (b) Stress vector and its components on y plane, (c) Stress vector and its components on z plane.

Substituting Eqs. (2.2-2.4) and (2.6), we get the component form of Eq. (2.5) as follows:

$$\begin{Bmatrix}(t_n)_x\\(t_n)_y\\(t_n)_z\end{Bmatrix} = \begin{bmatrix}\sigma_x & \sigma_{yx} & \sigma_{zx}\\ \sigma_{xy} & \sigma_y & \sigma_{zy}\\ \sigma_{xz} & \sigma_{yz} & \sigma_z\end{bmatrix} . \begin{Bmatrix}n_x\\n_y\\n_z\end{Bmatrix} \tag{2.7}$$

In array notation, this can be written as

$$\{t_n\} = [\sigma]^T . \{n\} \tag{2.8}$$

Where, the stress matrix $[\sigma]$ is

$$[\sigma] = \begin{bmatrix}\sigma_x & \sigma_{yx} & \sigma_{zx}\\ \sigma_{xy} & \sigma_y & \sigma_{zy}\\ \sigma_{xz} & \sigma_{yz} & \sigma_z\end{bmatrix} \tag{2.9}$$

Therefore, it is evident that the stress at a point can be completely described by means of just three stress vectors $\mathbf{t_x}$, $\mathbf{t_y}$ and $\mathbf{t_z}$ acting on mutually orthogonal planes or by their nine components: σ_x, σ_y, σ_z, σ_{xy}, σ_{yx}. σ_{yz}, σ_{zy}, σ_{xz}, and σ_{zx}. In the notation of stresses, the first index describes the direction of the normal to the plane on which the stress component acts while the second index represents the direction of the stress component itself, when both indices are same only one is kept. Thus, σ_{xy} indicates a stress component acting in y -direction on x -plane. When both the indices are same, then the second one simply omitted and, it means the stress component is along the normal to the plane on which it acts. It is called as the normal stress component. Thus, σ_x, σ_y and σ_z are the normal stress components. When the two indices are different, it means the direction of the component is within the plane. Such a component is called as the shear stress component.

2.3 Stress, Strain and Their Relationship

In order to provide the complete idea about the states of stresses, strains and displacements it is necessary to determine the nine components of stress (σ_x, σ_y, σ_z, σ_{xy}, σ_{yx}, σ_{yz}, σ_{zy}, σ_{xz} and σ_{zx}), six components of strain (ε_x, ε_y, ε_z, γ_{xy}, γ_{yz}, and γ_{zx}). Sometimes displacement components (u, v and w) are evaluated instead of strains components. These components can be better understood with reference to a cubic element as shown in figure 2.3. The first subscript of the symbol indicates the direction of the normal of the plane on which the stress is acting and the second subscript indicates the direction of the stress. By a simple consideration of the equilibrium of the element the number of symbols for shearing stresses can be reduced to three i.e. $\sigma_{xy} = \sigma_{yx}$, $\sigma_{yz} = \sigma_{zy}$ and $\sigma_{xz} = \sigma_{zx}$. As a result, the nine components of stress reduce to six independent components only.

The deformation of the elastic body is considered very small and by definition, the normal and shear strain can be given by

$$\varepsilon_x = \frac{\partial u_x}{\partial x}, \varepsilon_y = \frac{\partial u_y}{\partial y}, \varepsilon_z = \frac{\partial u_z}{\partial z} \tag{2.10}$$

$$\gamma_{xy} = \frac{\partial u_x}{\partial y} + \frac{\partial u_y}{\partial x}, \ \gamma_{yz} = \frac{\partial u_y}{\partial z} + \frac{\partial u_z}{\partial y}, \ \gamma_{zx} = \frac{\partial u_z}{\partial x} + \frac{\partial u_x}{\partial z} \tag{2.11}$$

Where, ε_x, ε_y and ε_z are the strain components parallel to the co-ordinate axis called normal strain and γ_{xy}, γ_{yz}, and γ_{zx} are strain components acting on the planes xy, yz and zx planes respectively, called shear strain.

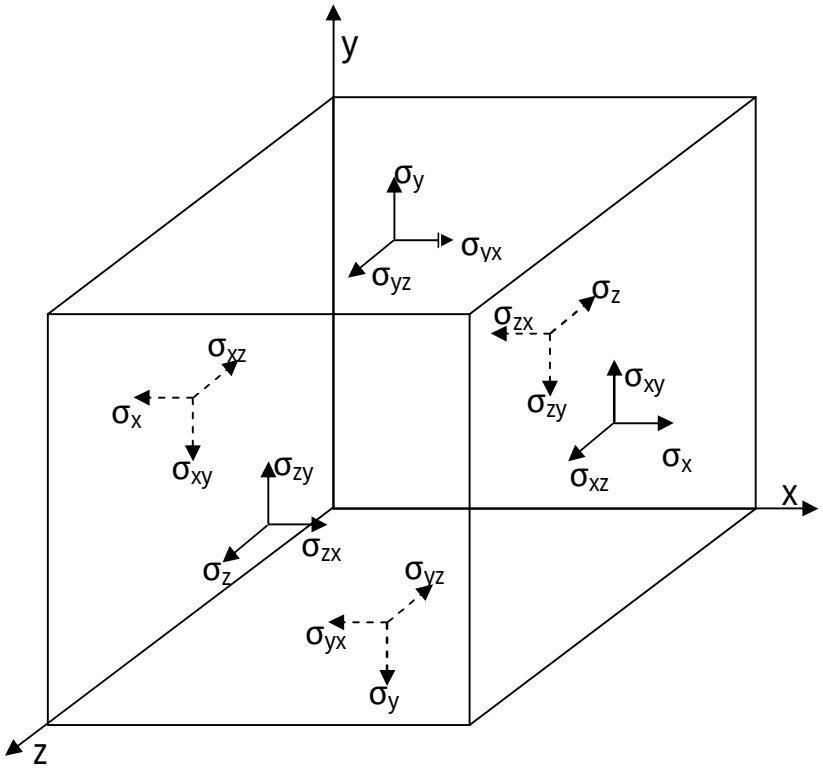

Figure 2.3: Stress components in a cubic element.

The stresses are related to the strains by the Hooke's law. The generalized Hooke's law suggests that each of the stress components is the linear function of the strain components. The stresses are related to the strains by the Hooke's law and Poisson's law as follows [43]:

$$\varepsilon_x = \frac{1}{E}\left[\sigma_x - \mu(\sigma_y + \sigma_z)\right]$$

$$\varepsilon_y = \frac{1}{E}\left[\sigma_y - \mu(\sigma_z + \sigma_x)\right] \qquad (2.12)$$

$$\varepsilon_z = \frac{1}{E}\left[\sigma_z - \mu(\sigma_x + \sigma_y)\right]$$

Where, E is the modulus of elasticity and μ is the Poison's ratio.

2.4 Plane Stress and Plane Strain

Although practically all the bodies are three dimensional, most of the practical problems of stress analysis could be reduced to two dimensional by applying two simplifying assumptions. One, the loading on the body is confined in a plane and the dimension of the body in the direction perpendicular to this plane is relatively small as compared to the others. In such cases, the stresses in the body perpendicular to the plane of loading are usually very small and thus can be neglected. As a result these problems become two dimensional, usually referred to as plane stress problems. Two, one of the three dimensions of the body is relatively large or straining in a particular direction is restrained. In such cases, the stresses in the large or restrained direction are zero. As a result these problems become two dimensional and usually referred to as plane strain problems.

If a thin plate is loaded by forces applied at the boundary, parallel to the plane of the plate and distributed over the thickness (Figure 2.4), the stress components σ_z, σ_{zx}, σ_{yz} become zero on both faces of the plate, and it may assumed that they are also zero within the plate. Thus in a plane stress problems the state of stress is defined by σ_x, σ_y, σ_{xy} only.

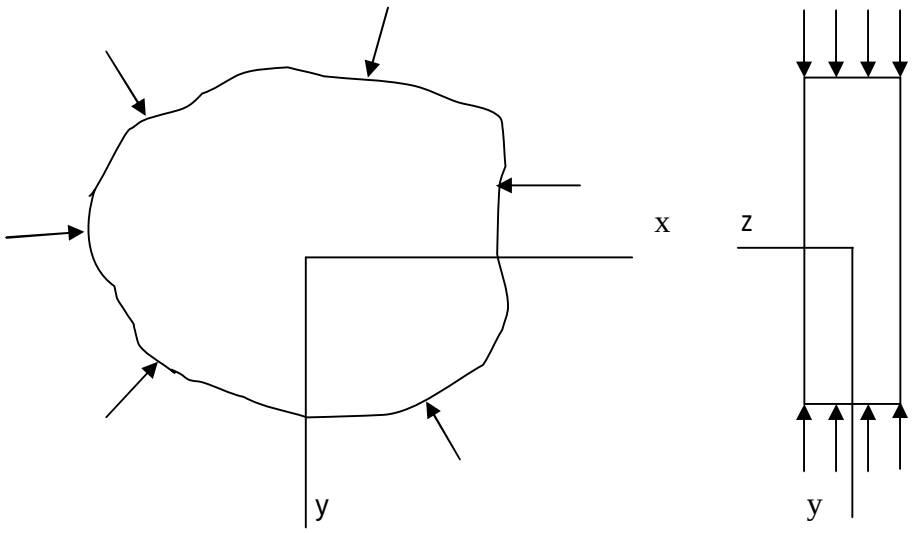

Figure 2.4: Plane stress.

A similar simplification is possible when the dimension of the body in the z-direction is very large. If a long cylindrical or prismatic body is loaded by forces that are perpendicular to the longitudinal elements and do not vary along the length, it may be assumed that all the cross sections are in the same condition. Problems like a retaining wall with lateral pressure (Figure 2.5a), a culvert or tunnel, a cylindrical tube with internal pressure (Figure 2.5b), a cylindrical roller compressed by forces in a diametric plane as in a roller bearing etc. can be considered of this kind and called plain strain problem.

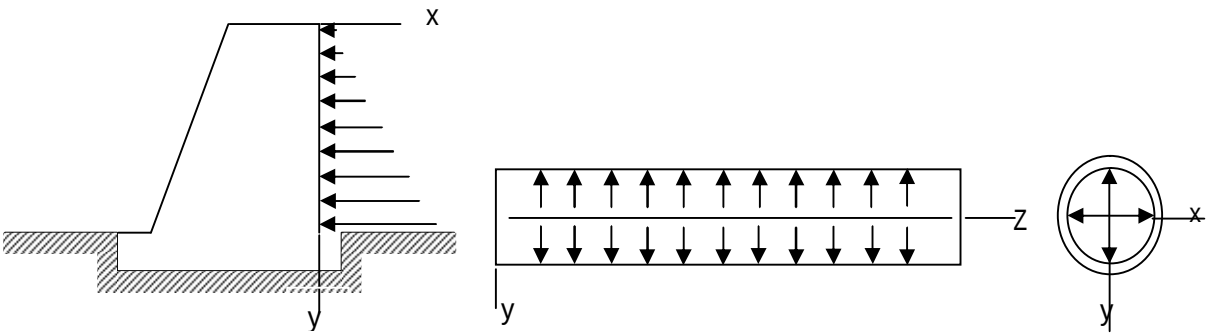

(a) Retaining wall with lateral pressure. (b) A cylindrical tube with internal pressure.

Figure 2.5: Plane strain.

2.5 Differential Equations of Equilibrium and Boundary Conditions

For static equilibrium of the infinitesimal cubic element as shown in figure 2.3, the following equations can be obtained, [43]

$$\frac{\partial \sigma_x}{\partial x} + \frac{\partial \sigma_{xy}}{\partial y} + \frac{\partial \sigma_{xz}}{\partial z} + X = 0$$

$$\frac{\partial \sigma_y}{\partial y} + \frac{\partial \sigma_{xy}}{\partial x} + \frac{\partial \sigma_{yz}}{\partial z} + Y = 0 \qquad (2.13)$$

$$\frac{\partial \sigma_z}{\partial z} + \frac{\partial \sigma_{xz}}{\partial x} + \frac{\partial \sigma_{yz}}{\partial y} + Z = 0$$

These equations (2.13) are known as the equations of equilibrium, where X, Y, and Z are the components of body force per unit volume of the element in x, y, and z-directions respectively. The body forces can be eliminated due to their negligible effect as compared to that of surface forces. For plane stress condition the cubic element reduces to a thin rectangular block and in the absence of body forces acting on that block, hence the equilibrium equations yields to

$$\frac{\partial \sigma_x}{\partial x} + \frac{\partial \sigma_{xy}}{\partial y} = 0 \qquad (2.14)$$

$$\frac{\partial \sigma_y}{\partial y} + \frac{\partial \sigma_{xy}}{\partial x} = 0$$

Above equations must be satisfied at all points throughout the body. The stress components vary over the volume of the block. At the boundary they must be in equilibrium with external forces on the boundary and the external forces may be considered as the continuation of the internal stress distribution. So the conditions of equilibrium at the boundary can be written as [43],

$$\sigma_n = \sigma_x l^2 + \sigma_y m^2 + 2\sigma_{xy} lm$$

$$\sigma_t = \sigma_{xy}(l^2 - m^2) + (\sigma_y - \sigma_x) lm \qquad (2.15)$$

Where, σ_n and σ_t are the normal and tangential components of the surface forces acting on the boundary per unit area and l, m are the direction cosines of the normal to the surface.

Similarly, normal component of displacement u_n and the tangential component u_t acting on the boundary surface can be expressed by

$$u_n = u.l + v.m$$

$$u_t = v.l - u.m \qquad (2.16)$$

Generally normal components (σ_n and u_n) are considered to be positive when act outward on the boundary and the tangential components (σ_t and u_t) are considered positive if they act in the anti-clockwise direction on the body.

2.6 Compatibility Equations

To determine the state of stress in the two-dimensional elastic body, it is necessary to find the solution of the equilibrium equations (Eq. 2.14), which must satisfy the boundary conditions (Eq. 2.15 and 2.16) at the boundary. Since these two equations contain three unknown stress components (σ_x, σ_y, and σ_{xy}), they are not sufficient to determine the three components. Therefore, the problem is a statically indeterminate one. As a result, to obtain the solution, the elastic deformations of the body must be taken into consideration. For two dimensional bodies, three strain components can be expressed in terms of the displacement components as

$$\varepsilon_x = \frac{\partial u}{\partial x}; \qquad \varepsilon_y = \frac{\partial v}{\partial y}; \qquad \gamma_{xy} = \frac{\partial u}{\partial y} + \frac{\partial v}{\partial x} \tag{2.17}$$

Since these three strain components are expressed by two functions only, they can be related arbitrarily among themselves. There exists a certain relationship among the strain components, which is expressed as,

$$\frac{\partial^2 \varepsilon_x}{\partial y^2} + \frac{\partial^2 \varepsilon_y}{\partial x^2} = \frac{\partial^2 \gamma_{xy}}{\partial x \, \partial y} \tag{2.18}$$

This differential relation is called the condition of compatibility. It must be satisfied by the strain components to ensure the existence of functions u and v connected with the strain components by Eq. 2.17.

Elimination of strains in terms of stresses, equation (Eq. 2.18) yields to

$$\left(\frac{\partial^2}{\partial x^2} + \frac{\partial^2}{\partial y^2}\right)(\sigma_x + \sigma_y) = 0 \tag{2.19}$$

The equations (Eq. 2.14) of equilibrium together with the boundary conditions (Eq. 2.15) and the above compatibility equation (Eq. 2.19) give us a system of equations that is usually sufficient for the complete solution of stress distribution in a two dimensional problem.

2.7 Solution Technique for 2-D Problems with Known Stresses at the Boundary

The solution of two dimensional elastic problems requires integration of the differential equations of equilibrium (Eq. 2.14) together with the compatibility equations (Eq. 2.19) and the boundary conditions (Eq. 2.15), [43] repeated for ready reference.

$$\frac{\partial \sigma_x}{\partial x} + \frac{\partial \sigma_{xy}}{\partial y} = 0$$

$$\frac{\partial \sigma_y}{\partial y} + \frac{\partial \sigma_{xy}}{\partial x} = 0 \qquad (2.14)$$

$$\left(\frac{\partial^2}{\partial x^2} + \frac{\partial^2}{\partial y^2}\right)(\sigma_x + \sigma_y) = 0 \qquad (2.19)$$

$$\sigma_n = \sigma_x . l^2 + \sigma_y . m^2 + 2\sigma_{xy} . l\, m$$

$$\sigma_t = \sigma_{xy} . (l^2 - m^2) + (\sigma_y - \sigma_x) . l\, m \qquad (2.15)$$

The usual method of solving these equations is through the introduction of a function $\varphi(x,y)$, known as Airy's stress function, defined as

$$\sigma_x = \frac{\partial^2 \phi}{\partial y^2}; \qquad \sigma_y = \frac{\partial^2 \phi}{\partial x^2}; \qquad \sigma_{xy} = \frac{\partial^2 \phi}{\partial x . \partial y} \qquad (2.20)$$

Which satisfies equations (Eq. 2.14) and transforms the equation (Eq. 2.19) into

$$\frac{\partial^4 \phi}{\partial x^4} + 2\frac{\partial^4 \phi}{\partial x^2 . \partial y^2} + \frac{\partial^4 \phi}{\partial y^4} = 0 \qquad (2.21)$$

Ultimately, equation (Eq. 2.21) has to be integrated satisfying equation (Eq. 2.15) at the boundary. But the solution approach stated above through the stress function $\varphi(x,y)$ is a special case of a general problem. Only a problem with pure known stress at the boundary can be solved by this approach. But, most of the practical engineering problems are with the mixed boundary conditions, that is, the conditions at the boundary might include known stresses, known displacements or combination of stresses and displacements with

different conditions in different segments at the boundary. A problem of this kind can't be solved through Airy's stress function φ(x,y), defined in equation (Eq. 2.20).

2.8 Mathematical Formulation in terms of Displacement Potential Function

In absence of body forces, the equilibrium equations for two dimensional elastic problems in terms of displacements components [9, 44] are as follows

$$\frac{\partial^2 u}{\partial x^2} + \left(\frac{1-\mu}{2}\right)\frac{\partial^2 u}{\partial y^2} + \left(\frac{1+\mu}{2}\right)\frac{\partial^2 v}{\partial x.\partial y} = 0$$

$$\frac{\partial^2 v}{\partial y^2} + \left(\frac{1-\mu}{2}\right)\frac{\partial^2 v}{\partial x^2} + \left(\frac{1+\mu}{2}\right)\frac{\partial^2 u}{\partial x.\partial y} = 0 \qquad (2.22)$$

These two homogeneous elliptic partial differential equations with the appropriate boundary conditions should be sufficient for the evaluation of the two functions u and v, and the knowledge of these functions over the region concerned will uniquely determine the stress components.

Although the above two differential equations are sufficient to solve mixed boundary value elastic problems but in reality it is difficult to solve for two functions simultaneously. So, to overcome this difficulty, investigations are necessary to convert equations (Eq. 2.22) into a single equation of a single function. If that function is defined in terms of the displacement function u and v, then the determination of that function uniquely determines the stress functions sought for.

A new potential function approach involves investigation of the existence of a function defined in terms of the displacement components. In this approach attempt had been made to reduce the problem to the determination of a single variable. A function ψ(x,y) is thus defined in terms of displacement components as, [3]

$$u = \frac{\partial^2 \psi}{\partial x.\partial y}$$

$$v = -\left[\left(\frac{1-\mu}{1+\mu}\right)\frac{\partial^2 \psi}{\partial y^2} + \left(\frac{2}{1+\mu}\right)\frac{\partial^2 \psi}{\partial x^2}\right] \qquad (2.23)$$

With this definition of $\psi(x,y)$, the first of the two equations (Eq. 2.22) is automatically satisfied. Therefore, ψ has only to satisfy the second equation. Thus, the condition that ψ has to satisfy is

$$\frac{\partial^4\psi}{\partial x^4} + 2\frac{\partial^4\psi}{\partial x^2.\partial y^2} + \frac{\partial^4\psi}{\partial y^4} = 0 \qquad (2.24)$$

Therefore, the problem is reduced to the evaluation of a single variable $\psi(x,y)$ from the above bi-harmonic partial differential equation.

2.9 Boundary Conditions for the Function ψ for Mixed Boundary Value Problems

In order to solve the problem by solving for the function ψ of the bi-harmonic equation (Eq. 2.24), the boundary conditions should be expressed in terms of ψ. The boundary conditions are known restraints and loadings, that is, known values of components of stresses and displacements at the boundary. The relation between known functions and the potential function ψ at the boundary are [3]:

$$u = \frac{\partial^2\psi}{\partial x.\partial y}$$

$$v = -\left[\left(\frac{1-\mu}{1+\mu}\right)\frac{\partial^2\psi}{\partial y^2} + \left(\frac{2}{1+\mu}\right)\frac{\partial^2\psi}{\partial x^2}\right] \qquad (2.25)$$

$$\sigma_x = \frac{E}{(1+\mu)^2}\left[\frac{\partial^3\psi}{\partial x^2\,\partial y} - \mu\frac{\partial^3\psi}{\partial y^3}\right]$$

$$\sigma_y = -\frac{E}{(1+\mu)^2}\left[\frac{\partial^3\psi}{\partial y^3} + (2+\mu)\frac{\partial^3\psi}{\partial x^2\,\partial y}\right] \qquad (2.26)$$

$$\sigma_{xy} = \frac{E}{(1+\mu)^2}\left[\mu\frac{\partial^3\psi}{\partial y^2\,\partial x} - \frac{\partial^3\psi}{\partial x^3}\right]$$

From the above expressions it is found that, as far as boundary conditions are concerned, either known restraints or known stresses or combinations of stresses and displacements, all can be converted to finite difference expressions in terms of ψ at the boundary.

Considering a pragmatic applicability, the rectangular components are converted into normal and tangential components, as these are actually known at the boundary using the following relationship (Eq. 2.15 and Eq. 2.16) [33].

$$u_n = u.l + v.m$$

$$u_t = v.l - u.m \qquad (2.16)$$

$$\sigma_n = \sigma_x.l^2 + \sigma_y.m^2 + 2\sigma_{xy}.l\,m$$

$$\sigma_t = \sigma_{xy}.(l^2 - m^2) + (\sigma_y - \sigma_x).l\,m \qquad (2.15)$$

2.10 Selection of Boundary Conditions

The possible known boundary components at a boundary point are any two out of four quantities, namely, u_n and u_t, the normal and tangential displacement components, σ_n and σ_t, the normal and tangential stress components. The possible sets of boundary conditions can be-

A. (i) Normal displacement component (u_n)
   (ii) Tangential displacement component (u_t)
   Or
B. (i) Normal displacement component (u_n)
   (ii) Normal stress component (σ_n)
   Or
C. (i) Normal displacement component (u_n)
   (ii) Tangential stress component (σ_t)
   Or
D. (i) Tangential displacement component (u_t)
   (ii) Normal stress component (σ_n)
   Or
E. (i) Tangential displacement component (u_t)
   (ii) Tangential stress component (σ_t)
   Or

F. (i) Normal stress component (σ_n)

(ii) Tangential stress component (σ_t)

But among the above six sets of boundary conditions, sets B and E do not usually occur in practical problems. So the remaining four possible sets of boundary conditions at any point on the boundary, which are considered in the present study are

1. (u_n, u_t)

2. (u_n, σ_t)

3. (u_t, σ_n) and

4. (σ_n, σ_t).

CHAPTER 3

NUMERICAL MODEL

3.1 Introduction

While the derivation of the governing equations for most of the problems is not unduly difficult, their solution by exact methods of analysis is often difficult due to geometric and material complexities. In such cases, numerical methods of analysis provide alternative means of findings solutions. Numerical methods are techniques by which mathematical problems are formulated so that they can be solved with arithmetic operations and always give an approximate solution. Although numerical methods can't give an exact result, it is used extensively by the researchers to save money and time, compromising with the accuracy, especially when analytical methods are not available. Numerical methods typically transform differential equations governing a continuum to a set of algebraic equations of a discreate model of the continuum that are to be solved using computers. The use of a numerical method and a computer to evalute the mathematical model of a process and estimate its characteristics is called numerical simulation. There are several reasons why an engineer or a scientist should study a numerical method: 1) Most practical problems involve complicated domains (both geometry and mateial constitution), loads, and nonlinearities that forbid the development of analytical solutions. Therefore, the only alternative is to find approximate solutions using numerical methods. 2) A numerical method, with the advent of a computer, can be used to investigate the effects of various parameters of the system on its response to gain a better understanding of the process/system being analyzed. 3) It is cost effective and saves time and material resources compaered to the multitude of physical experiments needed to gain the same level of understanding. 4) Because of the power of numerical methods and eletronic computation, it is possible to include all relevant features in a mathematical model of a physical process without worrying about its solution by exact means. 5) Those who are quick to use a computer program rather than think about the problem to be analyzed may find it difficult to interpret or explain the computer-generated results. Even to develop proper input data for the computer program, a good understanding of the underlying theory of the problem as well as the numerical method is required.

3.2 Finite Difference Method

The finite-difference method is one of the oldest numerical methods known for solving PDE's. In finite difference method, the derivatives of an original differential equation are replaced by the finite divided difference formulae for derivatives which are obtained by approximations of Tailor's series. So a differential equation is converted into a set of linear algebraic equation which can be solved by a suitable technique. Since all finite difference formulae are approximation of infinite series of differences, it is necessary that the series should converge or the error caused by the truncation should be sufficiently small to give a reliable result.

In this method, the region of the body under consideration is divided by lines parallel to the co-ordinate axes. And points hence formed at the intersection of the these lines are treated as a grid of finite number of discrete points which are called node points as shown in Figure 3.1. The continuous problem domain is discretized so that the dependent variables are considered to exist only at discrete nodal points. The finite difference form of governing partial differential equation is applied to all node points except the boundary node points and appropriate boundary conditions are applied to the boundary node points. To apply the boundary conditions at the boundary, a false or imaginary boundary is considered outside of real boundary as shown in figure 3.1. This imaginary boundary is necessary because each boundary point is subjected to a pair of boundary conditions such as u,v or u,σ_x or u,σ_{xy} etc. From these two boundary conditions one is applied to real boundary and other is applied to real boundary by using pivot at corresponding imaginary boundary points. This gives a complete set of simultaneous equations, i.e. number of equations in the set is equal to the number of grid points, which is solved by a suitable numerical technique.

In the remaining portion of the chapter, the conversion procedure of the partial differential equation (Eq. 2.24) and boundary conditions (Eq. 2.25 and 2.26) in the form of difference equations is provided.

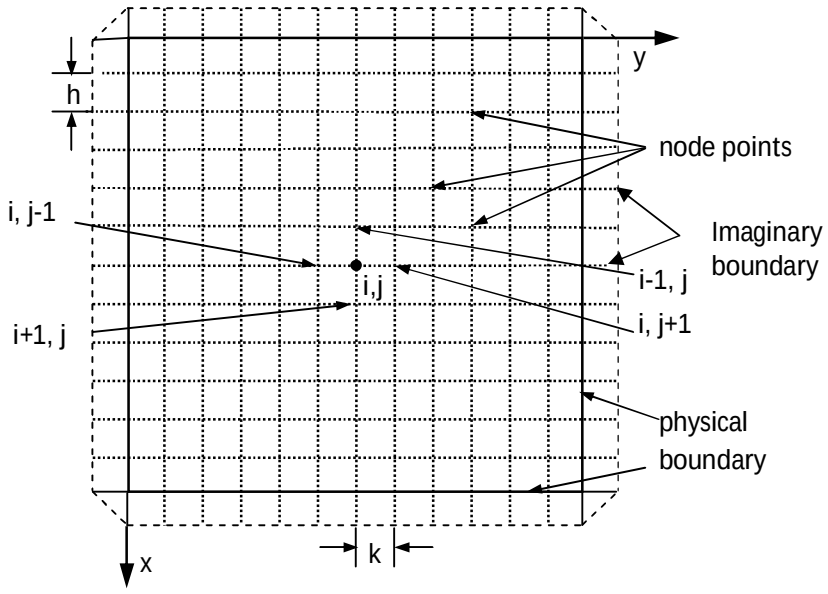

Figure 3.1: Discretization of rectangular body into a grid of points.

3.2.1 Finite Difference Formulae of the Derivatives

Finite difference approximations of the derivatives are actually truncated form of Taylor's series expansion. Three forms of finite-difference equations are very commonly used. The three forms are

- Forward Difference
- Backward Difference
- Central Difference

The level of accuracy of each form depends on the number of terms of the Taylor's series that are retained during the derivation of these formulas. To illustrate the derivation of the difference equations, a pivot point at (i, j) is considered and the neighboring points are designated as shown in the Figure 3.1. All points are at a finite distance of 'h' and 'k' form each other in x- and y-directions respectively. If a certain function f(x, y) has continuous partial derivatives of considerably higher order, then according to Taylor's series the value of function at a point (i+1, j) can be given by

$$f(i+1,j) = f(i,j) + h f'(i,j) + \frac{h^2}{2!} f''(i,j) + \frac{h^3}{3!} f'''(i,j) + ... + \frac{h^n}{n!} f^n(i,j) + ... \qquad (3.1)$$

Where, $h = (x_{i+1,\,j} - x_{i,\,j})$. Similarly the value of function at (i-1, j) can be expressed as,

$$f(i-1,j)=f(i,j)-hf'(i,j)+\frac{h^2}{2!}f''(i,j)-\frac{h^3}{3!}f'''(i,j)+.....+(-1)^n\frac{h^n}{n!}f^n(i,j)+... \quad (3.2)$$

Subtracting last equation from the previous equation gives

$$f'(i,j)=\left(\frac{\partial f}{\partial x}\right)_{i,j}=\frac{f(i+1,j)-f(i-1,j)}{2h}+O(h^2) \quad (3.3)$$

This equation is called central finite divided difference formula for first derivative and $O(h^2)$ represents the order of the truncation error. And some simple mathematical manipulation of Eq. 3.1 and Eq. 3.2 gives respectively

$$f'(i,j)=\left(\frac{\partial f}{\partial x}\right)_{i,j}=\frac{f(i+1,j)-f(i,j)}{h}+O(h) \quad (3.4)$$

$$f'(i,j)=\left(\frac{\partial f}{\partial x}\right)_{i,j}=\frac{f(i,j)-f(i-1,j)}{h}+O(h) \quad (3.5)$$

The former is called forward finite divided difference formula and later is called backward finite divided difference formula for first derivative. It is noticeable that last two equations are less accurate then the Eq. 3.3, though all three equations represent the difference equation of first derivative. Accuracy of forward and backward difference equation can be improved if more points are considered. The value of function at the points (i+2, j) and (i-2, j) can be expressed as

$$f(i+2,j)=f(i,j)+2hf'(i,j)+\frac{(2h)^2}{2!}f''(i,j)+\frac{(2h)^3}{3!}f'''(i,j)+\frac{(2h)^4}{4!}f''''(i,j)+... \quad (3.6)$$

$$f(i-2,j)=f(i,j)-2hf'(i,j)+\frac{(2h)^2}{2!}f''(i,j)-\frac{(2h)^3}{3!}f'''(i,j)+\frac{(2h)^4}{4!}f''''(i,j)-... \quad (3.7)$$

If these two equations (Eq. 3.6 and 3.7) are combined with the previous two equations (Eq. 3.1 and 3.2), then it is found that

$$f'(i,j)=\left(\frac{\partial f}{\partial x}\right)_{i,j}=\frac{-f(i+2,j)+4f(i+1,j)-3f(i,j)}{2h}+O(h^2) \quad (3.8)$$

$$f'(i,j)=\left(\frac{\partial f}{\partial x}\right)_{i,j}=\frac{3f(i,j)-4f(i-1,j)+f(i-2,j)}{2h}+O(h^2) \tag{3.9}$$

It is noticeable that last two equations involve three node points including the point of application which is called pivot point. So these three finite difference equations for first derivative (Eq. 3.3, 3.8 and 3.9), having same accuracy to order of h^2, can be expressed graphically (by using stencil) as in Figure 3.2.

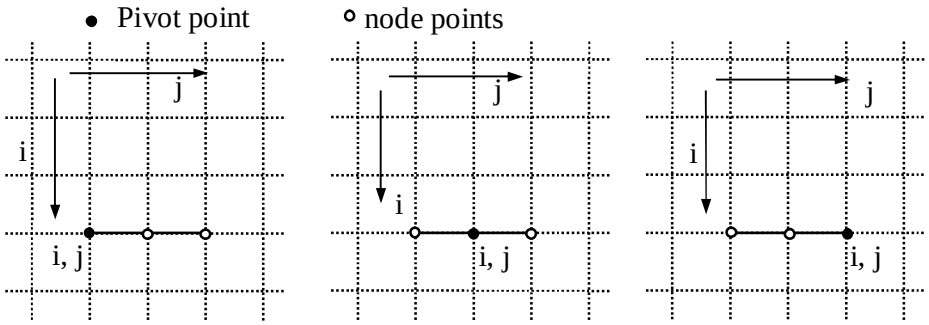

(a) forward (b) central (c) backward

Figure 3.2: Stencils for first derivative of various forms.

Again this accuracy level can be enhanced by considering more points in the formulation. So the difference equations of accuracy of order of h^2 or k^2 can be given as

Forward finite divided difference equations:

i) First derivative:

$$f'(i,j)=\left(\frac{\partial f}{\partial x}\right)_{i,j}=\frac{-f(i+2,j)+4f(i+1,j)-3f(i,j)}{2h}+O(h^2)$$

$$f'(i,j)=\left(\frac{\partial f}{\partial y}\right)_{i,j}=\frac{-f(i,j+2)+4f(i,j+1)-3f(i,j)}{2k}+O(k^2) \tag{3.10}$$

ii) Second derivative:

$$f''(i,j)=\left(\frac{\partial^2 f}{\partial x^2}\right)_{i,j}=\frac{-f(i+3,j)+4f(i+2,j)-5f(i+1,j)+2f(i,j)}{h^2}+O(h^2) \tag{3.11}$$

$$f''(i,j)=\left(\frac{\partial^2 f}{\partial y^2}\right)_{i,j}=\frac{-f(i,j+3)+4f(i,j+2)-5f(i,j+1)+2f(i,j)}{k^2}+O(k^2) \tag{3.12}$$

iii) Third derivative:

$$\left(\frac{\partial^3 f}{\partial x^3}\right)_{i,j} = \frac{-f(i+3,j)+6f(i+2,j)-12f(i+1,j)+10f(i,j)-3f(i-1,j)}{2h^3} + O(h^2) \tag{3.13}$$

$$\left(\frac{\partial^3 f}{\partial y^3}\right)_{i,j} = \frac{-f(i,j+3)+6f(i,j+2)-12f(i,j+1)+10f(i,j)-3f(i,j-1)}{2k^3} + O(k^2) \tag{3.14}$$

iv) Fourth derivative:

$$\left(\frac{\partial^4 f}{\partial x^4}\right)_{i,j} = \frac{1}{h^4}\begin{bmatrix} -2f(i+5,j)+11f(i+4,j)-24f(i+3,j) \\ +26f(i+2,j)-14f(i+1,j)+3f(i,j) \end{bmatrix} + O(h^2) \tag{3.15}$$

$$\left(\frac{\partial^4 f}{\partial y^4}\right)_{i,j} = \frac{1}{k^4}\begin{bmatrix} -2f(i,j+5)+11f(i,j+4)-24f(i,j+3) \\ +26f(i,j+2)-14f(i,j+1)+3f(i,j) \end{bmatrix} + O(k^2) \tag{3.16}$$

Central finite difference equations:

i) First derivative:

$$f'(i,j) = \left(\frac{\partial f}{\partial x}\right)_{i,j} = \frac{f(i+1,j)-f(i-1,j)}{2h} + O(h^2)$$

$$f'(i,j) = \left(\frac{\partial f}{\partial y}\right)_{i,j} = \frac{f(i,j+1)-f(i,j-1)}{2k} + O(k^2) \tag{3.17}$$

ii) Second derivative:

$$\left(\frac{\partial^2 f}{\partial x^2}\right)_{i,j} = \frac{f(i+1,j)-2f(i,j)+f(i-1,j)}{h^2} + O(h^2) \tag{3.18}$$

$$\left(\frac{\partial^2 f}{\partial y^2}\right)_{i,j} = \frac{f(i,j+1)-2f(i,j)+f(i,j-1)}{k^2} + O(k^2)$$

(3.19)

iii) Third derivative:

$$\left(\frac{\partial^3 f}{\partial x^3}\right)_{i,j} = \frac{f(i+2,j) - 2f(i+1,j) + 2f(i-1,j) - f(i-2,j)}{2h^3} + O(h^2) \tag{3.20}$$

$$\left(\frac{\partial^3 f}{\partial y^3}\right)_{i,j} = \frac{f(i,j+2) - 2f(i,j+1) + 2f(i,j-1) - f(i,j-2)}{2k^3} + O(k^2) \tag{3.21}$$

iv) Fourth derivative:

$$\left(\frac{\partial^4 f}{\partial x^4}\right)_{i,j} = \frac{f(i+2,j) - 4f(i+1,j) + 6f(i,j) - 4f(i-1,j) + f(i-2,j)}{h^4} + O(h^2) \tag{3.22}$$

$$\left(\frac{\partial^4 f}{\partial y^4}\right)_{i,j} = \frac{f(i,j+2) - 4f(i,j+1) + 6f(i,j) - 4f(i,j-1) + f(i,j-2)}{k^4} + O(k^2) \tag{3.23}$$

Backward finite divided difference equations:

i) First derivative:

$$f'(i,j) = \left(\frac{\partial f}{\partial x}\right)_{i,j} = \frac{3f(i,j) - 4f(i-1,j) + f(i-2,j)}{2h} + O(h^2)$$

$$f'(i,j) = \left(\frac{\partial f}{\partial y}\right)_{i,j} = \frac{3f(i,j) - 4f(i,j-1) + f(i,j-2)}{2k} + O(k^2) \tag{3.24}$$

ii) Second derivative:

$$f''(i,j) = \left(\frac{\partial^2 f}{\partial x^2}\right)_{i,j} = \frac{-f(i-3,j) + 4f(i-2,j) - 5f(i-1,j) + 2f(i,j)}{h^2} + O(h^2) \tag{3.25}$$

$$f''(i,j) = \left(\frac{\partial^2 f}{\partial y^2}\right)_{i,j} = \frac{-f(i,j-3) + 4f(i,j-2) - 5f(i,j-1) + 2f(i,j)}{k^2} + O(k^2) \tag{3.26}$$

iii) Third derivative:

$$\left(\frac{\partial^3 f}{\partial x^3}\right)_{i,j} = \frac{f(i-3,j) - 6f(i-2,j) + 12f(i-1,j) - 10f(i,j) + 3f(i+1,j)}{2h^3} + O(h^2) \tag{3.27}$$

$$\left(\frac{\partial^3 f}{\partial y^3}\right)_{i,j} = \frac{f(i,j-3) - 6f(i,j-2) + 12f(i,j-1) - 10f(i,j) + 3f(i,j+1)}{2k^3} + O(k^2) \qquad (3.28)$$

iv) Fourth derivative:

$$\left(\frac{\partial^4 f}{\partial x^4}\right)_{i,j} = \frac{1}{h^4}\begin{bmatrix} -2f(i-5,j) + 11f(i-4,j) - 24f(i-3,j) \\ +26f(i-2,j) - 14f(i-1,j) + 3f(i,j) \end{bmatrix} + O(h^2) \qquad (3.29)$$

$$\left(\frac{\partial^4 f}{\partial y^4}\right)_{i,j} = \frac{1}{k^4}\begin{bmatrix} -2f(i,j-5) + 11f(i,j-4) - 24f(i,j-3) \\ +26f(i,j-2) - 14f(i,j-1) + 3f(i,j) \end{bmatrix} + O(k^2) \qquad (3.30)$$

Besides these, the difference equations of the multiple derivatives are also required for the solution. These equations can be found from the combination of the equations from 3.8 to 3.30 and 3.3. An example is shown as follows-

$$\left(\frac{\partial^2 f}{\partial x \partial y}\right)_{i,j} = \left(\frac{\partial}{\partial x}\left(\frac{\partial f}{\partial y}\right)_{i,j}\right)_{i,j} + O(h^2, k^2) \qquad (3.31)$$

But this equation can have nine different forms as $(\partial f/\partial y)_{i,j}$ has three different forms, forward, central and backward which are shown in Eq. 3.10, 3.17 and 3.24 respectively, and $(\partial f/\partial x)_{i,j}$ also has three different forms of same types as shown in Eq. 3.8, 3.3, 3.9. Combination of these makes nine different forms which are-

1) i- forward, j- forward 2) i- forward, j- central 3) i- forward, j- backward

4) i- central, j- forward 5) i- central, j- central 6) i- central, j- backward

7) i- backward, j-forward 8) i- backward, j- central 9) i- backward, j- backward

Here expression for only i- forward, j- forward (form 1) is shown-

$$\left(\frac{\partial^2 f}{\partial x \partial y}\right)_{i,j} = \left(\frac{\partial}{\partial x}\left(\frac{\partial f}{\partial y}\right)_{i,j}\right)_{i,j}$$

$$= \left(\frac{\partial z}{\partial x}\right)_{i,j} \quad \text{taking } z = \left(\frac{\partial f}{\partial y}\right)_{i,j}$$

$$= \frac{-z(i+2, j) + 4z(i+1, j) - 3z(i, j)}{2h}$$

$$= \frac{1}{2h}\left[-\left(\frac{\partial f}{\partial y}\right)_{i+2,j} + 4\left(\frac{\partial f}{\partial y}\right)_{i+1,j} - 3\left(\frac{\partial f}{\partial y}\right)_{i,j}\right]$$

$$= \frac{1}{4hk}\begin{bmatrix} f(i+2, j+2) - 4f(i+2, j+1) + 3f(i+2, j) - 4f(i+1, j+2) \\ +16f(i+1, j+1) - 12f(i+1, j) + 3f(i, j+2) - 12f(i, j+1) + 9f(i, j) \end{bmatrix} \quad (3.32)$$

$$+O(h^2, k^2)$$

Stencil of this equation can be shown as in Figure 3.3a and that of i-backward, j-backward (form 9) is shown in Figure 3.3b.

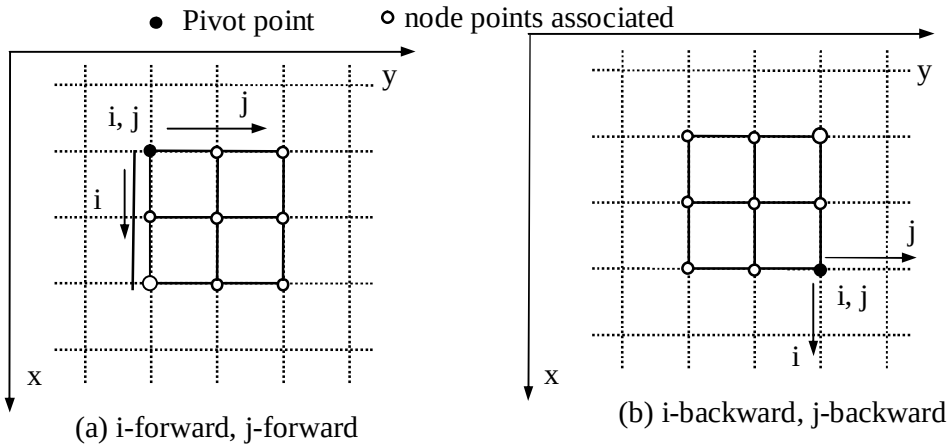

Figure 3.3: Stencils for ($\partial^2 f/\partial x \partial y$).

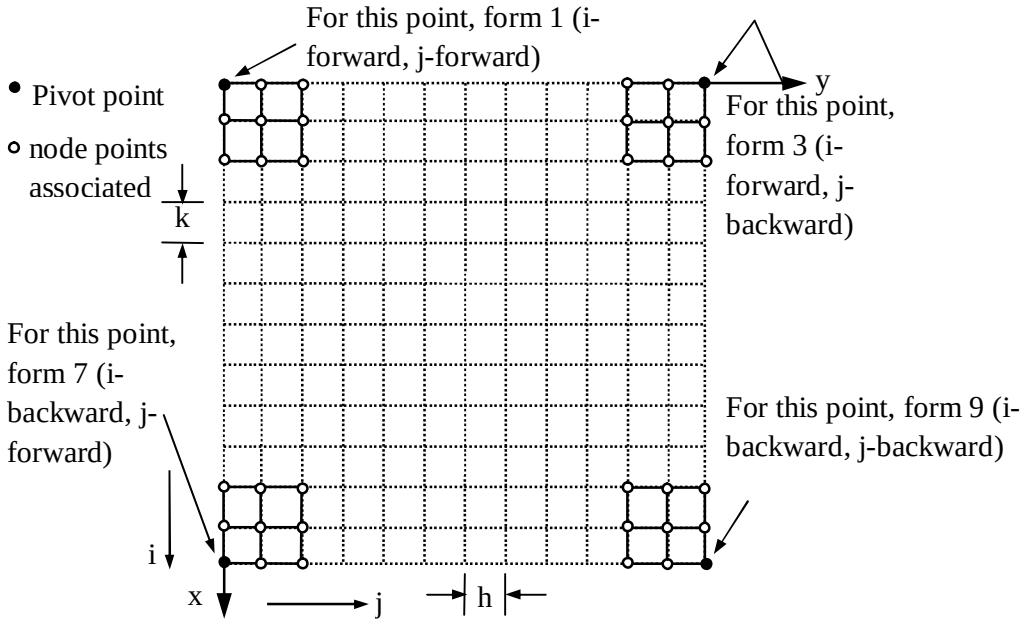

Figure 3.4: Application of different forms of $(\partial^2 f/\partial x \partial y)$.

These different types of forms are required for the solution, if $(\partial^2 f/\partial x \partial y)_{i,j}$ has to apply at different parts of the body. If a rectangular body is considered then application of different forms are shown in Figure 3.4. Here it will be worthy to mention that, the shape and the number of the node points of the stencils is same but the values of the coefficients of the associated node points may vary or remain same. Similarly the derivative $(\partial^3 f/\partial x^2 \partial y)_{i,j}$ can be discretized by using equation Eq. 3.18 and 3.10 and the difference equation thus found will be of the form i-central, j-forward.

$$\left(\frac{\partial^3 f}{\partial x^2 \partial y}\right)_{i,j} = \left(\frac{\partial^2}{\partial x^2}\left(\frac{\partial f}{\partial y}\right)_{i,j}\right)_{i,j}$$

$$= \left(\frac{\partial^2 z}{\partial x^2}\right)_{i,j} \quad \text{taking } z = \left(\frac{\partial f}{\partial y}\right)_{i,j}$$

$$= \frac{z(i+1,j) - 2z(i,j) + z(i-1,j)}{h^2}$$

$$= \frac{1}{h^2}\left[\left(\frac{\partial f}{\partial y}\right)_{i+1,j} - 2\left(\frac{\partial f}{\partial y}\right)_{i,j} + \left(\frac{\partial f}{\partial y}\right)_{i-1,j}\right]$$

$$= \frac{1}{2h^2k}\begin{bmatrix} -f(i+1,j+2)+4f(i+1,j+1)-3f(i+1,j)+2f(i,j+2) \\ -8f(i,j+1)+6f(i,j)-f(i-1,j+2)+4f(i-1,j+1)-3f(i-1,j) \end{bmatrix} \quad (3.33)$$
$$+O(h^2,k^2)$$

Similarly, i-forward j- central difference equation for $(\partial^3 f/\partial x\partial y^2)_{i,j}$ can be obtained from the manipulation of the equations 3.17 and 3.8.

$$\left(\frac{\partial^3 f}{\partial x\partial y^2}\right)_{i,j} = \left(\frac{\partial^2}{\partial y^2}\left(\frac{\partial f}{\partial x}\right)_{i,j}\right)_{i,j}$$

$$= \left(\frac{\partial^2 z}{\partial y^2}\right)_{i,j} \quad \text{taking } z = \left(\frac{\partial f}{\partial x}\right)_{i,j}$$

$$= \frac{z(i,j+1)-2z(i,j)+z(i,j-1)}{k^2}$$

$$= \frac{1}{k^2}\left[\left(\frac{\partial f}{\partial x}\right)_{i,j+1} - 2\left(\frac{\partial f}{\partial x}\right)_{i,j} + \left(\frac{\partial f}{\partial x}\right)_{i,j-1}\right]$$

$$= \frac{1}{k^2}\begin{bmatrix} \left(\dfrac{-f(i+2,j+1)+4f(i+1,j+1)-3f(i,j+1)}{2h}\right) \\ -2\left(\dfrac{-f(i+2,j)+4f(i+1,j)-3f(i,j)}{2h}\right) \\ +\left(\dfrac{-f(i+2,j-1)+4f(i+1,j-1)-3f(i,j-1)}{2h}\right) \end{bmatrix}$$

$$= \frac{1}{2k^2h}\begin{bmatrix} -f(i+2,j+1)+4f(i+1,j+1)-3f(i,j+1)+2f(i+2,j) \\ -8f(i+1,j)+6f(i,j)-f(i+2,j-1)+4f(i+1,j-1)-3f(i,j-1) \end{bmatrix} \quad (3.34)$$
$$+O(h^2,k^2)$$

Using equations 3.18 and 3.19 difference equation for $(\partial^4 f/\partial x^2\partial y^2)_{i,j}$, i-j both central, can be written as

$$\left(\frac{\partial^4 f}{\partial x^2\partial y^2}\right)_{i,j} = \left(\frac{\partial^2}{\partial y^2}\left(\frac{\partial^2 f}{\partial x^2}\right)_{i,j}\right)_{i,j}$$

$$= \left(\frac{\partial^2 z}{\partial y^2}\right)_{i,j} \quad \text{taking } z = \left(\frac{\partial^2 f}{\partial x^2}\right)_{i,j}$$

$$= \frac{z(i,j+1)-2z(i,j)+z(i,j-1)}{k^2}$$

$$= \frac{1}{h^2k^2}\begin{bmatrix} f(i+1,j+1) - 2f(i,j+1) + f(i-1,j+1) - 2f(i+1,j) \\ +4f(i,j) - 2f(i-1,j) + f(i+1,j-1) - 2f(i,j-1) + f(i-1,j-1) \end{bmatrix} \quad (3.35)$$
$$+O(h^2, k^2)$$

With the help of these formulas the governing differential equation (Eq. 2.22) and boundary conditions (Eq. 2.24 and 2.25) can be transformed into the desired finite difference equations.

3.2.2 Application Technique of Finite Difference Formulae in Rectangular Grid

Usually in the region of study, where the dependent function $\psi(x, y)$ has to be evaluated, the governing differential equation (Eq. 2.24) is applied at all node points except the boundary node points and boundary conditions (Eq. 2.25 and 2.26) are applied at boundary node points. For a rectangular shaped body usually two boundary conditions are known in each side of the rectangle. If a very simple problem of axially loaded member shown in figure 3.5a is considered then boundary conditions for this loading condition are shown in figure 3.5b. So each side has two boundary conditions and if this body is transformed into a grid of discrete points then it can be shown in figure 3.5c.

As shown in figure 3.5c each boundary node points experiences two boundary conditions. If both the two boundary conditions are applied at each boundary node points then the system of linear equations will have more number of algebraic equations than the number of points. Therefore, to yield a unique solution from the system of linear equations will be very difficult.

This problem can be solved if only one boundary condition is applied in each boundary node points. It can be accomplished by applying one boundary condition in a particular node point and the other boundary condition in the next neighboring node point and so on (figure 3.6a). But in that case, solving procedure of the problem becomes difficult in terms of applying governing equation (GE) because central difference form of GE cannot be applied at domain nodal points that are situated just next to the physical boundary.

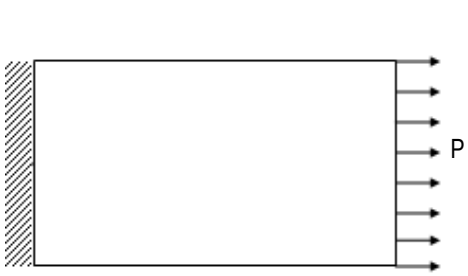

(a) Axially loaded member

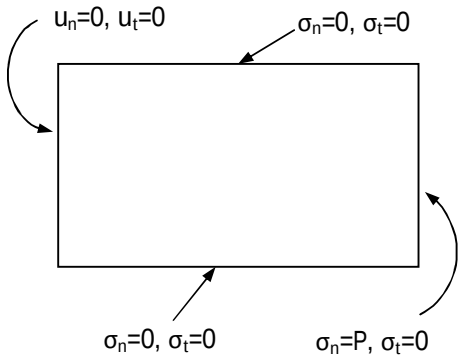

(b) Boundary conditions of problem (a)

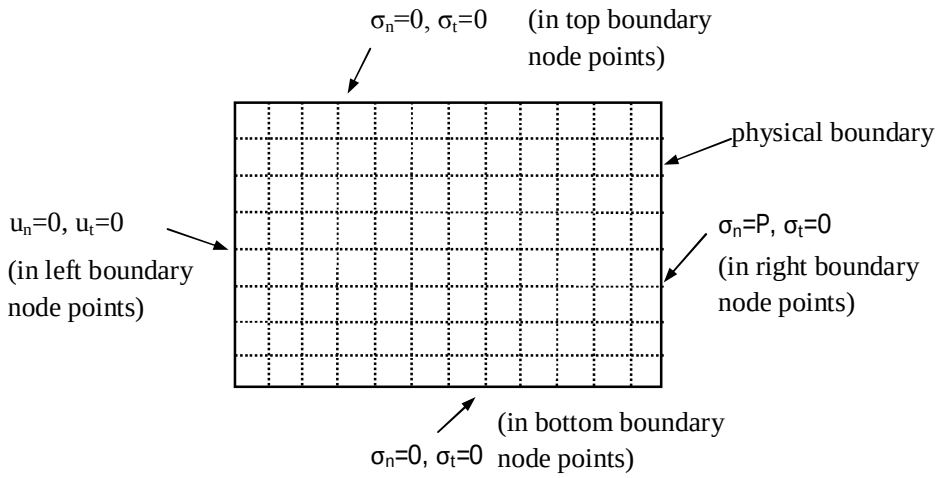

(c) Discretetization of domain

Figure 3.5: Boundary conditions for an axially loaded member.

To overcome this problem a boundary near the physical boundary is assumed to exist, which is named as the imaginary boundary. If only the top boundary is considered then it can be shown by figure 3.6b. Top boundary nodes have two boundary conditions to satisfy, i.e. $\sigma_n=0$, $\sigma_t=0$. Hence an imaginary boundary is assumed at the outside of top physical boundary, immediate top grid points of the top boundary node points, as well as at all other boundaries of the rectangle. So if one boundary condition $\sigma_n=0$ is satisfied by the physical boundary nodes, then other boundary condition $\sigma_t=0$ can be applied at same physical boundary nodes by taking help of imaginary boundary nodes, or vice versa. Actually for both of the boundary conditions, the finite difference formulae will be formulated by taking pivot point at physical boundary nodes but for the sake of the solution process one boundary condition is taken at imaginary node by

changing the pivot point from physical node to imaginary node while all of the coefficient of corresponding node will remain unchanged. This also helps to formulate GE with central difference formula for all domain nodal points by taking imaginary nodes in formulation. So, the system of linear equations will have same number of variables and equations. In this research work this technique is followed.

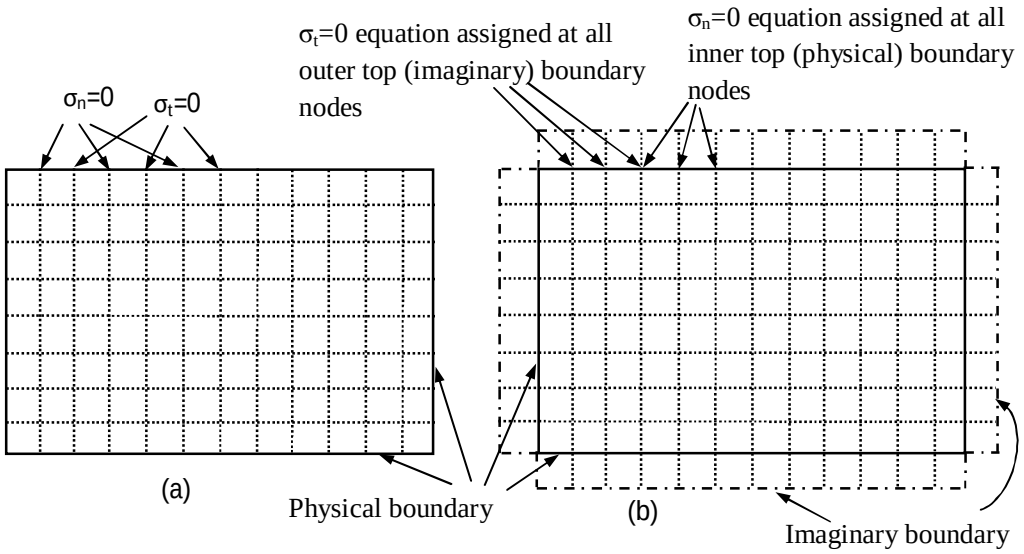

Figure 3.6: Boundary condition management (a) without and (b) with imaginary boundary.

So the difference equations have to develop in such a way that they would cover the physical boundary points, inner points and imaginary points also. These finite difference forms are described in the following sections.

3.3 The Mesh Refinement Methodology

In mesh refinement technique, the physical problem is discretized by taking different size of meshes at different regions of the physical problem in order to reduce computational efforts and resources and to improve the accuracy of the solutions at most critical section of the physical problem. This discretization of the physical problem into finer meshes can include either only domain or domain with a part of the boundary. Methodology of mesh refinement for both cases will be discussed in next section of this thesis under the heading Case-I and Case-II.

3.3.1 Case-I: Mesh Refinement includes only domain

A discretization of physical model under mesh refinement technique in which the finer mesh region includes only domain is shown in figure 3.7. In order to satisfy governing equation (GE) over the whole domain, a set of stencils have been made in the following section of this thesis. The finer mesh (length of h1) region lies only in the domain and it is identified by four arbitrary letters A, B, C and D (figure 3.7).

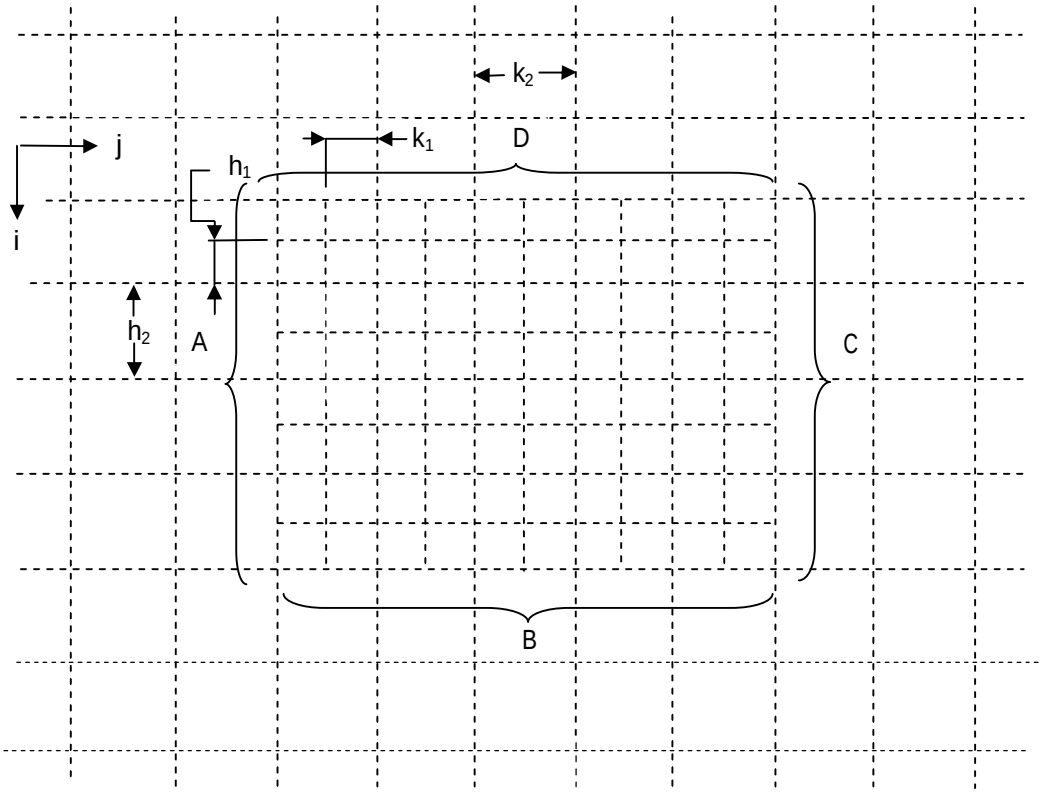

Figure 3.7: Discretization of physical model under mesh refinement technique which includes only domain.

3.3.1.1 Finite Difference Form of the Bi-harmonic Governing Equation (GE)

This section will illustrate the formulation of different stencils of GE that are necessary in order to satisfy GE whole over the domain referring to figure 3.7. By using combinations of forward, backward and central difference formula of second and fourth derivatives of displacement potential function, ψ some stencils for the bi-harmonic governing equation, from Eq. 3.36 to Eq. 3.41, have been developed in this section.

Stencil-1: Named as 'a' formula

The governing equation for the problem in terms of displacement potential function, Eq. 2.24

$$\frac{\partial^4\psi}{\partial x^4} + 2\frac{\partial^4\psi}{\partial x^2.\partial y^2} + \frac{\partial^4\psi}{\partial y^4} = 0$$

By using the difference formula of $\frac{\partial^4\psi}{\partial x^4}$, $\frac{\partial^4\psi}{\partial x^2.\partial y^2}$ and $\frac{\partial^4\psi}{\partial y^4}$ from the equations Eq. 3.29, 3.30 and 3.35 respectively, the above equation can be written as

$$\frac{1}{h^4}[\psi(i+2,j) - 4\psi(i+1,j) + 6\psi(i,j) - 4\psi(i-1,j) + \psi(i-2,j)] + \frac{2}{h^2k^2}[\psi(i+1,j+1) - 2\psi(i+1,j) + \psi(i+1,j-1) - 2\psi(i,j-1) + 4\psi(i,j) - 2\psi(i,j-1) + \psi(i-1,j+1) - 2\psi(i-1,j) + \psi(i-1,j-1)] + \frac{1}{k^4}[\psi(i,j+2) - 4\psi(i,j+1) + 6\psi(i,j) - 4\psi(i,j-1) + \psi(i,j-2)] = 0$$

$$\rightarrow zk1\{\psi(i-2,j) + \psi(i+2,j)\} - zk2\{\psi(i-1,j) + \psi(i+1,j)\} - zk3\{\psi(i.j+1) + \psi(i,j-1)\} + zk4\psi(i,j) + zk5\{\psi(i-1,j-1) + \psi(i-1,j+1) + \psi(i+1,j-1) + \psi(i+1,j+1) + \psi(i,j-2) + \psi(i,j+2)\} = 0 \quad (3.36)$$

Where, $zk1 = r^4$; $zk2 = 4(r^4 + r^2)$; $zk3 = 4(1 + r^2)$; $zk4 = (6r^4 + 8r^2 + 6)$; $zk5 = 2r^2$ and $r = \frac{k}{h}$

The above equation (Eq. 3.36) is the finite difference approximation of the bi-harmonic partial differential equation and has validity in the domain nodal points which have only uniform mesh. The stencil of this equation is shown in figure 3.8.

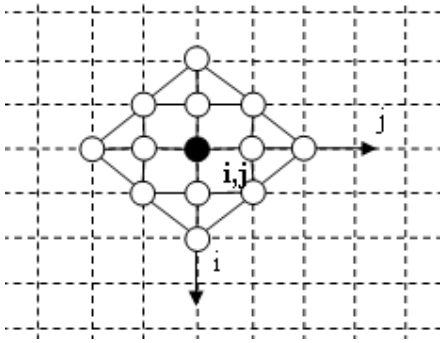

Figure 3.8: Stencil of the governing equation 'a' formula.

Stencil-2: Named as 'b' formula.

Starting from governing equation for the problem in terms of ψ, Eq. 2.24.

$$\frac{\partial^4\psi}{\partial x^4} + 2\frac{\partial^4\psi}{\partial x^2.\partial y^2} + \frac{\partial^4\psi}{\partial y^4} = 0$$

By using the combination of finite difference formula of $\frac{\partial^2\psi}{\partial x^2}$, $\frac{\partial^2\psi}{\partial y^2}$; $\frac{\partial^4\psi}{\partial y^4}$ from eq.3.18, 3.19 and 3.16 the above equation can be written as

$$\frac{1}{h1^2}\left[\frac{\partial^2\psi}{\partial x^2}_{i-1,j} - 2\frac{\partial^2\psi}{\partial x^2}_{i,j} + \frac{\partial^2\psi}{\partial x^2}_{i+1,j}\right] + \frac{2}{h1^2}\left[\frac{\partial^2\psi}{\partial y^2}_{i-1,j} - 2\frac{\partial^2\psi}{\partial y^2}_{i,j} + \frac{\partial^2\psi}{\partial y^2}_{i+1,j}\right] + \frac{1}{k1^4}[3\psi(i,j) - 14\psi(i,j+1) + 26\psi(i,j+2) - 24\psi(i,j+3) + 11\psi(i,j+4) - 2\psi(i,j+5)] = 0$$

Now using the combination of finite difference formula of $\frac{\partial^2\psi}{\partial x^2}$ and $\frac{\partial^2\psi}{\partial y^2}$ from eq.3.18, 3.19 and 3.12 give

$$\rightarrow \frac{1}{h1^2h2^2}[\psi(i-3,j) - 2\psi(i-1,j) + \psi(i+1,j)] - \frac{2}{h1^4}[\psi(i-1,j) - 2\psi(i,j) + \psi(i+1),j] + \frac{1}{h1^2h2^2}[\psi(i-1,j) - 2\psi(i+1,j) + \psi(i+3,j)] + \frac{2}{h1^2k2^2}[\psi(i-1,j-2) - 2\psi(i-1,j) + \psi(i-1,j+2)] - \frac{4}{h1^2k1^2}[2\psi(i,j) - 5\psi(i,j+1) + 4\psi(i,j+2) - \psi(i,j+3)] + \frac{2}{h1^2k2^2}[\psi(i+1,j-2) - 2\psi(i+1,j) + \psi(i+1,j+2)] + \frac{1}{k1^4}[3\psi(i,j) - 14\psi(i,j+1) + 26\psi(i,j+2) - 24\psi(i,j+3) + 11\psi(i,j+4) - 2\psi(i,j+5)] = 0$$

$$\rightarrow m2\{\psi(i-3,j) + \psi(i+3,j)\} + 2m4\{\psi(i-1,j+2) + \psi(i-1,j-2) + \psi(i+1,j-2) + \psi(i+1,j+2)\} - (m2 + 2m1 + 4m4)\{\psi(i-1,j) + \psi(i+1,j)\} + (4m1 - 8m3 + 3m5)\psi(i,j) + (20m3 - 14m5)\psi(i,j+1) + (26m5 - 16m3)\psi(i,j+2) + (4m3 - 24m5)\psi(i,j+3) + 11m5\psi(i,j+4) - 2m5\psi(i,j+5) = 0 \qquad (3.37)$$

Where, $m1 = \frac{1}{h1^4}$; $m2 = \frac{1}{h1^2h2^2}$; $m3 = \frac{1}{h1^2k1^2}$; $m4 = \frac{1}{h1^2k2^2}$; $m5 = \frac{1}{k1^4}$

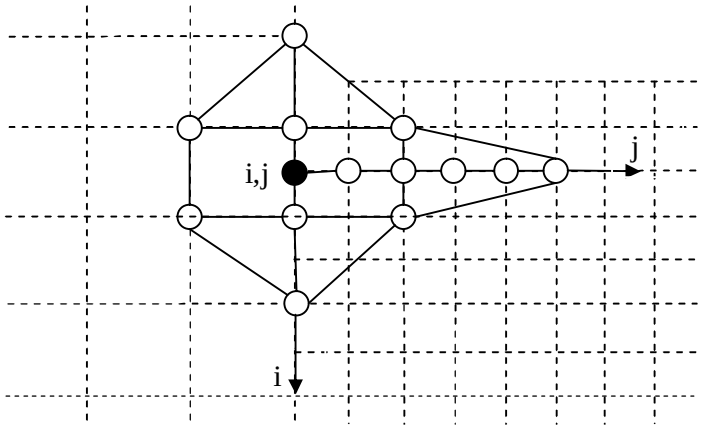

Figure 3.9: Stencil of the governing equation 'b' formula.

Stencil-3: Named as c formula

Starting from governing equation for the problem in terms of ψ, Eq. 2.24

$$\frac{\partial^4\psi}{\partial x^4} + 2\frac{\partial^4\psi}{\partial x^2.\partial y^2} + \frac{\partial^4\psi}{\partial y^4} = 0$$

Using the finite difference formula of $\frac{\partial^4\psi}{\partial x^4}$; $\frac{\partial^2\psi}{\partial x^2}$; $\frac{\partial^4\psi}{\partial y^4}$ from eq. 3.22, 3.18 and 3.16, the above equation can be written as-

$$\frac{1}{h1^4}[\psi(i-2,j) - 4\psi(i-1,j) + 6\psi(i,j) - 4\psi(i+1,j) + \psi(i+2,j)] + \frac{2}{h1^2}\left[\frac{\partial^2\psi}{\partial y^2}_{i-1,j} - 2\frac{\partial^2\psi}{\partial y^2}_{i-1,j} + \frac{\partial^2\psi}{\partial y^2}_{i+1,j}\right] + \frac{1}{k1^4}[3\psi(i,j) - 14\psi(i,j+1) + 26\psi(i,j+2) - 24\psi(i,j+3) + 11\psi(i,j+4) - 2\psi(i,j+5)] = 0$$

Now using finite difference formula of $\frac{\partial^2\psi}{\partial y^2}$ from eq. 3.12 and 3.19 gives

$$\rightarrow \frac{1}{h1^4}[\psi(i-2,j) - 4\psi(i-1,j) + 6\psi(i+1,j) - 4\psi(i+1,j) + \psi(i+2,j)] + \frac{2}{h1^2k2^2}[\psi(i-1,j-2) - 2\psi(i-1,j) + \psi(i-1,j+2)] - \frac{4}{h1^2k1^2}[2\psi(i,j) - 5\psi(i,j+1) + 4\psi(i,j+2) - \psi(i,j+3)] + \frac{2}{h1^2k2^2}[\psi(i+1,j-2) - 2\psi(i+1,j) + \psi(i+1,j+2)] + \frac{1}{k1^4}[3\psi(i,j) - 14\psi(i,j+1) + 26\psi(i,j+2) - 24\psi(i,j+3) + 11\psi(i,j+4) - 2\psi(i,j+5)] = 0$$

$$\rightarrow m1\{\psi(i-2,j) + \psi(i+2,j)\} + (-4m1 - 4m4)\{\psi(i-1,j) + \psi(i+1,j)\} + (6m1 - 8m3 + 3m5)\psi(i,j) + 2m4\{\psi(i-1,j-2) + \psi(i-1,j+2) + \psi(i+1,j-2) + \psi(i+1,j+2)\} + (20m3 - 14m5)\psi(i,j+1) + (26m5 - 16m3)\psi(i,j+2) + (4m3 - 24m5)\psi(i,j+3) + 11m5\psi(i,j+4) - 2m5\psi(i,j+5) = 0 \quad (3.38)$$

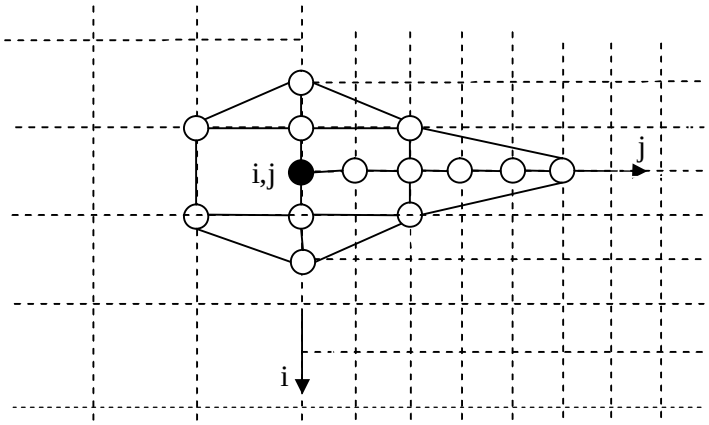

Figure 3.10: Stencil of the governing equation ‘c’ formula.

Stencil-4: Named as ‘d’ formula

Starting from governing equation for the problem in terms of ψ, Eq. 2.24

$$\frac{\partial^4\psi}{\partial x^4} + 2\frac{\partial^4\psi}{\partial x^2.\partial y^2} + \frac{\partial^4\psi}{\partial y^4} = 0$$

Using the finite difference formula of $\frac{\partial^4\psi}{\partial x^4}$; $\frac{\partial^2\psi}{\partial x^2}$; $\frac{\partial^2\psi}{\partial y^2}$ from eq. 3.22, 3.18 and 3.19, the above equation can be written as-

$$\frac{1}{h1^4}[\psi(i-2,j) - 4\psi(i-1,j) + 6\psi(i,j) - 4\psi(i+1,j) + \psi(i+2,j)] + \frac{2}{h1^2}\left[\frac{\partial^2\psi}{\partial y^2}_{i-1,j} - 2\frac{\partial^2\psi}{\partial y^2}_{i,j} + \frac{\partial^2\psi}{\partial y^2}_{i+1,j}\right] + \frac{1}{k1^2}\left[\frac{\partial^2\psi}{\partial y^2}_{i,j-1} - 2\frac{\partial^2\psi}{\partial y^2}_{i,j} + \frac{\partial^2\psi}{\partial y^2}_{i,j+1}\right] = 0$$

Now using finite difference formula of $\frac{\partial^2\psi}{\partial y^2}$ from eq. 3.19 gives

$$\rightarrow \frac{1}{h1^4}[\psi(i-2,j) - 4\psi(i-1,j) + 6\psi(i,j) - 4\psi(i+1,j) + \psi(i+2,j)] + \frac{2}{h1^2k1^2}[\psi(i-1,j-1) - 2\psi(i-1,j) + \psi(i-1,j+1) - 2\psi(i,j-1) + 4\psi(i,j) - 2\psi(i,j+1) + \psi(i+1,j-1) - 2\psi(i+1,j) + \psi(i+1,j+1)] + \frac{1}{k1^2k2^2}[\psi(i,j-3) - 2\psi(i,j-1) + \psi(i,j+1)] - \frac{2}{k1^4}[\psi(i,j-1) - 2\psi(i,j) + \psi(i,j+1)] + \frac{1}{k1^2k2^2}[\psi(i,j-1) - 2\psi(i,j+1) + \psi(i,j+3)] = 0$$

$$\rightarrow m1\{\psi(i-2,j) + \psi(i+2,j)\} + 2m3\{\psi(i-1,j-1) + \psi(i-1,j+1) + \psi(i+1.j-1) + \psi(i+1,j+1)\} + (-4m1 - 4m3)\{\psi(i-1,j) + \psi(i+1,j)\} + m6\{\psi(i,j-3) + \psi(i,j+3)\} + (-4m3 - 2m5 - m6)\{\psi(i,j-1) + (i,j+1)\} + (6m1 + 8m3 + 4m5)\psi(i,j) = 0 \quad (3.39)$$

Where, $m6 = \frac{1}{k1^2k2^2}$; other constant are already defined before.

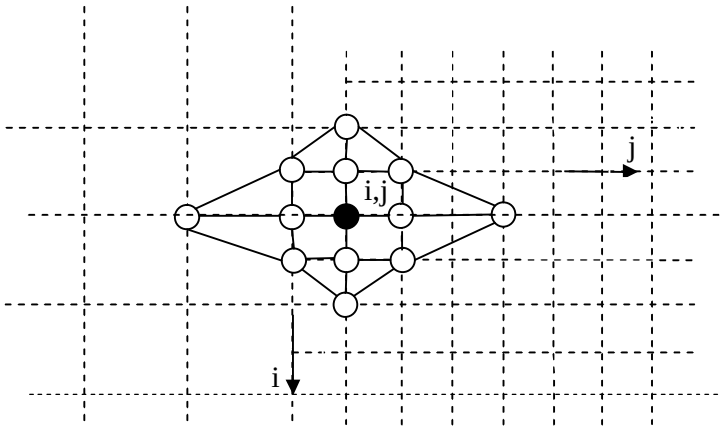

Figure 3.11: Stencil of the governing equation ‘d’ formula.

Stencil-5: Named as ‘e’ formula

Starting from governing equation for the problem in terms of ψ, Eq. 2.24

$$\frac{\partial^4\psi}{\partial x^4} + 2\frac{\partial^4\psi}{\partial x^2.\partial y^2} + \frac{\partial^4\psi}{\partial y^4} = 0$$

Using the finite difference formula of $\frac{\partial^4\psi}{\partial x^4}$; $\frac{\partial^2\psi}{\partial x^2}$; $\frac{\partial^2\psi}{\partial y^2}$ from eq. 3.22, 3.18 and 3.19, the above equation can be written as-

$$\frac{1}{h1^4}[\psi(i+2,j) - 4\psi(i+1,j) + 6\psi(i,j) - 4\psi(i-1,j) + \psi(i,j-2)] + \frac{2}{h1^1}\left[\frac{\partial^2\psi}{\partial y^2}_{i-1,j} - 2\frac{\partial^2\psi}{\partial y^2}_{i,j} + \frac{\partial^2\psi}{\partial y^2}_{i+1,j}\right] + \frac{1}{k1^2}\left[\frac{\partial^2\psi}{\partial y^2}_{i,j-1} - 2\frac{\partial^2\psi}{\partial y^2}_{i,j} + \frac{\partial^2\psi}{\partial y^2}_{i,j+1}\right] = 0$$

Now using finite difference form of $\frac{\partial^2\psi}{\partial y^2}$ from eq. 3.19 and 3.12 gives

$$\rightarrow \frac{1}{h1^4}[\psi(i+2,j) - 4\psi(i+1,j) + 6\psi(i,j) - 4\psi(i-1,j) + \psi(i-2,j)] + \frac{2}{h1^2k1^2}[\psi(i-1,j-1) - 2\psi(i-1,j) + \psi(i-1,j+1) - 2\psi(i,j-1) + 4\psi(i,j) - 2\psi(i,j+1) + \psi(i+1,j-1) - 2\psi(i+1,j) - \psi(i+1,j+1)] + \frac{1}{k1^4}[2\psi(i,j-1) - 5\psi(i,j) + 4\psi(i,j+1) - \psi(i,j+2) - 4\psi(i,j) + 10\psi(i,j+1) - 8\psi(i,j+2) + 2\psi(i,j+3) + 2\psi(i,j+1) - 5\psi(i,j+2) + 4\psi(i,j+3) - \psi(i,j+3)] = 0$$

$$\rightarrow 2m3\{\psi(i-1,j-1) + \psi(i+1,j-1) + \psi(i-1,j+1) + \psi(i+1,j+1)\} + m1\{\psi(i-2,j) + \psi(i+2,j)\} + (-4m1 - 4m3)\{\psi(i-1,j) + \psi(i+1,j)\} + (-4m1 + 2m5)\psi(i,j-1) + (6m1 + 8m3 - 9m5)\psi(i,j) + (-4m3 + 16m5)\psi(i,j+1) - 14m5\psi(i.j+2) + 6m5\psi(i,j+3) - m5\psi(i,j+4) = 0 \quad (3.40)$$

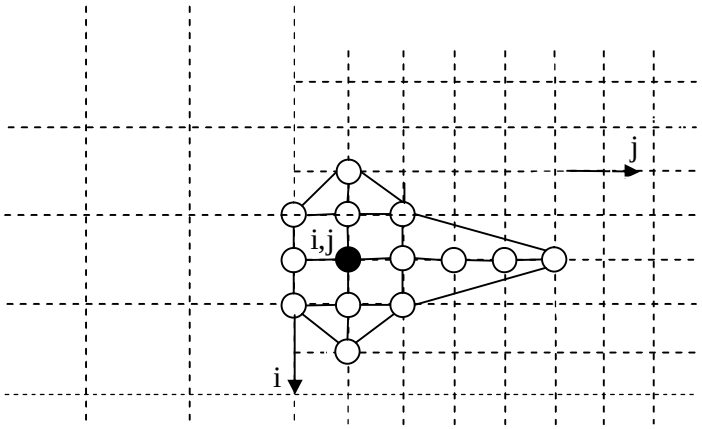

Figure 3.12: Stencil of the governing equation ‘e’ formula.

Stencil-6: Named as ‘f’ formula

Starting from governing equation for the problem in terms of ψ, Eq. 2.24

$$\frac{\partial^4\psi}{\partial x^4} + 2\frac{\partial^4\psi}{\partial x^2.\partial y^2} + \frac{\partial^4\psi}{\partial y^4} = 0$$

Using the different combination of finite difference formula of $\frac{\partial^2\psi}{\partial x^2}; \frac{\partial^2\psi}{\partial y^2}$ from eq. 3.18 and 3.19 respectively the above equation can be written as-

$$\frac{1}{h1^2}\left[\frac{\partial^2\psi}{\partial x^2}_{i-1,j} - 2\frac{\partial^2\psi}{\partial x^2}_{i,j} + \frac{\partial^2\psi}{\partial x^2}_{i+1,j}\right] + \frac{2}{h1^2}\left[\frac{\partial^2\psi}{\partial y^2}_{i-1,j} - 2\frac{\partial^2\psi}{\partial y^2}_{i,j} + \frac{\partial^2\psi}{\partial y^2}_{i+1,j}\right] + \frac{1}{k1^2}\left[\frac{\partial^2\psi}{\partial y^2}_{i,j-1} - 2\frac{\partial^2\psi}{\partial y^2}_{i,j} + \frac{\partial^2\psi}{\partial y^2}_{i,j+1}\right] = 0$$

Now using finite difference formula of $\frac{\partial^2\psi}{\partial x^2}; \frac{\partial^2\psi}{\partial y^2}$ from eq. 3.11, 3.19 and 3.12 gives

$$\rightarrow \frac{1}{h1^4}[2\psi(i-1,j) - 5\psi(i,j) + 4\psi(i+1,j) - \psi(i+2,j) - 4\psi(i,j) + 10\psi(i+1,j) - 8\psi(i+2,j) + 2\psi(i+3,j) + 2\psi(i+1,j) - 5\psi(i+2,j) + 4\psi(i+3,j) - \psi(i+4,j)] + \frac{2}{h1^2k1^2}[\psi(i-1,j-1) - 2\psi(i-1,j) + \psi(i-1,j+1) - 2\psi(i,j-1) + 4\psi(i,j) - 2\psi(i,j+1) + \psi(i+1,j-1) - 2\psi(i+1,j) + \psi(i+1,j+1)] + \frac{1}{k1^4}[2\psi(i,j-1) - 5\psi(i,j) + 4\psi(i,j+1) - \psi(i,j+2) - 4\psi(i,j) + 10\psi(i,j+1) - 8\psi(i,j+2) + 2\psi(i,j+3) + 2\psi(i,j+1) - 5\psi(i,j+2) + 4\psi(i,j+3) - \psi(i,j+4)] = 0$$

$$\rightarrow 2m3\{\psi(i-1,j-1) + \psi(i+1,j-1) + \psi(i-1,j+1) + \psi(i+1,j+1)\} + (-9m1 + 8m3 - 9m5)\psi(i,j) + (2m1 - 4m3)\psi(i-1,j) + (16m1 - 4m3)\psi(i+1,j) - 14m1\psi(i+2,j) + 6m1\psi(i+3,j) - m1\psi(i+4,j) + (-4m3 + 2m5)\psi(i,j-$$

$$1) + (-4m3 + 16m5)\psi(i,j+1) - 14m5\psi(i,j+2) + 6m5\psi(i,j+3) - m5\psi(i,j+4)] = 0 \quad (3.41)$$

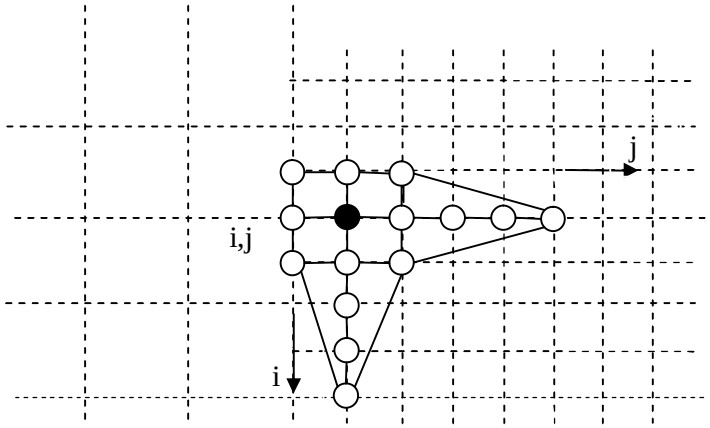

Figure 3.13: Stencil of the governing equation 'f' formula.

3.3.1.2 Application Technique of Finite Difference Formulae of GE

Referring to figure 3.7, in this section, the application method of different stencils of GE, those are formulated in the previous section, over the whole domain will be discussed. All the stencils have been formulated for sides A. For other sides, B, C and D, the stencils can be obtained only by changing some parameters e.g. any stencils of left sides (A) can be used for right sides (C) only by replacing j-* with j+* where * means 1, 2 …etc. The conversion procedure of stencils from one side to another side is listed in table-1. The stencils for each side are given in figure 3.14. Stencil-1 is symmetric about both vertical and horizontal axis, so it shape remain same in all sides. Since, it has applicability over uniform fine mesh and also over uniform coarse mesh; as a result it has two size of same shape which is shown in figure 3.15. The small one is applied over uniform fine mesh and large one is applied over uniform coarse mesh. The pivot of each stencil is filled with different color and also the domain nodal points are filled with same color of pivot points as shown in figure 3.16. The same color of a stencil pivot point and nodal points indicates that this stencil has applicability only on these nodal points. Thus the GE is satisfied all over the domain nodal points.

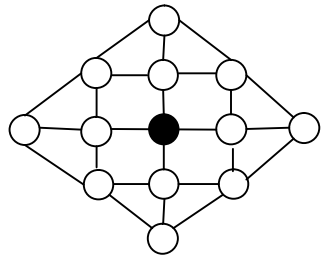

Stencil-1

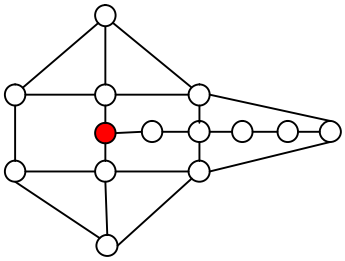

Stencil-2

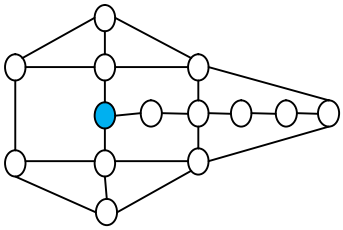

Stencil-3

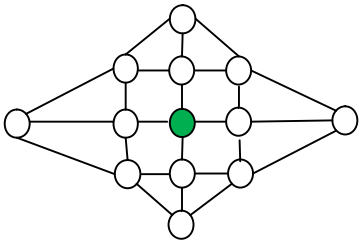

Stencil-4

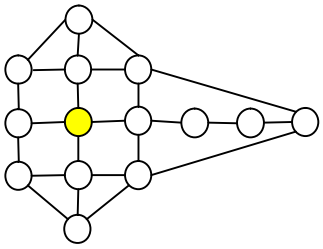

Stencil-5

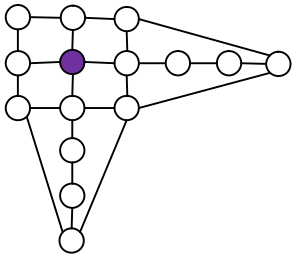

Stencil-6

a) Stencils of GE for sides A

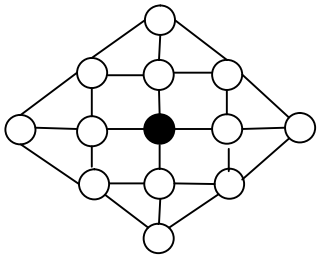

Stencil-1

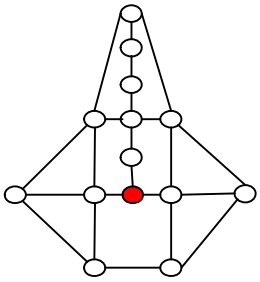

Stencil-2

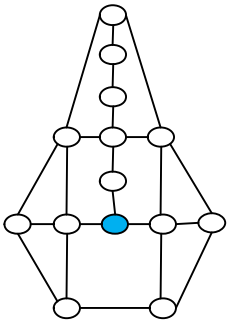

Stencil-3

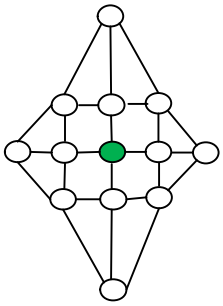

Stencil-4

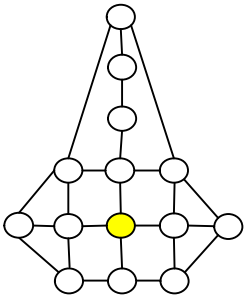

Stencil-5

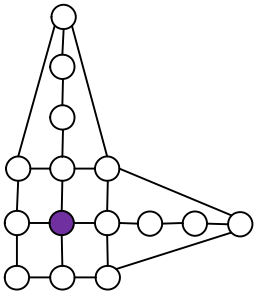

Stencil-6

b) Stencils of GE for sides B

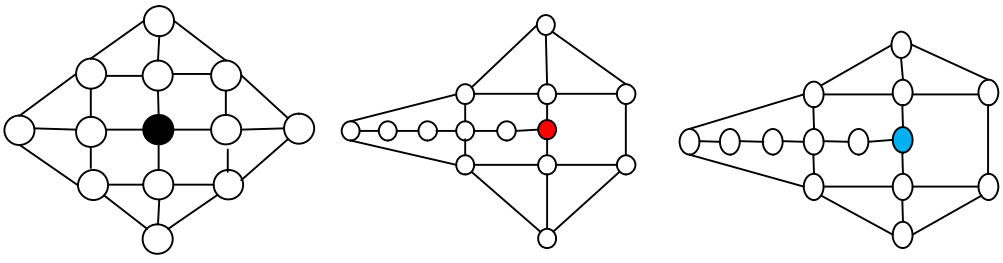

Stencil-1 Stencil-2 Stencil-3

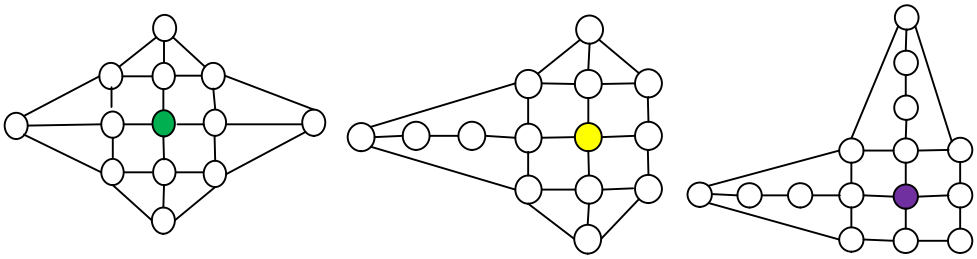

Stencil-4 Stencil-5 Stencil-6

c) Stencils of GE for sides C

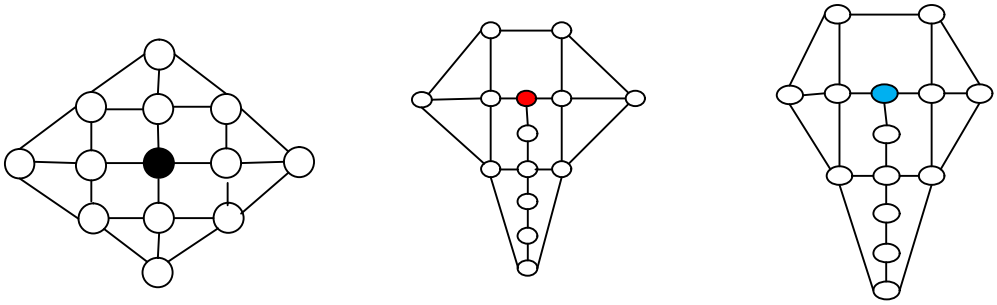

Stencil-1 Stencil-2 Stencil-3

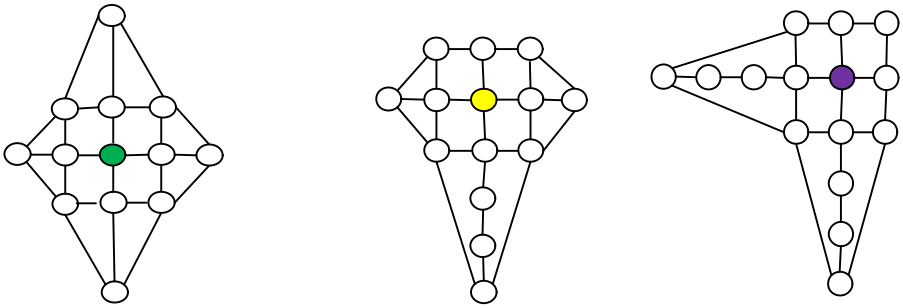

Stencil-4 Stencil-5 Stencil-6

d) Stencils of GE for side D

Figure 3.14: Different types of stencils of GE for over whole domain.

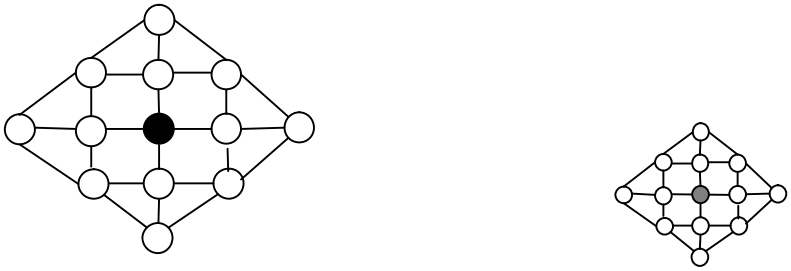

a) Large size b) Small size

Figure 3.15: Two different sizes of stencil-1 ‘a’ formula.

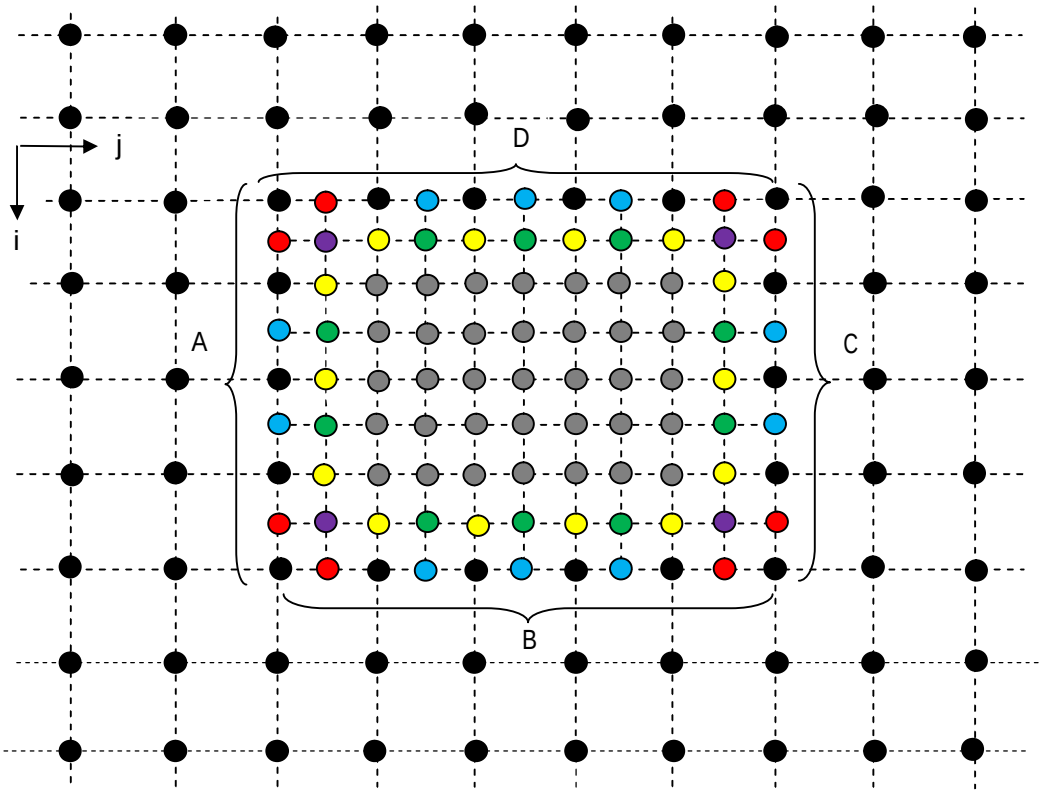

Figure 3.16: Applicability of different stencils of GE over whole domain.

Table 3.1: Conversion charts of finite difference formulas of GE for different sides of the fine mesh zone of domain.

Surfaces	Type of difference formula required	Replacement required
A	i-centered, j-forward	No change required
B	i-backward j-centered	i by j, h1 by k1, h2 by k2 and then i-* by i+* and vise versa
C	i-centered, j-backward	Only replace j+* by j-* and vice versa
D	i- forward, j-centered	i by j, h1 by k1 and h2 by k2

N.B: '*' means 1,2.3……..and this chart is valid for formula a,b,c,d and e.

By using this table one can convert the equation a, b, c, d, and e from one side to another. Actually, there is no need to convert equation c because it is symmetric about horizontal and vertical planes passing through its pivot point. To convert the equation f i.e. eq. 3.41, which is valid in top left corner marked by yellow pivot point (figure 3.16), changing of i and j by i-* and j-* respectively is required. To convert for bottom left corner yellow point (figure 3.10) change only i by i-*, for bottom right corner replace i by i-3* and j by j-* and for top right corner, replace j by j-*.

3.3.1.3 Finite Difference Form of the Boundary Conditions

The formulation of finite difference formulae of boundary conditions (BCs) will be presented in this section.

B.C.-1: Displacement in x-direction, u

Starting from the equation of displacement component, u in terms of ψ eq.2.25

$$u = \frac{\partial^2 \psi}{\partial x . \partial y}$$

Using the equation 3.9, the above equation reduces to

$$= \frac{1}{2h}\left[-3\frac{\partial \psi}{\partial y}_{i,j} + 4\frac{\partial \psi}{\partial y}_{i+1,j} - \frac{\partial \psi}{\partial y}_{i+2,j}\right]$$

Now using the finite difference formula of $\frac{\partial \psi}{\partial y}$ from eq.3.10

$$= \frac{1}{4hk}[-3\{-3\psi(i,j) + 4\psi(i,j+1) - \psi(i,j+2)\} + 4\{-3\psi(i+1,j) + 4\psi(i+1,j+1) - \psi(i+1,j+2)\} - \{-3\psi(i+2,j) + 4\psi(i+2,j+1) - \psi(i+2,j+2)\}]$$

$$= s1.\,[9\psi(i,j) - 12\{\psi(i,j+1) + \psi(i+1,j)\} + 16\psi(i+1,j+1) + \psi(i+2,j+2) + 3\{\psi(i,j+2) + \psi(i+2,j)\} - 4\{\psi(i+1,j+2) + \psi(i+2,j+1)\}] \quad (3.42)$$

Where s1=$\frac{1}{4hk}$

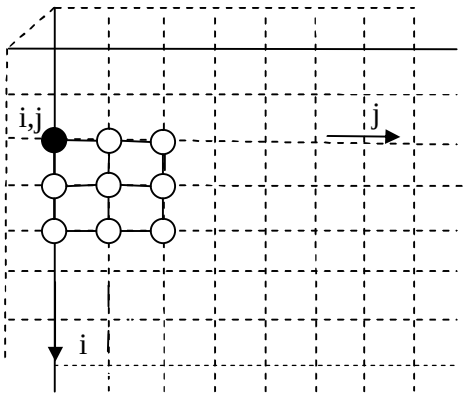

Figure 3.17: Stencil of displacement component, u

B.C.-2: Displacement in y-direction, v

Starting from the equation of displacement component, v in terms of ψ eq.2.25

$$v = -\left[\left(\frac{1-\mu}{1+\mu}\right)\frac{\partial^2 \psi}{\partial y^2} + \left(\frac{2}{1+\mu}\right)\frac{\partial^2 \psi}{\partial x^2}\right]$$

Using finite difference formula of $\frac{\partial^2 \psi}{\partial y^2}$ and $\frac{\partial^2 \psi}{\partial x^2}$ from equation 3.19 and 3.18 respectively

$$= -\frac{1}{1+\mu}\left[\frac{1-\mu}{k^2}\{\psi(i,j+1) - 2\psi(i,j) + \psi(i,j-1)\} + \frac{2}{h^2}\{\psi(i+1) - 2\psi(i,j) + \psi(i-1,j)\}\right]$$

$$=s2[c1\{\psi(i,j+1) + \psi(i,j-1)\} - (2c1 + 2zk5)\psi(i,j) + zk5\{\psi(i+1,j) + \psi(i-1,j)\}] \quad (3.43)$$

Where, $s2 = -\frac{1}{(1+\mu)k^2}$; $c1 = 1-\mu$

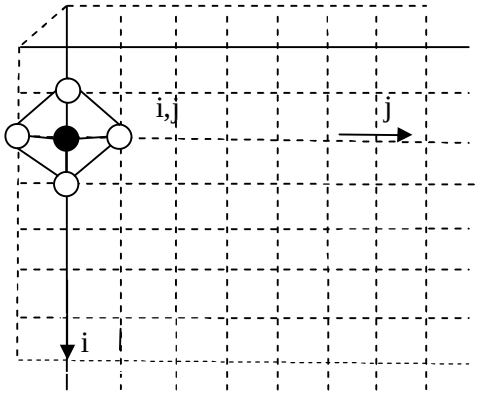

Figure 3.18: Stencil of displacement component, v

B.C.-3: Stress component in x-direction, σ_x

Starting from the equation of stress component, σ_x in terms of ψ eq.2.26

$$\sigma_x = \frac{E}{(1+\mu)^2}\left[\frac{\partial^3\psi}{\partial x^2\,\partial y} - \mu\frac{\partial^3\psi}{\partial y^3}\right]$$

$$\text{or,} \quad (1+\mu)^2\frac{\sigma_x}{E} = \left[\frac{\partial^3\psi}{\partial x^2\,\partial y} - \mu\frac{\partial^3\psi}{\partial y^3}\right]$$

Now using the eq.3.18 and 3.19, the above equation reduces to

$$(1+\mu)^2\frac{\sigma_x}{E} = \frac{1}{h^2}\left[\frac{\partial\psi}{\partial y}_{i-1,j} - 2\frac{\partial\psi}{\partial y}_{i,j} + \frac{\partial\psi}{\partial y}_{i+1,j}\right] - \frac{\mu}{k^2}\left[\frac{\partial\psi}{\partial y}_{i,j-1} - \frac{\partial\psi}{\partial y}_{i,j} + \frac{\partial\psi}{\partial y}_{i,j+1}\right]$$

Now using the eq.3.10 gives

$$(1+\mu)^2\frac{\sigma_x}{E}=\frac{1}{2h^2k}[-3\psi(i-1,j)+4\psi(i-1,j+1)-\psi(i-1,j+2)+6\psi(i,j)-8\psi(i,j+1)+2\psi(i,j+2)-3\psi(i+1,j)+4\psi(i+1,j+1)-\psi(i+1,j+2)]-\frac{\mu}{2k^3}[-3\psi(i,j-1)+4\psi(i,j)-\psi(i,j+1)+6\psi(i,j)-8\psi(i,j+1)+2\psi(i,j+2)-3\psi(i,j+1)+4\psi(i,j+2)-\psi(i,j+3)]$$

or, $$(1+\mu)^2\frac{\sigma_x}{E}=s3[zk9\{-3\psi(i-1,j)+4\psi(i-1,j+1)-\psi(i-1,j+2)-3\psi(i+1,j)+4\psi(i+1,j+1)-\psi(i+1),j+2\}+3\psi(i,j-1)-(6zk9-10)\psi(i,j)+(12-8zk9)\psi(i,j+1)+(2zk9-6)\psi(i,j+2)+\psi(i,j+3)] \quad (3.44)$$

Where, $s3=\frac{\mu}{2k^3}$; $zk9=\frac{r^2}{\mu}$

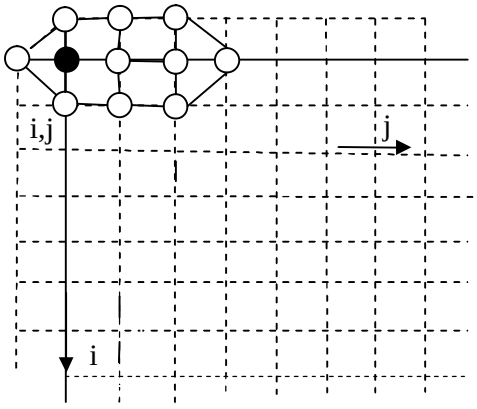

Figure 3.19: Stencil of stress component, σ_x

B.C.-4: Stress component in y-direction, σ_y

Starting from the equation of stress component, σ_y in terms of ψ eq.2.26

$$\sigma_y=-\frac{E}{(1+\mu)^2}\left[\frac{\partial^3\psi}{\partial y^3}+(2+\mu)\frac{\partial^3\psi}{\partial x^2\,\partial y}\right]$$

or, $$-(1+\mu)^2\frac{\sigma_y}{E}=\left[\frac{\partial^3\psi}{\partial y^3}+(2+\mu)\frac{\partial^3\psi}{\partial x^2\,\partial y}\right]$$

Now using the eq.3.18 and 3.19, the above equation reduces to

$$-(1+\mu)^2\frac{\sigma_y}{E}=\frac{1}{2k^3}\left[\frac{\partial\psi}{\partial y}_{i,j-1}-2\frac{\partial\psi}{\partial y}_{i,j}+\frac{\partial\psi}{\partial y}_{i,j+1}\right]+\frac{2+\mu}{h^2}\left[\frac{\partial\psi}{\partial y}_{i+1,j}-2\frac{\partial\psi}{\partial y}_{i,j}+\frac{\partial\psi}{\partial y}_{i-1,j}\right]$$

Now using the eq. 3.10 gives

$$-(1+\mu)^2\frac{\sigma_y}{E} = \frac{1}{2k^3}[-3\psi(i,j-1) - 4\psi(i,j) + 2\psi(i,j+1) + 6\psi(i,j) - 8\psi(i,j+1) + 2\psi(i,j+2) - 3\psi(i,j+1) + 4\psi(i,j+2) - \psi(i,j+3)] + \frac{2+\mu}{2h^2k}[-\psi(i+1,j+2) + 4\psi(i+1,j+1) - 3\psi(i+1,j) + 2\psi(i,j+2) - 8\psi(i,j+1) + 6\psi(i,j) - \psi(i-1,j+2) + 4\psi(i-1,j+1) - 3\psi(i-1,j)]$$

$$\text{or, } -(1+\mu)^2\frac{\sigma_y}{E} = s4\{[-3\psi(i,j-1) + 10\psi(i,j) - 12\psi(i,j+1) + 6\psi(i,j+2) - \psi(i,j+3)] + zk6[-\psi(i+1,j+2) + 4\psi(i+1,j+1) - 3\psi(i+1,j) + 2\psi(i,j+2) - 8\psi(i,j+1) + 6\psi(i,j) - \psi(i-1,j+2) + 4\psi(i-1,j+1) - 3\psi(i-1,j)]\} \quad (3.45)$$

Where, $s4 = \frac{1}{2k^3}$; $zk6 = r^2(2+\mu)$

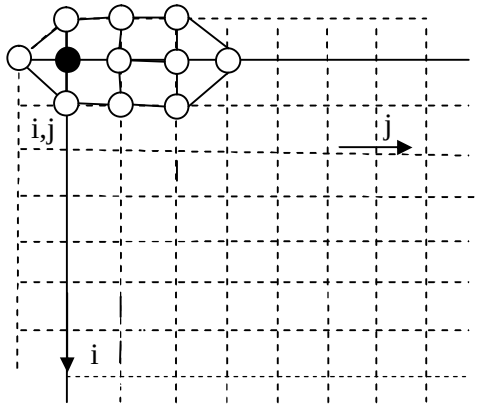

Figure 3.20: Stencil of stress component, σ_y

B.C.-5: Stress component in y-direction, σ_{xy}

Starting from the equation of stress component, σ_{xy} in terms of ψ eq.2.26

$$\sigma_{xy} = \frac{E}{(1+\mu)^2}\left[\mu\frac{\partial^3\psi}{\partial y^2\,\partial x} - \frac{\partial^3\psi}{\partial x^3}\right]$$

$$\text{or, } \quad (1+\mu)^2\frac{\sigma_{xy}}{E} = \left[\mu\frac{\partial^3\psi}{\partial y^2\,\partial x} - \frac{\partial^3\psi}{\partial x^3}\right]$$

Now using eq. 3.18 and 3.19 the above equation reduces to

$$\text{or, } (1+\mu)^2\frac{\sigma_{xy}}{E} = \frac{\mu}{k^2}\left[\frac{\partial\psi}{\partial x_{i,j-1}} - 2\frac{\partial\psi}{\partial x_{i,j}} + \frac{\partial\psi}{\partial x_{i,j+1}}\right] - \frac{1}{h^2}\left[\frac{\partial\psi}{\partial x_{i-1,j}} - 2\frac{\partial\psi}{\partial x_{i,j}} + \frac{\partial\psi}{\partial x_{i+1,j}}\right]$$

Now using eq. 3.8 the above equation reduces to

$$(1+\mu)^2\frac{\sigma_{xy}}{E} = \frac{\mu}{2hk^2}[-3\psi(i,j-1) + 4\psi(i+1,j-1) - \psi(i+2,j-1) + 6\psi(i,j) - 8\psi(i+1,j) + 2\psi(i+2,j) - 3\psi(i,j+1) + 4\psi(i+1,j+1) - \psi(i+2,j+1)] - \frac{1}{2h^3}[-3\psi(i-1,j) + 4\psi(i,j) - \psi(i+1,j) + 6\psi(i,j) - 8\psi(i+1,j) + 2\psi(i+2,j) - 3\psi(i+1,j) + 4\psi(i+2,j) - \psi(i+3,j)]$$

$$\text{or, } (1+\mu)^2\frac{\sigma_{xy}}{E} = s5[-3\psi(i,j-1) + 4\psi(i+1,j-1) - \psi(i+2,j-1) + 6\psi(i,j) - 8\psi(i+1,j) + 2\psi(i+2,j) - 3\psi(i,j+1) + 4\psi(i+1,j+1) - \psi(i+2,j+1) + zk7\{-3\psi(i-1,j) + 10\psi(i,j) - 12\psi(i+1,j) + 6\psi(i+2,j) - \psi(i+3,j)\}] \quad (3.46)$$

Where, $s5 = \frac{\mu}{2hk^2}$; $zk7 = \frac{r^2}{\mu}$

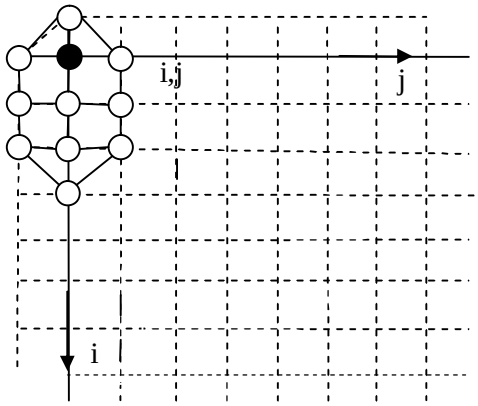

Figure 3.21: Stencil of stress component, σ_{xy}

3.3.1.4 Application Technique of Finite Difference Formulae of Boundary conditions

Recall the figure 3.7 with physical boundary and imaginary boundary lines as shown in figure 3.22. To apply the boundary conditions over the physical boundary, the whole field is divided into four sectors, which are i) top-left, ii) bottom-left, iii) bottom-right, and iv) top-right and shown in figure 3.22. The stencils of figure from 3.17 to 3.21 are formulated for top-left region of boundary. For other region, the stencils can be easily obtained by replacing some parameters. The conversion procedure from one region to

another region is given in table 3.2 and the corresponding stencils are shown in figure 3.23. The applicability of these boundary conditions over the whole boundary is shown in figure 3.24. The pivot point of stencils, applied in a particular region, are filled with single color and also the boundary nodal points of this particular region are filled with same color of pivot points as shown in figure 3.23 and 3.24. The same color of a stencil pivot point and nodal points indicates that this stencil has applicability only on these nodal points. Thus any combination of these boundary conditions can be satisfied all over the physical boundary nodal points.

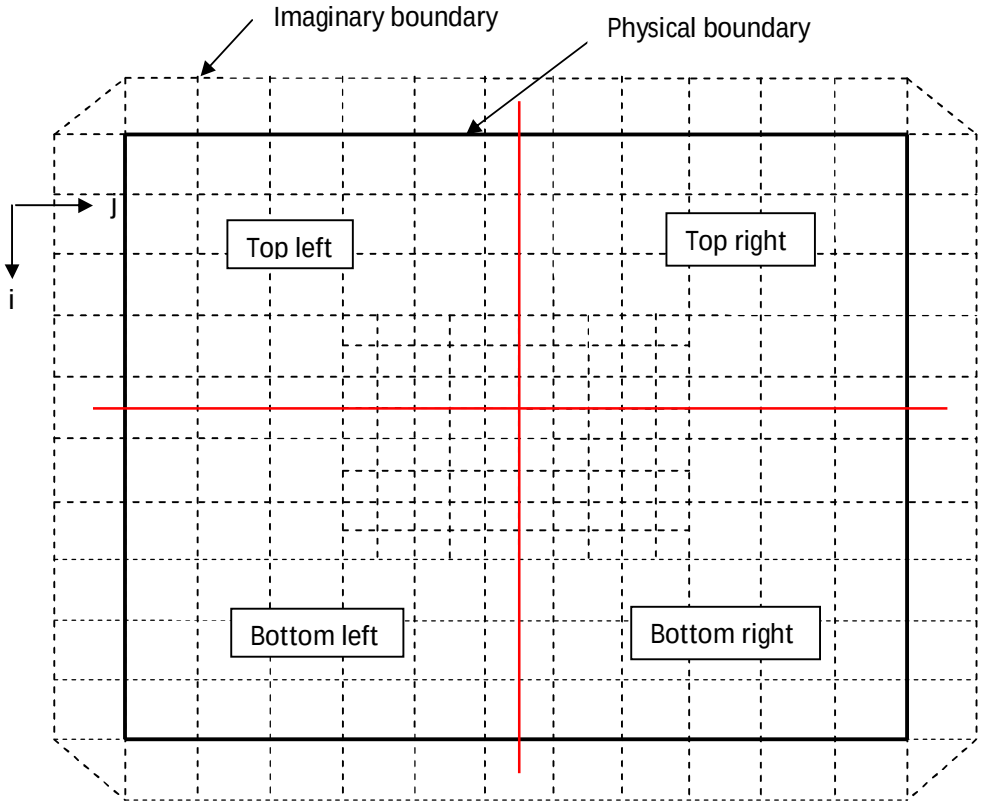

Figure 3.22: Mesh refinement of domain only.

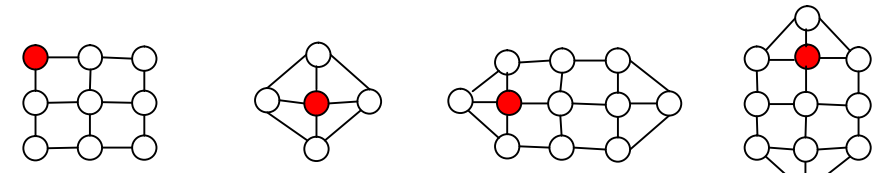

B.C.-1: u B.C.-2: v B.C.-3 or 4: σ_x or σ_y B.C.-5: σ_{xy}

a) Stencil of boundary conditions for top-left region.

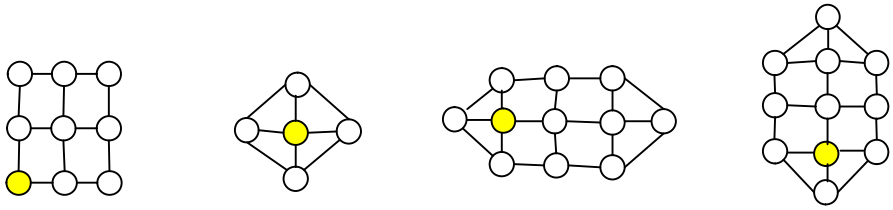

B.C.-1: u B.C.-2: v B.C.-3 or 4: σ_x or σ_y B.C.-5: σ_{xy}

b) Stencils of boundary conditions for bottom-left region.

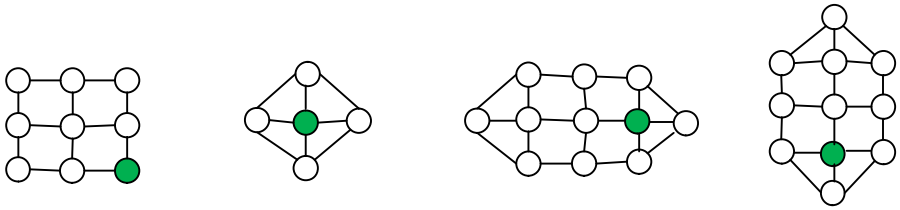

B.C.-1: u B.C.-2: v B.C.-3 or 4: σ_x or σ_y B.C.-5: σ_{xy}

c) Stencils of boundary conditions for bottom-right region.

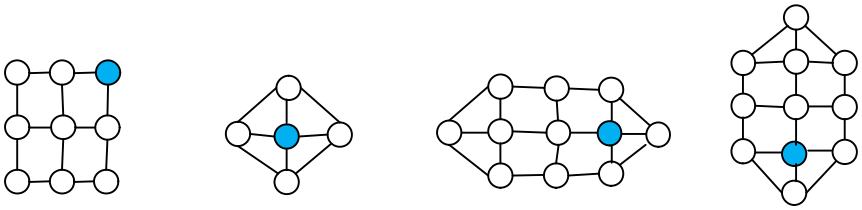

B.C.-1: u B.C.-2: v B.C.-3 or 4: σ_x or σ_y B.C.-5: σ_{xy}

d) Stencils of boundary conditions for top-right region.

Figure 3.23: Stencils of boundary conditions for different boundary regions.

Table 3.2: Conversion charts of finite difference formulas of boundary conditions for different region of the boundary.

Boundary region	Type of difference formula required	Replacement required
Top-left	i-forward j-forward	No change required
Bottom-left	i-backward j-forward	s1 by –s1, s5 by –s5, i-* by i+* and i+* by i-*

Bottom-right	i-backward j- backward	s3 by –s3, s4 by –s4, s5 by –s5, i-* by i+*, i+* by i-*, j-* by j+*, and j+* by j-*
Top-right	i- forward, j- backward	s1 by –s1, s3 by –s3, s4 by –s4, j-* by j+*, and j+* by j-*

Where, * stands for digits 1 or 2 or 3 etc.

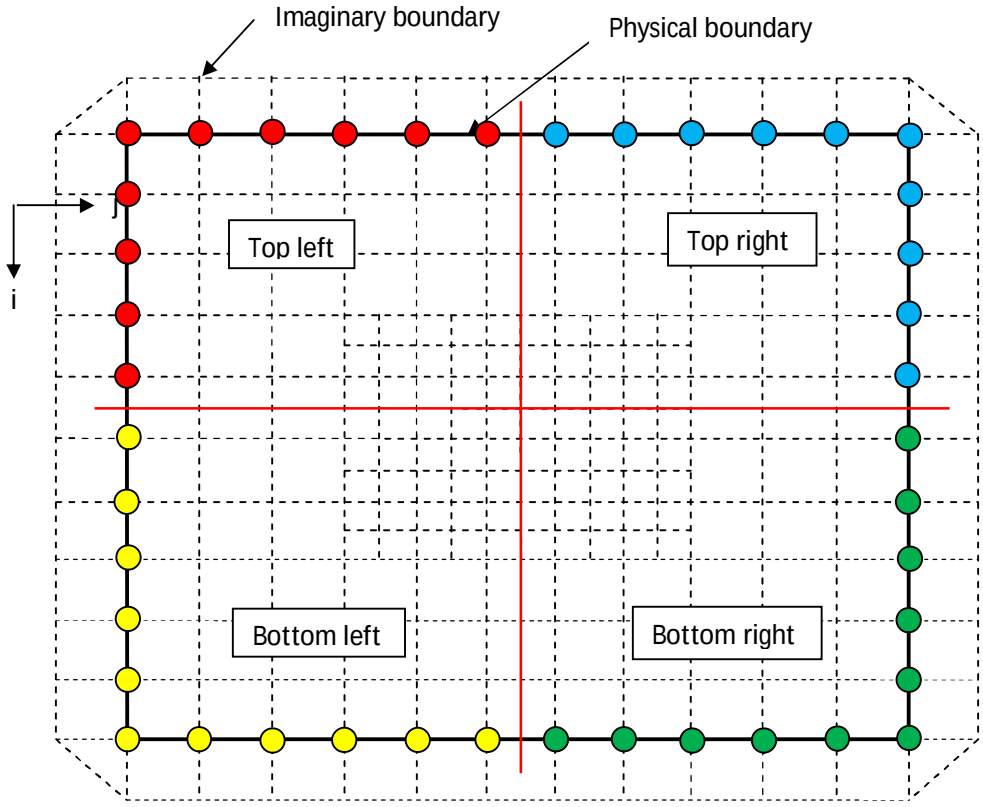

Figure 3.24: Applicability of different stencils of boundary conditions over the whole boundary.

3.3.2 Case-II: Mesh Refinement Includes Domain as well as Boundary

A discretization of physical model under mesh refinement technique in which the finer mesh region includes domain as well as boundary shown in figure 3.25.

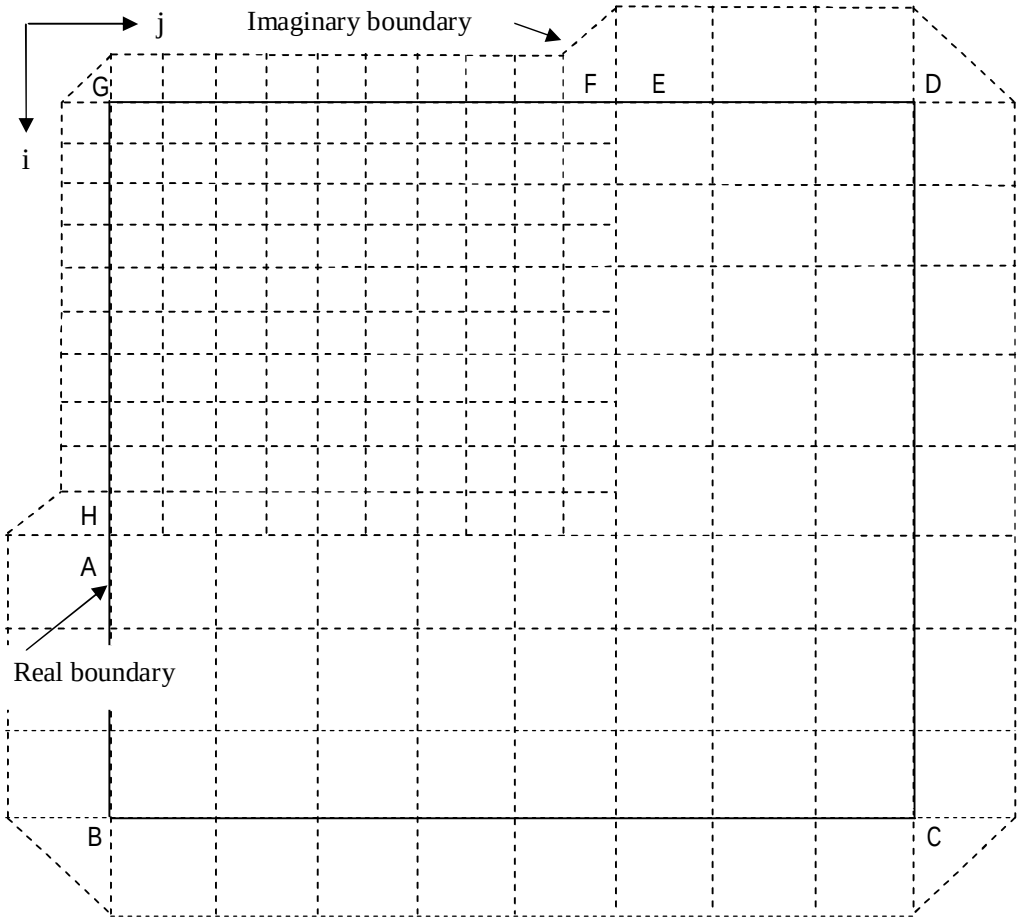

Figure 3.25: Discretization under mesh refinement which includes domain as well as boundary.

In this section, mesh refinement procedure for above type of discretization (figure 3.25) will be discussed. To satisfy GE over the whole domain, no extra stencils have to be developed because stencils that have been formulated in previous sections are sufficient for any type of discretization of the domain. But, for this type of discretization, some stencils of boundary conditions should have been formulated to satisfy the boundary conditions over the whole physical boundary. The following two sections will show the application procedure of GE and boundary equations over the whole field.

3.3.2.1 Application Technique of Finite Difference Formulae of GE

Recalling the figure 3.14 i.e. the different type of stencils of GE, in this section the applicability of these stencils over the whole domain will be discussed. Similar to the previous sections (Sec. 3.3.1.2), same color of a stencil pivot point and domain points indicates that this particular stencil will be applied in these domain points. The detail of this applicability of stencils of GE over the domain is shown in figure 3.26.

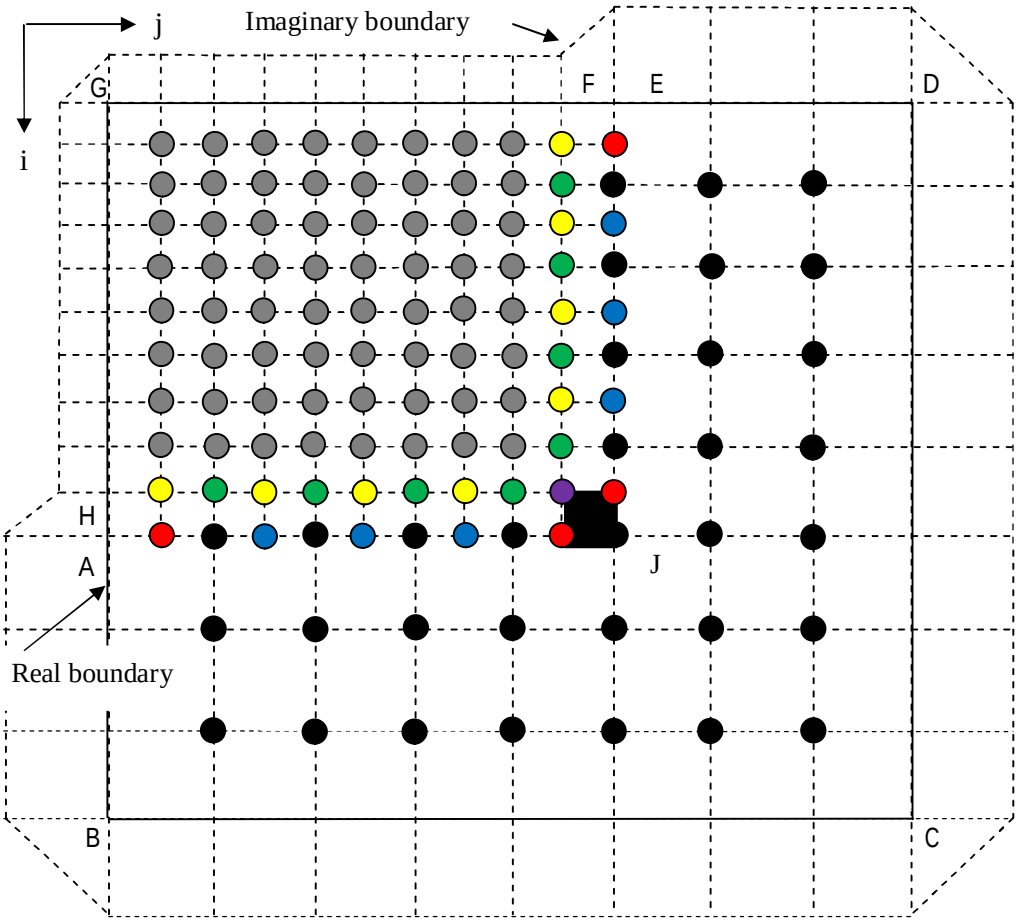

FGHI-Fine uniform mesh region; **ABCDEJA**-Coarse uniform mesh region**; AJEFIH**-Transition non-uniform mesh region

Figure 3.26: Application of finite difference formula of GE over whole domain.

3.3.2.2 Finite Difference Form of the Boundary Conditions and Application Technique

In previous sections (sec. 3.3.1.3), some finite difference formulae of boundary conditions have been formulated and corresponding stencils have been shown in figure from eq. 3.17 to 3.21. But, these stencils have applicability only over the uniform mesh (fine or coarse). Since in this time mesh refinement includes domain as well as boundary (figure 3.25), so the previously formulated finite difference formulae cannot be applied over the whole real boundary because of their limited applicability only over uniform mesh. The application technique of eq. 3.17 to 3.21 is shown in figure 3.27. Refer to the figure 3.23, same color of stencil pivot point and real boundary point indicates that corresponding stencil/stencils is/are applied on these points. In figure 3.27, it is seen that two points of mesh changing regions are identified by cross (X) marks. This cross mark indicates that the stencils of figure 3.23 or eq. 3.17 to 3.21 will not valid in these points. Sometimes, from mathematical view point, there is no problem to apply some stencils of boundary conditions, those were shown in figure 3.23, over the transition region but that do not provide better solution of the problem. As an example, consider the upper mesh changing region is subjected by boundary conditions $\sigma_x=0$ and $\sigma_{xy}=0$. Then eq. 3.19 and 3.21 i.e. stencil-3 and stencil-5 of figure 3.23a can be applied easily and mathematically there is no problem to apply these stencils or equation in this mesh changing region. But, author of this thesis examined that it did not provide satisfactory solution. So, in this section, some other formulae will be developed to apply the boundary conditions over the transition region. For displacement component u or v, no other form of finite difference formulae do not require because those stencils, formulated in previous section (sc. 3.3.1.3), are sufficient to apply boundary conditions in term of u or v in transition region and provide satisfactory results. For stress component, σ_x, σ_y and σ_{xy}, new stencils will formulate in the following paragraph of this section. The formulation finite difference formulae of boundary conditions for transition region require more inclusion of both coarse and fine meshes i.e. central difference formula of derivatives should get preference over backward or forward finite difference formula of same order of accuracy. Thus, the aligned numerical formulations that is combination of more forward and backward finite difference formulae at mesh size transition region could

not provide better solution rather the balanced numerical formulations that is combination of more central difference at mesh size transition region provide better solution. Sometimes, it may also necessary to apply treatment of stencils of boundary conditions for the adjacent point of mesh size transition region.

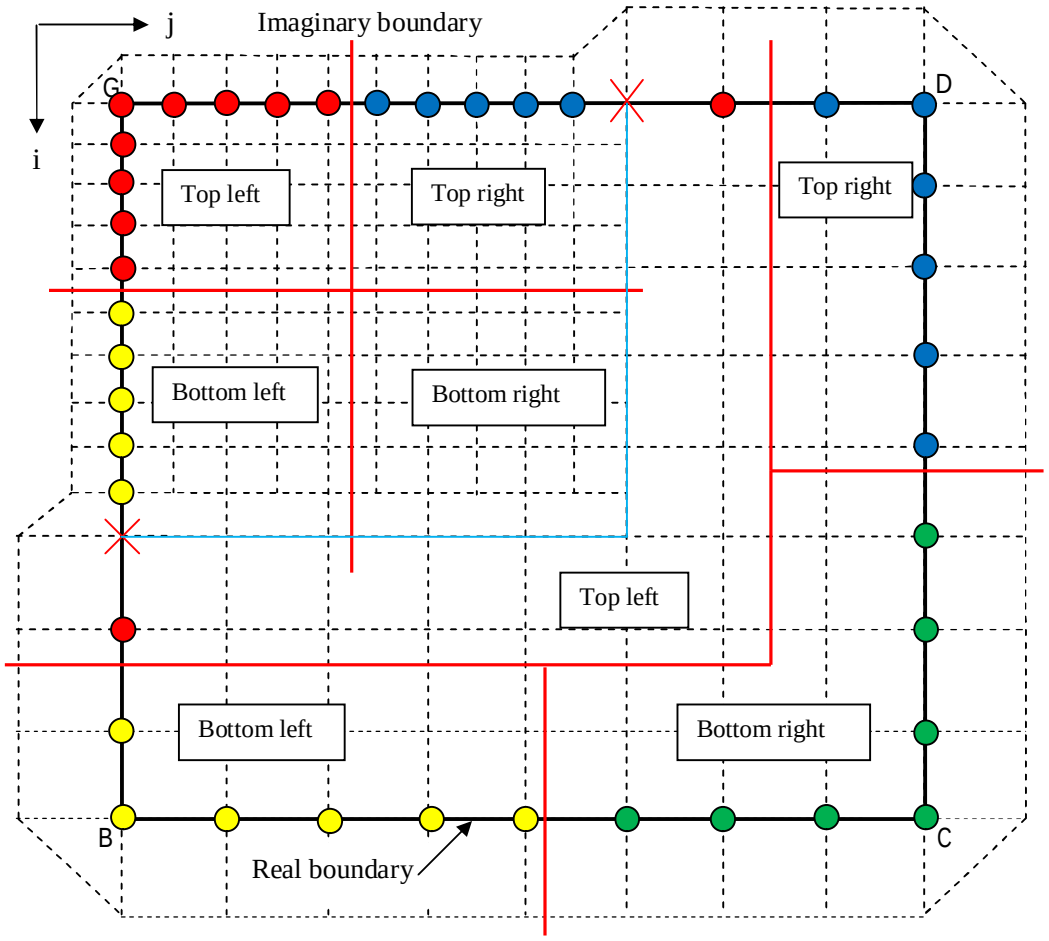

Figure 3.27: Application technique of different stencils of boundary conditions over the uniform mesh boundary region both fine and coarse.

Formulae of new stencils of stress components for the mesh size transition regions-

B.C.-3: Stress component in x-direction, σ_x

Starting from the equation of stress component, σ_x in terms of ψ eq.2.26

$$\sigma_x = \frac{E}{(1+\mu)^2}\left[\frac{\partial^3\psi}{\partial x^2\,\partial y} - \mu\frac{\partial^3\psi}{\partial y^3}\right]$$

$$\text{or,} \qquad (1+\mu)^2\frac{\sigma_x}{E} = \left[\frac{\partial^3\psi}{\partial x^2\,\partial y} - \mu\frac{\partial^3\psi}{\partial y^3}\right]$$

Now using eq. 3.9 and 3.21, the above equation reduces to

$$\text{or,}\ (1+\mu)^2\frac{\sigma_x}{E} = \frac{1}{2k1}\left[3\frac{\partial\psi}{\partial x^2}_{i,j} - 4\frac{\partial\psi}{\partial x^2}_{i,j-1} + \frac{\partial\psi}{\partial x^2}_{i,j-2}\right] - \frac{\mu}{2k2^3}[-\psi(i,j-4) + 2\psi(i,j-2) - 2\psi(i,j+2) + \psi(i,j+4)]$$

Now using eq.3.18, the above equation reduces to

$$(1+\mu)^2\frac{\sigma_x}{E} = \frac{3}{2k1h2^2}[\psi(i-2,j) - 2\psi(i,j) + \psi(i+2,j)] - \frac{2}{k1h1^2}[\psi(i-1,j-1) - 2\psi(i,j-1) + \psi(i+1,j-1)] + \frac{1}{2k1h1^2}[\psi(i-1,j-2) - 2\psi(i,j-2) + \psi(i+1,j-2)] - \frac{\mu}{2k2^3}[-\psi(i,j-4) + 2\psi(i,j-2) - 2\psi(i,j+2) + \psi(i,j+4)]$$

$$\text{or,}\quad (1+\mu)^2\frac{\sigma_x}{E} = \frac{3}{2}m7\{\psi(i-2,j) + (i+2,j)\} - 3m7\psi(i,j) - 2m8\{\psi(i-1,j-1) + \psi(i+1,j-1)\} + 4m8\psi(i,j-1) + \frac{1}{2}m8\{\psi(i-1,j-2) + \psi(i+1,j-2)\} - (m8+2m9)\psi(i,j-2) + 2m9\psi(i,j+2) - m9\psi(i,j+4) + m9\psi(i,j-4) \qquad (3.47)$$

Where, $m7 = \frac{1}{k1h2^2}$; $m8 = \frac{1}{k1h1^2}$; and $m9 = \frac{\mu}{2k2^3}$

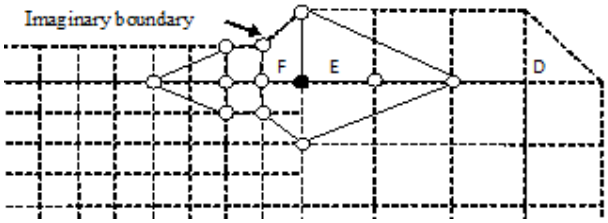

Figure 3.28: Stencil of stress component, σ_x for transition region.

B.C.-4: Stress component in y-direction, σ_y

Starting from the equation of stress component, σ_y in terms of ψ eq.2.26

$$\sigma_y = -\frac{E}{(1+\mu)^2}\left[\frac{\partial^3\psi}{\partial y^3} + (2+\mu)\frac{\partial^3\psi}{\partial x^2\,\partial y}\right]$$

$$\text{or,} \quad -(1+\mu)^2\frac{\sigma_y}{E} = \left[\frac{\partial^3\psi}{\partial y^3} + (2+\mu)\frac{\partial^3\psi}{\partial x^2\,\partial y}\right]$$

$$\text{or,} \quad -(1+\mu)^2\frac{\sigma_y}{E} = \frac{1}{2k2^3}[-\psi(i,j-4) + 2\psi(i,j-2) - 2\psi(i,j+2) + \psi(i,j+4)] + \frac{2+\mu}{2k1}\left[3\frac{\partial^2\psi}{\partial x^2}_{i,j} - 4\frac{\partial^2\psi}{\partial x^2}_{i,j-1} + \frac{\partial^2\psi}{\partial x^2}_{i,j-2}\right]$$

Now using eq.3.18, the above equation reduces to

$$-(1+\mu)^2\frac{\sigma_y}{E} = \frac{1}{2k2^3}[-\psi(i,j-4) + 2\psi(i,j-2) - 2\psi(i,j+2) + \psi(i,j+4)] + \frac{3(2+\mu)}{2k1h2^2}[\psi(i-2,j) - 2\psi(i,j) + \psi(i+2,j)] - \frac{2(2+\mu)}{k1h1^2}[\psi(i-1,j-1) - 2\psi(i,j-1) + \psi(i+1,j-1)] + \frac{(2+\mu)}{2k1h1^2}[\psi(i-1,j-2) - 2\psi(i,j-2) + \psi(i+1,j-2)]$$

$$\text{or,} \quad -(1+\mu)^2\frac{\sigma_y}{E} = \frac{3}{2}m10\{\psi(i-2,j) + (i+2,j)\} - 3m10\psi(i,j) - 2m11\{\psi(i-1,j-1) + \psi(i+1,j-1)\} + 4m11\psi(i,j-1) + \frac{1}{2}m11\{\psi(i-1,j-2) + \psi(i+1,j-2) - (m11-2m12)\psi(i,j-2) - 2m12\psi(i,j+2) + m12\psi(i,j+4) - m12\psi(i,j-4) \quad (3.48)$$

Where, $m10 = \frac{m7}{2+\mu}$; $m11 = \frac{m8}{2+\mu}$; $m12 = \frac{m9}{\mu}$

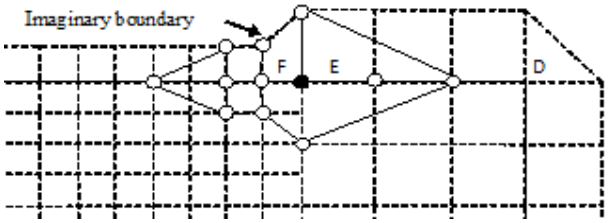

Figure 3.29: Stencil of stress component, σ_y for transition region.

B.C.-5: Stress component in y-direction, σ_{xy}

Starting from the equation of stress component, σ_{xy} in terms of ψ eq.2.26

$$\sigma_{xy} = \frac{E}{(1+\mu)^2}\left[\mu\frac{\partial^3\psi}{\partial y^2\,\partial x} - \frac{\partial^3\psi}{\partial x^3}\right]$$

$$\text{or,} \qquad (1+\mu)^2\frac{\sigma_{xy}}{E} = \left[\mu\frac{\partial^3\psi}{\partial y^2\,\partial x} - \frac{\partial^3\psi}{\partial x^3}\right]$$

Now using eq. 3.9 and 3.20, the above equation reduces to

$$(1+\mu)^2\frac{\sigma_{xy}}{E} = \frac{\mu}{2h1}\left[3\frac{\partial^2\psi}{\partial y^2}_{i,j} - \frac{\partial^2\psi}{\partial y^2}_{i-1,j} + \frac{\partial^2\psi}{\partial y^2}_{i-2,j}\right] - \frac{2}{2h2^3}[\psi(i+4,j) - 2\psi(i+2,j) + \psi(i-2,j) - \psi(i-4,j)]$$

$$\text{or,}\ (1+\mu)^2\frac{\sigma_{xy}}{E} = \frac{3\mu}{2h1k2^2}[\psi(i,j-2) - 2\psi(i,j) + \psi(i,j+2)] - \frac{2\mu}{h1k1^2}[\psi(i-1,j-1) - 2\psi(i-1,j) + \psi(i-2,j+1)] + \frac{\mu}{2h1k1^2}[\psi(i-2,j-1) - 2\psi(i-2,j) + \psi(i-2,j+1)] - \frac{2}{2h2^3}[\psi(i+4,j) - 2\psi(i+2,j) + \psi(i-2,j) - \psi(i-4,j)]$$

$$\text{or,}\quad (1+\mu)^2\tau_{xy}/E = \frac{3}{2}m13\{\psi(i,j+2) + (i,j-2)\} - 3m13\psi(i,j) - 2m14\{\psi(i-1,j-1) + \psi(i+1,j-1)\} + 4m14\psi(i-1,j) + \frac{1}{2}m14\{\psi(i-2,j+1) + \psi(i-2,j-1) - (m14+2m15)\psi(i,j-2) + 2m15\psi(i+2,j) - m15\psi(i+4,j) + m15\psi(i-4,j) \qquad (3.49)$$

Where, $m13 = \frac{\mu}{h1k2^2}$; $m14 = \frac{\mu}{h1k1^2}$; $m15 = \frac{1}{2h2^3}$

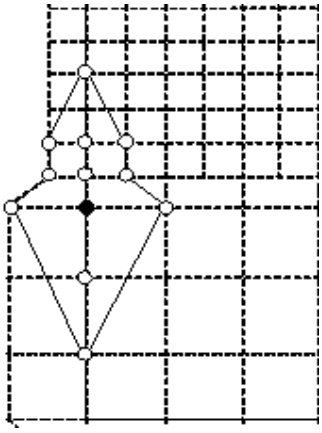

Figure 3.30: Stencil of stress component, σ_{xy} for transition region.

The application technique of these new stencils of stress components is shown in figure 3.31. At upper transition region, only treatment of stress components σ_x and σ_y is necessary because existing stencils (figure 3.23a) of other boundary conditions (u, v and σ_{xy}) provide satisfactory results when these are applied over coarse uniform mesh. One should apply these stencils over coarse mesh because that would results more inclusion of meshes of both fine and coarse mesh. Similarly, for left mesh transition region only treatment of stress components σ_{xy} is necessary because existing stencils (figure 3.23a) of other boundary conditions (u, v, σ_x and σ_y) provide satisfactory results when these are applied over coarse uniform mesh.

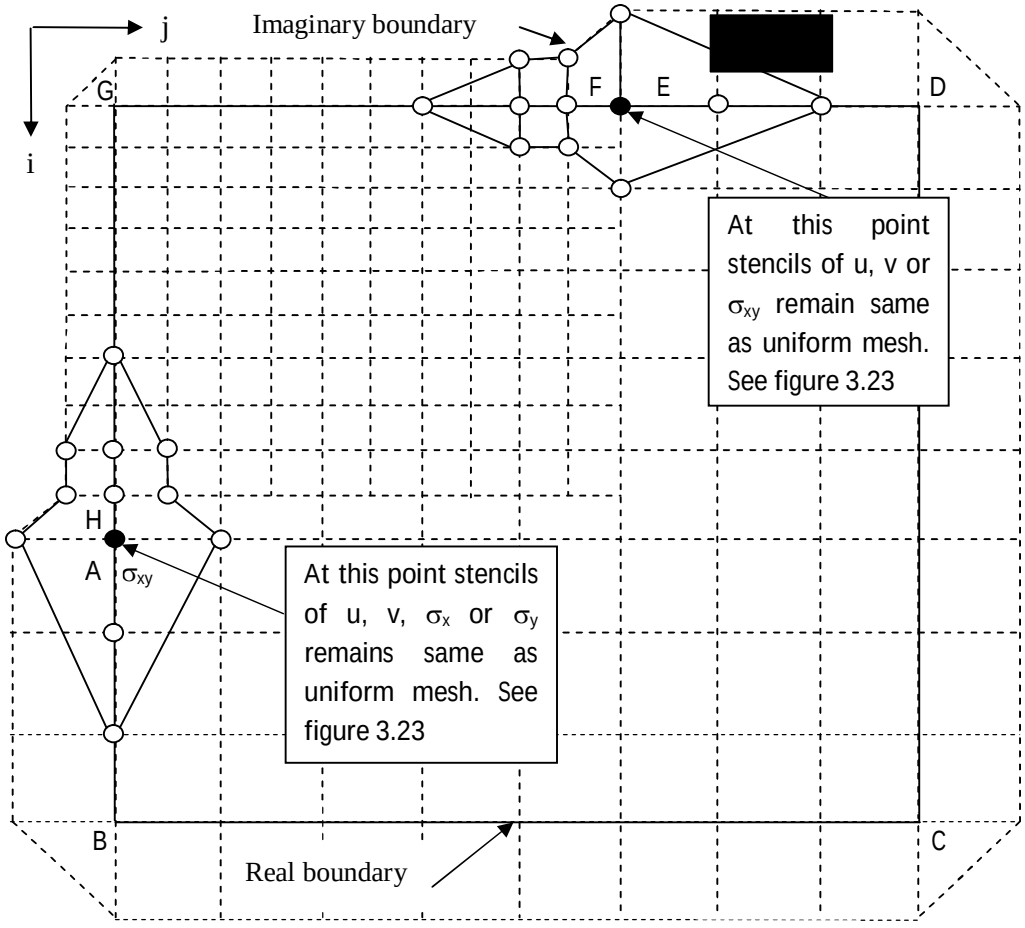

Figure 3.31: Application technique of boundary conditions stencils at transition region from fine to coarse mesh.

3.4 Solution of a Set of Algebraic Equations (Evaluation of ψ)

If the whole region is placed in a rectangular grid then the region gives a finite number of node points which include reference boundary points, imaginary boundary points and inner body points (node points other than the reference and imaginary boundary points). Finite difference expressions of the boundary conditions should be applied in all reference boundary and imaginary boundary node points. And Finite difference expressions of the governing equation should be applied in all inner body points. So every point gives rise to a linear algebraic equation and the whole region gives a set of linear algebraic equations equal to the number of total node points in the region. The set of linear equations can be shown as,

$$\begin{bmatrix} a_{11} & a_{12} & a_{13} & . & . & . & a_{1n} \\ a_{21} & a_{22} & a_{23} & . & . & . & a_{2n} \\ a_{31} & a_{32} & a_{33} & . & . & . & a_{3n} \\ . & . & . & . & . & . & . \\ . & . & . & . & . & . & . \\ a_{n1} & a_{n2} & a_{n3} & . & . & . & a_{nn} \end{bmatrix} \begin{Bmatrix} \psi_1 \\ \psi_2 \\ \psi_3 \\ . \\ . \\ \psi_n \end{Bmatrix} = \begin{Bmatrix} c_1 \\ c_2 \\ c_3 \\ . \\ . \\ c_n \end{Bmatrix} \tag{3.50}$$

or

$$[A]\{\psi\} = \{C\}$$

Where, a_{11}, a_{12} ……a_{nn} are coefficients, n is the number of total node points, [A] is called coefficient matrix and [C] is constant matrix.

In this equation only unknowns are the ψ's. Many numerical techniques are available to solve this type of equation such as L-U decomposition, Cholesky composition, gauss-Siedel method, matrix portioning, matrix inversion, relaxation method etc. Here L-U decomposition method is used and hence value of ψ at each node point will be found.

3.5 Determination of Stress and Displacement Component at Each Grid Point

Once value of ψ at every node points are evaluated the stress and displacement components at each point can be found from the equations (Eq. 2.25and 2.26) stated in the earlier chapter which are motioned here for convenience.

$$u = \frac{\partial^2 \psi}{\partial x . \partial y}$$

$$v = -\left[\left(\frac{1-\mu}{1+\mu}\right)\frac{\partial^2 \psi}{\partial y^2} + \left(\frac{2}{1+\mu}\right)\frac{\partial^2 \psi}{\partial x^2}\right]$$

$$\sigma_x = \frac{E}{(1+\mu)^2}\left[\frac{\partial^3 \psi}{\partial x^2\, \partial y} - \mu\frac{\partial^3 \psi}{\partial y^3}\right]$$

$$\sigma_y = -\frac{E}{(1+\mu)^2}\left[\frac{\partial^3 \psi}{\partial y^3} + (2+\mu)\frac{\partial^3 \psi}{\partial x^2\, \partial y}\right]$$

$$\sigma_{xy} = \frac{E}{(1+\mu)^2}\left[\mu\frac{\partial^3 \psi}{\partial x^2\, \partial y} - \frac{\partial^3 \psi}{\partial x^3}\right]$$

In order to calculate stress and displacement the finite difference expressions of these equations are required and as before the expressions depend on the section of the region where these should be applied. For top-right section (figure 3.27) the finite difference equations (eq. 3.42 to eq. 3.46) are given below:

$$u_x(i,j) = \left(\frac{\partial^2 \psi}{\partial x . \partial y}\right)_{i,j}$$

$$= s1.[9\psi(i,j) - 12\{\psi(i,j+1) + \psi(i+1,j)\} + 16\psi(i+1,j+1) + \psi(i+2,j+2) + 3\{\psi(i,j+2) + \psi(i+2,j)\} - 4\{\psi(i+1,j+2) + \psi(i+2,j+1)\}]$$

$$u_y = -\left[\left(\frac{1-\mu}{1+\mu}\right)\frac{\partial^2 \psi}{\partial y^2} + \left(\frac{2}{1+\mu}\right)\frac{\partial^2 \psi}{\partial x^2}\right]$$

$$= s2[c1\{\psi(i,j+1) + \psi(i,j-1)\} - (2c1 + 2zk5)\psi(i,j) + zk5\{\psi(i+1,j) + \psi(i-1,j)\}]$$

$$\frac{\sigma_x}{E} = \frac{1}{(1+\mu)^2}\left[\frac{\partial^3 \psi}{\partial x^2\, \partial y} - \mu\frac{\partial^3 \psi}{\partial y^3}\right]$$

$$\text{or, } (1+\mu)^2\frac{\sigma_x}{E} = s3[zk9\{-3\psi(i-1,j)+4\psi(i-1,j+1)-\psi(i-1,j+2)-3\psi(i+1,j)+4\psi(i+1,j+1)-\psi(i+1),j+2\}+3\psi(i,j-1)-(6zk9-10)\psi(i,j)+(12-8zk9)\psi(i,j+1)+(2zk9-6)\psi(i,j+2)+\psi(i,j+3)]$$

$$\frac{\sigma_y}{E} = -\frac{1}{(1+\mu)^2}\left[\frac{\partial^3\psi}{\partial y^3}+(2+\mu)\frac{\partial^3\psi}{\partial x^2\,\partial y}\right]$$

$$\text{or, } -(1+\mu)^2\frac{\sigma_y}{E} = s4\{[-3\psi(i,j-1)+10\psi(i,j)-12\psi(i,j+1)+6\psi(i,j+2)-\psi(i,j+3)]+zk6[-\psi(i+1,j+2)+4\psi(i+1,j+1)-3\psi(i+1,j)+2\psi(i,j+2)-8\psi(i,j+1)+6\psi(i,j)-\psi(i-1,j+2)+4\psi(i-1,j+1)-3\psi(i-1,j)]\}$$

$$\frac{\sigma_{xy}}{E} = \frac{1}{(1+\mu)^2}\left[\mu\frac{\partial^3\psi}{\partial x^2\,\partial y}-\frac{\partial^3\psi}{\partial x^3}\right]$$

$$\text{or, } (1+\mu)^2\frac{\sigma_{xy}}{E} = s5[-3\psi(i,j-1)+4\psi(i+1,j-1)-\psi(i+2,j-1)+6\psi(i,j)-8\psi(i+1,j)+2\psi(i+2,j)-3\psi(i,j+1)+4\psi(i+1,j+1)-\psi(i+2,j+1)+zk7\{-3\psi(i-1,j)+10\psi(i,j)-12\psi(i+1,j)+6\psi(i+2,j)-\psi(i+3,j)\}]$$

These equations can also be used for the other sections of the region by changing signs of the constants i, j, s1, s2, s3, and s4 as shown in table 3.2. The formula structures to calculate the stresses and displacements in the different sections of figure 3.22 and figure 3.25 of the member are shown in figure 3.32 and 3.34 respectively. Using the formula structures as shown in figure 3.33 one can calculate stresses and displacements over whole field except those nodal points which have ‘x’ mark. For those points new formula structures have been made in the next of this section and corresponding stencils are shown in figure 3.35. There are two shade of each color one each deep and other is light. In deep color stencils should be used over fine uniform mesh, on the other hand, in light color stencils should be used over uniform coarse mesh.

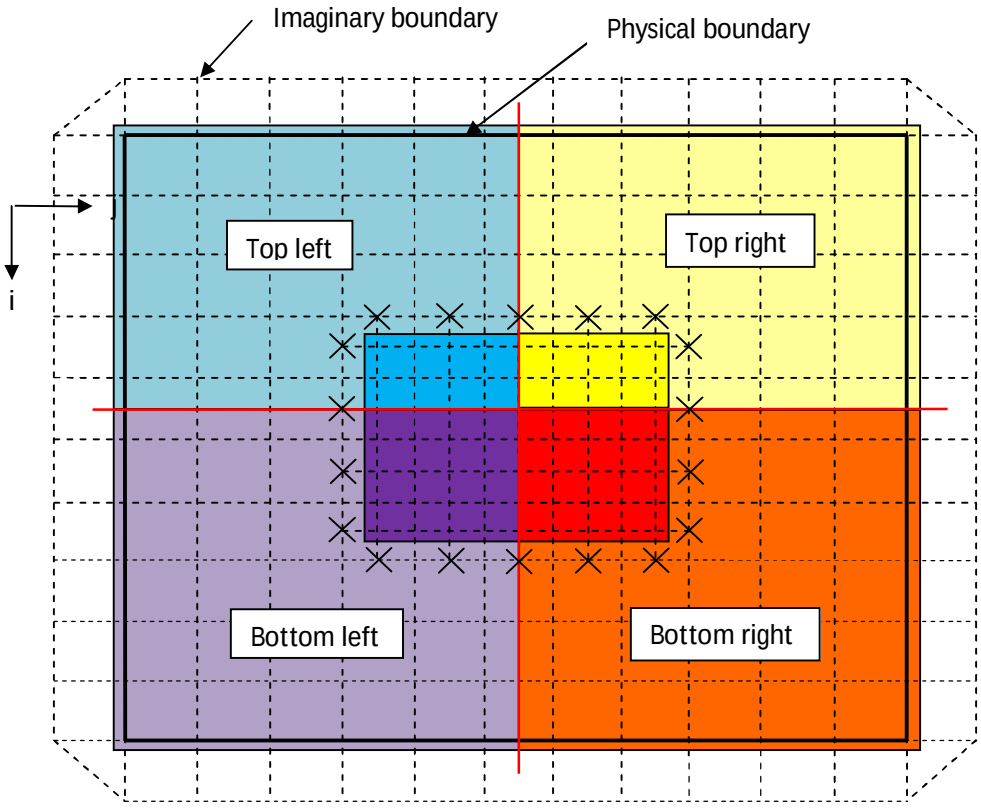

Figure 3.32: Different formula structures for stress and displacement calculation at different sections of the member for case-I.

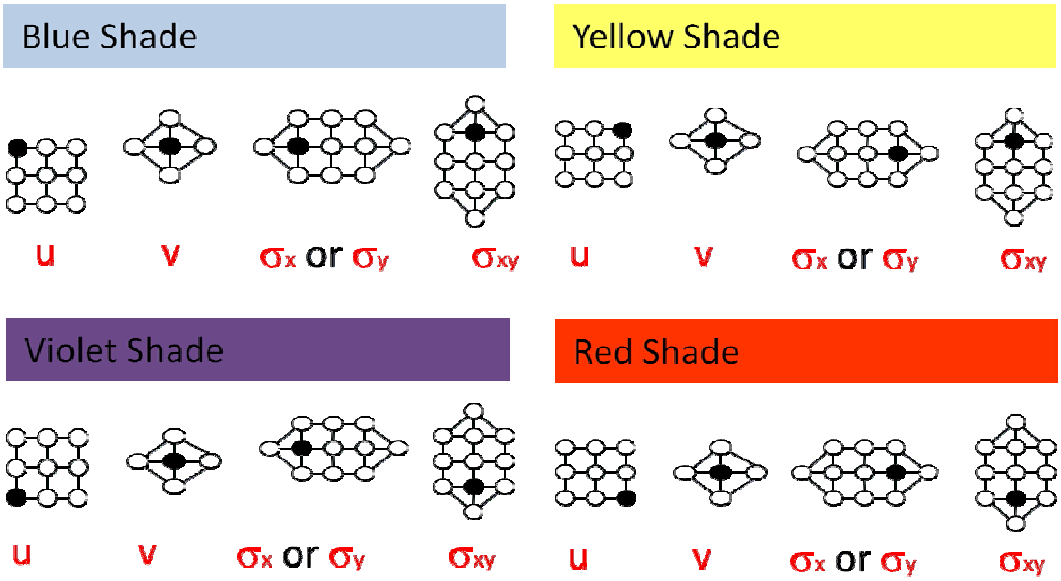

Figure 3.33: Stencils for calculation of displacement and stress at different regions of the member.

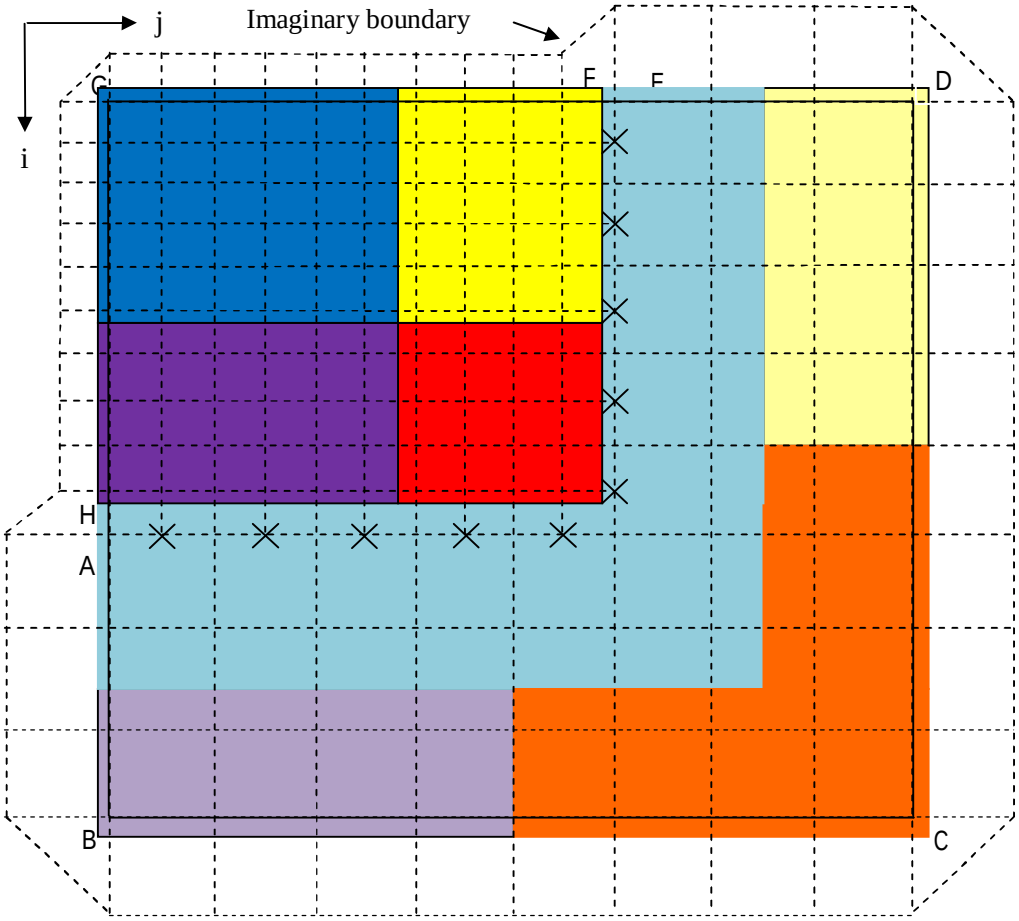

Figure 3.34: Different formula structures for stress and displacement calculation at different sections of the member for case-II.

Formulation of stencils for calculation stresses and displacements at cross marks (X):

There is no need to formulate stencil for displacement component, u because the existing stencils give better result for this reason eq. 3.42 is stated again.

$$u = \frac{\partial^2 \psi}{\partial x . \partial y}$$

$$= s1.\,[9\psi(i,j) - 12\{\psi(i,j+1) + \psi(i+1,j)\} + 16\psi(i+1,j+1) + \psi(i+2,j+2) + 3\{\psi(i,j+2) + \psi(i+2,j)\} - 4\{\psi(i+1,j+2) + \psi(i+2,j+1)\}]$$

$$u_y = -\left[\left(\frac{1-\mu}{1+\mu}\right)\frac{\partial^2 \psi}{\partial y^2} + \left(\frac{2}{1+\mu}\right)\frac{\partial^2 \psi}{\partial x^2}\right]$$

$$= (-3m16 + 2m17)\psi(i,j) + 5m16\psi(i,j-1) - 4m16\psi(i,j-2) + m16\psi(i,j-3) - m17\{\psi(i+1,j) + \psi(i-1,j) \quad (3.51)$$

Where, $m16 = \frac{1-\mu}{(1+\mu)k1^2}$; $m17 = \frac{2}{(1+\mu)h1^2}$

$$(1+\mu)^2 \frac{\sigma_x}{E} = \left[\frac{\partial^3\psi}{\partial x^2\,\partial y} - \mu\frac{\partial^3\psi}{\partial y^3}\right]$$

$$= \frac{1}{2}m18\{\psi(i+1,j+2) - \psi(i+1,j-2) + \psi(i-1,j+2) - \psi(i-1,j-2)\} - (3m19 + 5\mu * m20)\psi(i,j) + (4m19 + 18\mu * m20)\psi(i,j-1) - (m19 + \mu * m20)\psi(i,j-2) + 14\mu * m20\psi(i,j-3) - 3\mu * m20\psi(i,j-4) \quad (3.52)$$

Where, $m18 = \frac{1}{h1^2k2}$; $m19 = \frac{1}{h1^2k1}$; $m20 = \frac{1}{2k1^3}$

$$-(1+\mu)^2 \frac{\sigma_y}{E} = \left[\frac{\partial^3\psi}{\partial y^3} + (2+\mu)\frac{\partial^3\psi}{\partial x^2\,\partial y}\right]$$

$$= 5m20\psi(i,j) - 18m20\psi(i,j-1) + 24m20\psi(i,j-2) - 14m20\psi(i,j-3) + 3\psi(i,j-4) + \frac{2+\mu}{2}m18\{\psi(i-1,j+2) - \psi(i-1,j-2) + \psi(i+1,j+2) - \psi(i+1,j-2)\} - (2+\mu)\{3m19\psi(i,j) - 4m19\psi(i,j-1) + m19\psi(i,j-2)\} \quad (3.53)$$

$$(1+\mu)^2 \frac{\sigma_{xy}}{E} = \left[\mu\frac{\partial^3\psi}{\partial x^2\,\partial y} - \frac{\partial^3\psi}{\partial x^3}\right]$$

$$= \frac{1}{2}m18\{\psi(i+1,j+2) - \psi(i+1,j-2) + \psi(i-1,j+2) - \psi(i-1,j-2)\} - m19\{3\psi(i,j) - 4\psi(i,j-1) + \psi(i,j-2)\} - \mu m20\{5\psi(i,j) - 18\psi(i,j-1) + 24\psi(i,j-2) - 14\psi(i,j-3) + 3\psi(i,j-4)\} \quad (3.54)$$

These equations 3.42 and 3.51-3.54 are applied at cross marks of figure 3.32 and 3.34. Stencils of equations 3.42 and 3.51-3.54 for different region of the field are shown in figure 3.35. The application technique of these stencils for both case-I and case-II is shown in figure 3.36 and 3.37 with reference to the figure 3.35. Thus one can calculate stress and displacement at over the whole field by using the above procedure. In case-II, where the refine mesh includes both domain and boundary, may have four different scenarios. The refine mesh may locate either any corner of the field; in case-II refine

mesh locates at top-left corner of the field and the methodology is already discussed. For any other scenario i.e. for top-right, bottom-left and bottom-right, the methodology discussed above can be used with some intelligence. Detail procedure of mesh refinement methodology is shown in figure 3.37, which shows complete algorithm of mesh refinement methodology.

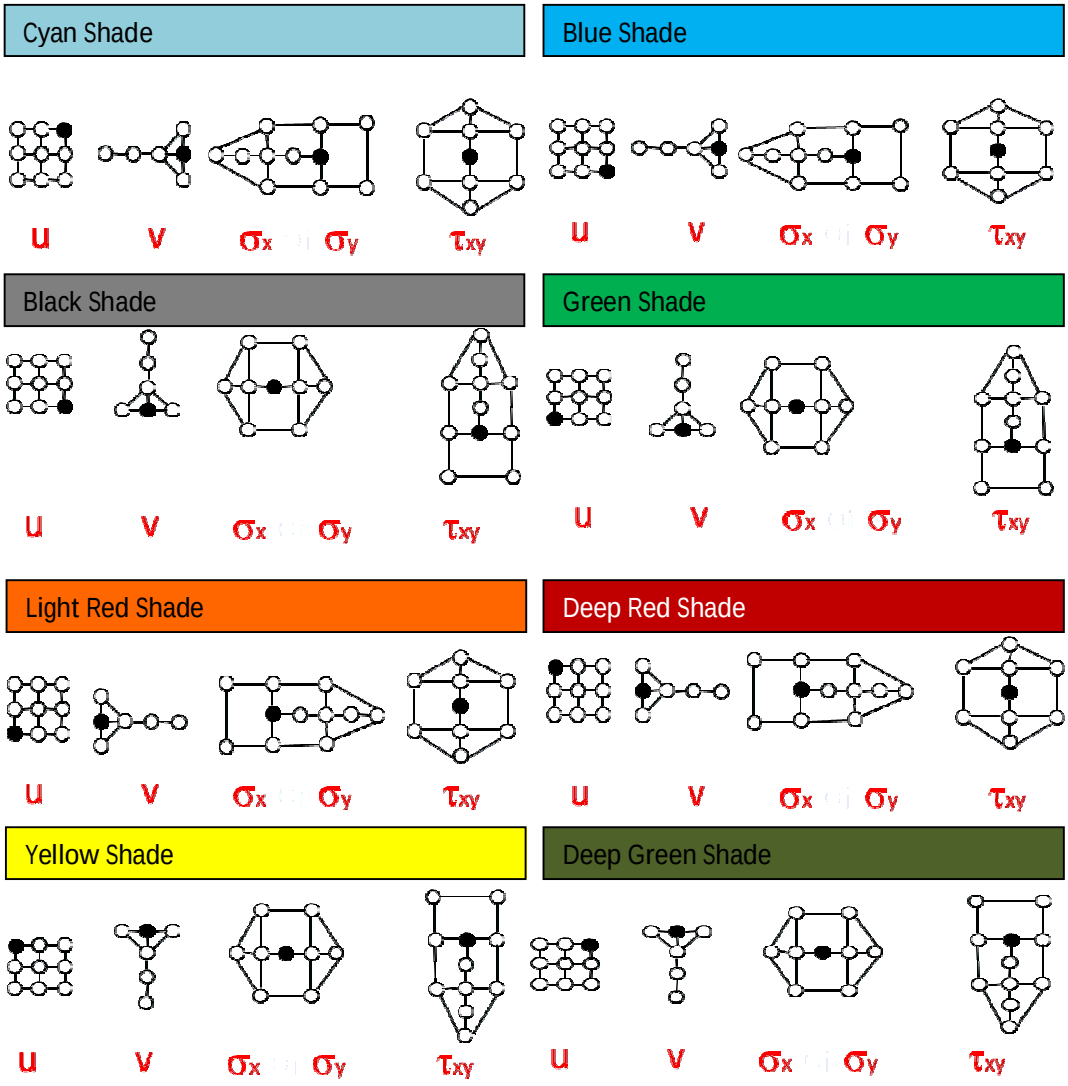

Figure 3.35: Stencils for stress calculation for cross mark nodes at different region of field (see figure 3.35 and 3.36).

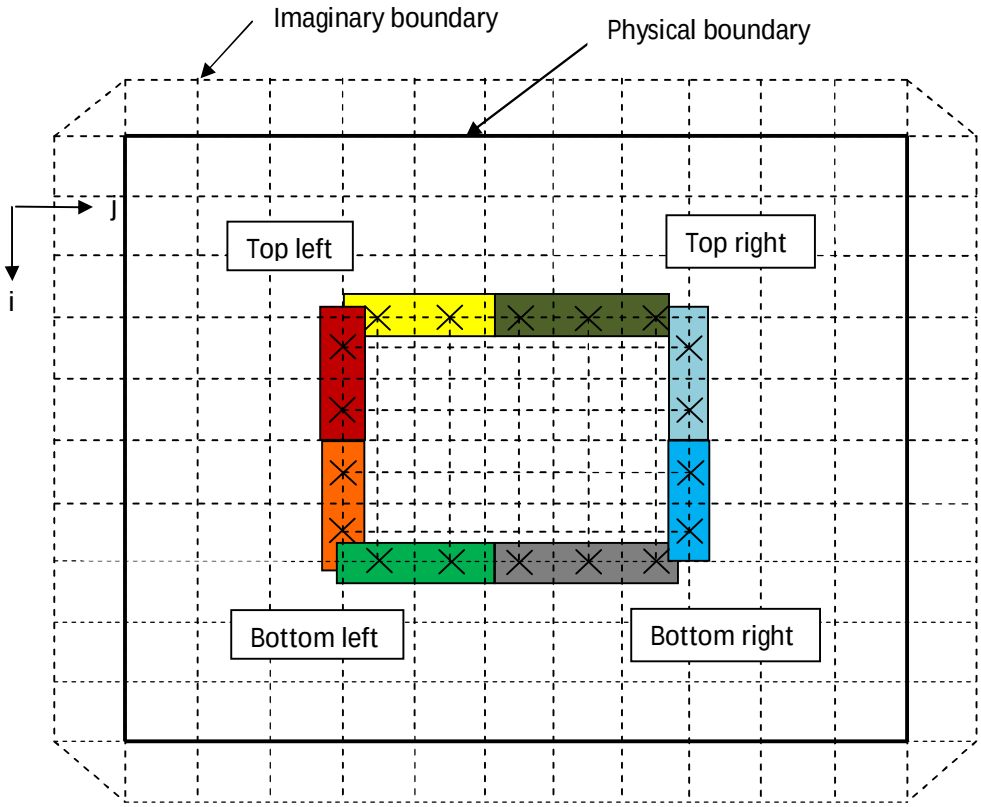

Figure 3.36: Calculation of stress and displacement at cross mark node for case-I.

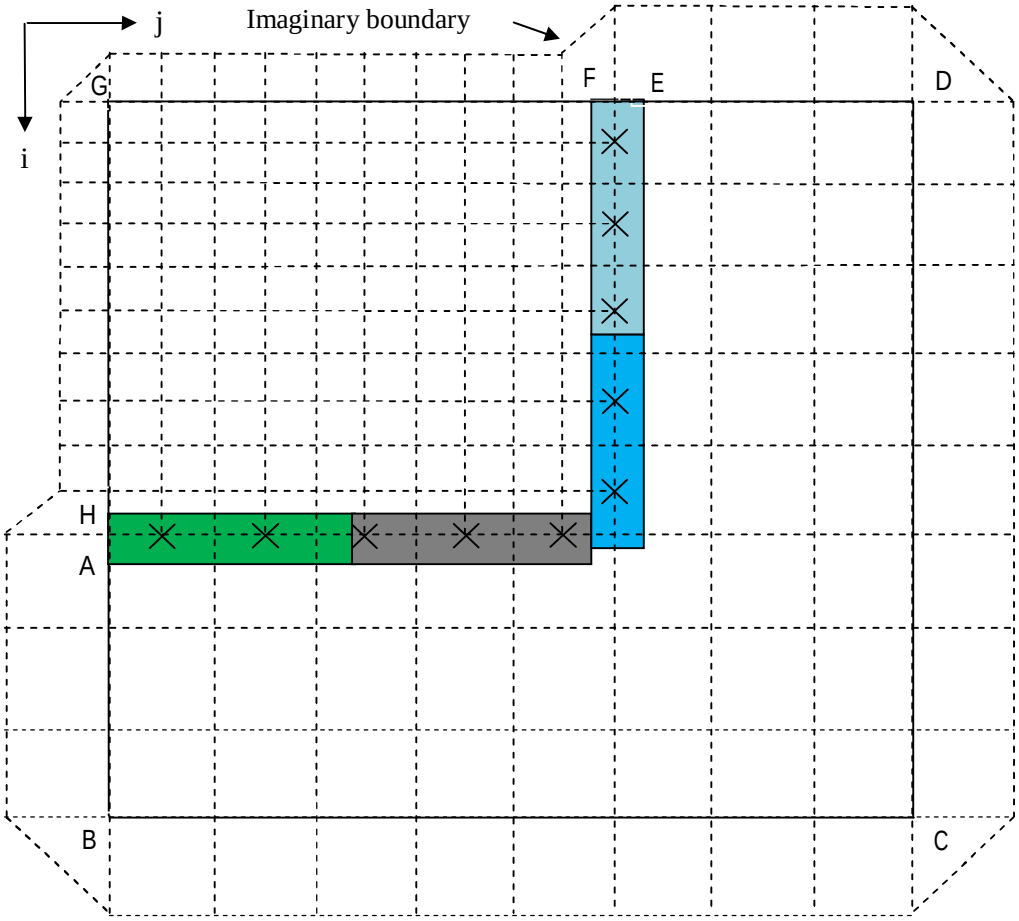

Figure 3.37: Calculation of stress and displacement at cross mark nodes for case-II.

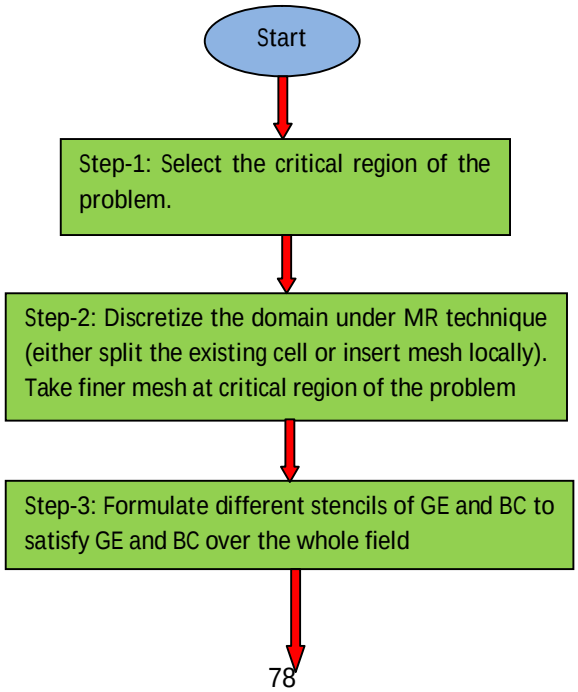

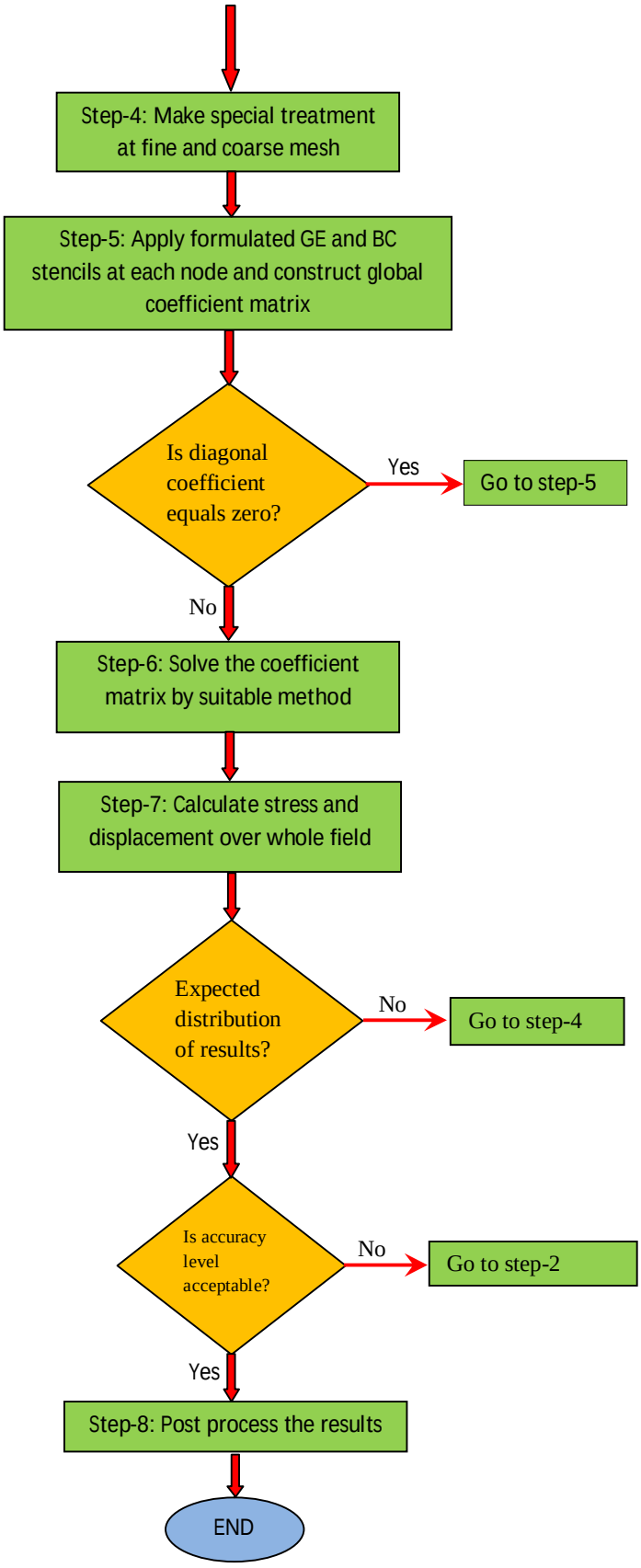

Figure 3.38: Flow chart of MR technique.

3.6 Computer Program for the Finite Difference Solution

A computer program based on the FORTRAN language is developed for the finite difference solution of the problem. The program has several subroutines to perform different tasks. In the flow chart as shown in figure 3.39, the whole program is briefly expressed. It is actually a parsimonious representation of the whole program. First the program reads data from one input files. Input file contains data about the coarse and fine mesh position in the region, its shape expressed in Cartesian coordinate, boundary conditions for different region and loading conditions etc. It is mentionable that the input files have to prepare in a prescribed way, otherwise the program won't read and will show error message. The main program first reads the data from input file and apply the BCs at real and imaginary boundary of the field. Then main program develops global coefficient matrix by applying GE over the whole domain. The coefficient matrix is solved by LU decomposition method. Then finally the stresses and displacements are calculated over the whole field.

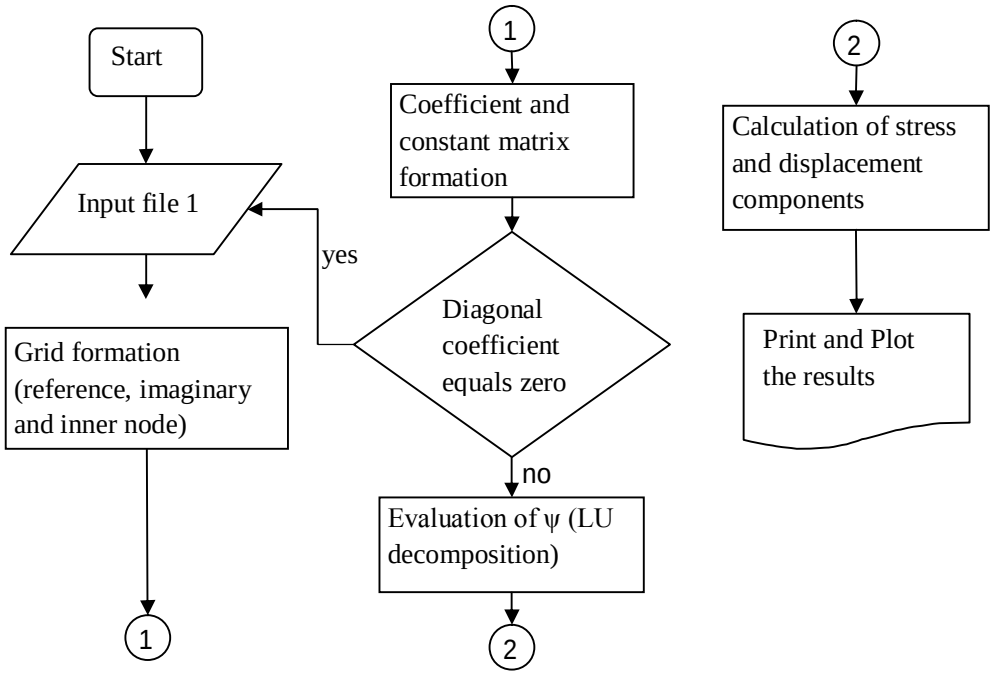

Figure 3.39: Flowchart of the computer program for finite difference solution

3.7 Finite Element Method

Finite element method is a very popular numerical method and used by many researchers over the world for solving a wide range of problems. In the previous method, finite difference method, the whole region is divided into a grid of discrete points or nodes and in each node finite difference form of the differential equation is applied which offers a point wise approximation. In contrast to the finite difference method, the finite element method divides the solution region into simply shaped regions or elements. An approximate solution for the differential equation is developed for each of these elements and the total solution is then generated by linking together the individual solutions to ensure the continuity at the inter-element boundary. So this technique provides piece wise approximation of the region rather than the point wise approximation found in the finite difference method. Based on finite element method several commercial software's are available such as ANSYS, NASTRAN & PATRAN, FEMLAB, LS DIANA etc. which are very reliable and equally popular. In this study ANSYS is used to solve the problems and hence gives a way to compare and validate the finite difference results. Since finite difference solution is the main target of this work, finite element method here performs as a supporting tool. Therefore details of the solution procedures by commercial software ANSYS (finite element method) are not mentioned here.

CHAPTER 4

APPLICATION OF THE SCHEME

4.1 Introduction

In this chapter, the mesh refinement scheme is applied to solve several applied mechanics problems. At first, numerical solutions of a specific problem are obtained by finite difference method with mesh refinement technique and finite element method considering same material properties and same boundary conditions. The solutions obtained by these methods are compared to each other to establish the reliability, soundness and accuracy level of the proposed technique. Once the finite difference method with mesh refinement technique results is verified, then some other problems are selected to solve by this method and the obtained results are analyzed and compared with uniform meshing technique to check the superiority of mesh refinement technique over uniform meshing technique. By checking the results of mesh refinement with uniform mesh technique, two exclusive feature of mesh refinement technique will be identified: one is mesh refinement reduces computational efforts and resources i.e. saves computational memory and the other one is for same number of nodal points mesh refinement technique provides better solutions of physical problem. The exclusive features of mesh refinement technique are verified by comparing the solutions with literature and with also with finite element method. After that the distribution of stress and displacement is obtained for some other problem by mesh refinement algorithm of finite difference technique. The results obtained from the mesh refinement finite difference technique for different boundary conditions are critically analyzed.

4.2 Case Study-I: Axially Loaded Member

A simple member under axial loading as shown in figure 4.1 has been solved for displacement and stress to validate the result of the proposed mesh refinement technique. The problem is considered as plane stress problem because the loadings on the body are applied at the boundary and are parallel to the plane of the plate/member and distributed over the thickness i.e. confined in the plane of the plate/member and the dimension of the body in the direction perpendicular to this plane is relatively small as compared to the others. In such cases, the stresses in the body perpendicular to the plane of loading are usually very small and thus can be neglected. As a result these

problems become two dimensional, usually referred to as plane stress problems. The left edge of the member is fixed and the right edge is under uniform normalized tensile stress. The other two edges (top and bottom) of the member are free surfaces. So, at the left edge displacement components should be zero i.e. u=0, v=0, at the right edge tangential stress is zero i.e. $\sigma_{xy} = 0$ and , the normal stress is equal to applied stress i.e. $\frac{\sigma_y}{E} = \frac{\sigma_o}{E} = 2.0x10^{-4}$; and at the top and bottom edges are stress free so normal stress, $\sigma_x = 0.0$, and also tangential stress, $\sigma_{xy} = 0.0$. σ_y is the dimension less stress; σ_o is the applied load in terms of stress directed to y-axis and E is the modulus of elasticity, μ is the Poison's ratio of the material of the member. The geometry of the problem is square having a/b=1.0 and a=b=25 unit. To check the validity of proposed technique, same problem is solved for stress and displacement distribution by using finite difference method with mesh refinement and also by finite element method taking μ=0.3. All stress components are normalized by applied stress, so it has no necessity to consider the value of E i.e. the results are valid for any material having Poisons ratio μ=0.3. For mesh refinement technique, three different sizes of mesh are taken for the study. This is shown in figure 4.2. From the knowledge of theory of elasticity, it is well known to all that for this above problem the support edge of the member is most critical in terms of stress intensity. For this reason, mesh refinement is done at this edge i.e. near this edge finest meshes are taken. Mesh sensitivity is done for the finest mesh size while the size of finest mesh is half of the size of fine mesh and the size of fine mesh is half of coarse mesh i.e. the size of finest mesh is one fourth of the coarse mesh. The results obtained by FDM and FEM are compared to each other. Mesh sensitivity analysis is performed for both of the methods. The mesh size of finest mesh selected for FDM analysis is h/a=0.02 as shown in figure 4.3a and figure 4.3b i.e. mesh length =0.5 unit (number of meshes =2805 i.e. 50x50 + imaginary nodes), as there is little variation of results if the mesh size is further smaller. But this program can solve a set of up to 4000 linear equations very efficiently; after this limit the computer memory becomes insufficient. Due to this limitation, further reduction in mesh size is not possible for the study. This thesis paper tries to solve this problem by redistributing the node i.e. mesh refinement and getting higher number of node at the critical zone while a small number of node at the other zones. Thus staying within the mesh no. limitation, better solutions are tried to obtain by MR technique at support end of the problem. In finite element method, uniform rectangular meshes are considered throughout the field. In mesh

sensitivity curve for FEM analysis as shown in figure 4.4, the optimum mesh size is 0.04 to 0.01875 where as the selected mesh size for the analysis is h/a=0.02. It would help to compare the two results at similar position of various sections of the specified problem. Since under FEM consideration 0.02X0.02 size meshes are taken throughout the field, FEM has around 30% greater no. of mesh points than MR technique.

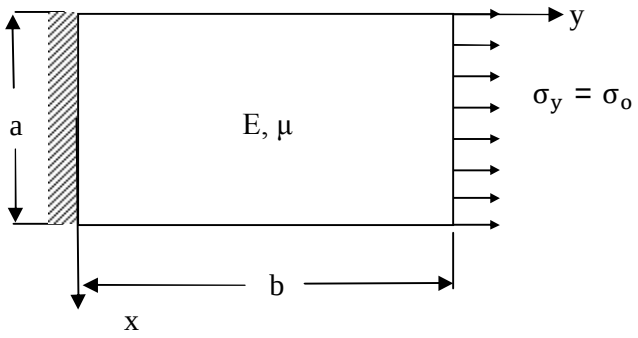

Figure 4.1: A simple member under axial loading.

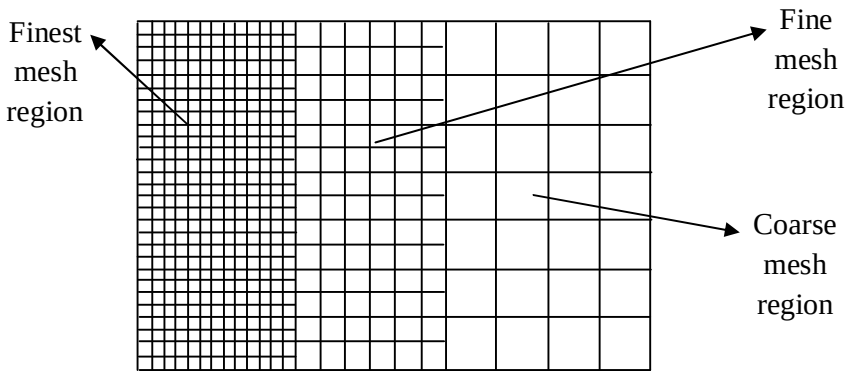

Figure 4.2: Discretization of field under mesh refinement technique.

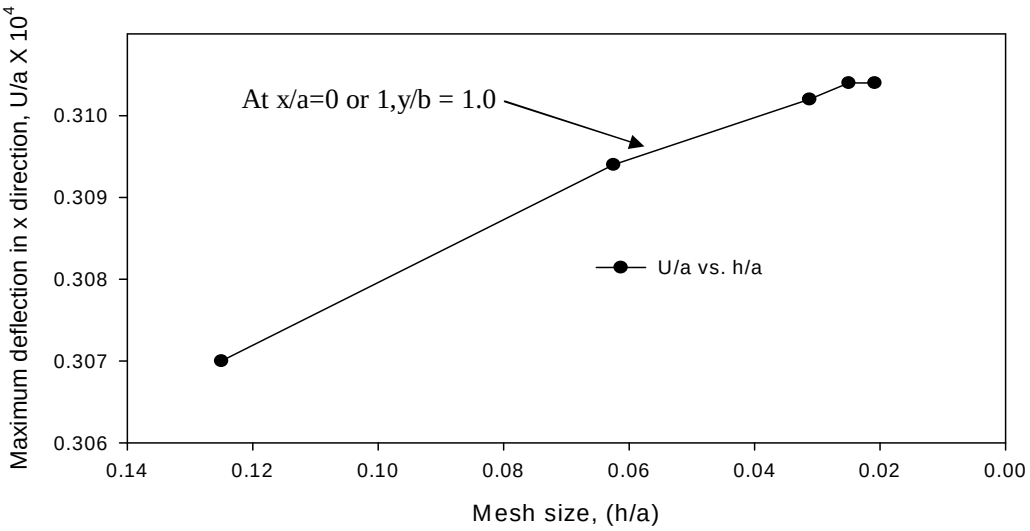

Figure 4.3a: Variation of normalized maximum displacement, u/a with mesh size by mesh refinement FDM scheme.

Figure 4.5 shows the comparison of displacement (v/b) distribution at various sections of the selected problem obtained by FDM and FEM analysis. At y/b=0.0, two results are exactly identical as the two lines merge together and both methods give displacement component v/b is zero at this section and resembles fixed support. As the value of y/b increases the value of displacements (v/b) increases and the right most edge experiences the maximum displacement as expected. Except section y/b=0.0, at other sections of the member there are very small differences in results obtained by above two methods. Near the fixed boundary (left side) sections of the problem the differences are much smaller than the right side sections of the problem. But the variation of the two results is not in significant amount.

The distribution of displacement component (u/a) as shown is figure 4.6 is of similar nature in both FDM and FEM method. The distribution of displacement component, u/a is observed to be in good agreement with the physical model of the plate. Only results at y/b=0.0 and y/b=0.24 are shown to understand the solutions clearly because after section y/b=0.24 the displacement component v/b at other sections is almost same and similar to that of section y/b=0.24. Such like graph for v/b there are insignificant amount of deviation of results by FDM and FEM. Result at y/b=0.0 is exactly same for both methods, although, in result at y/b=0.24 there is small amount of deviation between two methods but not in significant amount. Also in other sections (not shown graphically) of the member there present deviation between results of two methods but

again deviations are not significant amount. Due to material and loading symmetry of the problem about x/a=0.5 the distribution of any parameter should be symmetric about this section x/a=0.5. This phenomena is readily seen in the distribution of v/b and u/a.

The distribution of most significant stress, σ_y at section y/b=0.0 of the material by FDM and FEM methods is shown in figure 4.7. It indicates that for this particular problem stress at section y/b=0.0 is very significant. FDM results are higher that than of FEM results at singularity point which is obvious because FEM cannot get the accurate results at boundary point due to its limitation of taking nodes at the boundary. FEM uses average of element stress to find the results at boundary whereas FDM can take node points on boundary by which can conforms better results at the boundary. That is indicated by the figure 4.7. The distribution of normal stress, σ_y is also symmetric about the section x/a=0.5.

At other sections of the material, the variation of the stress σ_y is very small and nearly equal to the applied stress and this is shown by figure 4.8. This matching of results by these two methods conform the validity and accuracy of the proposed technique.

The distribution of normal stress, σ_x at support is shown in figure 4.9 as a comparative study. The FEM method gives a higher value of stress than that of FDM method. This is so because, the FDM method has limitation of applying boundary conditions properly at the singularity point. In this problem at top-left or bottom-left corner there should apply only two boundary conditions u=0, v=0, one on real boundary point and other on imaginary boundary point by taking the nodal point lies on left edge of the body . But there is another false boundary point at the top edge of the body in which we should apply another boundary conditions σ_x=0 or σ_{xy}=0. In this case we have applied σ_{xy}=0 and get a similar solution of FEM. The distribution of normal stress σ_x for other section is shown in figure 4.10 and observed that to be in good agreement with the physical model. The distribution of shear stress σ_{xy} is shown in figure 4.11 as a comparative study. The results of two methods do not match exactly at around x=0.0 and x=1.00. this is due to the limitation of application technique of boundary conditions at this corner of the member. At singular point, it is seen that the shear stress is zero this is due to the application of σ_{xy}=0 at this position of the problem. But the maximum shear stress is occurring near the vicinity of this singular point which is seen to be good agreement with the physical model. The distribution of shear stress at other section of

the member is shown in figure 4.12. It shows that the distribution matches with our expectation.

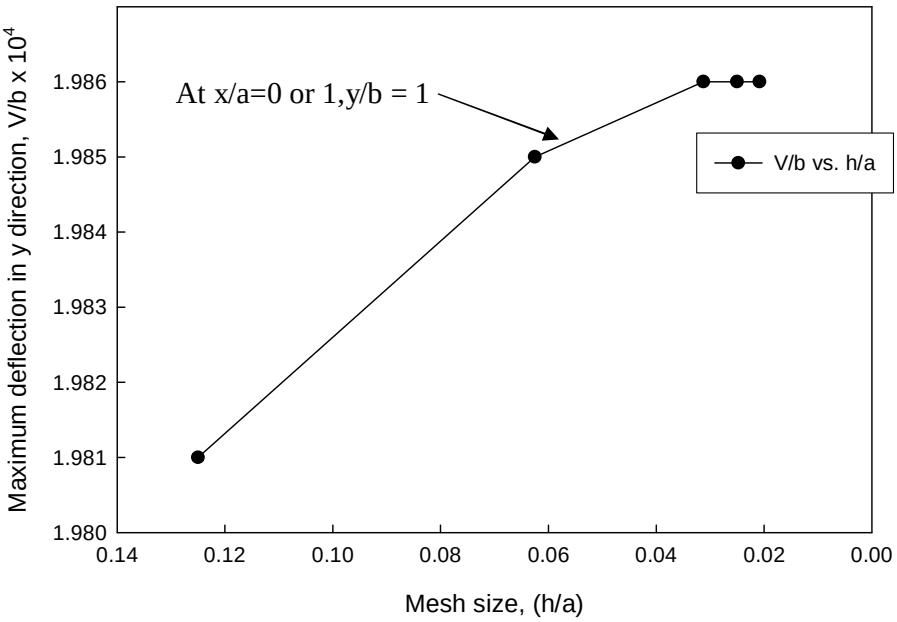

Figure 4.3b: Variation of normalized maximum displacement, v/b with mesh size by mesh refinement FDM scheme.

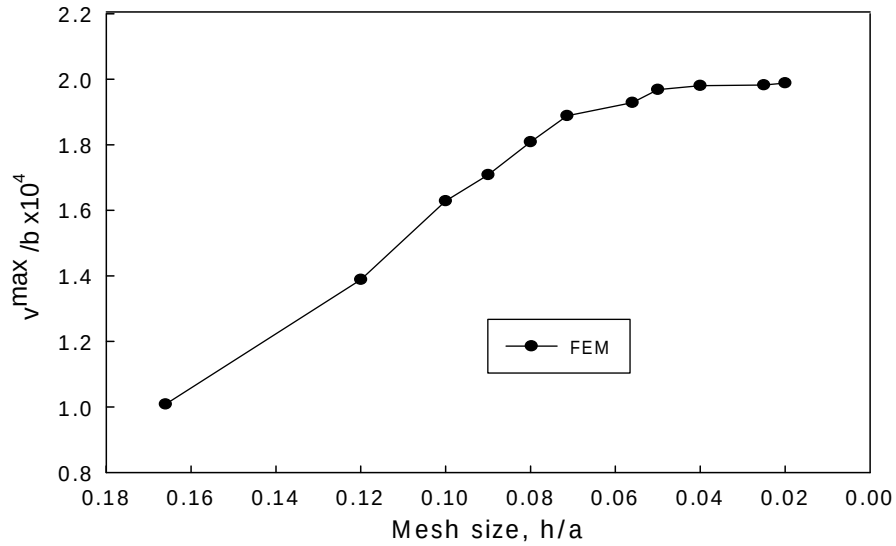

Figure 4.4: Variation of maximum normalized displacement (v^{max}/b) with mesh size by FEM.

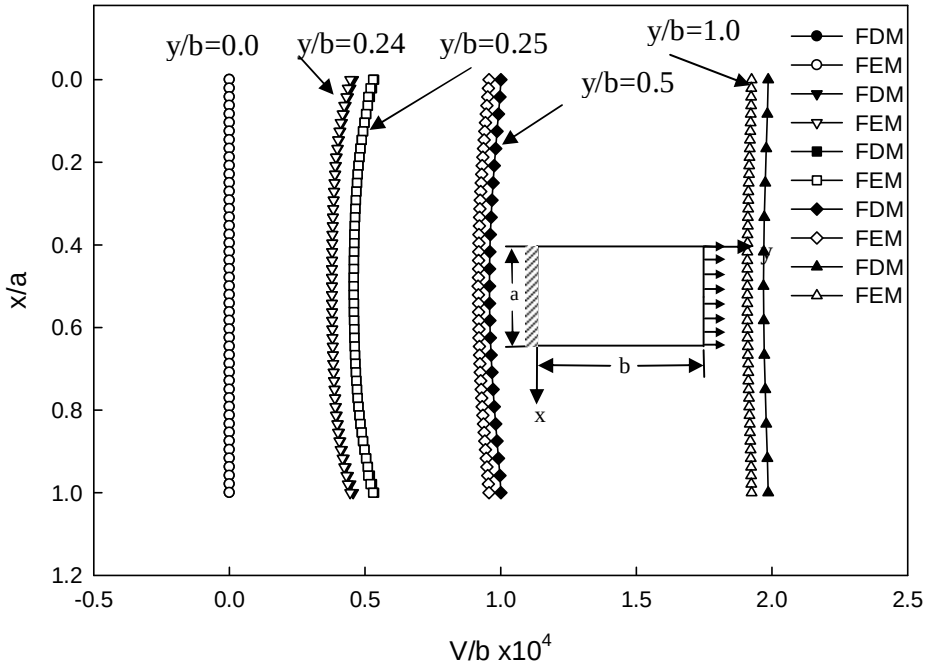

Figure 4.5: Comparison of normalized displacement (V/b) distribution at various sections of the material.

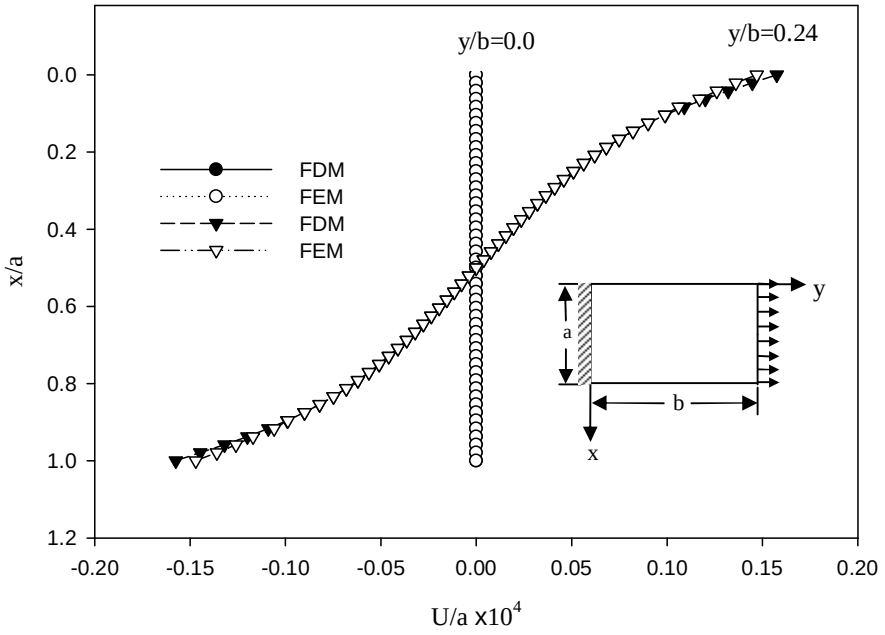

Figure 4.6: Comparison of normalized displacement (U/a) distribution at various sections of the material.

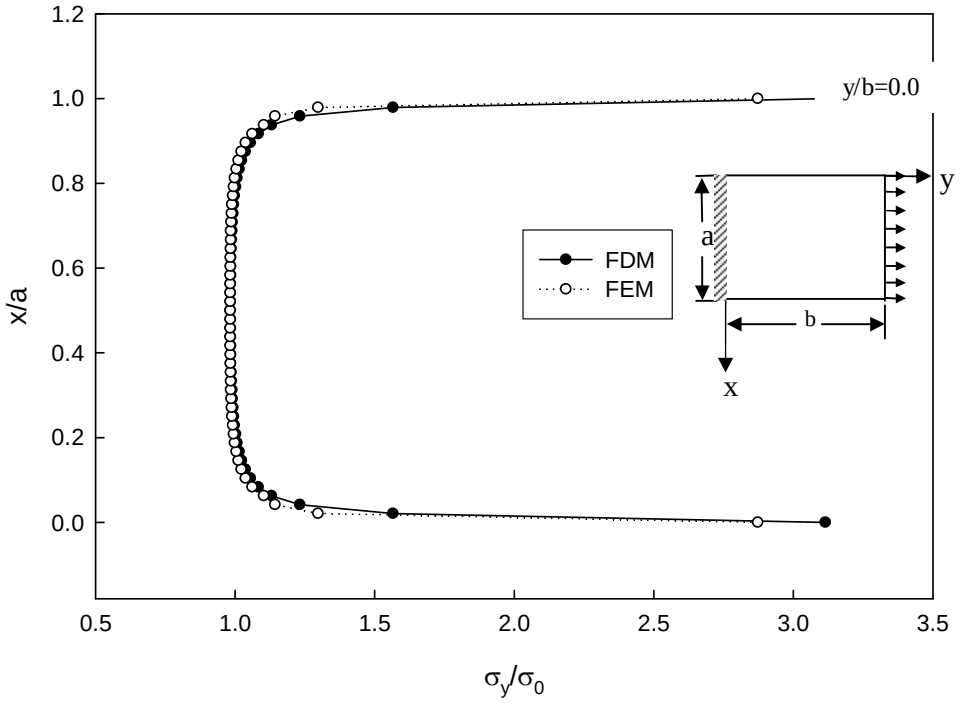

Figure 4.7: Comparison of normalized normal stress (σ_y/σ_o) distribution at y/b=0.0 of the simple bar by FDM and FEM.

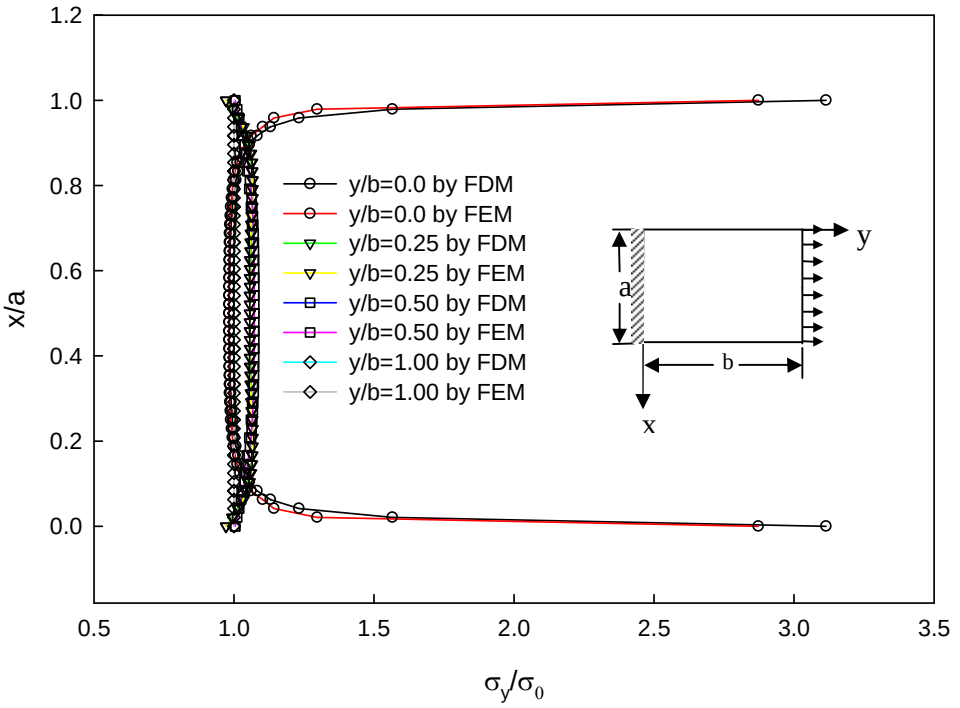

Figure 4.8: Normalized normal stress (σ_y/σ_o) distribution at different sections of the material by FDM with mesh refinement and FEM.

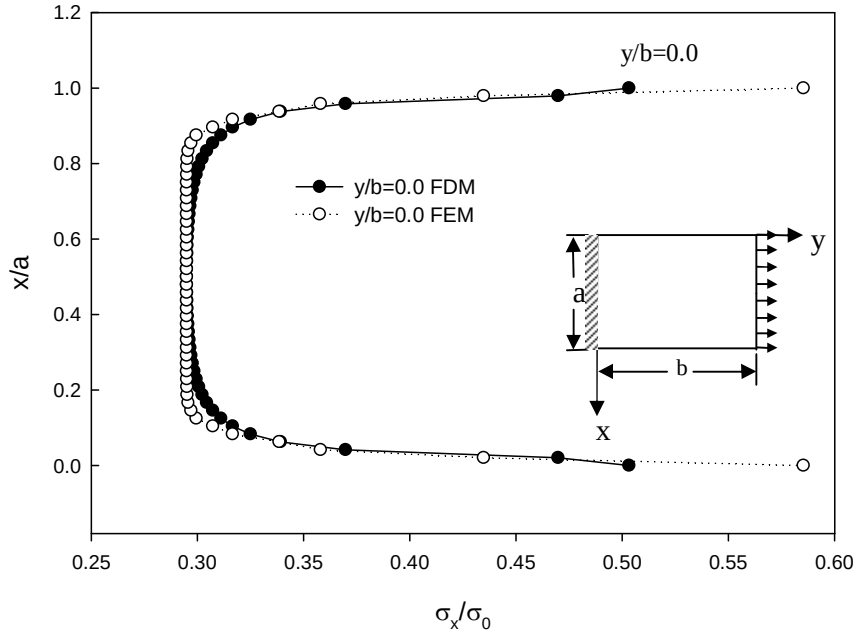

Figure 4.9: Comparison of normalized normal stress (σ_x/σ_o) distribution at y/b =0.0 by FDM with mesh refinement and FEM.

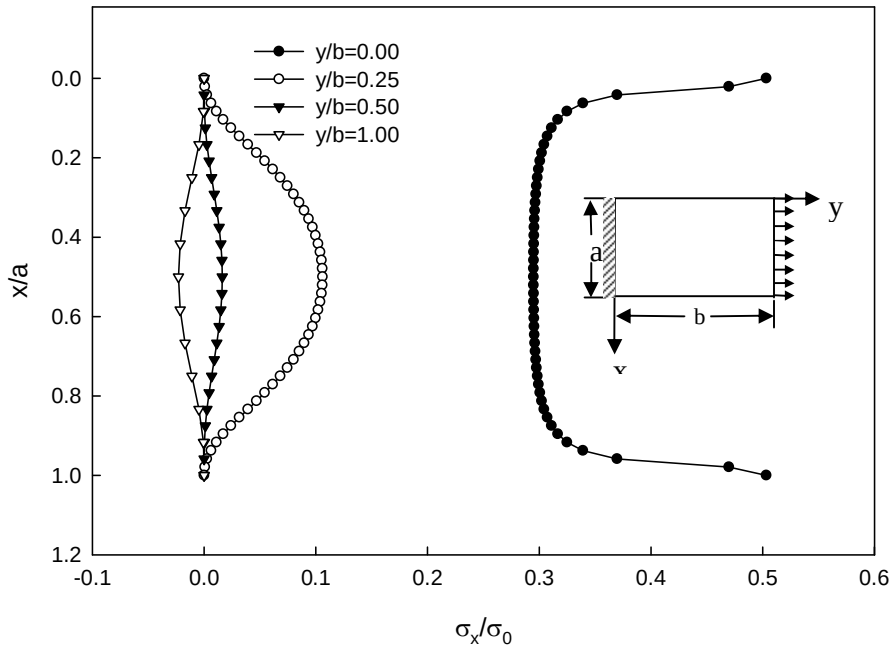

Figure 4.10: Normalized normal stress (σ_x/σ_o) distribution of a bar under uniform tension at different section by FDM with mesh refinement technique.

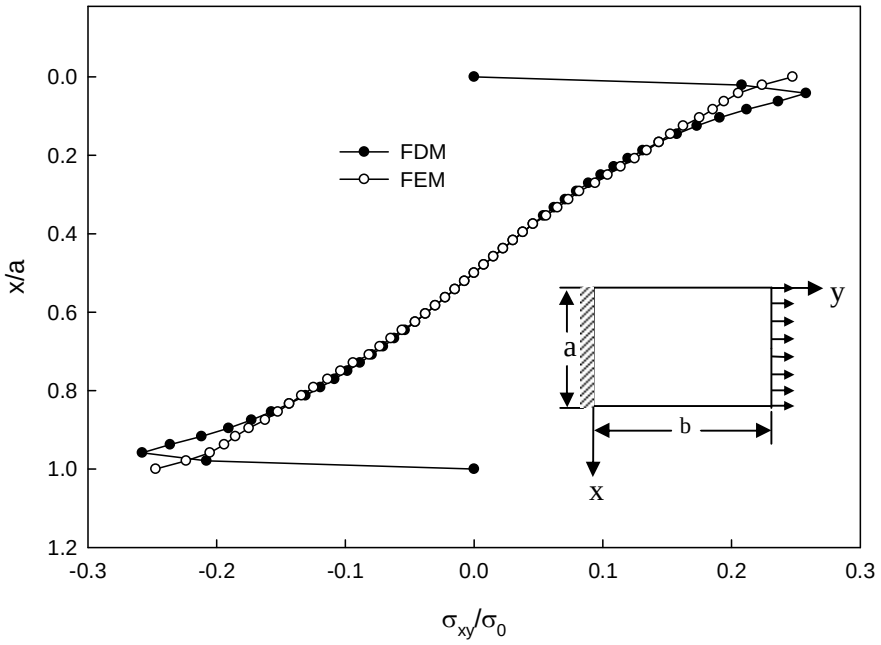

Figure 4.11: Comparison of normalized shear stress obtained by MR finite difference method and finite element method.

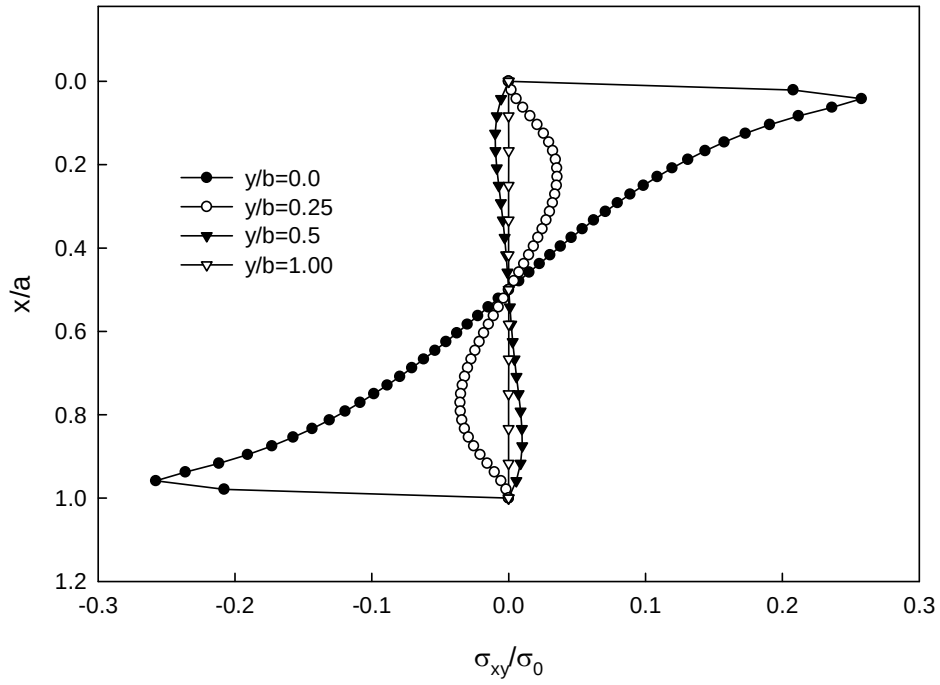

Figure 4.12: Normalized shear stress (σ_{xy}) distribution of a fixed bar under uniform tension by FDM with mesh refinement technique.

4.3 Case Study-II: Axially Loaded Member with Embedded Crack

4.3.1 Reduction of number of equation: A huge amount of memory saving

In this section of this thesis, embedded crack problem is solved by two different techniques of FDM: one is considering uniform mesh throughout the numerical field and other one is mesh refinement taking three different sizes of meshes at different regions of the member. Here, it would help to establish a feature of mesh refinement technique: reduction of meshes does not hamper the accuracy of the solutions i.e. a huge amount of computational effort and resources is saved by mesh refinement techniques. This is so because numerical simulations of physical phenomena under uniform mesh technique consume a significant amount of computational resources, since their domains are discretized on high resolution meshes throughout the numerical field. An enormous wastage of these resources occurs in refinement of sections of the domain where computation of the solution does not require high resolutions. On the other hand, mesh refinement technique takes different resolution of meshes at different regions of the problem depending on the requirement of good solutions. On the following section this problem of wastage of resources is effectively solved by mesh refinement technique. A simple problem containing embedded crack under uniform tensile stress as shown in figure 4.13 is selected for analysis this aspect of the mesh refinement technique. The material geometry of the problem is taken as a/b=1.0 and size of the crack is taken as one fourth of the width of the member. The material properties are taken as same that of the previous problem. Due to symmetric nature of the problem we represent the results only for half portion of the problem as shown in figure 4.14 with necessary boundary condition.

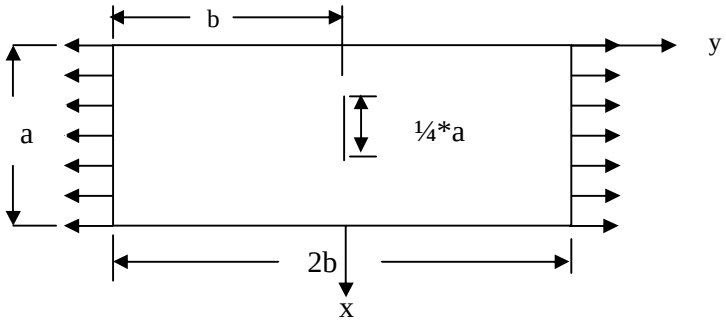

Figure 4.13: Simple bar with embedded crack under uniform tensile stress.

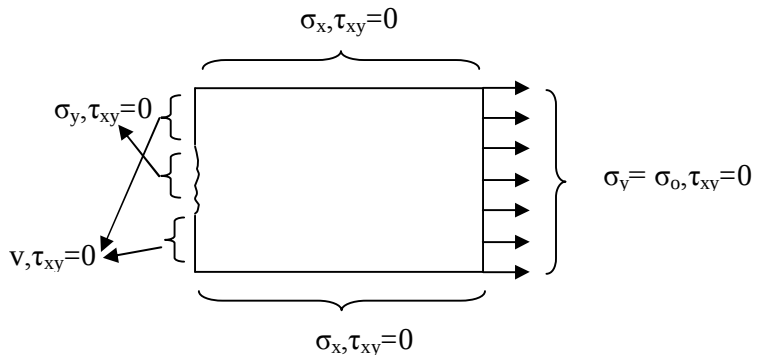

Figure 4.14: Half section of the problem with necessary boundary conditions.

The discretization process in mesh refinement technique is the most critical tasks because mesh refinement technique gives better result over uniform mesh technique if and only if discretization process can be done with some intelligence otherwise there will no improvement in accuracy of the solution. In mesh refinement technique, sections of the domain needing high resolution are generally determined by means of a criterion which may vary depending on the nature of the problem. Fairly straightforward criteria could include comparing the solution to a threshold or the gradient of a solution, that is, its local rate of change to a threshold or presents of stress concentrators or sharp change in cross section etc. Comparing the solution to a threshold is not particularly rigorous and hardly ever represents a physical phenomenon of interest, it is simple to implement. However, the gradient criterion is not as simple to implement as a direct comparison of values, but it is still quick and a good indicator of the effectiveness of the mesh refinement technique. Some other straightforward criteria can include the presence of cracks, void, hole etc., a sharp change in cross section, material flaws etc. Since the above problem contains a crack and work as a stress riser, mesh refinement is done in vicinity of the crack as shown in figure 4.15a, which contain three different mesh sizes, h_1, h_2 and h_3 in the direction of x-axis. For simplicity, this thesis takes $h_2=2*h_1$ and $h_3=2*h_2$. Same types and sizes meshes are also considered in y-axis direction i.e. $k_1=h_1$, $k_2=h_2$ etc. Total no of meshes in MR technique is around 2400. To compare the result obtained by mesh refinement technique with uniform meshing, the domain of uniform meshing is discretized with mesh having size equal to the smallest mesh size of mesh refinement technique throughout the field shown in figure 4.15b. Total no. of meshes in uniform technique is around 4000 (60X60 + imaginary nodes), which is around 40% greater than MR technique. Thus

great reductions in mesh number occur in mesh reduction technique. The mesh refinement technique has around 40% less nodal points than uniform mesh technique.

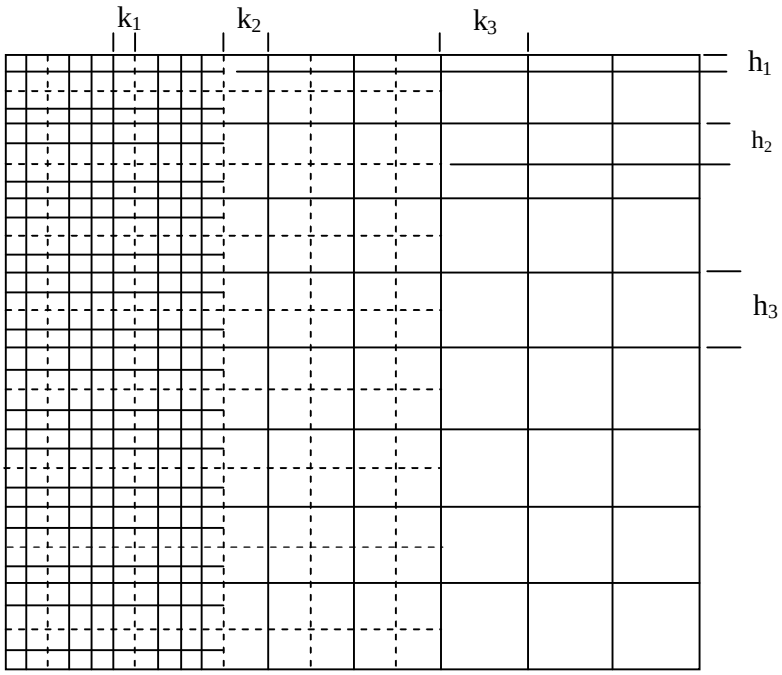

a) Discreatization of domain under mesh refinement technique.

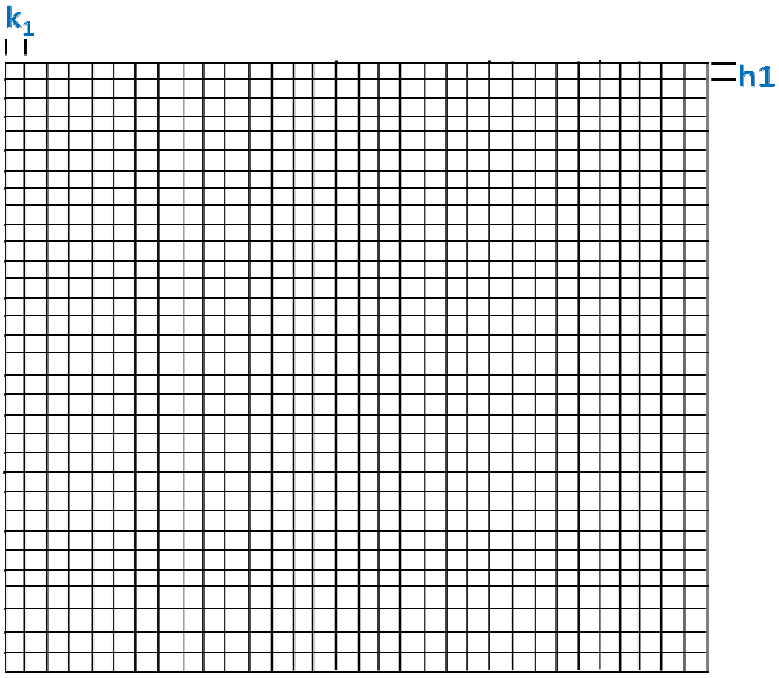

b) Discretization of domain under uniform mesh technique.

Figure 4.15: Discretization process of the field.

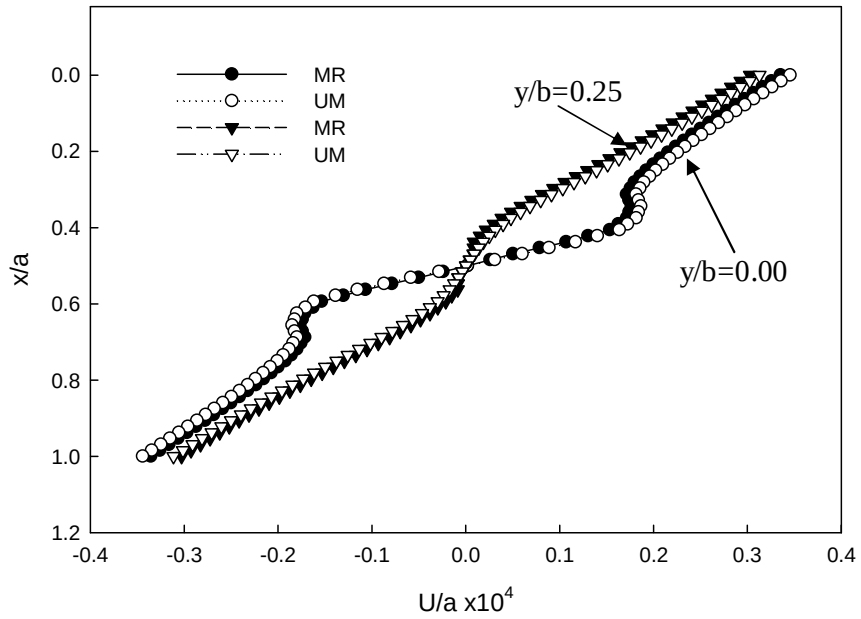

Figure 4.16: Comparison of results for normalized deflection, (u/a) by mesh refinement technique and uniform meshing.

Results obtained by two method mesh refinement technique and uniform meshing method of this above problem are shown in figure 4.16 to figure 4.22. Figure 4.16 shows the results for normalized deflection (u/a) for both methods at different sections. There are some differences in results obtained by two techniques but these are not very significant. The results obtained by uniform meshing are somewhat magnified than that of mesh refinement but difference is not very high. Results are shown only for two sections namely y/b=0.00 and y/b=0.25 for clear understanding of results because for other sections results are almost same and graphing these results will be crowded the figure. Figure 4.17 shows normalized deflection (v/b) for left most and right most section. In the right most section i.e. maximum deflection for the problem matches exactly, but at the left most section results do not match exactly. There are some differences in value of v/b at the position of crack and it is the maximum at the tip of the crack, although the difference is not very significant. The magnitude (10^{-5}) of the results by two different methods is same. The maximum deflection at y/b=0.0 for mesh refinement is 4.0711×10^{-5} whereas for uniform meshing is 4.7110×10^{-5}. The figure 4.18 shows normalized deflection (v/b) at different section. The maximum deflection is same for every nodal points at y/b=1.0 which is obvious because the effect of stress

concentrator i.e. crack diminishes at earlier section at around section y/b=0.5. Before the section y/b=0.5, for each and every section maximum displacement component v/b occurs at horizontal mid-section of the plate i.e. at x/a=0.5.

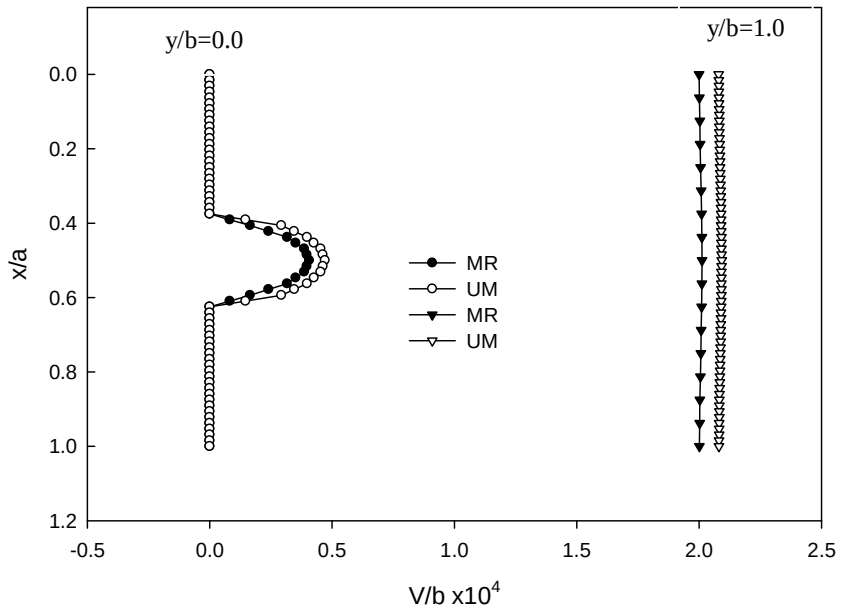

Figure 4.17: Comparison of results for normalized deflection, (v/b) at section y/b=0.0 and y/b=1.0 by mesh refinement technique and uniform meshing.

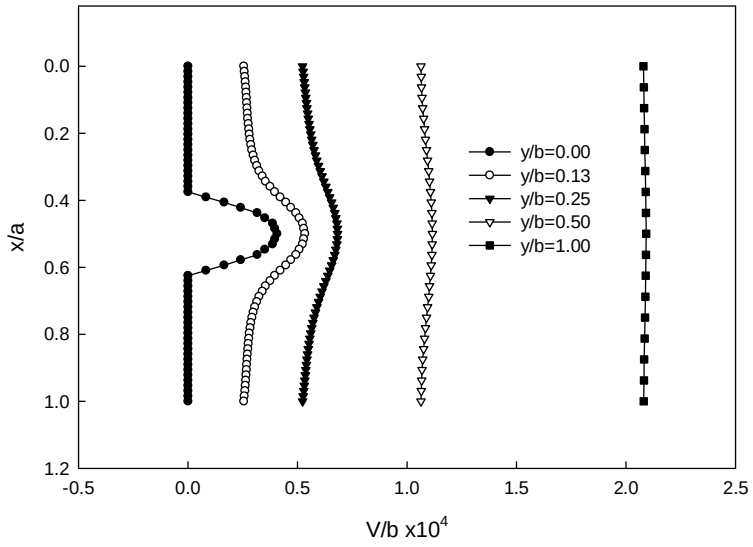

Figure 4.18: Results for normalized deflection, (v/b) at different section by mesh refinement technique.

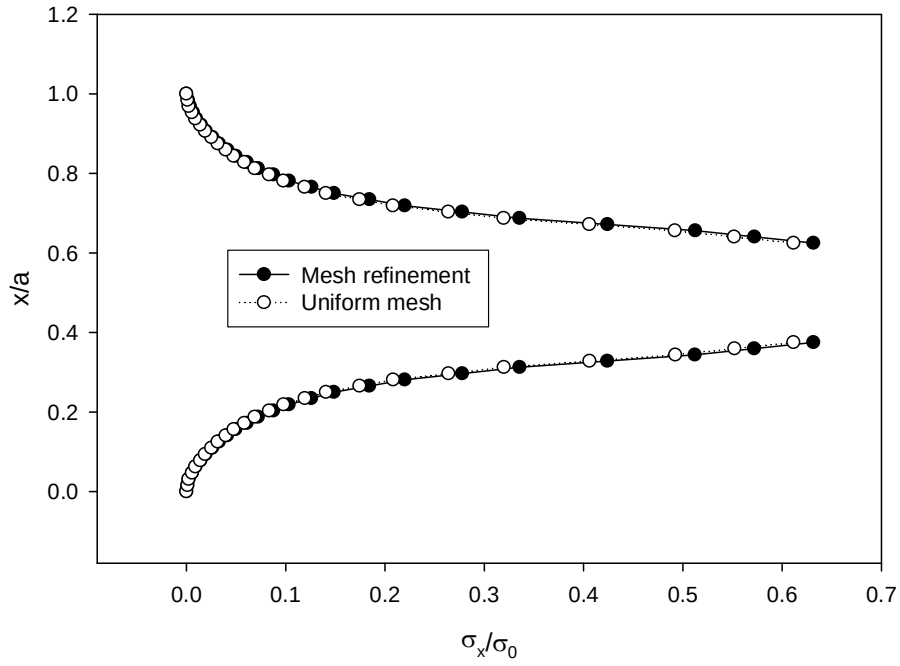

Figure 4.19: Comparison of results for normalized stress, (σ_x/σ_o) at section y/b=0.0 by mesh refinement technique and uniform meshing.

Figure 4.19 shows the normalized stress (σ_x/σ_o) distribution at section y/b=0.0. It shows that as node point increments from top edge or bottom edge to crack tips, the stress increases gradually and this matches with the theory of elasticity. Both the method gives same results for normalized stress (σ_x/σ_o) at the crack tips, so we can conclude that the method of mesh refinement saves a great amount of memory without compromising the accuracy of the solution. Normalized stress (σ_x/σ_o) at different section by mesh refinement technique is shown in figure 4.20. It shows that normalized stress (σ_x/σ_o) is almost zero at the right section of the materials which keeps the conformity of the solution with the basic theory of elasticity. Figure 4.21 shows comparison of results for normalized normal stress (σ_y/σ_o) at section y/b=0.0 i.e. at the crack section by mesh refinement technique and uniform mesh refinement technique. These two methods give same results, although, mesh refinement scheme play with around 40% reduction of node than uniform meshing scheme. The tip of the crack suffers the maximum stress and similarity with applied elasticity theory. Without the section near the crack all other section have suffered by a smaller stress almost equal to the stress applied stress $\sigma_1/E= 2.0e^{-4}$, that also conforms the theory of elasticity as shown in figure 4.22.

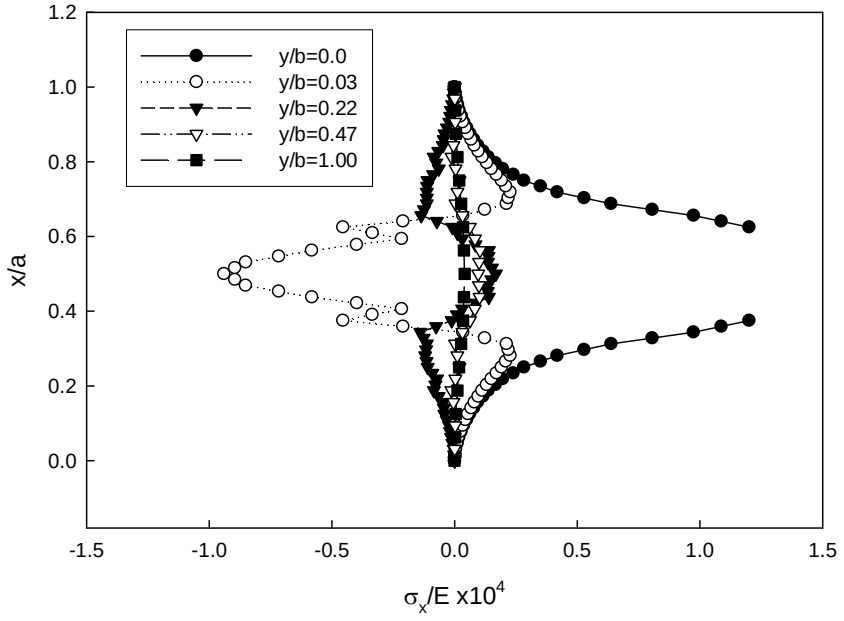

Figure 4.20: Results for normalized stress, (σ_x/σ_o) at section y/b=0.0 by mesh refinement technique and uniform meshing.

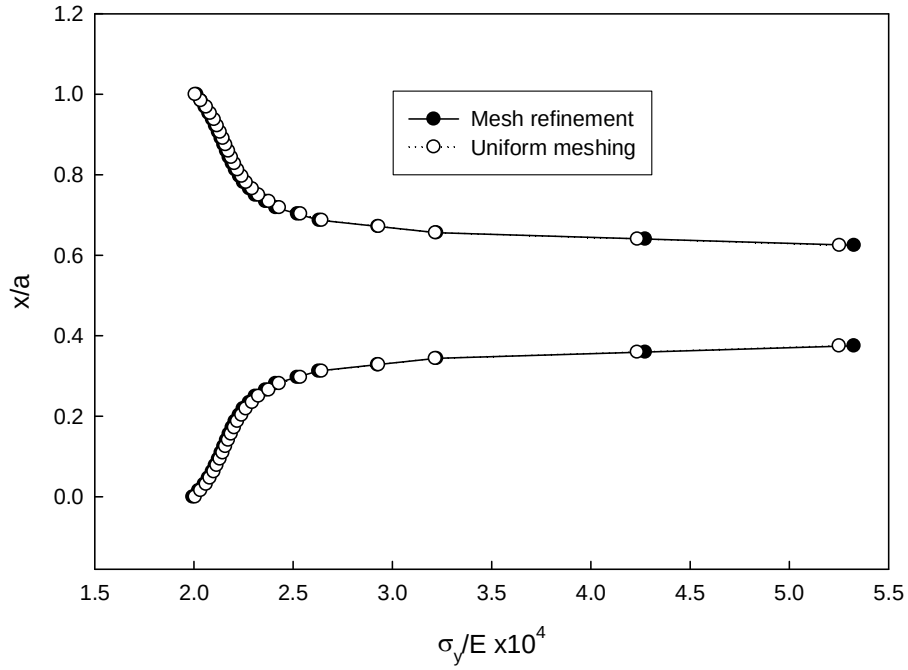

Figure 4.21: Comparison of results for normalized stress, (σ_x/σ_o) at section y/b=0.0 by mesh refinement technique and uniform meshing.

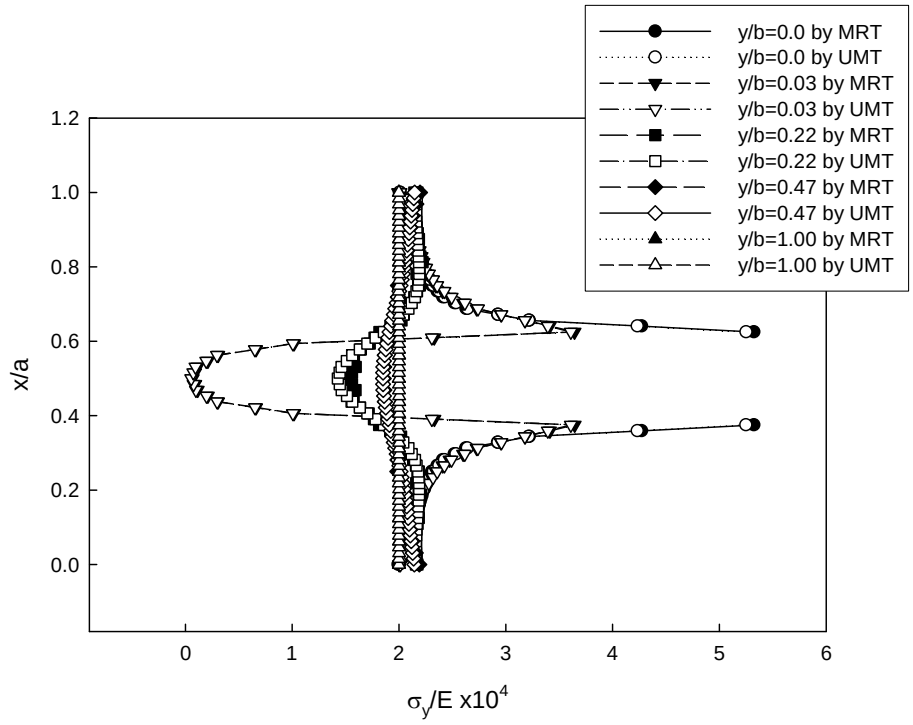

Figure 4.22: Comparison of results for normalized stress, (σ_y/σ_o) at different section by mesh refinement technique and uniform meshing.

4.3.2 Redistribution of Meshes Increases the Accuracy of the Solutions

As stated before, around 4000 linear equation can be solved effectively by this program due to the limitation of computer ability (Pentium(R) Dual Core CPU, E5200 @2.50GHz, 2.50GHz, 1.00GB of RAM). The previous section of this thesis tries to solve this problem of memory exhausting by reducing the no. of equation but not compromising the accuracy using mesh refinement technique in finite difference method. But one can claim that, using high performance computer or super computer will relieve from this problem, then, there will no limitation of using uniform mesh technique in terms of nodal points or number of linear equation, so why you use this new technique? This section of this thesis tries to express the concept that for equal no. of nodal points mesh refinement technique gives better results than uniform mesh technique i.e. redistribution of nodes increases the accuracy of the solutions. Consider the following same problem of previous section to establish the above thought. A plate having embedded crack under uniform tensile stress as shown in figure 4.13 is considered to verify this aspect of this new technique. Due to nature of symmetry of the problem only half section is considered for analysis and this is shown in figure 4.14 with necessary boundary condition.

Under uniform mesh consideration, the discretization is done by taking same sizes mesh over the whole field as shown in figure 4.15b. The discretization, under mesh refinement technique, is done only by changing some nodal points of a region of uniform meshing discretization to some other regions thus gives an opportunity to maintain equal no. of nodal points for both technique (for both technique around 4000 mesh are considered). The changing of nodal points from one region to other region must be done with some intelligence otherwise the benefits of mesh refinement will remain under question marks. Here, intensity of the solution of uniform meshing is taken as a criterion to change the position of the nodal points from one region to others region. Nodal points should be changed from lower intensify areas to higher intensify areas. From the results of uniform mesh technique, the left section of the material i.e. y/b=0.0 to y/b=0.25 can be taken as higher intensify area as shown in figure 4.23. So, nodal points from right section of the domain should be changed to left section of the material as shown in figure 4.24 as compared to figure 4.15b. Thus, uniform meshing become non-uniform and uniform meshing contain only one mesh length, h_2 in x-axis direction whereas mesh refinement particularly in this case contain three different mesh

length, h_1, h_2 and h_3 and both uniform mesh technique and mesh refinement technique has around equal no. of nodal points. There is a relation between h_1, h_2 and h_3 and this is $h_1=h_2/2=h_3/4$. This has been taken for simplifying the problems.

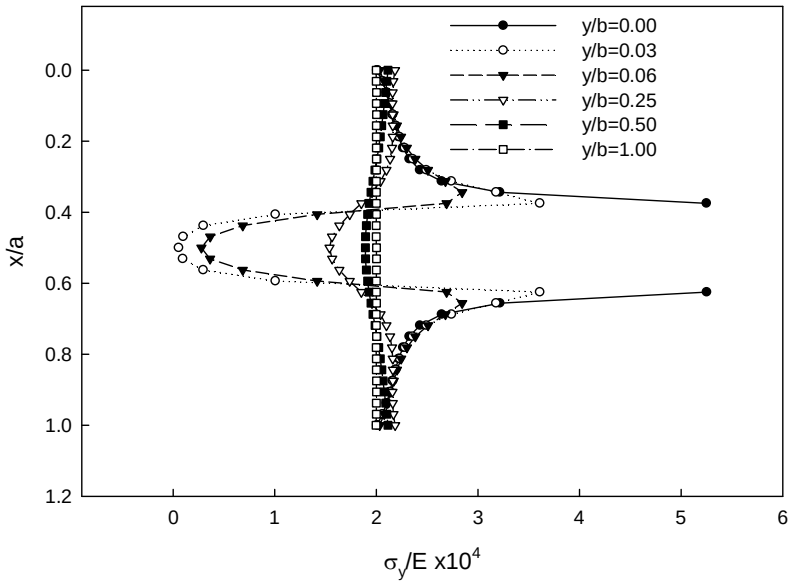

Figure 4.23: Results for normalized normal stress (σ_y/E) obtained by uniform meshing technique at various section of the material.

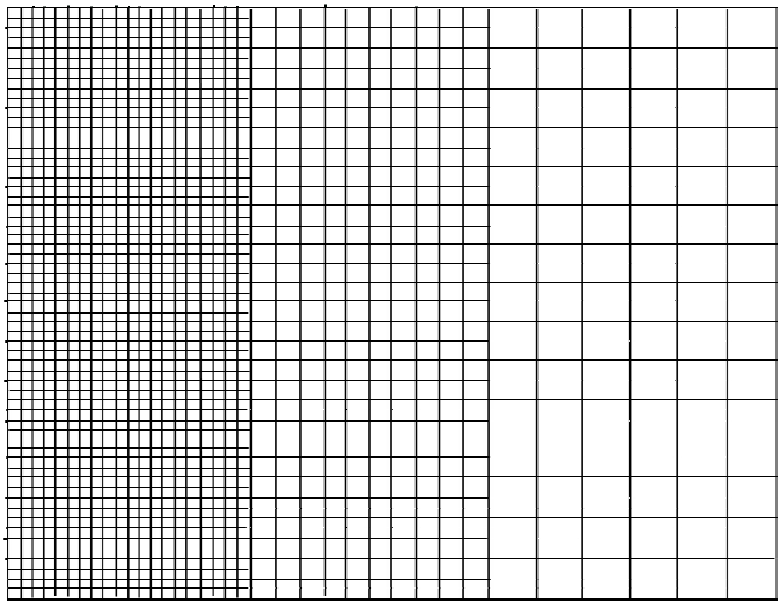

Figure 4.24: Redistribution of meshes in mesh refinement process to obtain better results.

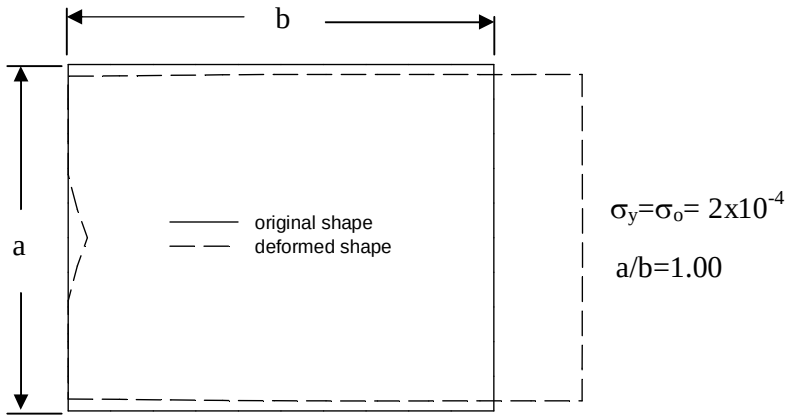

Figure 4.25: Original shape and deformed shape of the material. u and v are 1000 times magnified.

The results of this particular problem are shown in figure from 4.25 to 4.37. Figure 4.26, 4.28, 4.29, 4.31 and 4.33 shows a comparative study of results obtained by mesh refinement (MR) and uniform meshing (UM) techniques.

Figure 4.25 shows the original shape and deformed shape of the problem under the formulation of MR technique. Form qualitative inspection we see that solution is correct. The upper edge moves downward whereas bottom edge moves upward and these matches with our expectation. The material gets narrows down in vertical direction and elongated in horizontal direction.

Figure 4.26 deflection (u/a) for both methods and see that results of both techniques match numerically each other but MR technique gives a better distribution i.e. a more smother curve than UM method. Figure 4.27 shows deflection (u/a) at different section of the material by MR technique. Which shows that maximum deflection is occur at y/b=0.0. Figure 4.28 shows a comparative study of deflection (v/b) for both methods at section y/b=0.0 and shows that at the midpoint of crack the UM technique gives a higher value of displacement than MR technique. For all section MR technique gives always a smaller value of deflection than UM technique. The difference between two values of deflection (v/b) obtained by MR and UM technique increases as y/b value increases but the differences are not very significant. From these above discussion we cannot conclude that for equal no. of nodal points MR technique improve the accuracy.

Now we take a close look to the figure 4.33 which compare the results of normalized normal stress (σ_y/σ_o) obtained by MR and UM technique. From theory of elasticity we know that for this type of problem the important parameter is normalized normal stress σ_y/σ_o. Figure 4.33 shows this stress value is much larger for MR technique and from literature we know that it should have a large value. This verification is given in the next paragraph of this thesis from literature [45].

It is possible to analyze certain geometrical shapes by using the methods of the theory of elasticity to determine the values of stress concentration factors. Three distinct modes of crack propagation exist, as shown in figure 4.34. A tensile stress field gives rise to mode I, the *opening crack propagation mode,* as shown in figure 4.34a. This mode is the most common in practice. Mode II is the *sliding mode,* is due to in-plane shear, and can be seen in figure 4.34b. Mode III is the *tearing mode,* which arises from out-of-plane shear, as shown in figure 4.34c. Consider a mode I crack of length 2*a* in the infinite plate of figure 4.35. By using complex stress functions, it has been shown that the stress field on a *dx dy* element in the vicinity of the crack tip is given by [45]

$$\sigma_x = \sigma\sqrt{\frac{a}{2r}}\cos\frac{\theta}{2}\left(1-\sin\frac{\theta}{2}\sin\frac{3\theta}{2}\right) \tag{4.1}$$

$$\sigma_y = \sigma\sqrt{\frac{a}{2r}}\cos\frac{\theta}{2}\left(1+\sin\frac{\theta}{2}\sin\frac{3\theta}{2}\right) \tag{4.2}$$

$$\tau_{xy} = \sigma\sqrt{\frac{a}{2r}}\sin\frac{\theta}{2}\cos\frac{\theta}{2}\cos\frac{3\theta}{2} \tag{4.3}$$

$$\sigma_z = \begin{cases} 0 & \text{(for plane stress)} \\ \nu(\sigma_x+\sigma_y) & \text{(for plane strain)} \end{cases} \tag{4.4}$$

The stress σ_y near the tip, with $\theta = 0$, is

$$\sigma_y|_{\theta=0} = \sigma\sqrt{\frac{a}{2r}} \tag{4.5}$$

Thus as with the crack, we see that $\sigma_y|\theta=0 \rightarrow \infty$ as $r \rightarrow 0$, i.e. at the tip of the crack the stress σ_y should be infinite. But, in practical case the concept of an infinite stress concentration at the crack tip is inappropriate. Although, the infinite stress concept at the tip of the crack is appropriate, the crack tip should be experienced a large stress

concentration. It is already well known that for a circular hole stress should be three times higher than the applied stress. Thus, it can conclude that the method which gives larger stress at the tip of the crack and better distribution near the crack is an appropriate method in terms of solution. From figure 4.33, it is seen that for uniform mesh the stress concentration factor is 2.7 and for mesh refinement technique it is around 3.55. Thus it can be said that MR technique is more accurate than uniform mesh technique for analysis of stress near the vicinity of critical zone. There is an explanation why stress at tip of the crack is not infinite. This is so because one can never take a node at the tip of the crack, he always remains a half mesh length distance from the tip of the crack as shown in figure 4.36. Rectangular box indicates that any condition at this node will be applicable over this area. Dashed box shows crack tip condition implement area and solid box shows crack condition implement area. As a result, the original length of crack is reduced by half mesh length from both sides. The original crack is identified by dark line and reduced crack length is identified by length of all solid boxes in figure 4.36. Now applying r = half mesh length and $\theta = 0$, the eq. 4.2 gives normal stress value σ_y is 3.75 times of applied stress and this is very close to the result of MR technique. Thus MR technique gives better results than uniform mesh technique.

Figure 4.37 shows comparison of normalized normal stress (σ_y/E) at different section of the material. It shows that except y/b=0.0 for other value of y/b results of both techniques matches each other. So we can say that MR technique improves the accuracy of solution in the vicinity of a stress concentrator. Figure 4.38 shows the distribution of normalized normal stress (σ_y/σ_o) obtained by MR technique at different section of the member. It shows that at every section except the singularity section i.e. y/b=0.00, the average of the normal stress (σ_y/σ_o) over any section is equal to that of applied stress, which is another validation of the MR techniques results.

Figure 4.39 shows normalized shear stress distribution at various sections of the material. It shows the upper half of the material exerts a positive shear whereas lower half exerts a negative shear, thus total shear force is balanced. The maximum shear stress occurs at a section which lies immediate after section y/b=0.0

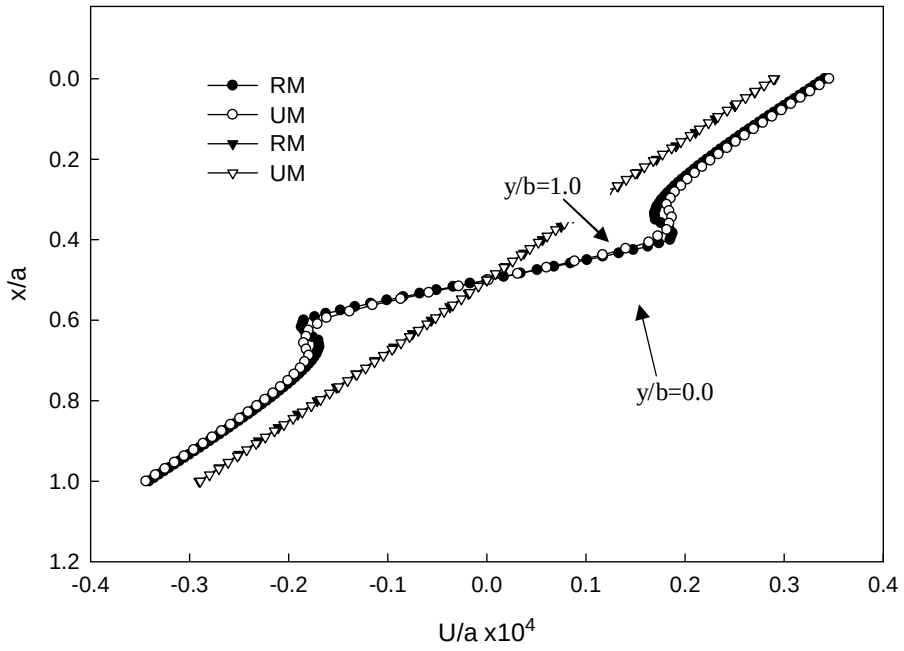

Figure 4.26: Comparison of the results for normalized displacement (u/a) obtained by mesh refinement (MR) technique and uniform mesh (UM) technique with almost equal no. of nodal points.

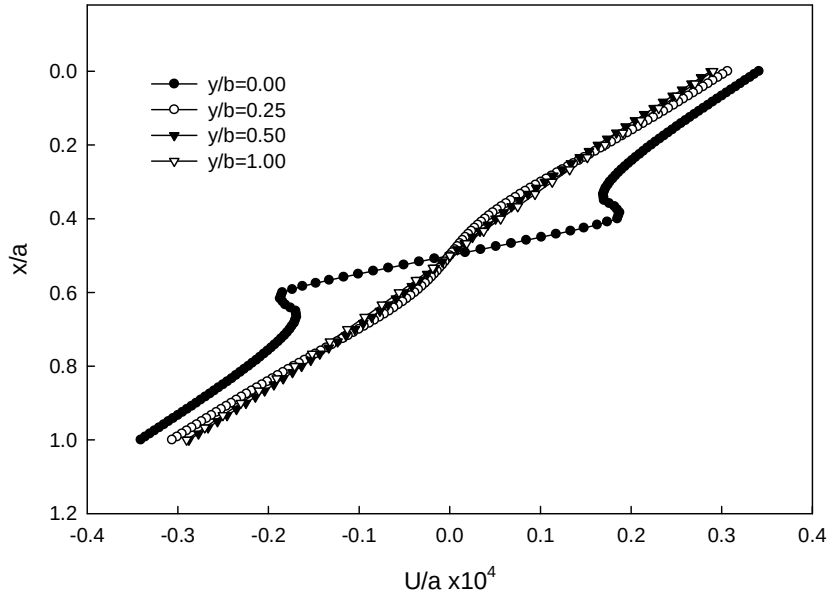

Figure 4.27: Normalized displacement (u/a) obtained by mesh refinement (MR) technique at different section of the member.

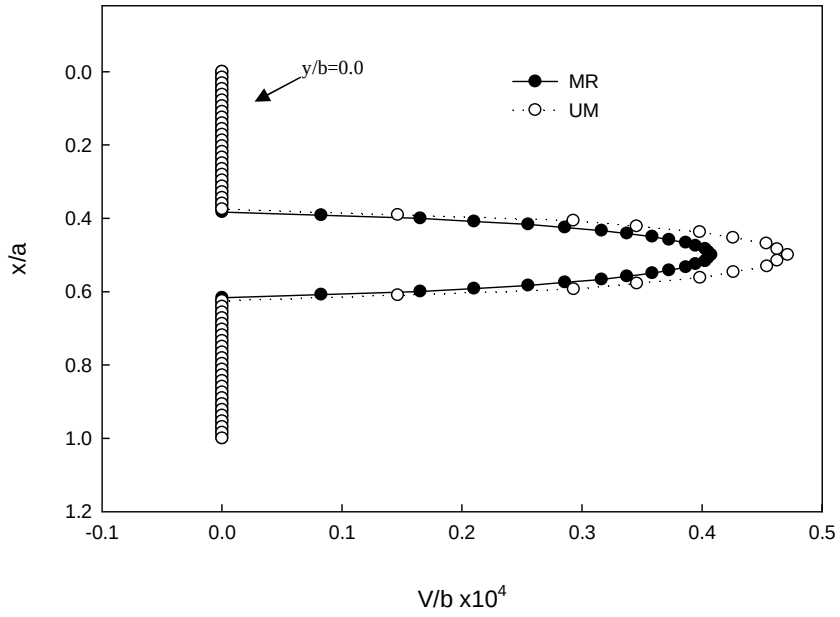

Figure 4.28: Comparison of the results for normalized displacement (v/b) obtained by MR technique and UM technique with almost equal no. of nodal points.

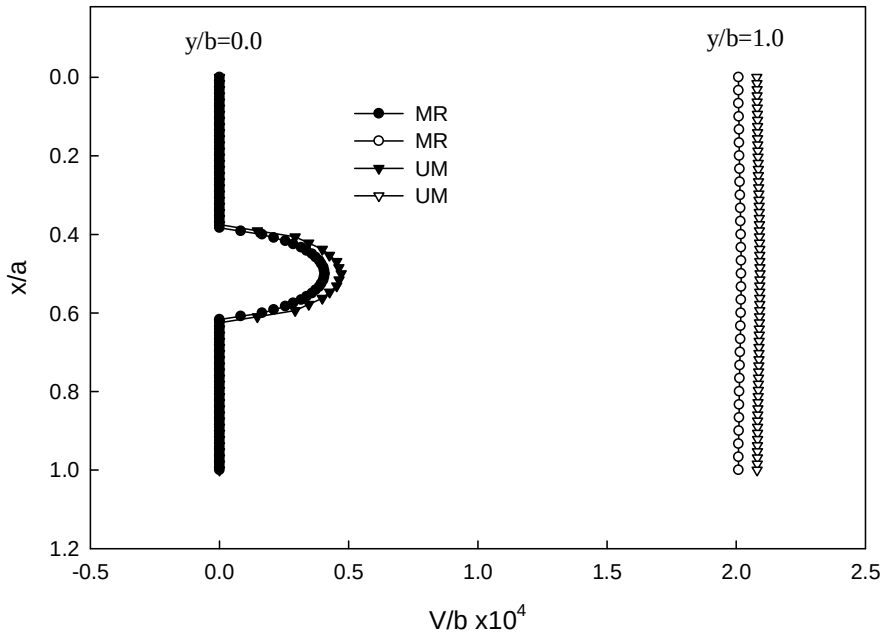

Figure 4.29: Comparison of the results for normalized displacement (v/b) obtained by MR technique and UM technique with almost same no. of nodal points.

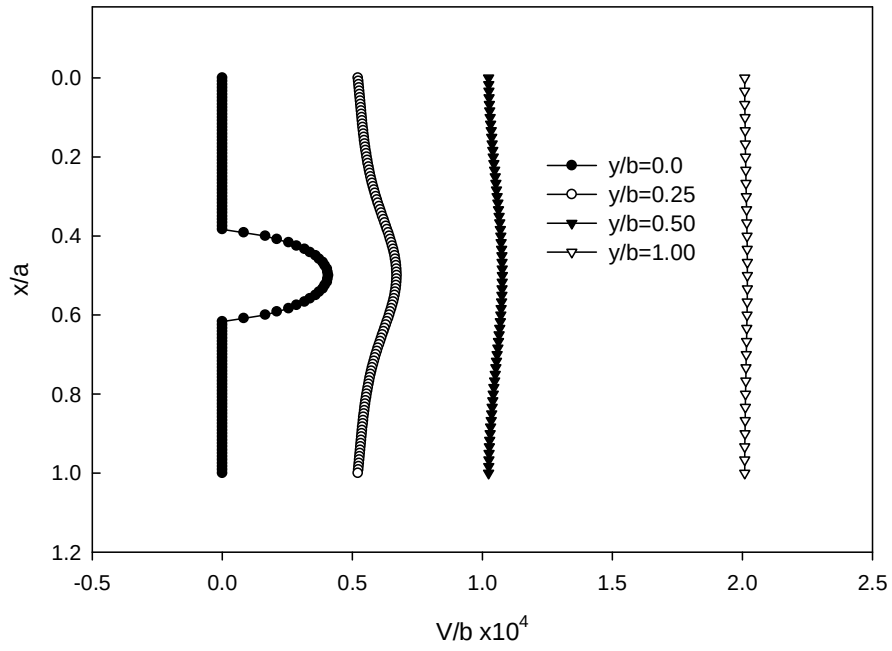

Figure 4.30: Normalized displacement (v/b) obtained by mesh refinement (MR) technique at different section of the material.

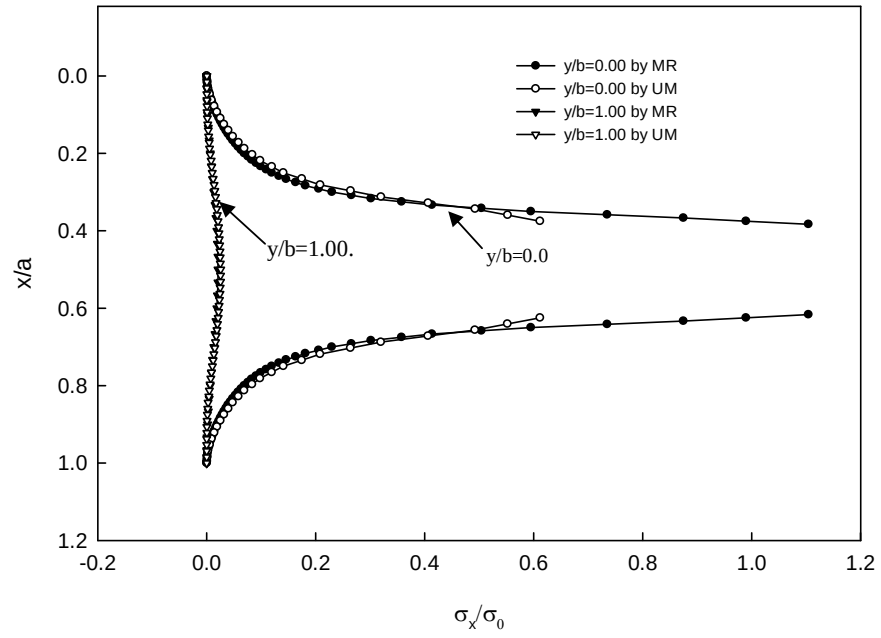

Figure 4.31: Comparison of the results for normalized normal stress (σ_x/σ_o) obtained by MR technique and UM technique with almost equal no. of nodal points.

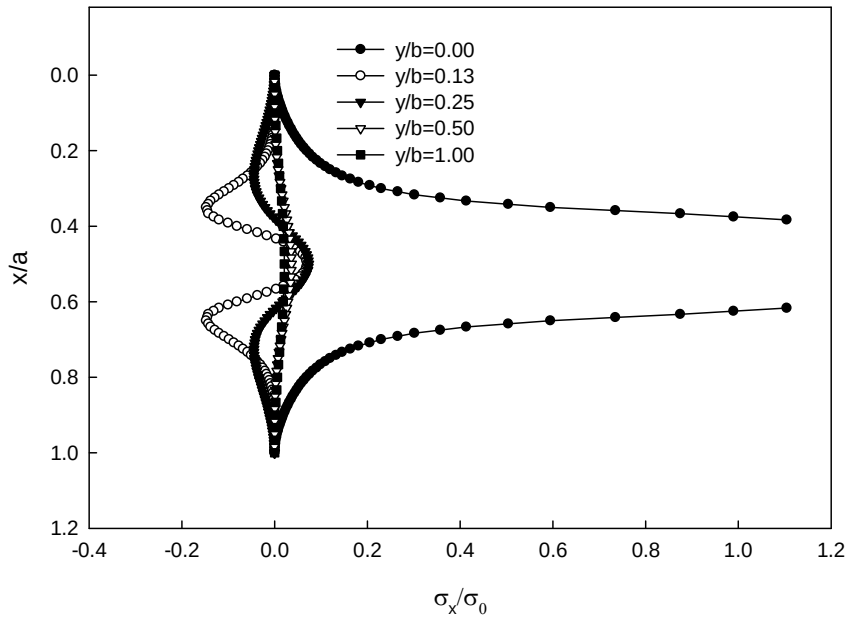

Figure 4.32: Distribution of normalized normal stress (σ_x/σ_o) obtained by MR technique at different section of the material.

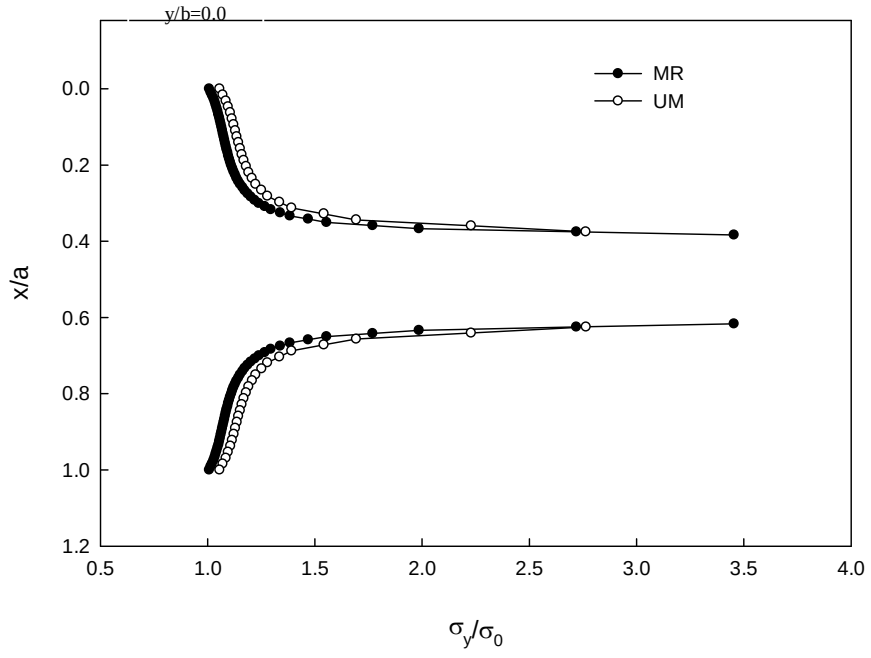

Figure 4.33: Comparison of the results for normalized normal stress (σ_y/σ_o) obtained by MR technique and UM technique with almost equal no. of nodal points.

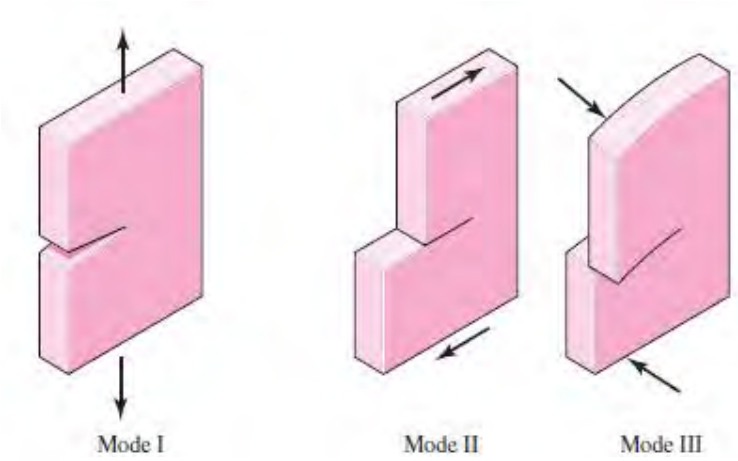

a) b) c)

Figure 4.34: Crack propagation modes.

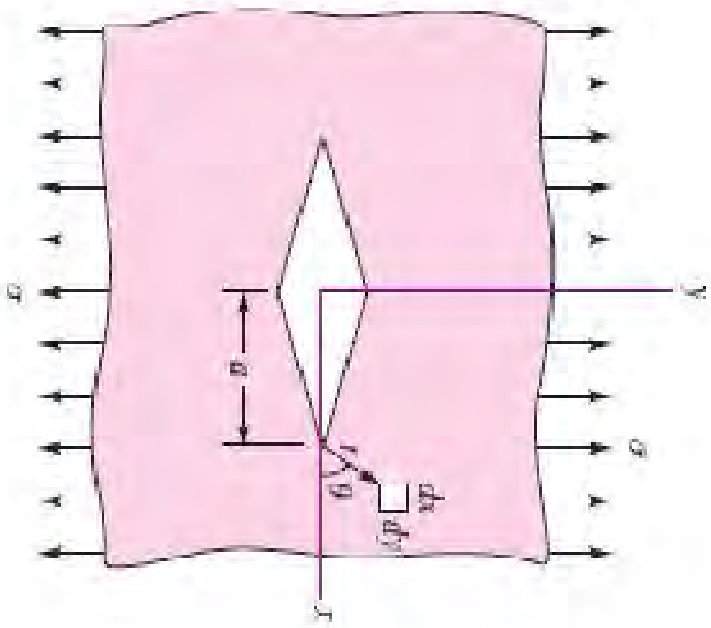

Figure 4.35: A transverse crack of mode-I in an infinite plate located in tension.

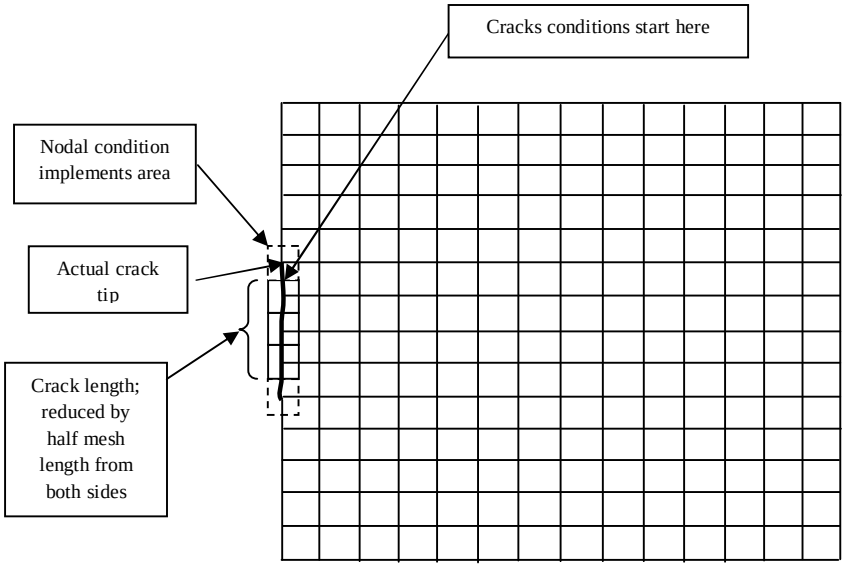

Figure 4.36: Effect of nodal condition on the length of the crack.

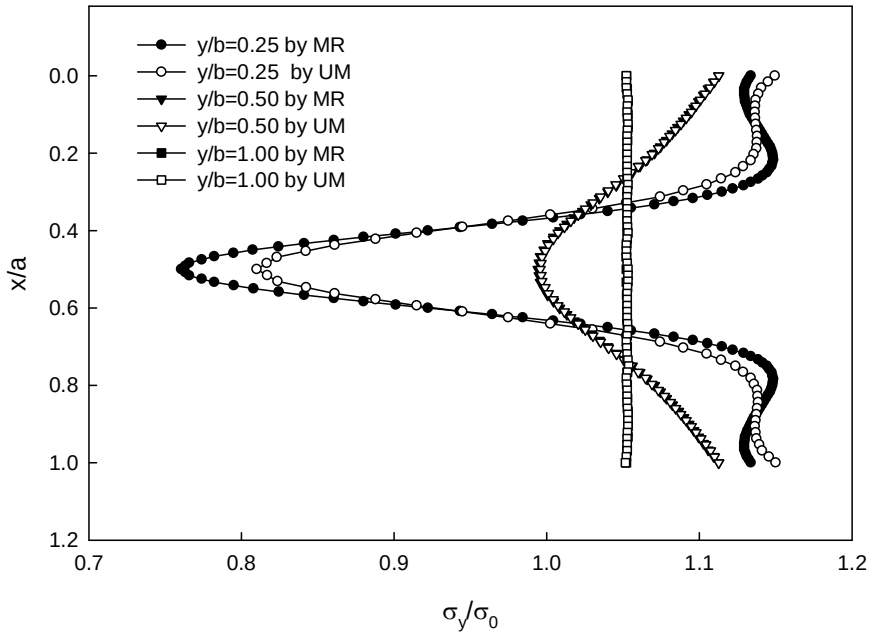

Figure 4.37: Comparison of the results for normalized normal stress (σ_y/σ_o) obtained by MR technique and UM technique with almost equal no. of nodal points at different section of member.

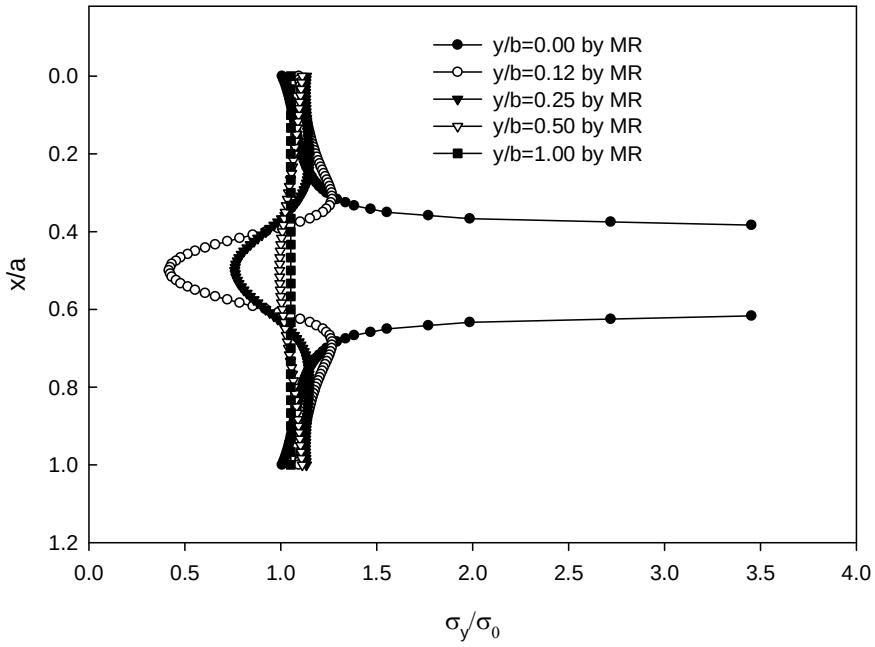

Figure 4.38: Distribution of normalized normal stress (σ_y/σ_o) obtained by MR technique at different section of the member.

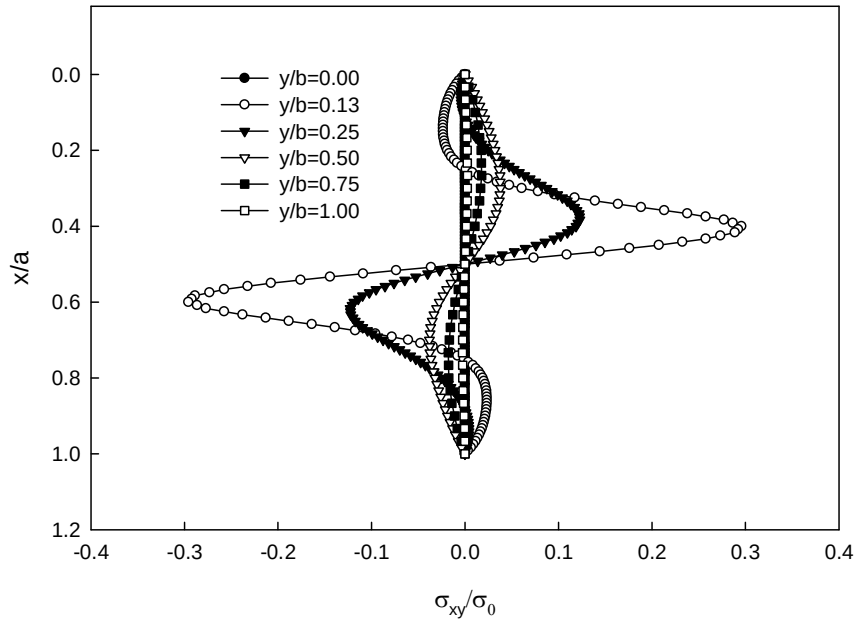

Figure 4.39: Distribution of normalized normal stress (σ_{xy}/σ_o) obtained by MR technique at different section of the member.

4.3.3 Comparison of results of embedded crack with literature and FEM

In previous two sections, results of MR technique are compared with uniform mesh technique and two exclusive features of MR technique have been established, namely: reductions of meshes save computational resources and for equal no. of nodal points increase the accuracy of the solution. In this section, results of MR technique of same problem (figure 4.13) will be compared with literature and FEM. The necessary boundary conditions for solving the problem are shown in figure 4.14. For comparison purpose, under FEM the numerical field is discretized 101x101 nodal points that is the mesh size (h/a x k/b) becomes 0.01 x 0.01. This gives around 10201 meshes and around 10000 elements. Under MR technique, three different sizes of mesh are considered. The finest mesh size is equal to 0.01 x 0.01 and it is taken at the crack end and is covered up to y/b=0.25. The size of the fine mesh is 0.02 x 0.02 and it covers from y/b=0.26 to y/b=0.50. The size of the coarse mesh is 0.04 x 0.04 and it covers from y/b>0.50 to y/b=1.00. The discretzation process is shown in figure 4.40, which contains around 3500 nodal points.

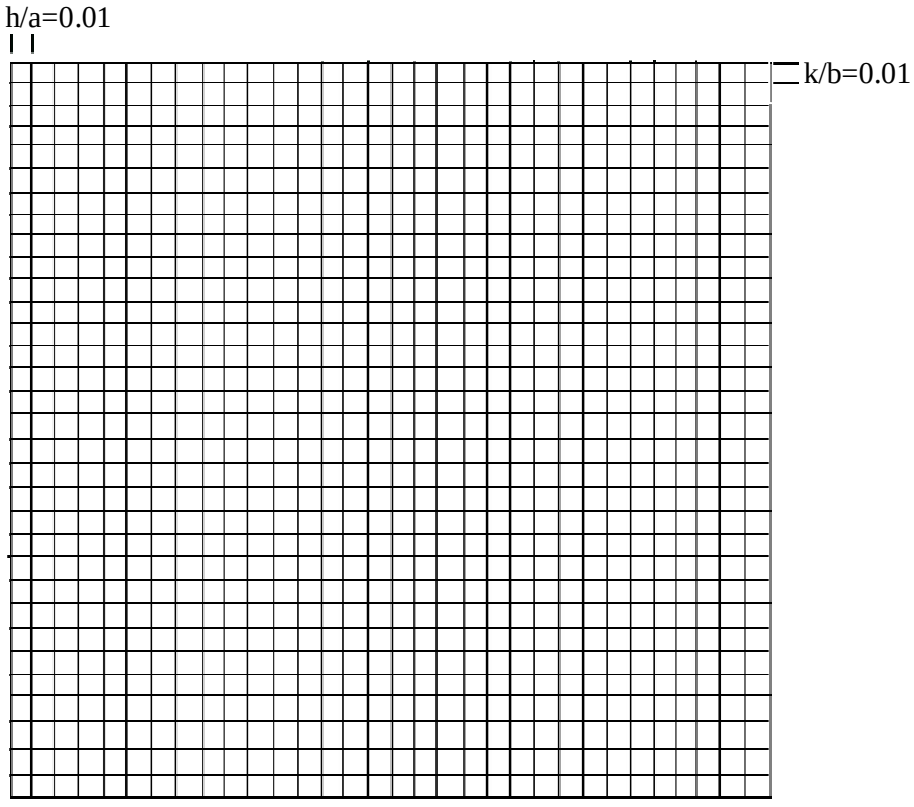

a) Discretization of domain under FEM.

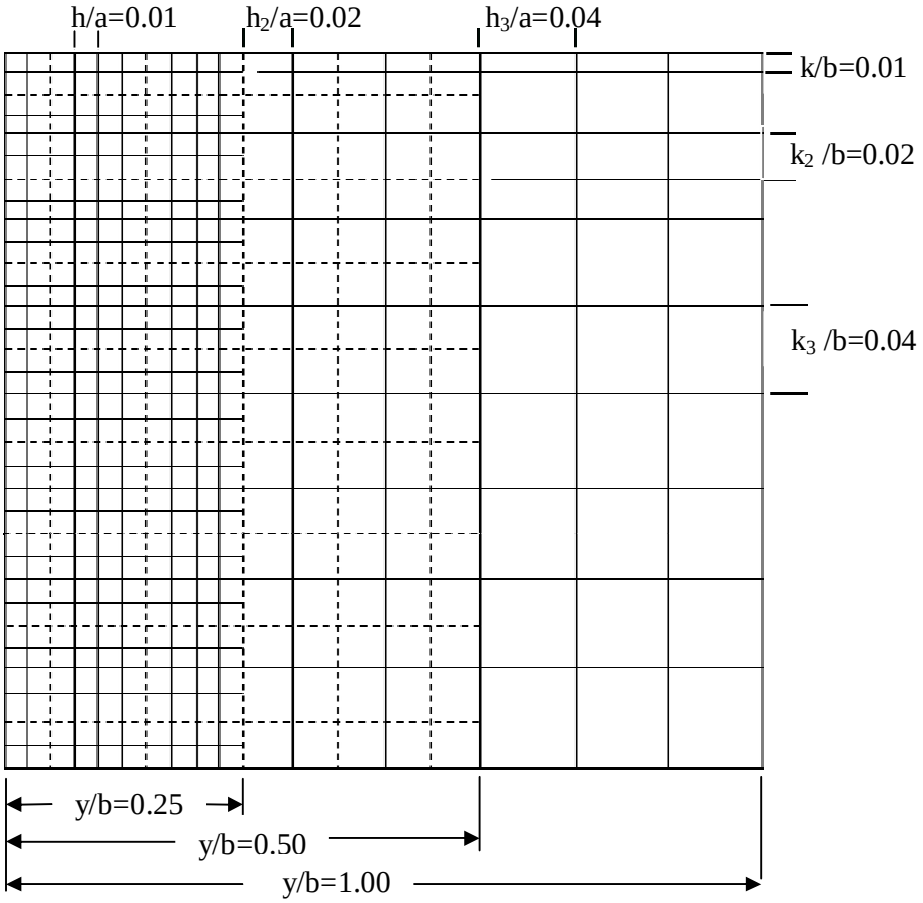

b) Discretiztion process under mesh refinement process.

Figure 4.40: Discretization process of domain under MR FDM and FEM.

The results of both methods are shown as a comparative study from figure 4.41 to 4.44. The figure 4.41 shows displacement component u/a at four different section of the material. Figure 4.41a shows u/a distribution at section y/b=0.0. It is seen that for both methods displacement at upper edge of the member is positive and that for lower end is negative. From our experience and theory of elasticity support this nature of the displacement. Results of both methods match each other although at the tip of the crack FEM gives higher displacement than mesh refinement technique. Figure 4.41b, 4.41c and 4.41d shows distribution of u/a at section y/b=0.25, 0.50 and 1.00 respectively. At every cases MR results matches with FEM results although FEM plays with much greater no of nodal points than MR technique.

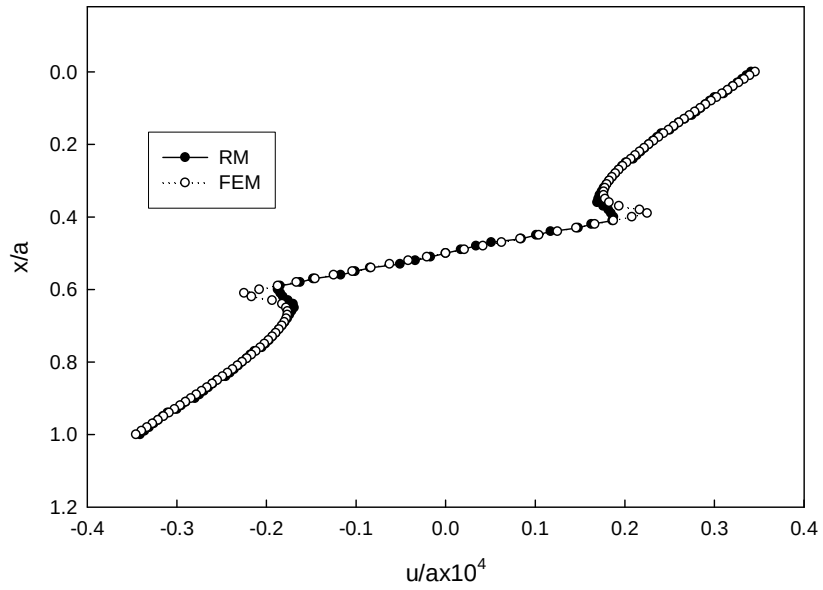

a) u/a distribution at y/b=0.00.

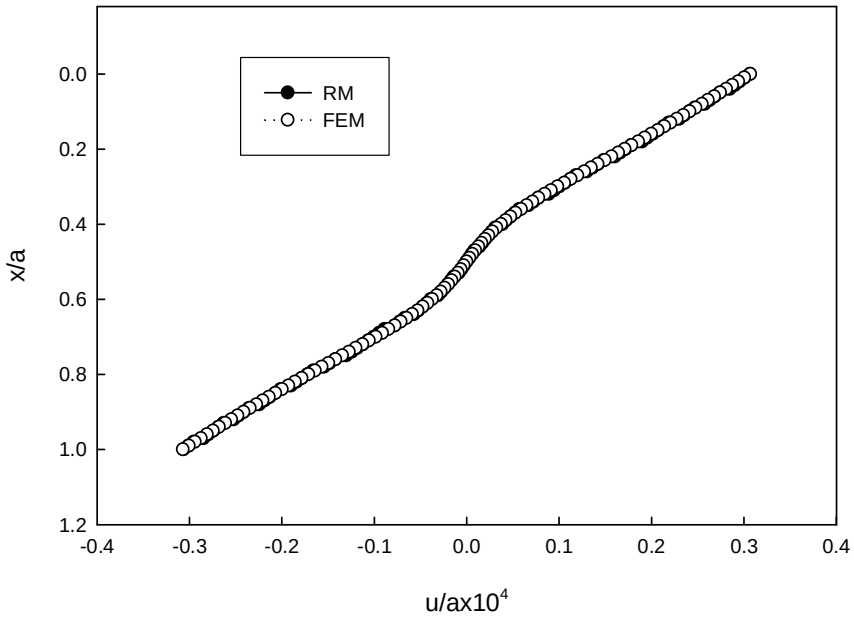

b) u/a distribution at y/b=0.25

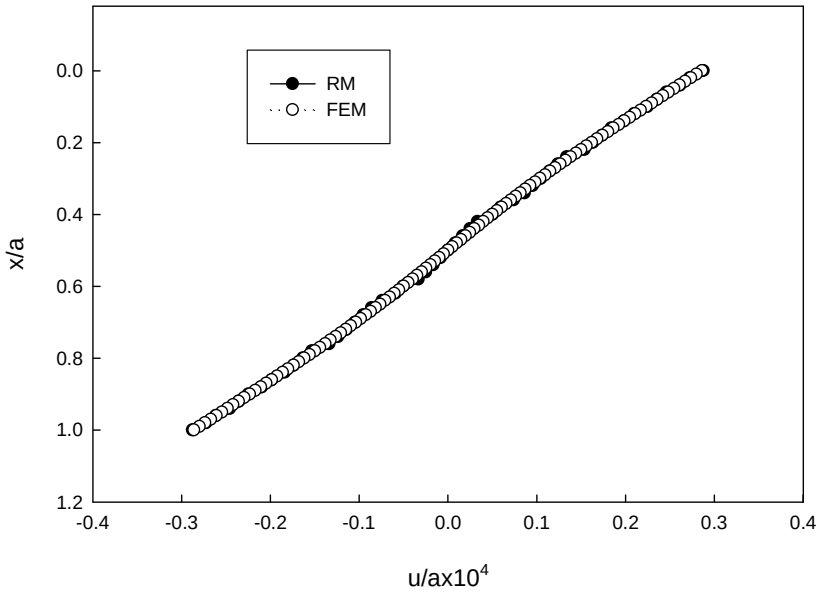

c) u/a distribution at y/b=0.50

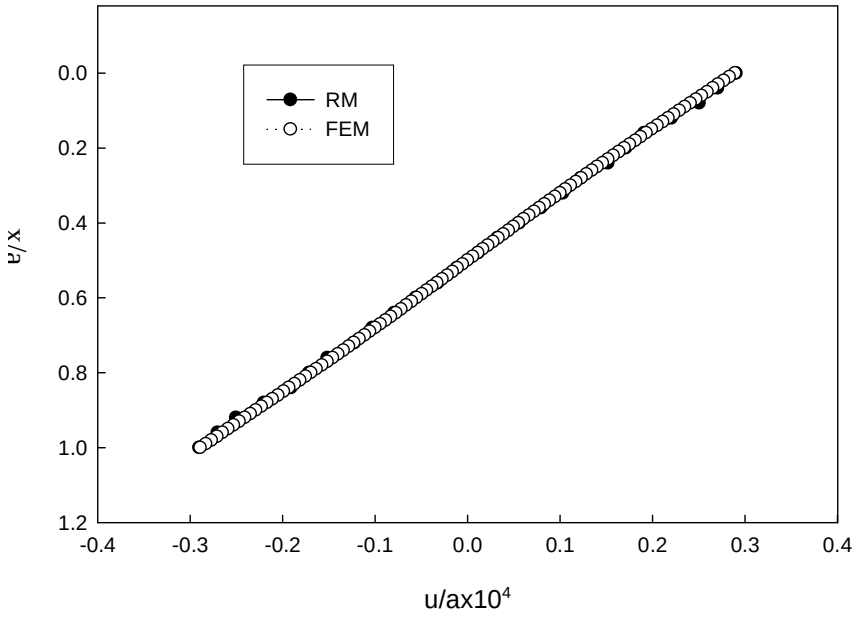

d) u/a distribution at y/b=1.00

Figure 3.41: Comparison of results u/a at different sections of the member of MR technique and FEM.

Figure 4.42 shows displacement component v/b at different sections of the member. Figure 4.42a and 4.42b show v/b distribution at sections y/b=0.00 and y/b=0.25 respectively. Whereas figure 4.42c shows v/b distribution at sections y/b=0.50 and y/b=1.00. In section y/b=0.00, both methods give almost same results but as the y/b increases the deviation in displacement of these two methods increase. And the largest deviation occurs at right edge of the member. In every section, the FEM gives somewhat larger displacement than MR technique. In section y/b=0.00 to y/b=0.50 the largest displacement occurs at the centre of the cracks i.e. x/a=0.50 for both methods and the displacement for these section reduces as x/a reduces or increases. Beyond the section y/b=0.50, the displacement v/b is almost constant for any value of x/a. This type of distribution occurs because after y/b=0.50 the effect of crack diminishes.

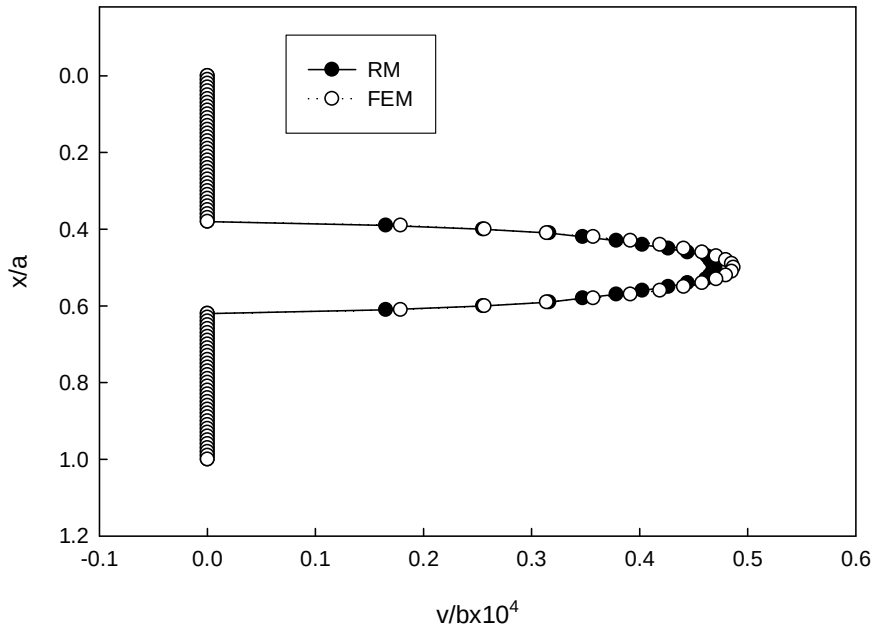

a) distribution of v/b at section y/b=0.00.

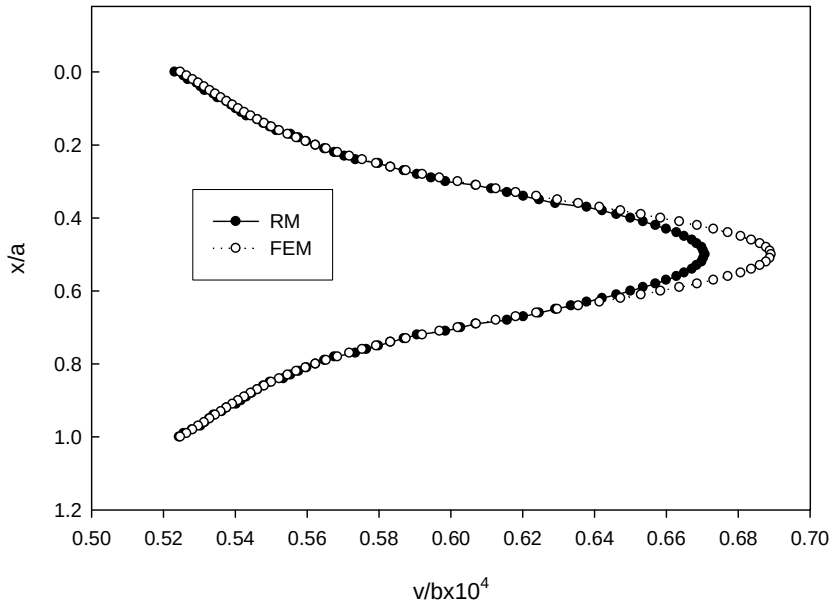

b) distribution of v/b at section y/b=0.25.

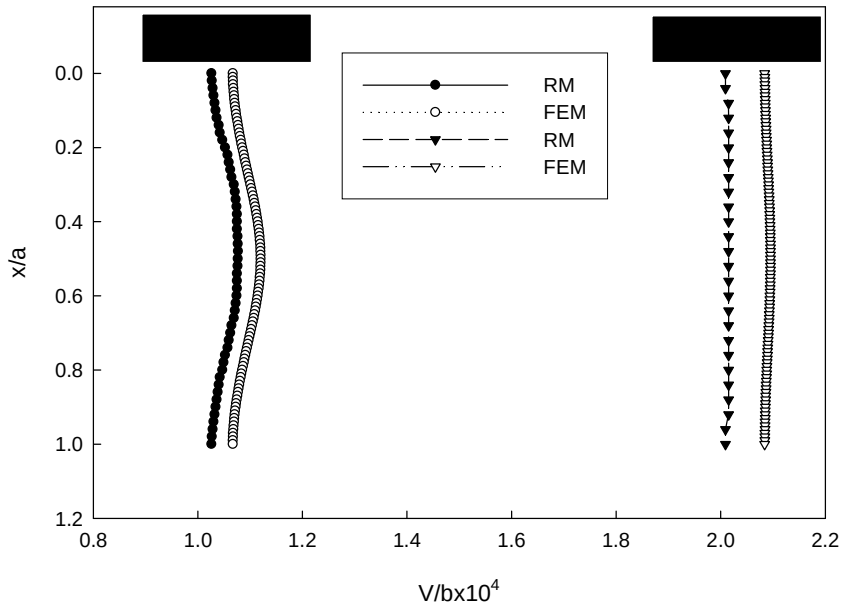

c) distribution of v/b at sections y/b=0.50 and y/b=1.00.

Figure 4.42: Distribution of displacement component, v/b at different sections of the member.

The most important result for this type of problem is the stress component in direction to applied stress and in this case it is σ_y which is shown in figure 4.43. In figure 4.43a, distribution of normal stress σ_y/σ_o at section y/b=0.00 is shown. From this figure it is seen that both methods give almost same results and also the distribution is follows same pattern. The maximum stress is observed as 3.75 for FEM and around 3.8 for MR technique. Following the concept of previous section i.e. one always remains half mesh length distance from the crack tip from eq. 4.2 it is found that the normal stress should become 3.54 times of the applied stress. Thus FEM and MR technique give almost comparable results although MR technique plays with around 40% nodal points of FEM method. Figure 4.44b shows distribution of normal stress σ_y/σ_o at section y/b=0.25. At mid section of the member, the results are almost same for both methods but at singularity points there presents deviation between the results of these two methods. This is results from the inability of FEM in management of boundary. At the boundary FEM cannot find solution directly, it first finds results on element near boundary and then extrapolates it at boundary edge. For this reason deviation occurs at boundary of the member.

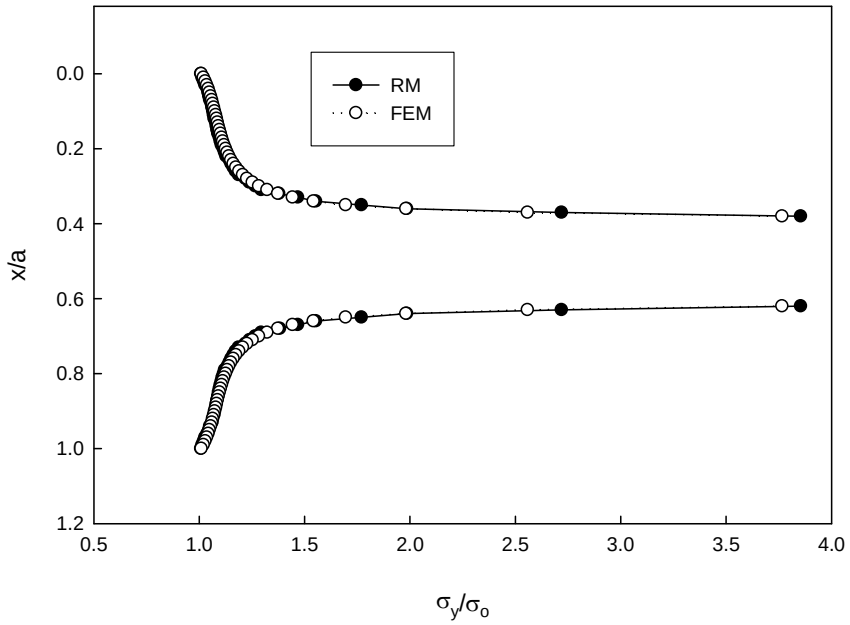

a) distribution of normal stress σ_y/σ_o at section y/b=0.00.

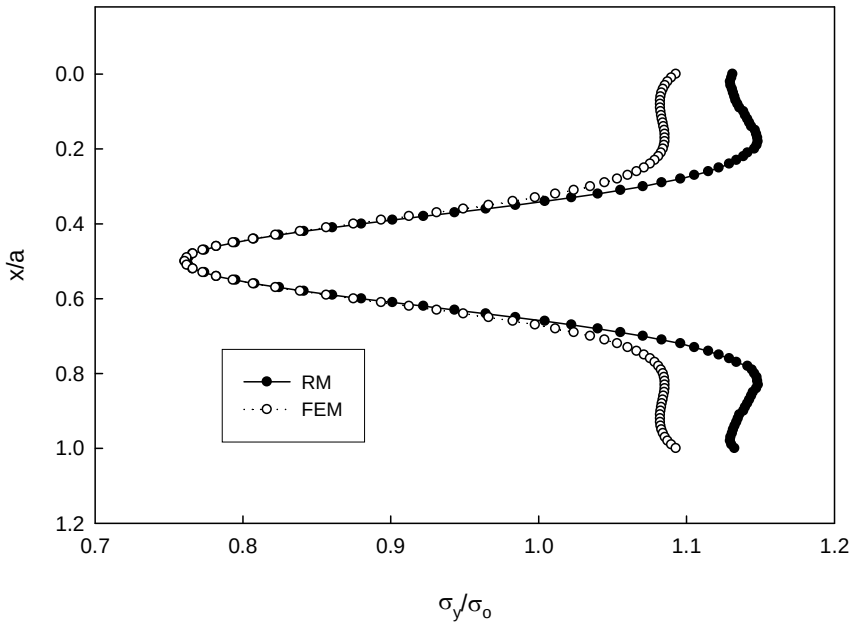

b) distribution of normal stress, σ_y/σ_o at section y/b=0.25.

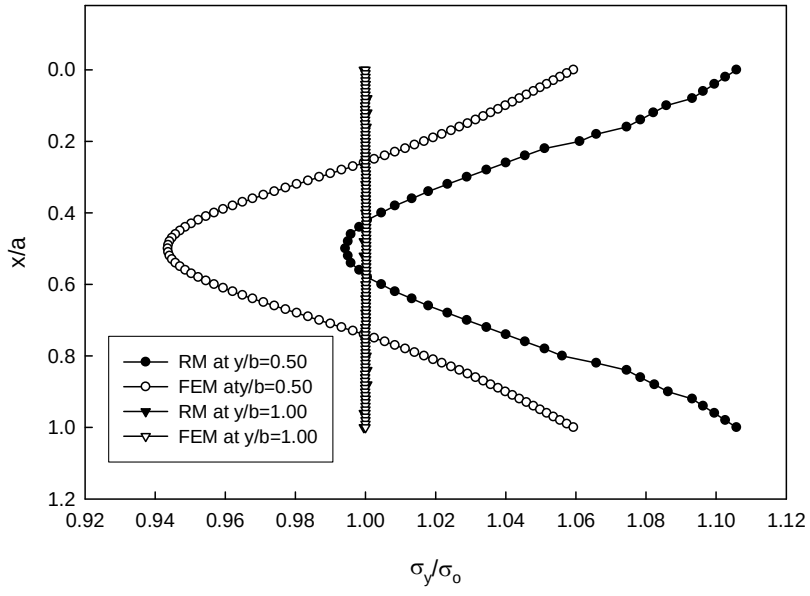

c) distribution of normal stress, σ_y/σ_o at sections y/b=0.50 and y/b=1.00.

Figure 4.43: Distribution of stress component, σ_y/σ_o at different sections of the member.

The normal stress, σ_x/σ_o distribution is shown in figure 4.44. From figure 4.44a, it is seen that the pattern of distribution is similar in both of the methods but FEM give somewhat larger stress than that of mesh refinement technique. The stress distribution of σ_x/σ_o at section y/b=0.00 is looks like the stress distribution of σ_y/σ_o at section y/b=0.00 but intensity of normal stress in y-direction i.e. σ_y/σ_o is larger compared to the stress of x-direction i.e. σ_x/σ_o. The tip of the crack experienced the maximum normal stress in both x- and y- direction (see figure 4.43a and 4.44a) but as x/a value decreases or increases from its value at tip of crack the stress tends to decreases and for both methods it becomes zero at the top and bottom edge of the member. The normal stress,σ_x/σ_o distribution in other sections are shown in figure 4.44b, 4.44c, and 4.44d. All data are presented in tabular form in table 4.1, 4.2 , 4.3 and 4.4.

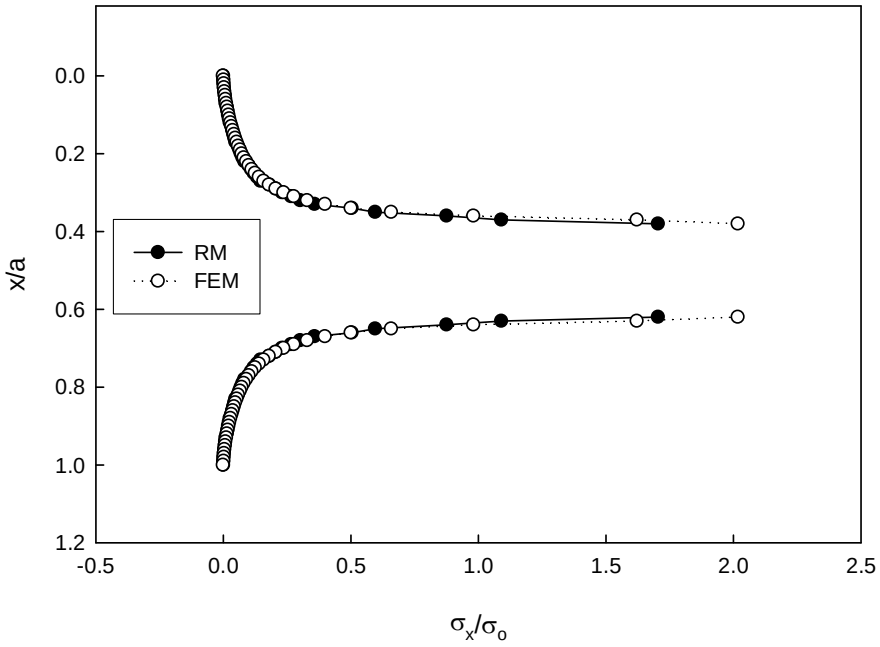

a) distribution of normal stress σ_x/σ_o at section y/b=0.00.

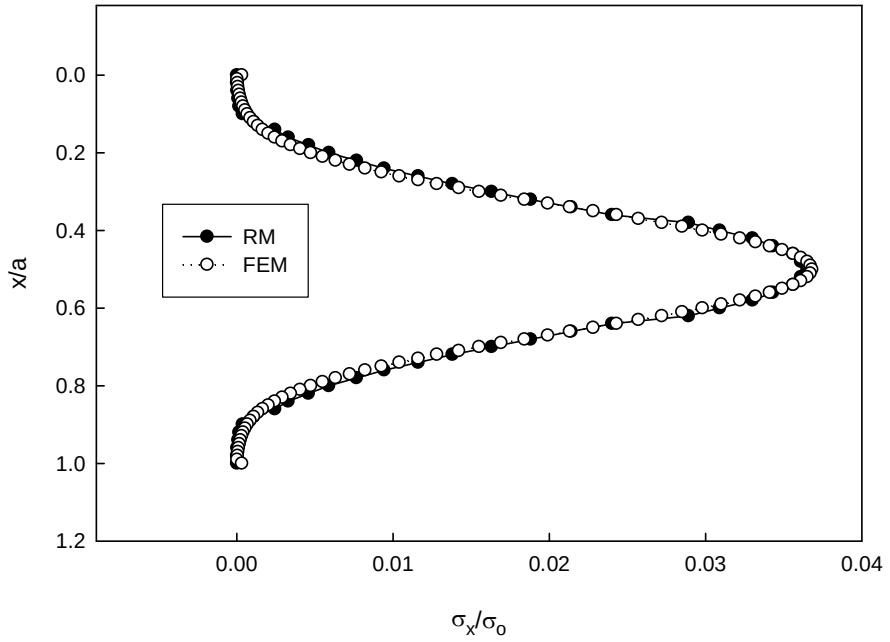

b) distribution of normal stress σ_x/σ_o at section y/b=0.25.

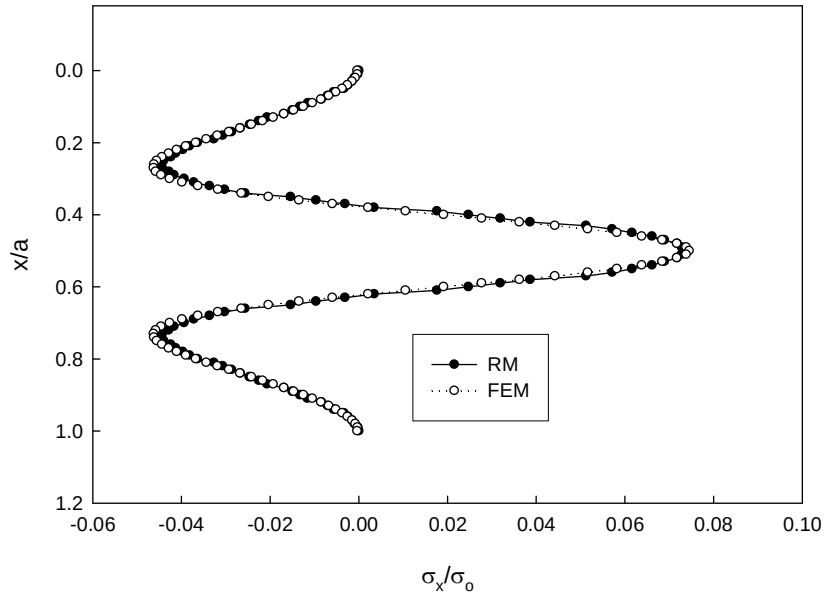

c) distribution of normal stress σ_x/σ_o at section y/b=0.50.

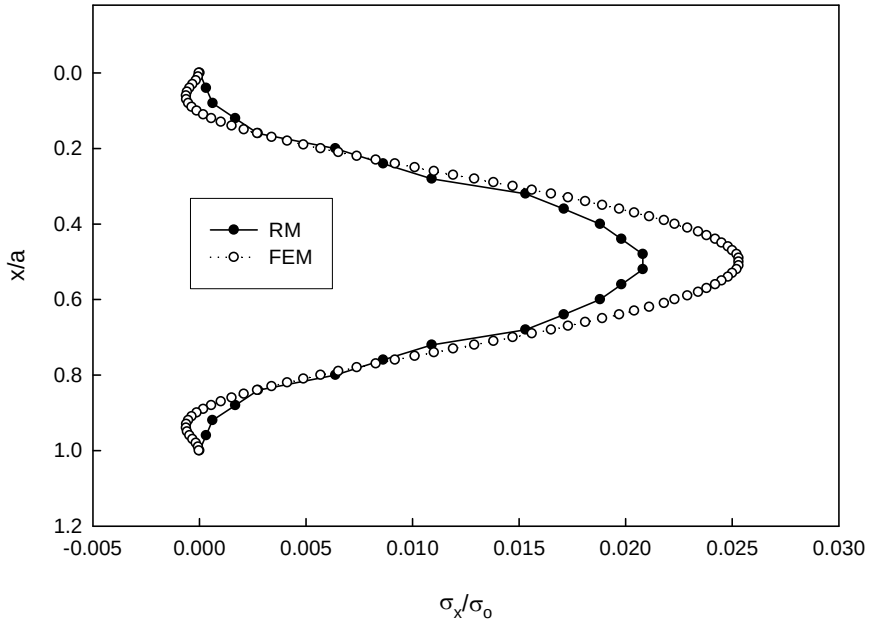

d) distribution of normal stress σ_x/σ_o at section y/b=1.00.

Figure 4.44: Distribution of stress component, σ_x/σ_o at different sections of the member.

Table 4.1: Comparison of results of displacement component u/a at various position of the member by FEM and MR technique.

x/a	u/a(y/b=0)		u/a(y/b=0.25)		u/a(y/b=0.50)		u/a(y/b=1.00)	
	FEM	FDM(MR)	FEM	FDM(MR)	FEM	FDM(MR)	FEM	FDM(MR)
0	3.45E-05	3.41E-05	3.07E-05	3.06E-05	2.86E-05	2.88E-05	2.89E-05	2.90E-05
0.01	3.39E-05	3.36E-05	3.01E-05	3.01E-05	2.80E-05		2.83E-05	
0.02	3.33E-05	3.31E-05	2.94E-05	2.96E-05	2.73E-05	2.72E-05	2.77E-05	
0.03	3.27E-05	3.26E-05	2.88E-05	2.90E-05	2.67E-05		2.71E-05	
0.04	3.21E-05	3.21E-05	2.81E-05	2.85E-05	2.61E-05	2.62E-05	2.65E-05	2.70E-05
0.05	3.15E-05	3.16E-05	2.74E-05	2.74E-05	2.55E-05		2.59E-05	
0.06	3.09E-05	3.10E-05	2.68E-05	2.69E-05	2.48E-05	2.46E-05	2.53E-05	
0.07	3.02E-05	3.00E-05	2.61E-05	2.63E-05	2.42E-05		2.47E-05	
0.08	2.96E-05	2.95E-05	2.55E-05	2.58E-05	2.36E-05	2.35E-05	2.41E-05	2.50E-05
0.09	2.90E-05	2.90E-05	2.48E-05	2.47E-05	2.29E-05		2.35E-05	
0.1	2.84E-05	2.85E-05	2.41E-05	2.41E-05	2.23E-05	2.25E-05	2.29E-05	
0.11	2.78E-05	2.80E-05	2.34E-05	2.36E-05	2.17E-05		2.23E-05	
0.12	2.72E-05	2.75E-05	2.28E-05	2.30E-05	2.11E-05	2.10E-05	2.17E-05	2.21E-05
0.13	2.66E-05	2.67E-05	2.21E-05	2.19E-05	2.05E-05		2.11E-05	
0.14	2.60E-05	2.60E-05	2.14E-05	2.13E-05	1.98E-05	1.98E-05	2.05E-05	
0.15	2.55E-05	2.55E-05	2.07E-05	2.07E-05	1.92E-05		1.99E-05	
0.16	2.49E-05	2.50E-05	2.00E-05	2.02E-05	1.86E-05	1.84E-05	1.93E-05	1.91E-05
0.17	2.43E-05	2.41E-05	1.93E-05	1.96E-05	1.80E-05		1.87E-05	
0.18	2.38E-05	2.36E-05	1.86E-05	1.90E-05	1.74E-05	1.74E-05	1.81E-05	
0.19	2.32E-05	2.31E-05	1.78E-05	1.78E-05	1.68E-05		1.75E-05	
0.2	2.27E-05	2.27E-05	1.71E-05	1.72E-05	1.62E-05	1.64E-05	1.69E-05	1.71E-05
0.21	2.22E-05	2.22E-05	1.64E-05	1.66E-05	1.56E-05		1.63E-05	
0.22	2.17E-05	2.18E-05	1.57E-05	1.60E-05	1.50E-05	1.54E-05	1.58E-05	
0.23	2.12E-05	2.14E-05	1.49E-05	1.48E-05	1.44E-05		1.52E-05	
0.24	2.07E-05	2.09E-05	1.42E-05	1.42E-05	1.38E-05	1.34E-05	1.46E-05	1.52E-05
0.25	2.02E-05	2.01E-05	1.35E-05	1.36E-05	1.32E-05		1.40E-05	
0.26	1.98E-05	1.97E-05	1.27E-05	1.30E-05	1.27E-05	1.24E-05	1.34E-05	
0.27	1.93E-05	1.93E-05	1.20E-05	1.18E-05	1.21E-05		1.29E-05	
0.28	1.89E-05	1.90E-05	1.13E-05	1.12E-05	1.15E-05	1.14E-05	1.23E-05	1.22E-05
0.29	1.86E-05	1.86E-05	1.06E-05	1.06E-05	1.09E-05		1.17E-05	
0.3	1.83E-05	1.83E-05	9.84E-06	1.01E-05	1.04E-05	1.05E-05	1.11E-05	
0.31	1.80E-05	1.80E-05	9.14E-06	9.47E-06	9.81E-06		1.06E-05	
0.32	1.78E-05	1.77E-05	8.45E-06	8.89E-06	9.26E-06	9.55E-06	1.00E-05	1.03E-05
0.33	1.77E-05	1.74E-05	7.78E-06	7.78E-06	8.71E-06		9.44E-06	
0.34	1.76E-05	1.72E-05	7.13E-06	7.24E-06	8.17E-06	8.61E-06	8.87E-06	
0.35	1.78E-05	1.71E-05	6.50E-06	6.71E-06	7.63E-06		8.31E-06	
0.36	1.82E-05	1.69E-05	5.89E-06	5.69E-06	7.09E-06	7.41E-06	7.75E-06	7.95E-06
0.37	1.93E-05	1.76E-05	5.31E-06	5.22E-06	6.56E-06		7.19E-06	
0.38	2.17E-05	1.82E-05	4.75E-06	4.75E-06	6.04E-06	5.93E-06	6.63E-06	

0.39	2.25E-05	1.85E-05	4.22E-06	4.32E-06	5.52E-06		6.07E-06	
0.4	2.08E-05	1.87E-05	3.72E-06	3.88E-06	5.00E-06	5.05E-06	5.51E-06	5.61E-06
0.41	1.87E-05	1.86E-05	3.25E-06	3.09E-06	4.49E-06		4.96E-06	
0.42	1.67E-05	1.63E-05	2.80E-06	2.73E-06	3.98E-06	3.34E-06	4.41E-06	
0.43	1.46E-05	1.48E-05	2.38E-06	2.37E-06	3.47E-06		3.85E-06	
0.44	1.25E-05	1.17E-05	1.99E-06	2.04E-06	2.97E-06	2.50E-06	3.30E-06	3.24E-06
0.45	1.04E-05	1.01E-05	1.62E-06	1.72E-06	2.47E-06		2.75E-06	
0.46	8.32E-06	8.44E-06	1.27E-06	1.41E-06	1.97E-06	1.66E-06	2.20E-06	
0.47	6.24E-06	5.09E-06	9.40E-07	8.33E-07	1.48E-06		1.65E-06	
0.48	4.16E-06	3.40E-06	6.19E-07	5.52E-07	9.86E-07	8.32E-07	1.10E-06	1.17E-06
0.49	2.08E-06	1.70E-06	3.07E-07	2.76E-07	4.93E-07		5.49E-07	
0.5	0	9.94E-09	3.12E-16	-7.00E-10	4.43E-16	2.41E-09	7.27E-16	
0.51	-2.08E-06	-1.69E-06	-3.07E-07	-2.72E-07	-4.93E-07		-5.49E-07	
0.52	-4.16E-06	-3.39E-06	-6.19E-07	-5.44E-07	-9.86E-07	-8.27E-07	-1.10E-06	-1.17E-06
0.53	-6.24E-06	-5.08E-06	-9.40E-07	-8.25E-07	-1.48E-06		-1.65E-06	
0.54	-8.32E-06	-8.43E-06	-1.27E-06	-1.41E-06	-1.97E-06	-1.66E-06	-2.20E-06	
0.55	-1.04E-05	-1.01E-05	-1.62E-06	-1.71E-06	-2.47E-06		-2.75E-06	
0.56	-1.25E-05	-1.17E-05	-1.99E-06	-2.03E-06	-2.97E-06	-2.49E-06	-3.30E-06	-3.24E-06
0.57	-1.46E-05	-1.48E-05	-2.38E-06	-2.36E-06	-3.47E-06		-3.85E-06	
0.58	-1.67E-05	-1.63E-05	-2.80E-06	-2.72E-06	-3.98E-06	-3.33E-06	-4.41E-06	
0.59	-1.87E-05	-1.85E-05	-3.25E-06	-3.08E-06	-4.49E-06		-4.96E-06	
0.6	-2.08E-05	-1.87E-05	-3.72E-06	-3.87E-06	-5.00E-06	-5.04E-06	-5.51E-06	-5.61E-06
0.61	-2.25E-05	-1.84E-05	-4.22E-06	-4.31E-06	-5.52E-06		-6.07E-06	
0.62	-2.17E-05	-1.82E-05	-4.75E-06	-4.74E-06	-6.04E-06	-5.92E-06	-6.63E-06	
0.63	-1.93E-05	-1.76E-05	-5.31E-06	-5.21E-06	-6.56E-06		-7.19E-06	
0.64	-1.82E-05	-1.70E-05	-5.89E-06	-5.69E-06	-7.09E-06	-7.40E-06	-7.75E-06	-7.95E-06
0.65	-1.78E-05	-1.69E-05	-6.50E-06	-6.70E-06	-7.63E-06		-8.31E-06	
0.66	-1.76E-05	-1.72E-05	-7.13E-06	-7.23E-06	-8.17E-06	-8.61E-06	-8.87E-06	
0.67	-1.77E-05	-1.74E-05	-7.78E-06	-7.77E-06	-8.71E-06		-9.44E-06	
0.68	-1.78E-05	-1.77E-05	-8.45E-06	-8.89E-06	-9.26E-06	-9.54E-06	-1.00E-05	-1.03E-05
0.69	-1.80E-05	-1.80E-05	-9.14E-06	-9.46E-06	-9.81E-06		-1.06E-05	
0.7	-1.83E-05	-1.83E-05	-9.84E-06	-1.00E-05	-1.04E-05	-1.05E-05	-1.11E-05	
0.71	-1.86E-05	-1.86E-05	-1.06E-05	-1.06E-05	-1.09E-05		-1.17E-05	
0.72	-1.89E-05	-1.89E-05	-1.13E-05	-1.12E-05	-1.15E-05	-1.14E-05	-1.23E-05	-1.22E-05
0.73	-1.93E-05	-1.93E-05	-1.20E-05	-1.18E-05	-1.21E-05		-1.29E-05	
0.74	-1.98E-05	-1.97E-05	-1.27E-05	-1.24E-05	-1.27E-05	-1.24E-05	-1.34E-05	
0.75	-2.02E-05	-2.01E-05	-1.35E-05	-1.30E-05	-1.32E-05		-1.40E-05	
0.76	-2.07E-05	-2.05E-05	-1.42E-05	-1.42E-05	-1.38E-05	-1.34E-05	-1.46E-05	-1.52E-05
0.77	-2.12E-05	-2.13E-05	-1.49E-05	-1.48E-05	-1.44E-05		-1.52E-05	
0.78	-2.17E-05	-2.18E-05	-1.57E-05	-1.54E-05	-1.50E-05	-1.53E-05	-1.58E-05	
0.79	-2.22E-05	-2.22E-05	-1.64E-05	-1.66E-05	-1.56E-05		-1.63E-05	
0.8	-2.27E-05	-2.27E-05	-1.71E-05	-1.72E-05	-1.62E-05	-1.63E-05	-1.69E-05	-1.71E-05
0.81	-2.32E-05	-2.31E-05	-1.78E-05	-1.78E-05	-1.68E-05		-1.75E-05	
0.82	-2.38E-05	-2.36E-05	-1.86E-05	-1.84E-05	-1.74E-05	-1.74E-05	-1.81E-05	

0.83	-2.43E-05	-2.41E-05	-1.93E-05	-1.90E-05	-1.80E-05		-1.87E-05	
0.84	-2.49E-05	-2.45E-05	-2.00E-05	-2.01E-05	-1.86E-05	-1.84E-05	-1.93E-05	-1.91E-05
0.85	-2.55E-05	-2.55E-05	-2.07E-05	-2.07E-05	-1.92E-05		-1.99E-05	
0.86	-2.60E-05	-2.60E-05	-2.14E-05	-2.13E-05	-1.98E-05	-1.98E-05	-2.05E-05	
0.87	-2.66E-05	-2.65E-05	-2.21E-05	-2.19E-05	-2.05E-05		-2.11E-05	
0.88	-2.72E-05	-2.70E-05	-2.28E-05	-2.24E-05	-2.11E-05	-2.10E-05	-2.17E-05	-2.21E-05
0.89	-2.78E-05	-2.75E-05	-2.34E-05	-2.35E-05	-2.17E-05		-2.23E-05	
0.9	-2.84E-05	-2.80E-05	-2.41E-05	-2.41E-05	-2.23E-05	-2.25E-05	-2.29E-05	
0.91	-2.90E-05	-2.90E-05	-2.48E-05	-2.47E-05	-2.29E-05		-2.35E-05	
0.92	-2.96E-05	-2.95E-05	-2.55E-05	-2.52E-05	-2.36E-05	-2.35E-05	-2.41E-05	-2.50E-05
0.93	-3.02E-05	-3.00E-05	-2.61E-05	-2.63E-05	-2.42E-05		-2.47E-05	
0.94	-3.09E-05	-3.10E-05	-2.68E-05	-2.68E-05	-2.48E-05	-2.46E-05	-2.53E-05	
0.95	-3.15E-05	-3.15E-05	-2.74E-05	-2.74E-05	-2.55E-05		-2.59E-05	
0.96	-3.21E-05	-3.21E-05	-2.81E-05	-2.79E-05	-2.61E-05	-2.61E-05	-2.65E-05	-2.70E-05
0.97	-3.27E-05	-3.26E-05	-2.88E-05	-2.85E-05	-2.67E-05		-2.71E-05	
0.98	-3.33E-05	-3.31E-05	-2.94E-05	-2.96E-05	-2.73E-05	-2.72E-05	-2.77E-05	
0.99	-3.39E-05	-3.36E-05	-3.01E-05	-3.01E-05	-2.80E-05		-2.83E-05	
1	-3.45E-05	-3.41E-05	-3.07E-05	-3.06E-05	-2.86E-05	-2.88E-05	-2.89E-05	-2.90E-05

Table 4.2: Comparison of results of displacement component u/a at various position of the member by FEM and MR technique.

x/a	v/b(y/b=0)		v/b(y/b=0.25)		v/b(y/b=0.50)		v/b(y/b=1.00)	
	FEM	FDM(MR)	FEM	FDM(MR)	FEM	FDM(MR)	FEM	FDM(MR)
0	0	7.21E-11	5.25E-05	5.23E-05	1.07E-04	1.03E-04	2.08E-04	2.01E-04
0.01	0	-8.56E-12	5.26E-05	5.26E-05	1.07E-04		2.08E-04	
0.02	0	-8.92E-11	5.28E-05	5.27E-05	1.07E-04	1.03E-04	2.08E-04	
0.03	0	-3.41E-11	5.30E-05	5.29E-05	1.07E-04		2.08E-04	
0.04	0	2.10E-11	5.31E-05	5.30E-05	1.07E-04	1.03E-04	2.08E-04	2.01E-04
0.05	0	-1.84E-11	5.33E-05	5.32E-05	1.07E-04		2.08E-04	
0.06	0	-5.77E-11	5.34E-05	5.34E-05	1.07E-04	1.03E-04	2.08E-04	
0.07	0	-3.02E-11	5.36E-05	5.35E-05	1.07E-04		2.09E-04	
0.08	0	-2.65E-12	5.38E-05	5.38E-05	1.07E-04	1.03E-04	2.09E-04	2.02E-04
0.09	0	2.49E-11	5.39E-05	5.39E-05	1.07E-04		2.09E-04	
0.1	0	5.25E-11	5.41E-05	5.40E-05	1.07E-04	1.03E-04	2.09E-04	
0.11	0	5.44E-11	5.43E-05	5.42E-05	1.07E-04		2.09E-04	
0.12	0	5.63E-11	5.44E-05	5.43E-05	1.07E-04	1.04E-04	2.09E-04	2.02E-04
0.13	0	1.70E-11	5.46E-05	5.46E-05	1.08E-04		2.09E-04	
0.14	0	-2.23E-11	5.48E-05	5.48E-05	1.08E-04	1.04E-04	2.09E-04	
0.15	0	3.08E-11	5.50E-05	5.50E-05	1.08E-04		2.09E-04	
0.16	0	8.39E-11	5.52E-05	5.51E-05	1.08E-04	1.04E-04	2.09E-04	2.02E-04
0.17	0	4.65E-11	5.55E-05	5.55E-05	1.08E-04		2.09E-04	
0.18	0	9.13E-12	5.57E-05	5.58E-05	1.08E-04	1.05E-04	2.09E-04	
0.19	0	-2.64E-12	5.60E-05	5.60E-05	1.08E-04		2.09E-04	
0.2	0	-1.44E-11	5.62E-05	5.62E-05	1.09E-04	1.05E-04	2.09E-04	2.02E-04
0.21	0	4.07E-11	5.65E-05	5.65E-05	1.09E-04		2.09E-04	
0.22	0	9.58E-11	5.68E-05	5.68E-05	1.09E-04	1.06E-04	2.09E-04	
0.23	0	3.08E-11	5.72E-05	5.70E-05	1.09E-04		2.09E-04	
0.24	0	-3.41E-11	5.75E-05	5.73E-05	1.09E-04	1.06E-04	2.09E-04	2.02E-04
0.25	0	-4.62E-12	5.79E-05	5.80E-05	1.09E-04		2.09E-04	
0.26	0	2.49E-11	5.83E-05	5.83E-05	1.09E-04	1.06E-04	2.09E-04	
0.27	0	-2.63E-11	5.88E-05	5.87E-05	1.10E-04		2.09E-04	
0.28	0	-7.74E-11	5.92E-05	5.91E-05	1.10E-04	1.06E-04	2.09E-04	2.02E-04
0.29	0	-3.61E-11	5.97E-05	5.95E-05	1.10E-04		2.09E-04	
0.3	0	5.24E-12	6.02E-05	5.99E-05	1.10E-04	1.07E-04	2.09E-04	
0.31	0	-6.59E-12	6.07E-05	6.07E-05	1.10E-04		2.09E-04	
0.32	0	-1.84E-11	6.13E-05	6.11E-05	1.10E-04	1.07E-04	2.09E-04	2.02E-04
0.33	0	-2.68E-12	6.18E-05	6.16E-05	1.11E-04		2.09E-04	
0.34	0	1.31E-11	6.24E-05	6.20E-05	1.11E-04	1.07E-04	2.09E-04	
0.35	0	5.44E-11	6.30E-05	6.25E-05	1.11E-04		2.09E-04	
0.36	0	9.58E-11	6.36E-05	6.29E-05	1.11E-04	1.07E-04	2.09E-04	2.02E-04
0.37	0	5.64E-11	6.41E-05	6.38E-05	1.11E-04		2.09E-04	
0.38	0	1.71E-11	6.47E-05	6.42E-05	1.11E-04	1.08E-04	2.09E-04	

0.39	1.79E-05	1.65E-05	6.53E-05	6.46E-05	1.11E-04		2.09E-04	
0.4	2.56E-05	2.55E-05	6.58E-05	6.50E-05	1.11E-04	1.08E-04	2.09E-04	2.02E-04
0.41	3.14E-05	3.16E-05	6.64E-05	6.54E-05	1.12E-04		2.09E-04	
0.42	3.57E-05	3.47E-05	6.69E-05	6.57E-05	1.12E-04	1.08E-04	2.09E-04	
0.43	3.91E-05	3.78E-05	6.73E-05	6.60E-05	1.12E-04		2.09E-04	
0.44	4.19E-05	4.02E-05	6.77E-05	6.63E-05	1.12E-04	1.08E-04	2.09E-04	2.02E-04
0.45	4.41E-05	4.26E-05	6.81E-05	6.65E-05	1.12E-04		2.10E-04	
0.46	4.58E-05	4.44E-05	6.84E-05	6.67E-05	1.12E-04	1.08E-04	2.10E-04	
0.47	4.71E-05	4.62E-05	6.86E-05	6.68E-05	1.12E-04		2.10E-04	
0.48	4.80E-05	4.65E-05	6.88E-05	6.70E-05	1.12E-04	1.08E-04	2.10E-04	2.02E-04
0.49	4.85E-05	4.68E-05	6.89E-05	6.70E-05	1.12E-04		2.10E-04	
0.5	4.87E-05	4.70E-05	6.89E-05	6.71E-05	1.12E-04	1.08E-04	2.10E-04	
0.51	4.85E-05	4.68E-05	6.89E-05	6.70E-05	1.12E-04		2.10E-04	
0.52	4.80E-05	4.65E-05	6.88E-05	6.70E-05	1.12E-04	1.08E-04	2.10E-04	2.02E-04
0.53	4.71E-05	4.61E-05	6.86E-05	6.68E-05	1.12E-04		2.10E-04	
0.54	4.58E-05	4.44E-05	6.84E-05	6.67E-05	1.12E-04	1.08E-04	2.10E-04	
0.55	4.41E-05	4.26E-05	6.81E-05	6.65E-05	1.12E-04		2.10E-04	
0.56	4.19E-05	4.02E-05	6.77E-05	6.63E-05	1.12E-04	1.08E-04	2.09E-04	2.02E-04
0.57	3.91E-05	3.78E-05	6.73E-05	6.60E-05	1.12E-04		2.09E-04	
0.58	3.57E-05	3.47E-05	6.69E-05	6.57E-05	1.12E-04	1.08E-04	2.09E-04	
0.59	3.14E-05	3.16E-05	6.64E-05	6.54E-05	1.12E-04		2.09E-04	
0.6	2.56E-05	2.55E-05	6.58E-05	6.50E-05	1.11E-04	1.07E-04	2.09E-04	2.02E-04
0.61	1.79E-05	1.65E-05	6.53E-05	6.46E-05	1.11E-04		2.09E-04	
0.62	0	-1.05E-10	6.47E-05	6.42E-05	1.11E-04	1.07E-04	2.09E-04	
0.63	0	1.35E-12	6.41E-05	6.38E-05	1.11E-04		2.09E-04	
0.64	0	1.08E-10	6.36E-05	6.34E-05	1.11E-04	1.07E-04	2.09E-04	2.02E-04
0.65	0	7.81E-11	6.30E-05	6.29E-05	1.11E-04		2.09E-04	
0.66	0	4.86E-11	6.24E-05	6.25E-05	1.11E-04	1.07E-04	2.09E-04	
0.67	0	7.21E-12	6.18E-05	6.20E-05	1.11E-04		2.09E-04	
0.68	0	-3.41E-11	6.13E-05	6.16E-05	1.10E-04	1.06E-04	2.09E-04	2.02E-04
0.69	0	-3.61E-11	6.07E-05	6.07E-05	1.10E-04		2.09E-04	
0.7	0	-3.81E-11	6.02E-05	6.03E-05	1.10E-04	1.06E-04	2.09E-04	
0.71	0	-2.63E-11	5.97E-05	5.99E-05	1.10E-04		2.09E-04	
0.72	0	-1.44E-11	5.92E-05	5.91E-05	1.10E-04	1.06E-04	2.09E-04	2.02E-04
0.73	0	3.67E-11	5.88E-05	5.87E-05	1.10E-04		2.09E-04	
0.74	0	8.79E-11	5.83E-05	5.83E-05	1.09E-04	1.06E-04	2.09E-04	
0.75	0	3.48E-11	5.79E-05	5.80E-05	1.09E-04		2.09E-04	
0.76	0	-1.84E-11	5.75E-05	5.77E-05	1.09E-04	1.05E-04	2.09E-04	2.02E-04
0.77	0	7.21E-12	5.72E-05	5.73E-05	1.09E-04		2.09E-04	
0.78	0	3.28E-11	5.68E-05	5.68E-05	1.09E-04	1.05E-04	2.09E-04	
0.79	0	-2.03E-11	5.65E-05	5.65E-05	1.09E-04		2.09E-04	
0.8	0	-7.35E-11	5.62E-05	5.62E-05	1.09E-04	1.05E-04	2.09E-04	2.02E-04
0.81	0	-8.53E-12	5.60E-05	5.60E-05	1.08E-04		2.09E-04	
0.82	0	5.64E-11	5.57E-05	5.58E-05	1.08E-04	1.04E-04	2.09E-04	

0.83	0	5.64E-11	5.55E-05	5.55E-05	1.08E-04		2.09E-04	
0.84	0	5.64E-11	5.52E-05	5.53E-05	1.08E-04	1.04E-04	2.09E-04	2.02E-04
0.85	0	4.07E-11	5.50E-05	5.50E-05	1.08E-04		2.09E-04	
0.86	0	2.49E-11	5.48E-05	5.48E-05	1.08E-04	1.04E-04	2.09E-04	
0.87	0	3.67E-11	5.46E-05	5.46E-05	1.08E-04		2.09E-04	
0.88	0	4.85E-11	5.44E-05	5.45E-05	1.07E-04	1.04E-04	2.09E-04	2.02E-04
0.89	0	2.10E-11	5.43E-05	5.43E-05	1.07E-04		2.09E-04	
0.9	0	-6.54E-12	5.41E-05	5.42E-05	1.07E-04	1.03E-04	2.09E-04	
0.91	0	1.90E-11	5.39E-05	5.40E-05	1.07E-04		2.09E-04	
0.92	0	4.46E-11	5.38E-05	5.38E-05	1.07E-04	1.03E-04	2.09E-04	2.02E-04
0.93	0	4.46E-11	5.36E-05	5.36E-05	1.07E-04		2.09E-04	
0.94	0	4.46E-11	5.34E-05	5.34E-05	1.07E-04	1.03E-04	2.08E-04	
0.95	0	3.08E-11	5.33E-05	5.33E-05	1.07E-04		2.08E-04	
0.96	0	1.70E-11	5.31E-05	5.32E-05	1.07E-04	1.03E-04	2.08E-04	2.01E-04
0.97	0	3.25E-12	5.30E-05	5.30E-05	1.07E-04		2.08E-04	
0.98	0	-1.05E-11	5.28E-05	5.28E-05	1.07E-04	1.03E-04	2.08E-04	
0.99	0	-1.05E-11	5.26E-05	5.26E-05	1.07E-04		2.08E-04	
1	0	-1.05E-11	5.25E-05	5.24E-05	1.07E-04	1.03E-04	2.08E-04	2.01E-04

Table 4.3: Comparison of results of stress component, (σ_y/σ_o) at various position of the member by FEM and MR technique.

x/a	σ_y/σ_o(y/b=0.00)		σ_y/σ_o (y/b=0.25)		σ_y/σ_o (y/b=0.50)		σ_y/σ_o (y/b=1.00)	
	FEM	FDM(MR)	FEM	FDM(MR)	FEM	FDM(MR)	FEM	FDM(MR)
0	1.01E+00	1.01E+00	1.09E+00	1.13E+00	1.06E+00	1.11E+00	1.00E+00	1.00E+00
0.01	1.02E+00	1.01E+00	1.09E+00	1.13E+00	1.06E+00		1.00E+00	
0.02	1.03E+00	1.02E+00	1.09E+00	1.13E+00	1.06E+00	1.10E+00	1.00E+00	
0.03	1.04E+00	1.03E+00	1.09E+00	1.13E+00	1.05E+00		1.00E+00	
0.04	1.04E+00	1.04E+00	1.08E+00	1.13E+00	1.05E+00	1.10E+00	1.00E+00	1.00E+00
0.05	1.05E+00	1.04E+00	1.08E+00	1.13E+00	1.05E+00		1.00E+00	
0.06	1.05E+00	1.05E+00	1.08E+00	1.13E+00	1.05E+00	1.10E+00	1.00E+00	
0.07	1.06E+00	1.05E+00	1.08E+00	1.13E+00	1.05E+00		1.00E+00	
0.08	1.06E+00	1.06E+00	1.08E+00	1.13E+00	1.04E+00	1.09E+00	1.00E+00	1.00E+00
0.09	1.07E+00	1.06E+00	1.08E+00	1.14E+00	1.04E+00		1.00E+00	
0.1	1.07E+00	1.06E+00	1.08E+00	1.14E+00	1.04E+00	1.09E+00	1.00E+00	
0.11	1.08E+00	1.07E+00	1.08E+00	1.14E+00	1.04E+00		1.00E+00	
0.12	1.08E+00	1.07E+00	1.08E+00	1.14E+00	1.04E+00	1.08E+00	1.00E+00	1.00E+00
0.13	1.09E+00	1.08E+00	1.08E+00	1.14E+00	1.03E+00		1.00E+00	
0.14	1.09E+00	1.08E+00	1.08E+00	1.14E+00	1.03E+00	1.08E+00	1.00E+00	
0.15	1.10E+00	1.08E+00	1.08E+00	1.15E+00	1.03E+00		1.00E+00	
0.16	1.10E+00	1.09E+00	1.09E+00	1.15E+00	1.03E+00	1.07E+00	1.00E+00	1.00E+00
0.17	1.11E+00	1.10E+00	1.09E+00	1.15E+00	1.02E+00		1.00E+00	
0.18	1.11E+00	1.10E+00	1.09E+00	1.15E+00	1.02E+00	1.07E+00	1.00E+00	
0.19	1.12E+00	1.11E+00	1.08E+00	1.15E+00	1.02E+00		1.00E+00	
0.2	1.12E+00	1.12E+00	1.08E+00	1.15E+00	1.02E+00	1.06E+00	1.00E+00	1.00E+00
0.21	1.13E+00	1.12E+00	1.08E+00	1.14E+00	1.01E+00		1.00E+00	
0.22	1.14E+00	1.13E+00	1.08E+00	1.14E+00	1.01E+00	1.05E+00	1.00E+00	
0.23	1.15E+00	1.14E+00	1.08E+00	1.13E+00	1.01E+00		1.00E+00	
0.24	1.16E+00	1.15E+00	1.08E+00	1.13E+00	1.01E+00	1.05E+00	1.00E+00	1.00E+00
0.25	1.17E+00	1.16E+00	1.07E+00	1.12E+00	1.00E+00		1.00E+00	
0.26	1.19E+00	1.17E+00	1.07E+00	1.11E+00	1.00E+00	1.04E+00	1.00E+00	
0.27	1.21E+00	1.19E+00	1.06E+00	1.11E+00	9.96E-01		1.00E+00	
0.28	1.23E+00	1.22E+00	1.05E+00	1.10E+00	9.93E-01	1.03E+00	1.00E+00	1.00E+00
0.29	1.25E+00	1.24E+00	1.04E+00	1.08E+00	9.90E-01		1.00E+00	
0.3	1.28E+00	1.27E+00	1.03E+00	1.07E+00	9.87E-01	1.03E+00	1.00E+00	
0.31	1.32E+00	1.29E+00	1.02E+00	1.06E+00	9.84E-01		1.00E+00	
0.32	1.37E+00	1.38E+00	1.01E+00	1.04E+00	9.80E-01	1.02E+00	1.00E+00	1.00E+00
0.33	1.44E+00	1.47E+00	9.98E-01	1.02E+00	9.77E-01		1.00E+00	
0.34	1.54E+00	1.55E+00	9.83E-01	1.00E+00	9.74E-01	1.02E+00	1.00E+00	
0.35	1.69E+00	1.77E+00	9.66E-01	9.84E-01	9.71E-01		1.00E+00	
0.36	1.98E+00	1.99E+00	9.49E-01	9.64E-01	9.68E-01	1.01E+00	1.00E+00	1.00E+00
0.37	2.56E+00	2.72E+00	9.31E-01	9.43E-01	9.65E-01		1.00E+00	
0.38	3.77E+00	3.85E+00	9.12E-01	9.22E-01	9.62E-01	1.01E+00	1.00E+00	

0.39			8.94E-01	9.01E-01	9.59E-01		1.00E+00	
0.4			8.75E-01	8.80E-01	9.57E-01	1.00E+00	1.00E+00	1.00E+00
0.41			8.56E-01	8.61E-01	9.55E-01		1.00E+00	
0.42			8.39E-01	8.41E-01	9.52E-01	1.00E+00	1.00E+00	
0.43			8.22E-01	8.24E-01	9.50E-01		1.00E+00	
0.44			8.07E-01	8.07E-01	9.49E-01	9.98E-01	1.00E+00	1.00E+00
0.45			7.93E-01	7.95E-01	9.47E-01		1.00E+00	
0.46			7.82E-01	7.82E-01	9.46E-01	9.96E-01	1.00E+00	
0.47			7.73E-01	7.74E-01	9.45E-01		1.00E+00	
0.48			7.66E-01	7.66E-01	9.44E-01	9.95E-01	1.00E+00	1.00E+00
0.49			7.62E-01	7.63E-01	9.44E-01		1.00E+00	
0.5			7.61E-01	7.61E-01	9.44E-01	9.94E-01	1.00E+00	
0.51			7.62E-01	7.63E-01	9.44E-01		1.00E+00	
0.52			7.66E-01	7.66E-01	9.44E-01	9.95E-01	1.00E+00	1.00E+00
0.53			7.73E-01	7.74E-01	9.45E-01		1.00E+00	
0.54			7.82E-01	7.82E-01	9.46E-01	9.96E-01	1.00E+00	
0.55			7.93E-01	7.95E-01	9.47E-01		1.00E+00	
0.56			8.07E-01	8.08E-01	9.49E-01	9.98E-01	1.00E+00	1.00E+00
0.57			8.22E-01	8.25E-01	9.50E-01		1.00E+00	
0.58			8.39E-01	8.41E-01	9.52E-01	1.00E+00	1.00E+00	
0.59			8.56E-01	8.61E-01	9.55E-01		1.00E+00	
0.6			8.75E-01	8.80E-01	9.57E-01	1.00E+00	1.00E+00	1.00E+00
0.61			8.94E-01	9.01E-01	9.59E-01		1.00E+00	
0.62	3.77E+00	3.85E+00	9.12E-01	9.22E-01	9.62E-01	1.01E+00	1.00E+00	
0.63	2.56E+00	2.72E+00	9.31E-01	9.43E-01	9.65E-01		1.00E+00	
0.64	1.98E+00	1.99E+00	9.49E-01	9.64E-01	9.68E-01	1.01E+00	1.00E+00	1.00E+00
0.65	1.69E+00	1.77E+00	9.66E-01	9.84E-01	9.71E-01		1.00E+00	
0.66	1.54E+00	1.55E+00	9.83E-01	1.00E+00	9.74E-01	1.02E+00	1.00E+00	
0.67	1.44E+00	1.47E+00	9.98E-01	1.02E+00	9.77E-01		1.00E+00	
0.68	1.37E+00	1.38E+00	1.01E+00	1.04E+00	9.80E-01	1.02E+00	1.00E+00	1.00E+00
0.69	1.32E+00	1.29E+00	1.02E+00	1.06E+00	9.84E-01		1.00E+00	
0.7	1.28E+00	1.27E+00	1.03E+00	1.07E+00	9.87E-01	1.03E+00	1.00E+00	
0.71	1.25E+00	1.24E+00	1.04E+00	1.08E+00	9.90E-01		1.00E+00	
0.72	1.23E+00	1.22E+00	1.05E+00	1.10E+00	9.93E-01	1.03E+00	1.00E+00	1.00E+00
0.73	1.21E+00	1.19E+00	1.06E+00	1.11E+00	9.96E-01		1.00E+00	
0.74	1.19E+00	1.17E+00	1.07E+00	1.11E+00	1.00E+00	1.04E+00	1.00E+00	
0.75	1.17E+00	1.16E+00	1.07E+00	1.12E+00	1.00E+00		1.00E+00	
0.76	1.16E+00	1.15E+00	1.08E+00	1.13E+00	1.01E+00	1.05E+00	1.00E+00	1.00E+00
0.77	1.15E+00	1.14E+00	1.08E+00	1.13E+00	1.01E+00		1.00E+00	
0.78	1.14E+00	1.13E+00	1.08E+00	1.14E+00	1.01E+00	1.05E+00	1.00E+00	
0.79	1.13E+00	1.12E+00	1.08E+00	1.14E+00	1.01E+00		1.00E+00	
0.8	1.12E+00	1.12E+00	1.08E+00	1.15E+00	1.02E+00	1.06E+00	1.00E+00	1.00E+00
0.81	1.12E+00	1.11E+00	1.08E+00	1.15E+00	1.02E+00		1.00E+00	
0.82	1.11E+00	1.11E+00	1.09E+00	1.15E+00	1.02E+00	1.07E+00	1.00E+00	

0.83	1.11E+00	1.10E+00	1.09E+00	1.15E+00	1.02E+00		1.00E+00	
0.84	1.10E+00	1.10E+00	1.09E+00	1.15E+00	1.03E+00	1.07E+00	1.00E+00	1.00E+00
0.85	1.10E+00	1.09E+00	1.08E+00	1.15E+00	1.03E+00		1.00E+00	
0.86	1.09E+00	1.0882	1.08E+00	1.14E+00	1.03E+00	1.08E+00	1.00E+00	
0.87	1.09E+00	1.0845	1.08E+00	1.1424	1.03E+00		1.00E+00	
0.88	1.08E+00	1.0813	1.08E+00	1.1411	1.04E+00	1.08E+00	1.00E+00	1.00E+00
0.89	1.08E+00	1.078	1.08E+00	1.1397	1.04E+00		1.00E+00	
0.9	1.07E+00	1.0745	1.08E+00	1.1384	1.04E+00	1.09E+00	1.00E+00	
0.91	1.07E+00	1.071	1.08E+00	1.1358	1.04E+00		1.00E+00	
0.92	1.06E+00	1.0645	1.08E+00	1.1347	1.04E+00	1.09E+00	1.00E+00	1.00E+00
0.93	1.06E+00	1.0612	1.08E+00	1.1337	1.05E+00		1.00E+00	
0.94	1.05E+00	1.05E+00	1.08E+00	1.1326	1.05E+00	1.10E+00	1.00E+00	
0.95	1.05E+00	1.05E+00	1.08E+00	1.1316	1.05E+00		1.00E+00	
0.96	1.04E+00	1.04E+00	1.08E+00	1.1308	1.05E+00	1.10E+00	1.00E+00	1.00E+00
0.97	1.04E+00	1.03E+00	1.09E+00	1.1297	1.05E+00		1.00E+00	
0.98	1.03E+00	1.02E+00	1.09E+00	1.1295	1.06E+00	1.10E+00	1.00E+00	
0.99	1.02E+00	1.01E+00	1.09E+00	1.1303	1.06E+00		1.00E+00	
1	1.01E+00	1.01E+00	1.09E+00	1.1324	1.06E+00	1.11E+00	1.00E+00	1.00E+00

Table 4.4: Comparison of results of stress component, (σ_x/σ_o) at various position of the member by FEM and MR technique.

x/a	σ_x/σ_o (y/b=0.00)		σ_x/σ_o (y/b=0.25)		σ_x/σ_o (y/b=0.50)		σ_x/σ_o (y/b=1.00)	
	FEM	FDM(MR)	FEM	FDM(MR)	FEM	FDM(MR)	FEM	FDM(MR)
0	-1.35E-03	1.20E-06	-3.89E-04	-1.21E-06	3.08E-04	4.84E-07	-2.02E-05	1.08E-05
0.01	5.56E-04	3.25E-04	-3.28E-04	-1.93E-04	1.28E-05		-6.12E-05	
0.02	1.35E-03	6.48E-04	-8.01E-04	-9.70E-04	3.09E-05	9.88E-07	-1.70E-04	
0.03	2.60E-03	2.58E-03	-1.55E-03	-1.55E-03	6.02E-05		-3.21E-04	
0.04	4.24E-03	4.06E-03	-2.56E-03	-2.44E-03	1.00E-04	5.46E-06	-4.66E-04	3.17E-04
0.05	6.24E-03	5.54E-03	-3.78E-03	-3.34E-03	1.52E-04		-5.74E-04	
0.06	8.54E-03	7.45E-03	-5.20E-03	-5.66E-03	2.16E-04	7.32E-05	-6.26E-04	
0.07	1.11E-02	9.36E-03	-6.80E-03	-7.04E-03	2.97E-04		-6.11E-04	
0.08	1.40E-02	1.39E-02	-8.56E-03	-8.41E-03	3.97E-04	1.41E-04	-5.24E-04	6.23E-04
0.09	1.71E-02	1.65E-02	-1.05E-02	-1.15E-02	5.20E-04		-3.64E-04	
0.1	2.04E-02	1.91E-02	-1.25E-02	-1.33E-02	6.70E-04	3.66E-04	-1.28E-04	
0.11	2.40E-02	2.20E-02	-1.47E-02	-1.50E-02	8.52E-04		1.80E-04	
0.12	2.79E-02	2.49E-02	-1.69E-02	-1.69E-02	1.07E-03	1.08E-03	5.59E-04	1.68E-03
0.13	3.21E-02	3.15E-02	-1.93E-02	-2.07E-02	1.33E-03		1.01E-03	
0.14	3.65E-02	3.53E-02	-2.17E-02	-2.26E-02	1.64E-03	2.43E-03	1.52E-03	
0.15	4.13E-02	3.90E-02	-2.42E-02	-2.46E-02	2.00E-03		2.09E-03	
0.16	4.65E-02	4.32E-02	-2.68E-02	-2.67E-02	2.42E-03	3.29E-03	2.71E-03	2.75E-03
0.17	5.21E-02	4.75E-02	-2.93E-02	-2.87E-02	2.89E-03		3.39E-03	
0.18	5.82E-02	5.72E-02	-3.19E-02	-3.07E-02	3.44E-03	4.59E-03	4.12E-03	
0.19	6.49E-02	6.29E-02	-3.44E-02	-3.27E-02	4.05E-03		4.88E-03	
0.2	7.22E-02	6.86E-02	-3.68E-02	-3.64E-02	4.73E-03	5.89E-03	5.69E-03	6.38E-03
0.21	8.04E-02	7.54E-02	-3.90E-02	-3.82E-02	5.48E-03		6.52E-03	
0.22	8.94E-02	8.22E-02	-4.11E-02	-3.97E-02	6.31E-03	7.66E-03	7.39E-03	
0.23	9.96E-02	9.86E-02	-4.29E-02	-4.13E-02	7.22E-03		8.27E-03	
0.24	1.11E-01	1.09E-01	-4.44E-02	-4.24E-02	8.20E-03	9.43E-03	9.18E-03	8.62E-03
0.25	1.24E-01	1.19E-01	-4.56E-02	-4.40E-02	9.26E-03		1.01E-02	
0.26	1.40E-01	1.32E-01	-4.62E-02	-4.45E-02	1.04E-02	1.16E-02	1.10E-02	
0.27	1.58E-01	1.46E-01	-4.63E-02	-4.43E-02	1.16E-02		1.19E-02	
0.28	1.79E-01	1.81E-01	-4.58E-02	-4.28E-02	1.28E-02	1.38E-02	1.29E-02	1.09E-02
0.29	2.05E-01	2.05E-01	-4.46E-02	-4.17E-02	1.42E-02		1.38E-02	
0.3	2.36E-01	2.30E-01	-4.27E-02	-3.94E-02	1.55E-02	1.63E-02	1.47E-02	
0.31	2.76E-01	2.65E-01	-3.99E-02	-3.72E-02	1.69E-02		1.56E-02	
0.32	3.28E-01	3.01E-01	-3.63E-02	-3.37E-02	1.84E-02	1.88E-02	1.65E-02	1.53E-02
0.33	3.98E-01	3.57E-01	-3.18E-02	-3.03E-02	1.99E-02		1.73E-02	
0.34	4.99E-01	5.04E-01	-2.65E-02	-2.57E-02	2.13E-02	2.14E-02	1.81E-02	
0.35	6.58E-01	5.95E-01	-2.04E-02	-1.54E-02	2.28E-02		1.89E-02	
0.36	9.81E-01	8.75E-01	-1.35E-02	-9.68E-03	2.43E-02	2.40E-02	1.97E-02	1.71E-02
0.37	1.62E+00	1.09E+00	-5.96E-03	-3.13E-03	2.57E-02		2.04E-02	
0.38	2.02E+00	1.70E+00	2.09E-03	3.43E-03	2.72E-02	2.89E-02	2.11E-02	

0.39			1.05E-02	1.76E-02	2.85E-02		2.18E-02	
0.4			1.91E-02	2.47E-02	2.98E-02	3.09E-02	2.23E-02	1.88E-02
0.41			2.77E-02	3.19E-02	3.10E-02		2.29E-02	
0.42			3.62E-02	3.86E-02	3.22E-02	3.30E-02	2.34E-02	
0.43			4.42E-02	5.12E-02	3.32E-02		2.38E-02	
0.44			5.16E-02	5.71E-02	3.41E-02	3.43E-02	2.42E-02	1.98E-02
0.45			5.82E-02	6.16E-02	3.49E-02		2.45E-02	
0.46			6.38E-02	6.61E-02	3.56E-02	3.56E-02	2.48E-02	
0.47			6.84E-02	6.89E-02	3.61E-02		2.50E-02	
0.48			7.17E-02	7.18E-02	3.65E-02	3.61E-02	2.52E-02	2.08E-02
0.49			7.38E-02	7.28E-02	3.67E-02		2.53E-02	
0.5			7.45E-02	7.37E-02	3.68E-02	3.65E-02	2.53E-02	
0.51			7.38E-02	7.28E-02	3.67E-02		2.53E-02	
0.52			7.17E-02	7.18E-02	3.65E-02	3.61E-02	2.52E-02	2.08E-02
0.53			6.84E-02	6.89E-02	3.61E-02		2.50E-02	
0.54			6.38E-02	6.61E-02	3.56E-02	3.56E-02	2.48E-02	
0.55			5.82E-02	6.16E-02	3.49E-02		2.45E-02	
0.56			5.16E-02	5.71E-02	3.41E-02	3.43E-02	2.42E-02	1.98E-02
0.57			4.42E-02	5.12E-02	3.32E-02		2.38E-02	
0.58			3.62E-02	3.86E-02	3.22E-02	3.30E-02	2.34E-02	
0.59			2.77E-02	3.19E-02	3.10E-02		2.29E-02	
0.6			1.91E-02	2.47E-02	2.98E-02	3.09E-02	2.23E-02	1.88E-02
0.61			1.05E-02	1.76E-02	2.85E-02		2.18E-02	
0.62	2.02E+00	1.70E+00	2.09E-03	3.44E-03	2.72E-02	2.89E-02	2.11E-02	
0.63	1.62E+00	1.09E+00	-5.96E-03	-3.12E-03	2.57E-02		2.04E-02	
0.64	9.81E-01	8.75E-01	-1.35E-02	-9.68E-03	2.43E-02	2.40E-02	1.97E-02	1.71E-02
0.65	6.58E-01	5.95E-01	-2.04E-02	-1.54E-02	2.28E-02		1.89E-02	
0.66	4.99E-01	5.04E-01	-2.65E-02	-2.57E-02	2.13E-02	2.14E-02	1.81E-02	
0.67	3.98E-01	3.57E-01	-3.18E-02	-3.03E-02	1.99E-02		1.73E-02	
0.68	3.28E-01	3.01E-01	-3.63E-02	-3.37E-02	1.84E-02	1.88E-02	1.65E-02	1.53E-02
0.69	2.76E-01	2.65E-01	-3.99E-02	-3.72E-02	1.69E-02		1.56E-02	
0.7	2.36E-01	2.30E-01	-4.27E-02	-3.94E-02	1.55E-02	1.63E-02	1.47E-02	
0.71	2.05E-01	2.05E-01	-4.46E-02	-4.17E-02	1.42E-02		1.38E-02	
0.72	1.79E-01	1.81E-01	-4.58E-02	-4.29E-02	1.28E-02	1.38E-02	1.29E-02	1.09E-02
0.73	1.58E-01	1.46E-01	-4.63E-02	-4.43E-02	1.16E-02		1.19E-02	
0.74	1.40E-01	1.32E-01	-4.62E-02	-4.45E-02	1.04E-02	1.16E-02	1.10E-02	
0.75	1.24E-01	1.19E-01	-4.56E-02	-4.40E-02	9.26E-03		1.01E-02	
0.76	1.11E-01	1.09E-01	-4.44E-02	-4.24E-02	8.20E-03	9.42E-03	9.18E-03	8.63E-03
0.77	9.96E-02	9.86E-02	-4.29E-02	-4.13E-02	7.22E-03		8.27E-03	
0.78	8.94E-02	8.22E-02	-4.11E-02	-3.97E-02	6.31E-03	7.65E-03	7.39E-03	
0.79	8.04E-02	7.54E-02	-3.90E-02	-3.82E-02	5.48E-03		6.52E-03	
0.8	7.22E-02	6.86E-02	-3.68E-02	-3.64E-02	4.73E-03	5.88E-03	5.69E-03	6.38E-03
0.81	6.49E-02	6.29E-02	-3.44E-02	-3.27E-02	4.05E-03		4.88E-03	
0.82	5.82E-02	5.72E-02	-3.19E-02	-3.07E-02	3.44E-03	4.58E-03	4.12E-03	

0.83	5.21E-02	4.75E-02	-2.93E-02	-2.87E-02	2.89E-03		3.39E-03	
0.84	4.65E-02	0.0432	-2.68E-02	-2.67E-02	2.42E-03	3.29E-03	2.71E-03	2.75E-03
0.85	4.13E-02	0.039	-2.42E-02	-0.0247	2.00E-03		2.09E-03	
0.86	3.65E-02	0.0353	-2.17E-02	-0.0226	1.64E-03	2.43E-03	1.52E-03	
0.87	3.21E-02	0.0315	-1.93E-02	-0.0207	1.33E-03		1.01E-03	
0.88	2.79E-02	0.0249	-1.69E-02	-0.0169	1.07E-03	1.08E-03	5.59E-04	1.68E-03
0.89	2.40E-02	0.022	-1.47E-02	-0.015	8.52E-04		1.80E-04	
0.9	2.04E-02	0.0191	-1.25E-02	-0.0133	6.70E-04	3.64E-04	-1.28E-04	
0.91	1.71E-02	0.0165	-1.05E-02	-0.0116	5.20E-04		-3.64E-04	
0.92	1.40E-02	0.0139	-8.56E-03	-8.42E-03	3.97E-04	1.40E-04	-5.24E-04	6.17E-04
0.93	1.11E-02	9.36E-03	-6.80E-03	-7.04E-03	2.97E-04		-6.11E-04	
0.94	8.54E-03	7.47E-03	-5.20E-03	-5.66E-03	2.16E-04	7.29E-05	-6.26E-04	
0.95	6.24E-03	5.57E-03	-3.78E-03	-3.34E-03	1.52E-04		-5.74E-04	
0.96	4.24E-03	4.07E-03	-2.56E-03	-2.45E-03	1.00E-04	5.52E-06	-4.66E-04	3.09E-04
0.97	2.60E-03	2.57E-03	-1.55E-03	-1.55E-03	6.02E-05		-3.21E-04	
0.98	1.35E-03	6.53E-04	-8.01E-04	-9.65E-04	3.09E-05	7.45E-07	-1.70E-04	
0.99	5.56E-04	3.25E-04	-3.28E-04	-1.91E-04	1.28E-05		-6.12E-05	
1	-1.35E-03	-3.10E-06	-3.89E-04	-8.27E-07	3.08E-04	1.73E-07	-2.02E-05	1.98E-06

4.4 Case Study-III: Analysis with Surface Crack

In this section of this thesis, another problem is analyzed for the equal no. of nodes by both MR and UM techniques. The statement of the problem is shown in figure 4.45a, which shows a simple bar having surface crack under uniform tensile stress. Due to symmetric nature of the problem only half section of the problem is considered and this half section with necessary boundary condition is shown in figure 4.45b. Under uniform mesh consideration, the discretization is done by using only one sizes mesh over the whole body. The discretization, under mesh refinement technique, is done only by changing some nodal points of a region of uniform meshing discretization to some other regions. The changing of nodal points from one region to other region must be done with some intelligent otherwise the benefits of mesh refinement will remain under question marks. Here, intensity of the solution of uniform meshing is taken as a criterion to change the position of the nodal points from one region to others region. Nodal points should be changed from lower intensify areas to higher intensify areas. From the results of uniform mesh technique, the left section of the material (figure 4.45b) i.e y/b=0.0 to y/b=0.25 can be taken as higher intensify area as shown in figure 4.46. So, nodal points from right section of the domain should be changed to left section of the material as shown in figure 4.47a and b. Thus, uniform meshing become non-uniform and uniform meshing contain only one mesh length, h_2 in x-axis direction whereas mesh refinement contain three different mesh length, h_1, h_2 and h_3. There is a relation between h_1, h_2 and h_3 and this is $h_1=h_2/2=h_3/4$. This has been taken for simplifying the problems.

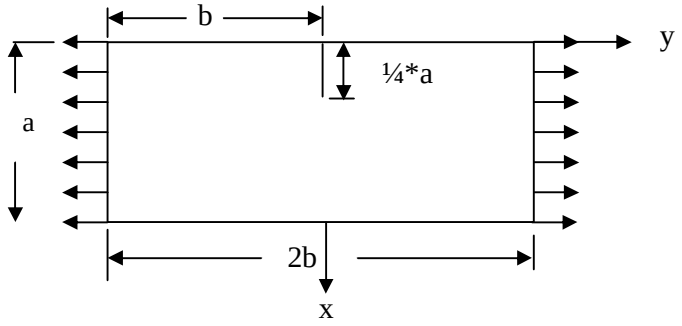

Figure 4.45a: A simple bar under uniform tensile loading.

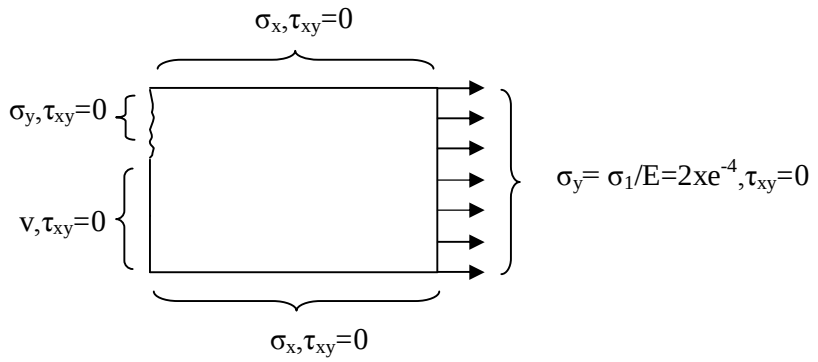

Figure 4.45b: Half section of the problem with necessary boundary condition.

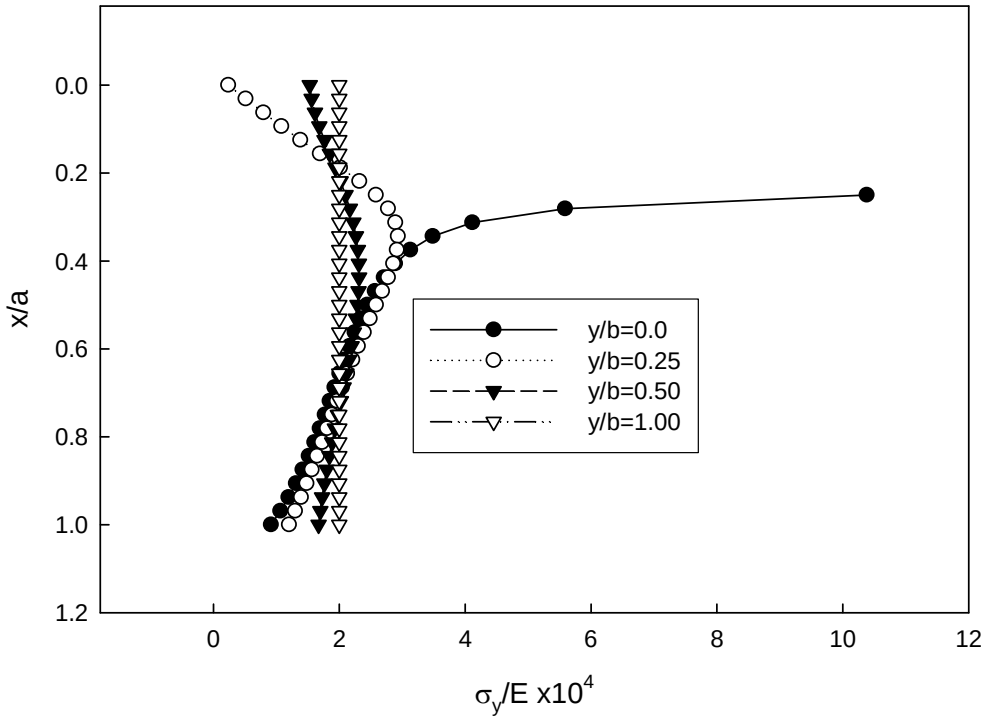

Figure 4.46: Results for normalized normal stress (σ_y/E) obtained by uniform meshing technique at various section of the material.

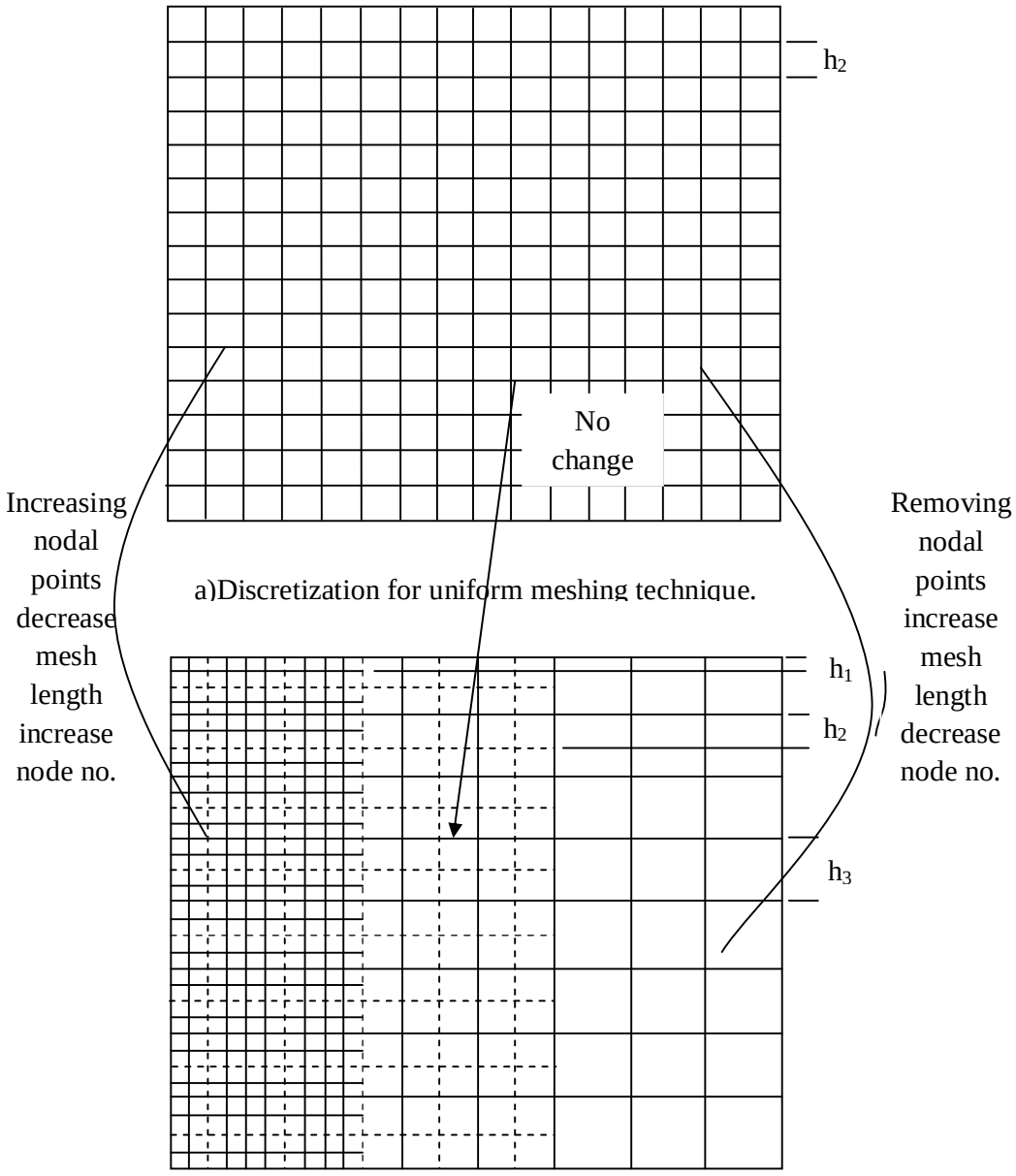

Figure 4.47: Discretization of the domain for finite difference method.

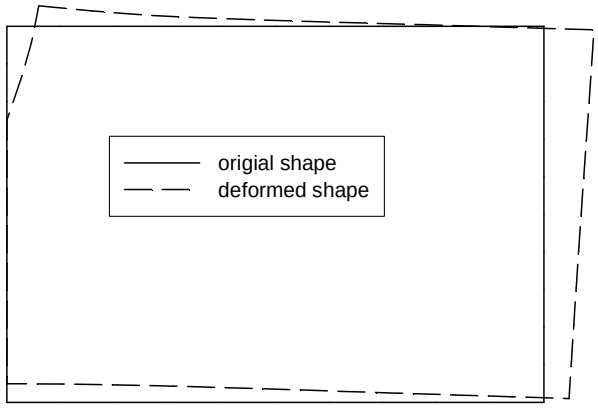

Figure 4.48: Original shape and deformed shape of the body. u and v are 300 times magnified.

Figure 4.48 shows the original shape and deformed shape of the body. From qualitative view the result is correct. From this figure we see that bending occurs in the clockwise direction. This is due to eccentricity of forces. Due to the presence of crack the neutral axis and centroidal axis does not coincide each other and as a result there creates a moment that causes the material to rotate in clockwise direction.

The results, of this above problem, obtained by these two techniques are shown from figure 4.49 to 4.56. The figure 4.49 shows normalized displacement (v/b) at y/b=0.0 by these two methods as a comparative study. At y/b=0.0 for mesh refinement technique there is greater number of nodal points (almost double) than that of uniform meshing technique as shown in figure 4.47. From figure 4.49, at y/b=0.0 the displacement obtained by two methods almost same but distribution of displacements points is much better in mesh refinement technique. Also maximum displacement is somewhat larger by mesh refinement technique. Figure 4.50 shows same results for a section at y/b=1.00. This figure shows that deflection varies linearly with x/a for both of these two methods. Again results of both techniques are similar in nature but results obtained by uniform meshing are smaller in magnitude than that of obtained by mesh refinement technique. Figure 4.51 shows normalized displacement v/b for another two sections y/b=0.25 and y/b=0.5 and the results of both methods matches each other in nature. But there is small difference in results of these two method in magnitude and as we move

from y/b=0.0 to y/b=1.00 the differences increases. However, the differences is always is lies in acceptable range. This displacement obtained by mesh refinement technique does not show any improvement over uniform mesh refinement technique in terms of accuracy. So take a closer look to figure 4.52. Which shows Comparison of the results for normalized normal stress (σ_y/E) obtained by mesh refinement technique and uniform mesh technique with almost same no. of nodal points at two section y/b=0.0 and y/b=1.00. This figure shows that at y/b=1.00 the results of both methods is exactly same and equal to applied stress $\sigma_1/E= 2.00x10^{-4}$. But at y/b=1.00, the results obtained by mesh refinement technique is larger than that of uniform meshing technique and this is the improvement of results by mesh refinement technique over uniform meshing technique because literatures say that at the tip of the crack the stress should higher than other section of the material. Since mesh refinement technique gives higher results than that of uniform meshing technique, so it can be stated that for same amount of nodal points mesh refinement technique improve the accuracy of results over uniform meshing technique in the vicinity of a stress riser.

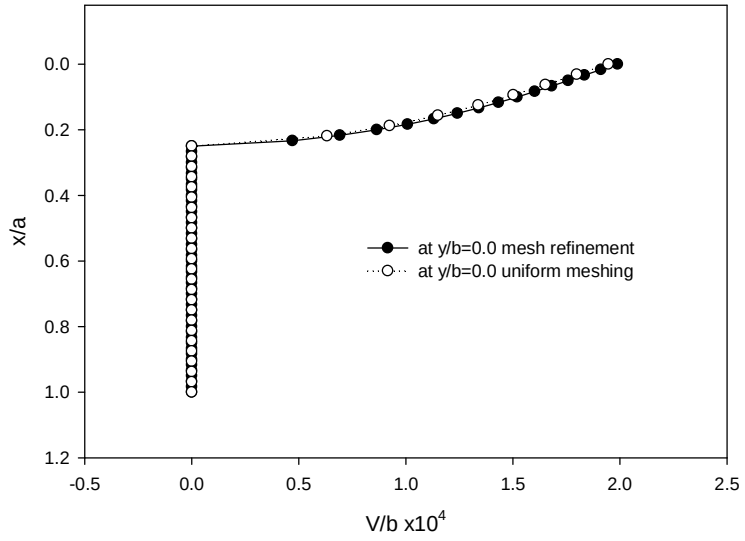

Figure 4.49: Comparison of the results for normalized displacement (v/b) obtained by mesh refinement technique and uniform mesh technique with almost equal no. of nodal points.

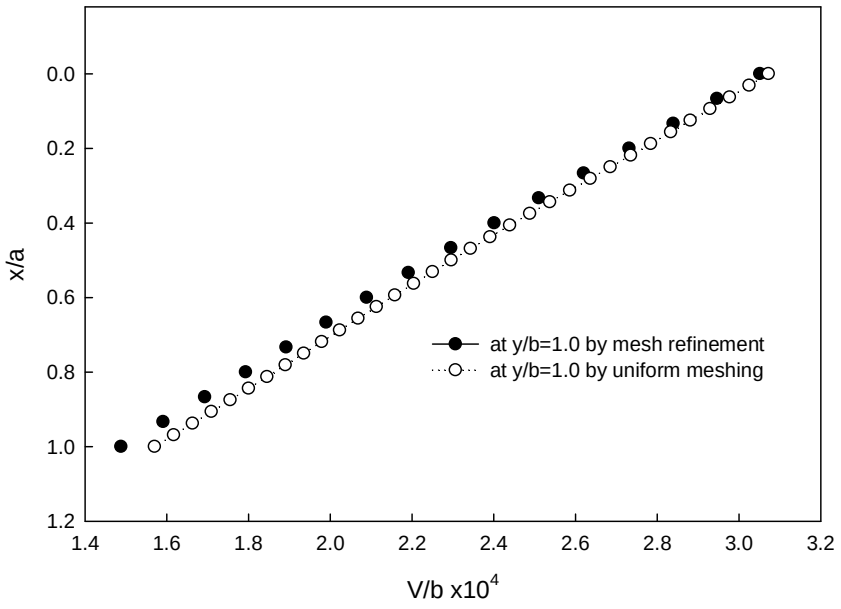

Figure 4.50: Comparison of the results for normalized displacement (v/b) obtained by mesh refinement technique and uniform mesh technique with almost equal no. of nodal points.

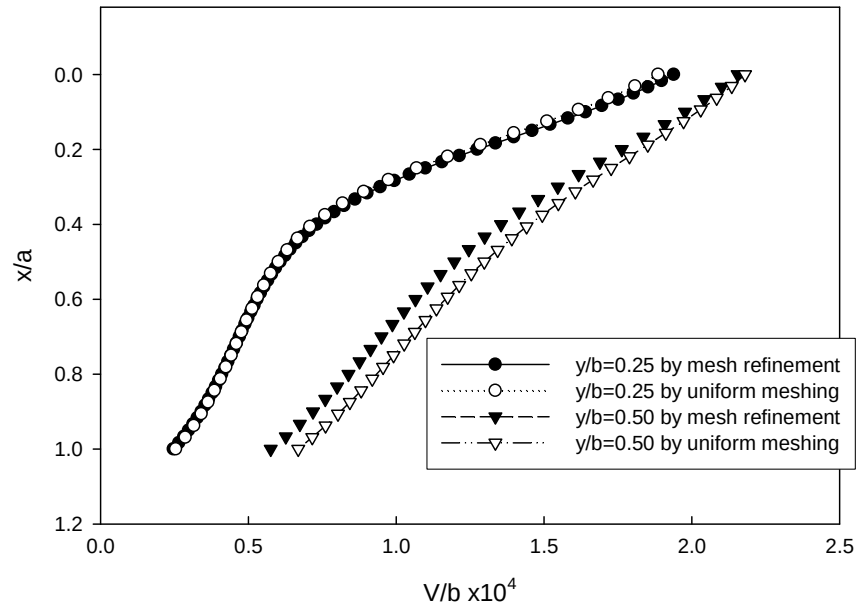

Figure 4.51: Comparison of the results for normalized displacement (v/b) obtained by mesh refinement technique and uniform mesh technique with almost equal no. of nodal points.

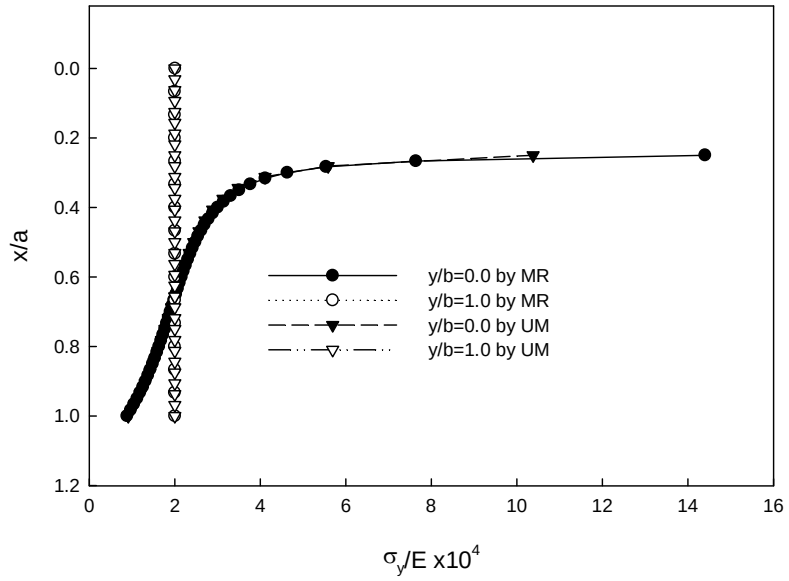

Figure 4.52: Comparison of the results for normalized normal stress (σ_y/E) obtained by mesh refinement technique and uniform mesh technique with almost equal no. of nodal points.

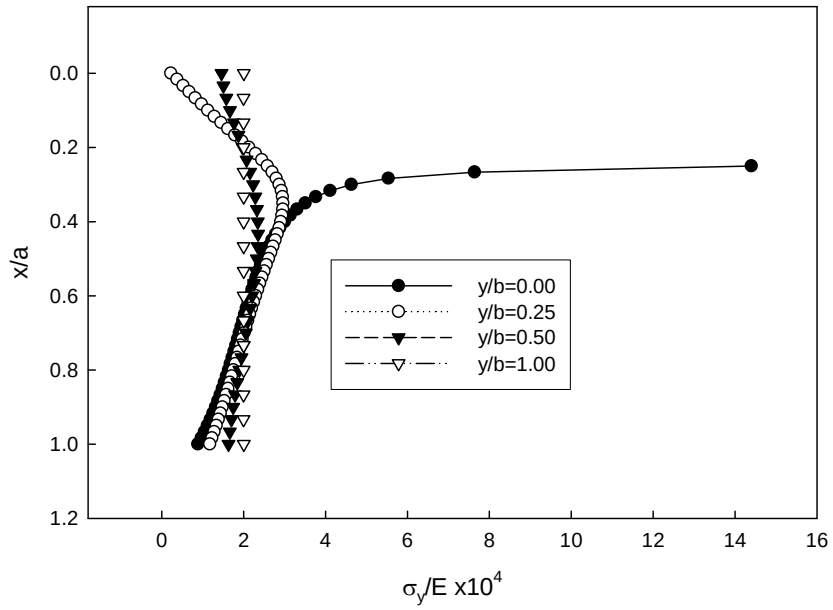

Figure 4.53: Results for normalized normal stress (σ_y/E) obtained by mesh refinement technique at various section of the material.

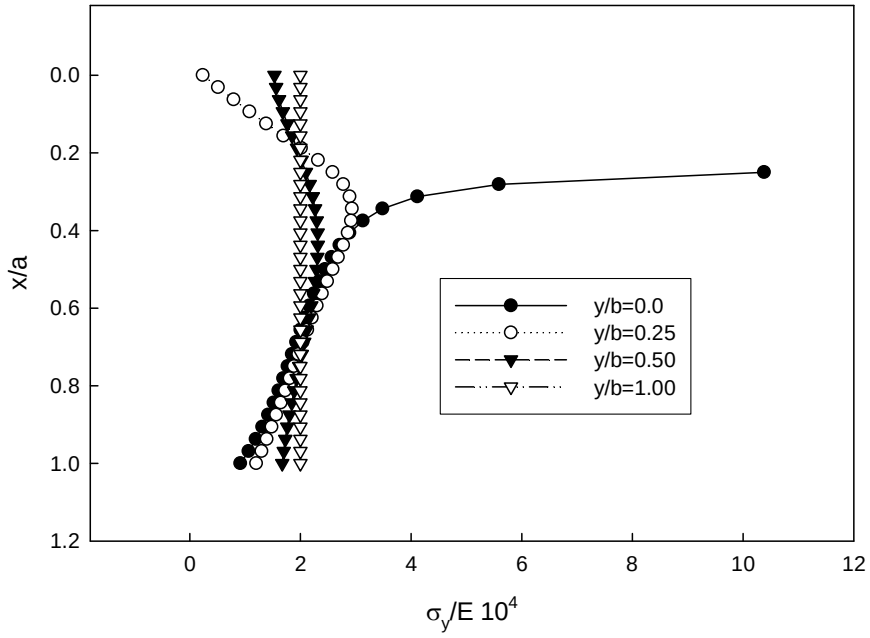

Figure 4.54: Results for normalized normal stress (σ_y/E) obtained by uniform meshing technique at various section of the material.

Figure 4.55 and 4.56 shows normalized normal stress in x-direction, σ_x/E with x/a. Figure 4.55 show a comparative study of stress obtained by MR and UM technique. For both techniques stress is maximum at the crack tips and it reduces as x/a increases. The MR technique gives a larger value of σ_x at the crack tip than obtained by UM technique.

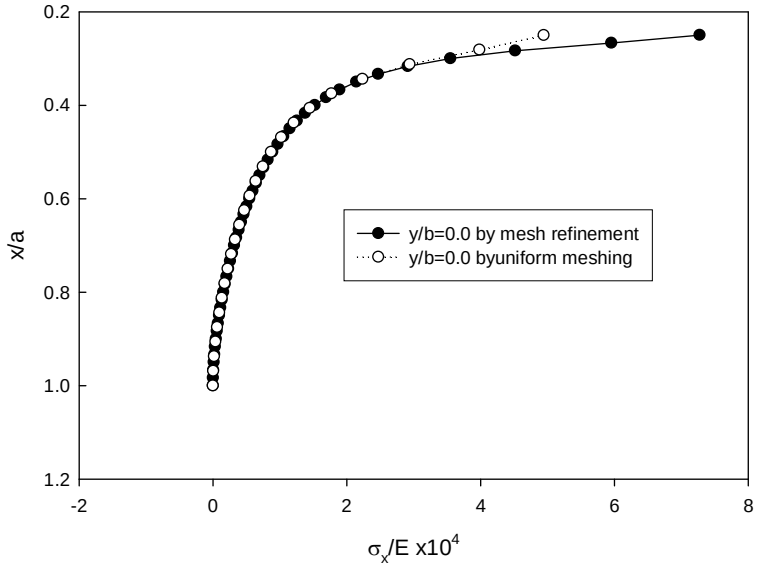

Figure 4.55: Comparison of the results for normalized normal stress (σ_x/E) obtained by mesh refinement technique and uniform mesh technique with almost equal no. of nodal points.

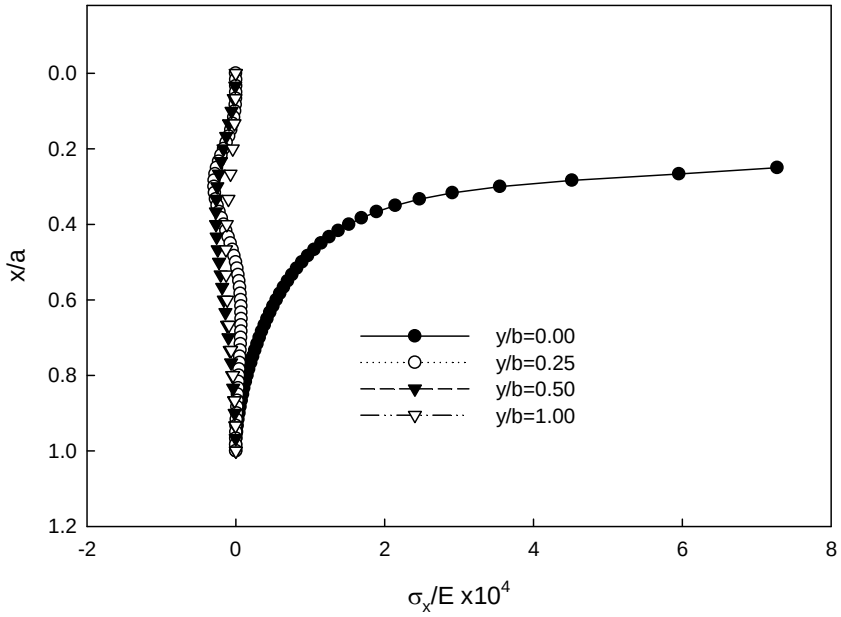

Figure 4.56: Results for normalized normal stress (σ_x/E) obtained by mesh refinement technique at various section of the material.

CHAPTER 5

CONCLUSIONS AND RECOMMENDATIONS

5.1 Conclusions

In this study a finite difference approach based on the displacement potential function formulation has been developed for the solution of two-dimensional elastic problems of simple homogeneous material under different boundary conditions. Since this approach deals with a single variable displacement potential function (ψ), it is found to be convenient to work with. The purpose of this thesis had not to solve this above type of problem but to develop a new mesh refinement technique for fourth order bi-harmonic partial differential equation by which problems that contain sharp change in cross section, stress concentrator or riser, material flaws and voids, cracks, holes etc. can be solved very effectively and efficiently. From this point of view this work reaches its goal successfully. A general algorithm has been made by which one can easily choose any part of the field to analysis critically by taking finer mesh in that part. Six different stencils for bi-harmonic governing equation and some other stencils for boundary conditions have been made and applicability on nodes of these stencils has been shown by figures. An efficient management technique is successfully developed to manage the boundary conditions and GE at position where mesh sizes transition regions. Also an efficient way has been created to apply fourth order bi-harmonic partial differential equation over non-uniform mesh. A programming code in the FOTRAN language is developed for this finite difference approach. Finite element results are carried out by using the commercial software. Results are presented in the graphs as non-dimensional form. Finally, the following conclusions are drawn in relation to the present research work:

1. The recently available methodology for the numerical solutions of mixed boundary-value elastic problem based on the ψ-formulation can be applied to the body of isotropic mechanical properties. An extended and completely new computational approach of this ψ-formulation for stress analysis is presented in this thesis removing the limitations uniform meshing of domain and boundary.

2. Completely new numerical formulations are developed in this thesis to handle to apply governing equation and boundary conditions for the mesh size transition regions. The numerical formulations with greater inclusion points at the mesh size transition region provide better solution i.e. the aligned numerical formulations like combination of more forward backward finite difference formulae at mesh size transition region could not provide better solution rather the balanced numerical formulations like combination of more central difference at mesh size changing region provide better solution.
3. The obtained solutions from the finite difference method are verified in numerous ways like comparison with the solution from finite element method, well-known published results, and uniform meshing by FDM, by seeing the symmetric and anti-symmetric nature of the solutions and by qualitative intuition.
4. Comparison between the results by the mesh refinement finite difference method and the existing standard commercial software based on finite element method provide the good superiority of the MR technique over FEM.
5. This mesh refinement technique i.e. taking high resolution in mesh size where necessary overcome the limitation of classical FDM which uses uniform mesh length and size. This new technique reduces the number of nodal points thus number of linear equation which makes the solution faster i.e. reduces the time consuming to run the program and due to lowering the number of nodal points, saves a huge amount computer memory.
6. To study the benefits of new technique one single problem is solved by two method, one is classical FDM which uses uniform mesh size and length and other one is this new technique and see that for almost equal number of nodal points i.e. linear algebraic equation, this new technique gives better results i.e. improves the accuracy of the results.

5.2. Recommendations for further research

The present study is perhaps the first attempt for the analysis of stresses by displacement potential function for two-dimensional elastic problems by introducing mesh refinement technique. Due to this reason the present study is limited to simple

elastic problem one can spread this technique to solve much more complex problem by writing new program.

- This thesis is limited to applying three different sizes mesh, attempts should be made to increase the total number of mesh refinement zone for more accurate results i.e. taking four, five, etc different sizes mesh and making ultra fine mesh around the part where results have to be known accurately. Moreover, it will be appropriate to use smaller mesh size all along the boundary and near the vicinity of crack this will produce better result.
- .This thesis has limited application of this new technique over some simple problem but one can apply this technique on very complex problem such as stress analysis of gear teeth, at wing of air plane etc. In these cases one has to incorporate the direction cosine to apply boundary conditions because for such cases the geometry will not rectangular.
- This new technique can be applied to solve stress around a hole by taking finer mesh around hole which gives a chance of checking accuracy of this new technique because stress concentration factor for a circular hole or ellipse is a well known value.
- This thesis work obtained *h*-refinement by splitting the existing mesh in smaller one, so there presents opportunity to develop another MR algorithm of *h*-refinement by inserting mesh locally in the existing mesh and could compare the results with each other to check which one is better in terms of computational efforts and memory consuming.

CHAPTER 6

REFERENCES

[1] Akanda, M. A. S., Ahmed, S.R., Khan, M. R., and Uddin, M. W., "A finite-difference scheme for mixed boundary-value problems of arbitrary-shaped elastic bodies", Advances in Engineering Software, 31(2000), No. 3, 173-184.

[2] Akanda, M. A. S., Ahmed, S.R. and Uddin, M. W., "Stress analysis of gear teeth using displacement potential function and finite-differences", International Journal for Numerical Methods in Engineering, 53(2001), No. 7, 1629-1649.

[3] Berger M. and Oliger J., "Adaptive mesh refinement for hyperbolic partial differential equation". - J. Comput. Phys., vol. 53, pp. 484-512, 1984.

[4] Mayo A., "The fast solution of poisson's and the biharmonic equations on irregular regions". – SIAM J. Numer. Anal., vol. 21, pp. 285-299, 1984.

[5] Berger M. and Colella P., "Local adaptive mesh refinement for shock hydrodynamics". - J. Comput. Phys., vol. 82, pp. 64-84, 1989.

[6] Berger M. and Leveque R., "Adaptive mesh refinement using wave-propagation algorithms for hyperbolic systems". – SIAM J. Numer. Anal., Vol. 35, No. 6, pp. 2298-2316,1998.

[7] Uddin, M. W., "Finite difference solution of two-dimensional elastic problems with mixed boundary conditions", M. Sc. Thesis, Carleton University, Canada, 1966.

[8] Idris A.B.M, "A new approach to solution of mixed boundary value elastic problem", M. Sc. Thesis, Bangladesh University of Engineering and Technology, Bangladesh, 1993.

[9] Ahmed, S. R., "Numerical solution of mixed boundary value elastic problems", M. Sc. Thesis, Bangladesh University of Engineering and Technology, Bangladesh, 1993.

[10] Ahmed SR, Khan MR, Islam KMS, Uddin MW. "Analysis of stresses in deep beams using displacement potential function", Journal of Institution of Engineers (India) 1996; 77: 141-7.

[11] Airy, G. B., Report of the British Association for the Advancement of Science, 1862.

[12] Mesnager, A., Stress analysis of bending of beams of narrow rectangular cross section using stress function, Comptes Rendus, Vol. 132, pp. 1475, 1901.

[13] Timpe, A., Z. Math. Physik., Vol. 52, pp. 348, 1905.

[14] Levy, M., Stress analysis in masonary dams using Airy's stress function, Comptes Rendus, Vol. 126, pp. 1235, 1898.

[15] Scewald, F., Stress analysis in masonary dams using polynomial expressions for Airy's stress function Abhandl. Aerodynam. Inst. Tech. Hochschule, Aachen, Vol. 7, pp. 11, 1927.

[16] Saint- Venant, B., Stress analysis in masonary dams near the foundation, Mem. Savants Estrangers, Vol. 14, 1855

[17] Timoshenko, S. P., "The approximate solution of two-dimensional problems in elasticity", *Philosophical Magazine*, Vol. 47, pp. 1095, 1924.

[18] Runge, C., Solution of torsional problems by finite difference equations, Z. Math. Physik., Vol. 56, pp. 225, 1908.

[19] Conway, H. D., Chow, L. and Morgan, G. W., "Analysis of deep beams", Journal of applied mechanics Trans. ASME, Vol. 18, No. 2, pp. 163-172, 1951.

[20] Akanda, M. A. S., "Stress analysis of gear teeth", M. Sc. Thesis, Bangladesh University of Engineering and Technology, Bangladesh, 1997.

[21] Ahmed, S.R., Idris, A. B. M. and Uddin, M. W., "Numerical Solution of Both Ends Fixed Deep Beams", Computers & Structures, Vol. 61, No. 1, pp. 21-29, 1996.

[22] Quddus, N. A., "Development of a boundary management technique in finite difference method of solution", M. Sc. Thesis, Bangladesh University of Engineering and Technology, Bangladesh, 2003.

[23] Hossain, M. Z., "A new approach to numerical solution of three dimensional mixed-boundary-value elastic problems", M. Sc. Thesis, Bangladesh University of Engineering and Technology, Bangladesh, 2004.

[24] Hossain, M. Z., Ahmed, S. R. and Uddin, M. W., "Generalized mathematical model for the solution of mixed-boundary-value elastic problems", Applied Mathematics and Computation, Vol. 169, Issue 2, pp. 1247-1275, 2005.

[25] Rahman, M. A., "A finite difference scheme for mixed boundary values of two dimensional elastic problems with internal hole", M. Sc. Thesis, Bangladesh University of Engineering and Technology, Bangladesh, 2006.

[26] Turner, M. J., Clough, R. W., Martin, H. C. and Topp, L. J., "Stiffness and deflection analysis of complex structures", J. aero. Sci, Vol. 23, pp. 805-823, 1956.

[27] Clough, R. W., "The finite element in plane stress analysis", Proc. 2nd A.S.C.E Conf. on electronic Computation, Pitsburg, Sept. 1960.

[28] Zienkiewicz, O. C. and Cheung, Y. K., “The finite element method in structural and continuum mechanics”, McGraw-Hill Publishing Company Ltd., England, 1967.

[29] Min C., Gibou F. and Ceniceros H. D. “A supra-convergent finite difference scheme for the variable coefficient Poisson equation on non-graded grids”. - J. Comput. Phys., submitted 2006.

[30] Gibou F., Fedkiw R., Cheng L.T. and Kang M., “A second-order accurate symmetric discretization of the poisson equation on irregular domains”. - J. Comput. Phys., vol. 176, pp. 205-227, 2002.

[31] Ceniceros H. D. and Roma A. M., “Study of long-time dynamics of a viscous vortex sheet with a fully adaptive non-stiff method”. – J. Comput. Phys., vol. 16, No.12, pp. 4285-4318, 2004.

[32] Johansen H. and Colella P., “A Cartesian grid embedded boundary method for poisson’s equation on irregular grids”. – J. Comput. Phys., vol. 147, pp. 60-85,1998.

[33] McCorquodale P., Colella P., Grote D. and Vay J. L., “A node-centered local refinement algorithm for poisson’s equation in complex geometries”. – J. Comput. Phys., vol. 201, pp. 34-60, 2004.

[34] Bieniasz L.K., “Experiments with a local adaptive grid h-refinement for the finite-difference solution of BVPs in singularly perturbed second-order ODEs”. Applied Mathematics and Computation 195 (2008) 196–219.

[35] Unterweger K., Weinzierl T., Ketcheson D. and Ahmadia A., “Spacetree-Based Adaptive Mesh Refinement for Hyperbolic Partial Differential Equations”. Numerical Software: Design, Analysis and Verification, 4-6 July 2012, Santander (Spain).

[36] Hiester H.R., Piggott M.D., Farrell P.E., Allison P.A., “Assessment of spurious mixing in adaptive mesh simulations of the two-dimensional lock-exchange”. Ocean Modelling 73 (2014) 30–44.

[37] T. Plewa, T. Linde, e. Gregory Weirs, V., Adaptive mesh refinement – theory and applications, in: Proceedings of the Chicago workshop on adaptive mesh refinement methods, Springer, 2003.

[38] Mehl S. and Hill M.C., “Development and evaluation of a local grid refinement method for block centered finite difference groundwater models using shared nodes”. Advances in water resources 25 (2002) 497-511.

[39] Ding H. and Shu C., “A stencil adaptive algorithm for finite difference solution of incompressible viscous flows”. Journal of Computational Physics 214 (2006) 397-420.

[40] T. Basebi, R.M. Thomas, A study of moving mesh methods applied to a thin flame propagating in a detonator delay element, Comput. Math. Appl. 45 (2003) 131–163.

[41] E.D. Wilkes, S.D. Phillips, O.A. Basaran, Computational and experimental analysis of dynamics of drop formation, Phys. Fluids 11 (12) (1999) 3577–3598.

[42] D.M Greaves, A.G.L. Borthwick, G.X. Wu, R.E. Taylor, A moving boundary finite element method for fully non-linear wave simulations, J. Ship Res. 41 (1997) 181–194.

[43] Timoshenko, S. P. and Goodier, J. N., Theory of Elasticity, 3rd Ed., McGraw-Hill Book Company, New York, N. Y., 1979.

[44] Sokolnikoff, I.S., Mathematical Theory of Elasticity, McGraw-Hill Book Company Inc., New York, 1956.

[45] Kolosoff, G.V. Application of a complex variable to the theory of elasticity, Moscow, objed, nauchno-tekhn, izd, 1935.

[46] Shigley J.E., Mechanical Engineering Design, First metric edition, McGraw-Hill Book Company Inc., New York, 1986.